NASA CR-165224
TRW ER-8001-F

DEVELOPMENT OF MATERIALS AND PROCESS TECHNOLOGY FOR DUAL ALLOY DISKS

FINAL REPORT

OCTOBER 1981

C. S. KORTOVICH
J. M. MARDER

Prepared For

NATIONAL AERONAUTICS and SPACE ADMINISTRATION
NASA LEWIS RESEARCH CENTER

CONTRACT NAS 3-21351

F. H. HARF, Project Manager

1. Report No. NASA-CR-165224	2. Government Accession No.	3. Recipient's Catalog No.

4. Title and Subtitle	5. Report Date
DEVELOPMENT OF MATERIALS AND PROCESS TECHNOLOGY FOR DUAL ALLOY DISKS	October 1981
	6. Performing Organization Code
7. Author(s) James M. Marder, Charles S. Kortovich	8. Performing Organization Report No. TRW ER-8000F
	10. Work Unit No.
9. Performing Organization Name and Address TRW Inc. TRW Materials Technology 23555 Euclid Avenue Cleveland, Ohio 44117	11. Contract or Grant No. NAS3-21351
	13. Type of Report and Period Covered Contractor Report
12. Sponsoring Agency Name and Address National Aeronautics and Space Administration Washington, D.C. 20546	14. Sponsoring Agency Code

15. Supplementary Notes

Project Manager, Fredric H. Harf, Materials & Structures Division, NASA Lewis Research Center, Cleveland, Ohio 44135

16. Abstract

A program was conducted to develop and evaluate techniques for the preparation of dual alloy disks. Four material combinations were evaluated in the form of HIP consolidated and heat treated cylindrical and plate shapes in terms of elevated temperature tensile, stress rupture and low cycle fatigue properties. The process evaluation indicated that the pre-HIP AF-115 rim/loose powder Rene' 95 hub combination offered the best overall range of mechanical properties for dual alloy disk applications.

The feasibility of this dual alloy concept for the production of more complex components was demonstrated by the scale-up fabrication of a prototype CFM-56 disk made from this AF-115/Rene' 95 combination. The hub alloy ultimate tensile strength was approximately 92% of the program goal of 1520 MPa (220 ksi) at 480°C (900°F) and the rim alloy stress rupture goal of 300 hours at 675°C (1250°F)/925 MPa (134 ksi) was exceeded by 200 hours. The low cycle fatigue properties were equivalent to those exhibited by HIP and heat treated alloys. There was an absence of rupture notch sensitivity in both alloys. The joint tensile properties were approximately 85% of the weaker of the two materials (Rene' 95) and the stress rupture properties were equivalent to those of the weaker of the two materials (Rene' 95).

17. Key Words (Suggested by Author(s))	18. Distribution Statement
Nickel Alloys Powder Disk Applications Hot Isostatic Pressing Vacuum Sintering	Unclassified - Unlimited

19. Security Classif. (of this report)	20. Security Classif. (of this page)	21. No. of Pages	22. Price*
Unclassified	Unclassified		

* For sale by the National Technical Information Service, Springfield, Virginia 22151

FOREWORD

The work described in this final report was performed in the Materials Technology Laboratory of TRW Inc. under NASA Contract NAS 3-21351, TRW Project No. 512-002988-88. The work was performed under the direction of Dr. C. S. Kortovich, the Program Manager, with J. M. Marder as the Principal Investigator. Technical assistance was provided by Mr. J. W. Sweeney and Mr. R. E. Ebert. The contract was administered under the management of the NASA Project Manager, Mr. F. H. Harf, Materials and Structures Division, NASA Lewis Research Center. Dr. R. V. Miner served as the NASA Research Advisor.

TABLE OF CONTENTS

LIST OF TABLES

LIST OF TABLES (continued)

LIST OF FIGURES

LIST OF FIGURES (continued)

LIST OF FIGURES (continued)

LIST OF FIGURES (continued)

LIST OF FIGURES (continued)

1.0 SUMMARY

The objective of this program was the development and evaluation of techniques for the preparation of dual alloy disks. The program was divided into two tasks. Task I involved process and mechanical property screening evaluations of promising dual alloy materials combinations. Task II included the scale-up of one of the material combinations to a large disk configuration for more extensive evaluations.

In Task I, four material combinations were evaluated in the form of HIP consolidated cylindrical shapes and then two material combinations were evaluated in the form of thick rectangular plates. The four material combinations are listed as follows:

Vacuum pre-sintered Rene' 95 rim/loose powder Rene' 95 hub

Loose powder L/C Astroloy rim/loose powder MERL 76 hub

Pre-HIP AF-115 rim/loose powder Rene' 95 hub

Vacuum pre-sintered PA-101 rim/loose powder MERL 76 hub

The process evaluations indicated that the pre-HIP AF-115 rim/loose powder Rene' 95 hub combination offered the best overall potential to meet the program mechanical property goals. The optimum processing of this combination included pre-HIP of the AF-115 rim candidate material at 1190°C (2175°F)/4 hours/105 MPa (15 ksi) followed by HIP consolidation with the Rene' 95 material at 1120°C (2050°F)/4 hours/105 MPa (15 ksi). The subsequent heat treatment included: 1205°C (2200°F)/2 hours salt quench to 650°C (1200°F) plus 760°C (1400°F)/16 hours.

In Task II, the feasibility of this dual alloy concept for the production of more complex components was demonstrated by the scale-up manufacture of a prototype CFM-56 disk and extensive mechanical property evaluations of this disk. Processing modifications for the large disk included a reduction in the solution heat treatment temperature from 1205°C (2200°F) to 1190°C (2175°F) in order to minimize the occurrence of triple point melting in the AF-115 observed with the 1205°C (2200°F) solution temperature and quench cracking observed primarily at the interface between the two alloys. The triple point melting was eliminated while the quench cracking was not. These cracks were usually associated with the portions of the AF-115 interface not specifically prepared for the HIP consolidation operation with the Rene' 95 powder. The mechanical property results indicated that the hub alloy ultimate tensile strength was approximately 92% of the program goal of 1520 MPa (220 ksi) at 480°C (900°F) and the rim alloy stress rupture goal of 300 hours at 675°C (1250°F)/925 MPa (134 ksi) was exceeded by 200 hours. The low cycle fatigue properties were equivalent to those exhibited by HIP and heat treated alloys. There was an absence of rupture notch sensitivity in both alloys. The joint tensile properties were approximately 85% of the weaker of the two materials (Rene' 95) and the stress rupture properties were equivalent to those of the weaker of the two materials (Rene' 95).

2.0 INTRODUCTION

The development of advanced high temperature materials and processing systems has been primarily responsible for the improvements in the performance of advanced gas turbine engines. Recent emphasis upon reductions in life cycle costs through reduced fuel consumption and operating costs and increased engine reliability has imposed more stringent combined requirements for higher operating temperatures and longer component lives (1). Traditionally, materials engineers have responded to such requirements by developing new alloys as well as novel production methods for optimized control of part geometry and microstructure.

A particularly significant response has been in the advancement of turbine disk technology. Specifically, the application of advanced powder metallurgy alloys and processing techniques to disk fabrication has resulted in two distinct advantages which complement each other. In the first place, prealloyed powder processing provides superalloys with the capability for improved mechanical properties (2). Powder metallurgy alloys can be specifically tailored to accomodate quantities of strengthening elements which would result in large scale phase segregation if produced in cast and wrought form. The presence of the strengthening elements imparts enhanced mechanical properties to these microstructurally homogeneous alloys (3). In the second place, powder metallurgy methods provide the potential for significant cost reductions compared to conventionally cast and wrought parts through efficient material utilization (4). Processing methods such as hot isostatic pressing (HIP) provide a technique to go directly from raw material to a near net shape in disk products.

In spite of these advantages, however, there is a serious limitation to the application of powder metallurgy techniques for future, advanced commercial gas turbine engines. Compared to current engines, turbine disks of advanced designs will have to withstand higher rotational speeds and gas temperatures (5). Typical operating conditions for the advanced engines may result in stresses at the disk bores exceeding 1400 MPa (200 ksi) while rim operating temperatures may approach 760^{o}C (1400^{o}F). A number of the promising candidate powder metallurgy disk alloys such as AF-115, NASA 11B-7, and AF2-1DA can be processed to have yield strengths approaching 1400 MPa (200 ksi) at temperatures as high as 650^{o}C (1200^{o}F) (6-8). In addition to improved short time strength compared to conventional forged alloys, significant improvements in long time creep rupture strength at high temperatures can also be obtained (3); it has been observed, however, that the large grain sizes required for high creep rupture strength necessitate higher solution treatment temperatures than should be used to achieve the greater short time tensile strength. Therefore a compromise has to be made in the processing to achieve acceptable mechanical property levels in the various disk areas. Thus, powder metallurgy processing, similar to other uniform processing approaches, is limited by the inability of currently available alloys to provide the wide range of properties needed for the various disk areas.

Dual alloy processing offers the potential to overcome this limitation and accomplish the fabrication of disks with a hitherto unachieved scope of mechanical properties. The feasibility of combining two different alloys has been demonstrated for bi-cast integral turbine wheels (9,10) and powder metallurgy integral turbine wheels (11,12). In all of these cases the blades were first produced separately and then combined with a different disk alloy by either casting or powder metallurgy operations. These processes are thus limited in that the entire disk material is uniform in composition and does not offer the required range of properties.

Other approaches exist which can provide a fabricated disk with a wide range of mechanical properties. Selective thermomechanical processing, for example, can be applied so that the hub area receives more deformation than the rim area. Induction heat treatments are then applied to the rim areas to develop enhanced creep properties (13). A more direct approach is the manufacture of disks by joining via HIP two different materials, which, when given a uniform heat treatment, should meet the property requirements of advanced disk designs. In addition to the cost advantages associated with direct HIP to shape fabrication (4), the concept offers increased flexibility to achieve the range of properties required in the end product. Prior to the present investigation, processing necessary to join the dissimilar materials had not been defined, nor had the microstructure and property characteristics of the rim, hub and joint areas been evaluated.

The present investigation was conducted to develop and evaluate techniques for the preparation, joining and heat treatment of dual alloy disks to satisfy the anticipated requirements of advanced commercial aircraft turbine engines. Emphasis was placed upon the utilization of existing alloys, which were to be neither forged nor otherwise thermomechanically processed. HIP processing was used to accomplish the joining and uniform heat treatments were applied to achieve optimum mechanical properties for both rim and hub applications. The experimental approach involved two tasks. In Task I - Process Evaluation, various alloy/processing combinations were investigated. Mechanical property screening tests included tensile, stress rupture and low cycle fatigue tests as well as characterization of the microstructures of the rim and hub candidate materials and the joint regions of the dual components. Small prototype disks from selected combinations were produced to determine how the location of the joint would be affected by the HIP processing. In Task II - Sub-Scale Disk Evaluation, a single material/process combination was scaled-up to a larger disk configuration and subjected to a more extensive evaluation.

This report summarizes the results obtained on the NASA-Lewis Research Center Contract NAS3-21351. It includes a review of the program to develop materials and process technology for dual alloy disks, a review of the experimental procedures, a summary of the experimental results, a discussion of these results, and recommendations for future work to optimize processing for dual alloy disks.

3.0 PROGRAM OUTLINE

The basic aim of the program was the development and evaluation of techniques for the preparation, joining and heat-treatment of two materials for use in the production of disks satisfying property requirements of advanced commercial aircraft turbine engines. These requirements represented the goals of the program and included the following:

1. In the hub material a tensile strength of 1520 MPa (220 ksi) at 480°C (900°F).

2. In the rim material at 925 MPa (134 ksi) stress a 300 hour rupture life at 675°C (1250°F).

3. Joint properties not less than 90 percent of the weaker of the two component materials.

4. Absence of notch-brittle conditions in the rim material.

5. Low cycle fatigue resistance in the hub material equal or superior to that in currently used disk materials.

The approach used to accomplish the program objectives included the manufacture of components made by joining by HIP techniques two different materials which were given a uniform heat treatment in order to meet the property requirements of advanced turbine disks. Initially, the study consisted of HIP joining evaluations conducted on candidate alloy pairs. It was augmented by heat treatment evaluations to develop optimized mechanical properties in test panels. Based on the results of these initial studies, one material-heat treatment combination was selected for the production of a scaled-up disk which was subjected to more detailed property evaluations.

The program was divided into two tasks as shown in Figure 1, the Work Breakdown Structure. The Task I of the investigation consisted of process evaluations and included the detailed study of shapes made from four different material/heat treatment combinations. Also included in Task I was the production of small prototype disks from selected combinations used to determine how the location of the joint was affected by the HIP operation. Task II consisted of the scale-up of one material-heat treatment combination to a larger disk configuration for more complete evaluations.

3.1 Task I - Process Evaluation

During Task I, process evaluations were performed to enable selection of a method of fabricating a full scale dual alloy disk. Mechanical property, microstructure, and joint location studies were carried out to accomplish these objectives.

3.1.1 Alloy Combination Selection

A number of different candidate nickel-base superalloys were available which could meet, in part, the goals of this program. None of the alloys, however, could meet

the entire spectrum of property requirements. The specific alloy combinations or pairs selected for the program were a function of the optimized property levels which could be expected from the various alloys.

3.1.1.1 Rim Alloy Candidates

The operating environment of turbine disk rims is one of high temperature, in the 760°C (1400°F) range, accompanied by stresses of intermediate magnitude imposed by the centrifugal loading of the turbine airfoils. This environment results in limitation on creep and stress rupture life (14). The chemical compositions of the rim alloy candidates selected for this program are listed in Table 1 and a Larson-Miller parameter curve comparing the stress rupture behavior of these alloys is presented in Figure 2. It should be pointed out that these mechanical properties are presented only for powder metallurgy material in the HIP plus heat treated condition.

Rene' 95 was initially developed to provide high strength in the highly stressed hub area of turbine disks. Because of the necessity to produce high strength, current processing techniques generally result in a finished component grain size of ASTM 8-10 (17). Analysis of the data available for fine grained Rene' 95 HIP'ed powder indicated that the stress rupture properties were not suitable for the rim of a dual alloy disk. However, grain coarsening treatments such as high temperature HIP or vacuum sintering could be used to increase the stress rupture properties to a higher level (17).

Low Carbon (LC) Astroloy is a chemical modification of U-700, an alloy originally developed as a forged turbine blade material (20). Because the primary impetus toward turbine blade development is improved creep and stress rupture, the U-700 family of alloys exhibits, as would be expected, excellent properties in this regard. A large amount of data available for powder metallurgy Astroloy (15) indicated that in the HIP'ed and heat treated condition, adequate stress rupture properties for use in the rim of a dual alloy disk could be achieved.

PA-101 is a modification of IN-792, which relies upon hafnium additions to provide improved ductility and strength. IN-792, like U-700, was originally formulated as a stress and creep rupture resistant turbine blade alloy. In the course of powder processing, however, PA-101 generally develops a fine grain size, which limits stress-rupture strength. The application of a grain growth treatment has been shown to restore a large portion of the rupture life, at the expense of tensile properties (17,18), thus making the PA-101 suitable as a rim alloy candidate.

AF-115 is an alloy developed as a powder metallurgy product uitlizing a HIP consolidation, and requiring a subsequent forging operation to develop strength. Evaluation of the alloy in the as-HIP condition, however, revealed that the stress rupture properties at this processing stage were suitable for the rim of a dual material disk (19).

3.1.1.2 Hub Alloy Candidates

The hub of a turbine disk operates in a low temperature-high stress regime. Disk designs are often constrained by burst or low cycle limitation of the hub material. Both burst and LCF properties can be improved by decreasing grain size and increasing strength (21). The target goal of the hub area for this program was an ultimate tensile strength of 1520 MPa (220 ksi) at 480°C (900°F) without benefit of forging or thermomechanical treatment. Only a limited number of alloys exhibited sufficient strength capability in the HIP'ed and heat treated condition for consideration as the hub of a dual alloy disk, including fine grain Rene' 95 and MERL 76. The composition of MERL 76 is listed in Table 1 and the ultimate tensile strength properties of both alloys as well as those of the rim candidate alloys are compared in Figure 3.

HIP'ed Rene' 95, processed to a fine grained ASTM 8 grain size, has exhibited very high tensile strength capability in the solution treated and aged condition (16,17). Data for this material were obtained in the form of tensile test results on specimens machined from a T-700 turbine disk. MERL 76 is a developmental alloy based upon a powder metallurgy version of IN-100 (14). Hafnium and columbium levels are varied from the standard IN-100 P/M composition to minimize the formation of prior particle carbide boundaries. These boundaries can result in stress rupture notch embrittlement and poor tensile ductility in the HIP product. The tensile data shown in Figure 3 indicate that this alloy is capable of attaining a desirable hub strength property level.

3.1.1.3 Material Combination Selection

The four material combinations selected for evaluation in this program were the following:

Combination	Rim Material	Hub Material
A	Preconsolidated (Vacuum Sintered) Rene' 95	Loose Powder Rene' 95
B	Loose Powder Low Carbon (L/C) Astroloy	Loose Powder MERL 76
C	Preconsolidated (HIP AF-115)	Loose Powder Rene' 95
D	Preconsolidated (Vacuum Sintered) PA-101	Loose Powder MERL 76

The materials in these combinations were all determined to have acceptable hub and rim mechanical properties. In addition to this primary selection criterion, the material combinations were also chosen to provide the greatest amount of information regarding the effect of various processing conditions upon base material and joint mechanical properties.

3.1.1.3.1 Combination A - Fine Grain Rene' 95 Hub Coarse Grain Rene' 95 Rim

The use of a single alloy for both rim and hub is quite attractive from the standpoint of the uniformity of physical properties. Quenching or operating stresses which might arise as a result of differences in thermal conductivity and thermal expansion characteristics of the rim and hub alloys, would necessarily be eliminated by the utilization of a single alloy in both locations. Rene' 95 has exhibited acceptable hub strength properties when processed to a fine grain size and acceptable rim properties when processed to a coarse grain size. This alloy was, therefore the primary candidate for a single alloy dual-microstructure disk.

3.1.1.3.2 Combination B - MERL 76 Hub - L/C Astroloy Rim

This alloy combination provided a unique set of processing options because of the relation of the gamma-prime solvus temperature of one alloy to another. The MERL 76 hub alloy solvus temperature is above that of the L/C Astroloy rim material. As a general rule for powder metallurgy superalloys, HIP below the gamma-prime solvus is beneficial for strength, whereas HIP above the solvus is beneficial for stress rupture properties. For this combination, therefore, a single powder consolidation step at a temperature between the two solvus temperatures was investigated. This single step consolidation technique would also result in significant cost savings in comparison to the processing schemes which require two consolidation steps.

3.1.1.3.3 Combination C - Fine Grain Rene' 95 Hub - AF-115 Rim

This material combination was selected because of the high temperature strength of fine grained Rene' 95 and the reported stress rupture capability of as-HIP plus heat treated AF-115.

3.1.1.3.4 Combination D - MERL 76 Hub - PA-101 Rim

The ability to coarsen the grain size and thereby effect an improvement in the stress rupture life of PA-101 has been well documented. The suitability of MERL 76 as a hub material has also been demonstrated. These alloys, however, differ significantly in composition and therefore were expected to exhibit differences in physical properties. Testing of this combination of alloys was expected to indicate whether severe stress would develop during heat treatment, particularly as the result of the quenching operation from the solution temperature.

3.1.2 Simple Shape Study

The Simple Shape Study was conducted to develop optimum processing methods for the HIP joining and heat treatment of the four material combinations. A flow chart describing this activity is shown in Figure 4 and shows the iterative approach that was followed. The initial processing studies included HIP joining and heat treatment studies carried out on round bars of consolidated material pairs. Based upon a screening of mechanical properties resulting from a variety of HIP cycles and heat treatments, four

material pair-HIP-heat treatment combinations were selected for more extensive evaluations. This more detailed evaluation was carried out on flat rectangular panels. Schematic diagrams of the cylindrical and flat panel configurations are shown in Figure 5. On the basis of this mechanical property evaluation, one material processing combination was selected for the Task II evaluation as a sub-scale prototype disk shape.

3.1.2.1 Processing of Shapes

Initial efforts were directed towards the fabrication of round bars and involved the preconsolidation of the rim material for Combinations A, C and D, which was then followed by HIP consolidation of all four material combinations. After the HIP cycle metallographic examination was carried out on the as-HIP material in the hub, rim and joint locations and then longitudinal sections of the consolidated cylinders were uniformly heat treated according to the currently recommended rim or hub alloy treatment. The microstructural response of each combination to the applied heat treatment was determined and a single, uniform heat treatment was selected for each alloy combination. Mechanical property screening including 480°C (900°F) tensile tests of the hub and joint material and 760°C (1400°F) stress rupture tests of the rim and joint material were conducted.

The mechanical property evaluation of each alloy combination was repeated, using different HIP joining conditions and heat treatments, as required. HIP conditions were adjusted to improve joint soundness and optimize properties for each material combination. The heat treatments were modified when found to seriously degrade the joint, hub or rim candidate materials. The tensile and stress rupture screening test results and associated metallographic analysis were used to select four material pair-HIP-heat treatment combinations for more detailed evaluation. These combinations were selected primarily on their capability to meet program goals, but potential fabrication cost differences were also considered, particularly when mechanical property levels were similar for two different combinations.

3.1.2.2 Testing of Shapes

This portion of the program involved a more complete evaluation of the most promising combinations of material pairs fabricated into a rectangular shape. Upon completion of the HIP operations the panels were heat treated and nondestructively tested to ensure the integrity of the base material and the joint between them. Upon completion of the nondestructive testing, mechanical property tests were conducted on various portions of the flat panels. Hub candidate material tests included tensile tests at 480°C (900°F), low cycle fatigue tests at 480°C (900°F), and stress rupture tests at 650°C (1200°F). Rim candidate material tests included stress rupture tests in the temperature range 540-815°C (1000-1500°F) and tensile tests at 760°C (1400°F). The joint area tests included stress rupture tests at 650°C (1200°F).

3.1.3 Disk Shape Study

The Disk Shape Study included the production of small prototype disks of selected pairs of material combinations. The disks were examined to determine how the location of the interface or joint was affected by the HIP operation. A simulated version

of the T-700 disk sonic shape was used as the disk shape demonstrator of the dual alloy processing concept. The sonic shape configuration was designed to facilitate nondestructive evaluation and demonstrate the sensitivity of the final disk shape to variations in the fabrication method. To accomplish this, X-radiographic inspection was conducted subsequent to the HIP consolidation operation. The disks were then sectioned to reveal the circumference of the joint between the materials.

3.1.4 Materials Selection for Task II

An analysis was made of all mechanical property testing data, microstructural information, nondestructive testing evaluations and joint location determinations. Based on these results a single material-HIP-heat treatment combination was selected for the production of the Task II prototype dual alloy disk. This disk was subjected to a more detailed property evaluation.

3.2 Task II - Sub-Scale Disk Evaluation

The Sub-Scale Disk Evaluation included the scale-up of a single material-heat treatment combination to a larger prototype disk configuration for more complete evaluation. The effect of the large size upon mechanical properties, shape retention and inspectability was evaluated for this task.

3.2.1 HIP/Inspect Sub-Scale Disk

The CFM-56 5-8 disk configuration was used as the shape for property demonstration in Task II of this program. This disk was selected because it offered several advantages. First, it has hub and rim regions of sufficient thickness to reveal any substantial variations in properties from the surface to the center of these regions. Second, this shape is also well characterized in terms of shape variation resulting from a simple powder HIP to sonic shape fabrication approach. This data offered a basis for the comparison with any shape variation resulting from this program as a means of determining the accuracy of the fabrication techniques. A single disk was fabricated for this program using HIP parameters identical to those resulting from Task I - Process Evaluation. Inspection of the HIP'ed disk included standard Zyglo and X-ray analysis subsequent to the HIP operations. A thermally induced porosity (TIP) evaluation was conducted on disk material which included a two hour exposure at 1205^{o}C (2200^{o}F).

3.2.2 Heat Treatment Verification

A verification of the heat treatment developed for the test panels was conducted in the large cross-section of the CFM-56 disk. This included the application of the optimized heat treatment developed in Task I to a section cut from the disk and conducting 480^{o}C (900^{o}F) tensile tests and 760^{o}C (1400^{o}F) stress rupture tests on specimens machined from this section. Modifications were made to this heat treatment as required to improve the tensile and stress rupture properties.

3.2.3 Mechanical Property Testing/Microstructure Study

Upon completion of the heat treatment verification, mechanical property tests were conducted on various portions of the CFM-56 disk. Those tests included the following:

Hub Material Tests

Tensile Tests	Stress Rupture Tests	Low Cycle Fatigue Tests
Room Temperature	595°C (1100°F)/1170 MPa (170 ksi)	480°C (900°F), $\Delta\varepsilon_t$ = 0.7, 0.85
480°C (900°F)	Notch Smooth	
650°C (1200°F)	650°C (1200°F)/1035 MPa (150 ksi)	
675°C (1250°F)	Notch Smooth	
	650°C (1200°F)/1035 MPa (150 ksi)	
	705°C (1300°F)/830 MPa (120 ksi)	

Rim Material Tests

Tensile Tests	Notch/Smooth Stress Rupture Tests	Creep Rupture Tests	Low Cycle Fatigue Tests
480°C (900°F)	650°C (1200°F)/	650°C (1200°F)/	650°C (1200°F), $\Delta\varepsilon_t$ = 0.7, 0.85
650°C (1200°F)	1035 MPa (150 ksi)	1035 MPa (150 ksi)	
760°C (1400°F)	760°C (1400°F)/	760°C (1400°F)/	
	690MPa (100 ksi)	690 MPa (100 ksi)	
		815°C (1500°F)/	
		520 MPa (75 ksi)	

Joint Material Tests

Tensile Tests	Stress Rupture Tests
650°C (1200°F)	650°C (1200°F)/1035 MPa (150 ksi)

4.0 TASK I - PROCESS EVALUATION

This task was conducted to perform the material combination and process evaluations required to select a method of fabricating a prototype dual alloy disk. Mechanical property, microstructure, and joint location studies were carried out to accomplish this evaluation.

4.1 Simple Shape Study

The Simple Shape Study concerned the development of optimum processing methods for the HIP joining and heat treatment of the four selected material combinations. The initial processing studies were conducted on round cylinders of consolidated material pairs. Based upon mechanical property screening evaluations, more detailed evaluations were carried out on flat panel shapes of selected material combinations. On the basis of this evaluation, one material processing combination was selected for the Task II evaluation of the scaled up prototype dual alloy disk.

4.1.1 Experimental Procedures

4.1.1.1 Powder Preparation

Hydrogen gas atomization was used to produce the MERL 76, PA-101, AF-115 and L/C Astroloy powders, while both hydrogen and argon gas atomization were used to produce the Rene' 95 powders for this program. For the hydrogen powders, vacuum induction melted-vacuum arc remelted ingots were procured and sent to Homogeneous Metals, Inc., of Herkimer, New York for atomization in their 20 kg (44 pound) pilot facility. There, the ingots of superalloy material were melted and then supersaturated with hydrogen gas under high pressure. The liquid metal was introduced to a vacuum chamber through an orifice, causing the pressurized liquid to erupt into particles. This argon free procedure was used to minimize the potential for thermally induced porosity during subsequent processing steps. The powder product of each ingot atomization was size classified to separate the -60 mesh fraction for use in this program. For the argon atomized Rene' 95, approximately 9 kg (20 pounds) of -60 mesh powder from a production lot was procured from the Udimet Powder Division of the Special Metals Corporation of Ann Arbor, Michigan. The chemical analyses of the ingots and the atomized powders are presented in Table 2, along with the nominal composition for each alloy. All of the alloys exhibited chemistries close to the desired nominal compositions.

4.1.1.2 Powder Consolidation

Powder consolidation for the initial processing studies was conducted on round cylinders of material pairs while the more detailed mechanical property evaluations were conducted on flat rectangular test panels. The powder consolidation included direct HIP (for Combination B), a combination of two HIP runs (for Combination C), and a combination of a vacuum sintering run with a HIP run (for Combinations A and D), depending upon the material combination under study.

4.1.1.2.1 Vacuum Presintering

The vacuum presintering runs on the Rene' 95 and PA-101 rim candidate materials for Combinations A and D, respectively, were conducted in a Vacuum Industries Series 2100, 35 KVA vacuum heat treatment furnace. Preliminary sintering runs with 17 g of powder, loaded into 9 x 6 x 80 mm (3/8 inch x 1/4 inch x 3 inches) ceramic boats, were used to define time and temperature sintering parameters to achieve maximum grain coarsening and densification, while minimizing incipient melting in these two alloys. The sintering procedure involved furnace loading at room temperature, followed by heat-up to 650°C (1200°F) at approximately 165°C/hour (300°F/hour). The furnace was held at this temperature for approximately 24 hours to allow outgassing after which the temperature was raised to the sintering temperature at the same heat-up rate. The vacuum level at the beginning of the sintering runs was 1×10^{-4} torr, which decreased to about 1×10^{-5} torr during the operation. The specimens were furnace cooled to 120°C (250°F) at a rate of 250°C (450°F/hour) and the specimens were then removed from the furnace.

Once the proper sintering conditions were characterized with the aid of metallographic analysis, sintered compacts were prepared for subsequent HIP joining with the required hub candidate powders. These compacts were prepared using cast Thermo-Sil castable silica molding material to form cylindrical shapes approximately 25 mm (one inch) in diameter by 100 mm (4 inches) long. The surface of the compacts which were to be bonded to the hub powders were surface ground using 60 grit grinding wheels to a finish of 50 RMS. The sintered and surface ground compacts were then ultrasonically degreased with acetone, washed in methyl alcohol and distilled water and shipped to Industrial Materials Technology (IMT) of Lawrence, Massachusetts, for final canning and HIP bonding to the hub alloy powders.

4.1.1.2.2 HIP Consolidation

HIP consolidation, conducted at IMT, was initially directed towards the fabrication of cylindrical shapes of approximately 25 mm (one inch) internal diameter by 250 mm (10 inches) in length. For all four of the material combinations, the canning material consisted of 25 mm (one inch) internal diameter 3 mm (1/8 inch) thick AISI 1018 mild steel tubing. Canning procedures varied, however, depending upon the particular material combination being consolidated. For the loose powder-loose powder Combination B, first one powder was placed in a can, vibrated, and then the second powder was placed in the can and vibrated. The can was evacuated at 650°C (1200°F) for 24 hours to drive off adsorbed gases and then the fill tube was welded shut for the consolidation operation. For the combinations with the vacuum presintered Rene' 95 and PA-101 rim materials, first the sintered compacts were inserted into the lower half of the HIP cans, then appropriate hub alloy powders were added, and the cans were vibrated, and outgassed and sealed as described previously. For the combination involving the HIP'ed AF-115 rim material, a 100 mm (4 inch) long compact was HIP consolidated using a canning procedure similar to that described for the loose powder combinations. This HIP compact was decanned by machining, and the surface to be bonded to the hub powder surface ground to a finish of 50 RMS prior to insertion into the can for bonding. Powder filling, outgassing and can sealing was accomplished using the same procedures as described previously. All containers were leak checked prior to initiating the HIP consolidation cycles.

On the basis of mechanical property tests conducted on the cylindrical shapes, more detailed evaluations were carried out on flat panel shapes of selected material combinations. The combinations chosen for these more extensive evaluations included the loose powder L/C Astroloy-loose powder MERL 76 Combination B and the HIP'ed AF-115 loose powder Rene' 95 Combination C. The flat panel configurations each measured approximately 230 mm (9 inches) x 90 mm (3.5 inches) x 25 mm (one inch) and were fabricated in cans made of 3 mm (1/8 inch) thick seam welded AISI 1018 mild steel sheets. Can loading, outgassing and sealing procedures were similar to those used for the cylindrical shapes. For Combination C, involving the HIP'ed AF-115 rim candidate material, the rectangular HIP'ed compact of AF-115 was decanned by machining and the surface to be bonded to the Rene' 95 hub powder surface ground to a finish of 50 RMS All containers were leak checked prior to initiating the HIP consolidation cycles.

4.1.1.3 Mechanical Property Testing

Prior to the mechanical property screening evaluations, a heat treatment study was conducted to determine the optimum test microstructures for each material combination. This consisted of solution and aging heat treatments to produce a large grain size in the rim candidate material, while maintaining a fine grain size in the hub candidate material. Initially, sections of the consolidated cylinders were uniformly heat treated according to the currently recommended rim or hub alloy treatment. The microstructural response of each combination to the applied heat treatment was determined, and a single, uniform heat treatment was selected for mechanical property screening evaluations of each alloy combination. Post test metallographic examinations were as used to determine what adjustments in the heat treatments were necessary in order to improve the mechanical property results. For the consolidated cylinders, mechanical property screening tests included tensile and stress rupture tests. For the flat panel configurations testing included tensile, stress rupture as well as low cycle fatigue tests. The test specimen configurations for the tensile, stress rupture and low cycle fatigue tests are shown schematically in Figure 6.

Tensile testing was performed in air on an Instron Universal Test machine with a crosshead speed of 0.1 mm/minute (0.005 in/minute) until yielding occurred. Temperature was controlled to within 2°C (3°F). Ultimate tensile strength, 0.2% offset yield strength, percent elongation and percent reduction of area were recorded. The specimen configuration and test procedures corresponded to the ASTM E21-70 specification and the extensometers for these tests corresponded to E83 specification.

Stress rupture tests were performed in air in Satec constant load, lever arm units and temperature was maintained to within a 2°C (3°F) tolerance. Failure time, percent reduction of area and percent elongation were recorded, with failure being measured from the time of application of the load (approximately 15 minutes after temperature equilization). The specimen configuration and test procedures corresponded to the ASTM E139-70 specification.

Low cycle fatigue tests were conducted at 480°C (900°F), under strain control at a total strain range of 0.7. A frequency of 20 cycles per minute was used. These tests were conducted with closed loop diametral strain control programmed to a closed loop electrohydraulic Gilmore servo system. A Hewlett-Packard Model 202A function generator was used to control the diametral strain. A double collar arrangement clamped the threaded part of the specimen to each grip with sufficient preload to prevent backlash under reversed loading conditions. Heating by direct resistance used a programmable thyratron controlled 50 kva power source. Specimen diameter was measured using a scissors-action controlled LVDT type of extensometer. The specimen diameter was compensated electronically for thermal expansion to directly control the net mechanical strain.

4.1.1.4 Metallographic Evaluation

Metallographic analyses including optical metallographic, SEM and electron microprobe analyses were used to aid in the interpretation of the processing and mechanical property results. The preparation procedure included grinding on 180 to 600 grit silicon carbide papers with water as a lubricant, polishing on billiard cloth with Linde A abrasive (Al_2O_3 -3 microns) and in a Syntron Automatic polisher on gamel cloth with Linde B abrasive (Al_2O_3 -.05 micron). Kalling's etch (50 ml HCl, 50 ml methyl alcohol 2.5 g $CuCl_2$) was used as required to delineate microstructural features. The optical metallographic analysis was conducted with a Bausch and Lomb Research II Metallograph, the SEM analysis with an AMR-900 scanning electron microscope and the electron microprobe analysis with a Phillips AMR/3 electron microprobe analyzer.

4.1.2 Processing of Shapes

The effort in this portion of the program was directed towards the definition of the rim preconsolidation operations, the HIP cycle for the consolidation and joining of the different material components of the disk hub and rim and their subsequent heat treatment. Cylindrical shapes were HIP consolidated for these evaluations.

4.1.2.1 Combination A (Vacuum Sintered Rene' 95 Rim - Rene' 95 Hub)

4.1.2.1.1 Vacuum Pre-Sintering Operations

The first step in the fabrication of the Combination A dual alloy cylindrical shape consisted of the preconsolidation of the Rene' 95 rim material. Vacuum sinter preconsolidation studies were conducted on small amounts of -60 mesh Rene' 95 powder loaded into short ceramic boats. The aims of the preconsolidation studies were to achieve the largest grain size and highest density possible with a minimum of incipient melting throughout the microstructure. A large grain size should achieve the optimum stress rupture properties in the rim material and a high density minimize dimensional changes during the subsequent HIP joining operation. A minimum of incipient melting was desired to (1) avoid attendant areas of microporosity which could contribute to premature stress rupture failure and (2) prevent large scale redistribution of alloying elements which also might compromise the properties of the alloy.

The Rene' 95 vacuum sintering trials were conducted for six hours at 1300°C (2375°F) and 1265°C (2310°F). The 1300°C (2375°F) sintering temperature resulted in excessive incipient melting, although a grain size of ASTM 1 was achieved. Reducing the sintering temperature to 1265°C (2310°F) produced a density in excess of 90% and a significant decrease in incipient melting without significantly reducing the ASTM grain size. A similar grain size response for Rene' 95, vacuum sintered at 1290°C (2350°F), has been reported by Reichman (16). The microstructures of powders exposed to these sintering treatments are shown in Figure 7. The structure of the material sintered at 1265°C (2310°F) exhibits an ASTM 1-2 grain size, Figure 7b. Residual pores and a small amount of incipient melting, less than approximately 5%, are present at the grain boundaries. Since this structure was considered satisfactory for rim preconsolidation in this combination, the six hour 1265°C (2310°F) vacuum sintering condition was selected for the Rene' 95 preconsolidation.

4.1.2.1.2 HIP Consolidation Operations

The vacuum preconsolidation step was followed by an operation in which the Rene' 95 powder hub material and the preconsolidated Rene' 95 rim material were HIP'ed together. The objective here was to fully consolidate the hub material at a low enough temperature to prevent excessive grain growth, join the rim and hub materials into a single component, and eliminate any residual porosity remaining in the vacuum sintered preconsolidated rim material. The prevention of excessive grain growth during this operation was required to develop optimum tensile and fatigue properties in the hub material.

The initial HIP consolidation operation for Combination A was carried out at IMT using a 25 mm (one inch) diameter 1018 mild steel tube can containing both the rim and hub materials. A typical HIP consolidated cylindrically shaped can is shown in Figure 8. The preliminary consolidation conditions for Combination A included four hours at 1120°C (2050°F) and 105 MPa (15 ksi) and were selected because these conditions have commonly been used for HIP Rene' 95 intended for disk applications (17). The microstructures of the joint and the surrounding rim and hub materials after HIP consolidation are shown in Figure 9. The vacuum sintered Rene' 95 rim material exhibited a grain size of ASTM 1-2, evidence of the grain growth which occurred as a result of the vacuum sinter operation. No additional grain growth during HIP consolidation was observed. However, an appreciable amount of porosity which was present after the vacuum sinter still remained after the HIP operation. This suggested that too low a HIP consolidation temperature was used and that a higher HIP temperature would be required to seal this porosity. For example, Reichman (16) has shown that a 1230°C (2250°F) HIP operation can heal this porosity in coarse grained vacuum sintered Rene' 95. This particular temperature, however, may be too high to maintain a fine grain size in the Rene' 95 hub powder. The loose powder hub material shown in Figure 9 exhibited a fine grained microstructure typical of Rene' 95 HIP'ed at 1120°C (2050°F) for disk applications (17). The interface between the rim and hub materials was generally clean and exhibited no unique features.

Because the 1120°C (2050°F)/105 MPa (15 ksi) HIP condition used initially was not effective in eliminating the porosity in the vacuum presintered Rene' 95, studies were initiated to determine the proper HIP conditions required to obtain more complete consolidation in the rim material. For these studies two HIP runs were investigated and the operations were conducted at the NASA-Lewis Research Center utilizing a 4 hour exposure under 140 MPa (20 ksi) pressure conditions. In the first operation, material which had previously been HIP'ed at 1120°C (2050°F) was re-HIP'ed at 1165°C (2125°F). In the second operation, vacuum presintered material was HIP'ed at 1145°C (2090°F). Light photomicrographs of the microstructures of material HIP'ed at these two conditions are shown in Figure 10. It was apparent that both of the HIP operations were successful in sealing the residual porosity in the presintered Rene' 95. In addition, in the compact which had been HIP'ed previously, the 1165°C (2125°F) HIP treatment also caused grain growth to approximately ASTM No. 5-6 grain size in the loose powder Rene' 95 hub material. This grain size was considered satisfactory to develop the desired hub material strength properties. This fact, in conjunction with the greater degree of pore sealing in the presintered Rene' 95 rim material led to the selection of the 1165°C (2125°F) HIP joining temperature for the fabrication of the second Combination A can for mechanical property testing. The 1145°C (2090°F) HIP temperature represented an alternative HIP joining condition should the grain growth of the hub material be found to adversely affect mechanical properties.

4.1.2.1.3 Heat Treatment Operations

The objective of the heat treatment study was to evaluate various uniform heat treatments applied to the joined materials to select the optimum microstructures for mechanical property evaluations. The initial choices were a heat treatment recommended for fine grained hub material and another recommended for large grained rim material and are listed as follows:

Hub Material Heat Treatment	Rim Material Heat Treatment
1150°C (2100°F)/2 Hours, Salt Quench to 540°C (1000°F) + 870°C (1600°F)/1 Hour Air Cool +650°C (1200°F)/24 Hours Air Cool	1150°C (2100°F)/2 Hours, Salt Quench to 540°C (1000°F) + 870°C (1600°F)/8 Hours Air Cool + 1040°C (1900°F)/4 Hours Air Cool + 650°C (1200°F)/24 Hours Air Cool + 760°C (1400°F)/8 Hours

The hub material heat treatment was designed to develop optimum tensile properties and consisted of a solution treatment approximately 20°C (30°F) below the gamma-prime solvus followed by a molten salt quench and a double age (6). The second heat treatment was applied to maximize the rupture life of the rim material and included the same solution treatment, but with a different aging cycle which results in the generation of several gamma-prime sizes, thereby increasing rupture life and ductility (6).

4.1.2.1.3.1 Hub Material Heat Treatment Results

The resulting microstructure of material given the standard Rene' 95 heat treatment, used to develop optimum strength and fatigue properties in the hub material, is shown in Figure 11. The rim material exhibited the coarse grain size, ASTM 0-1, resulting from the vacuum sinter and a single, relatively fine, intragranular gamma-prime size. The grain boundaries exhibited some increase in gamma-prime concentration, most notable at the triple points. Discrete carbide and gamma-prime particles were also found the grain boundaries. The gamma-prime morphology reflects the suprasolvus preconsolidation temperature, 1265^{o}C (2310^{o}F), and the concentration of gamma-prime at the triple points suggests that a small amount of incipient melting may have occurred during the preconsolidation operation.

The hub material exhibited a very fine grain size, approximately ASTM 5-6, unchanged from the as-HIP grain size. The only gamma-prime in evidence was relatively coarse. This precipitate morphology resulted from the near solvus HIP and subsolvus solution treatment employed. The gamma-prime which precipitated during the aging treatments was not resolvable by light microscopy. As shown in Figure 11d, there were certain regions within the hub material microstructure which were characterized by the remnants of the dendritic structures of the original powder particles. This indicates that processing employed for this combination did not achieve complete solutioning. While this type of microstructural feature has commonly been observed in as-HIP'ed Rene' 95, it has not been shown to be detrimental to high temperature mechanical properties (22). The interface between the hub and rim materials was delineated by fine discrete gamma-prime and carbide particles. In summary, there was no evidence of any detrimental microstructural constituents as a result of the HIP joining or heat treatments employed. This type of structure would therefore be considered desirable for mechanical property testing.

4.1.2.1.3.2 Rim Material Heat Treatment Results

The rim material heat treatment was designed to produce optimum stress rupture properties through the precipitation of several generations of gamma-prime particles. The resulting microstructures of the rim, joint and hub materials are presented in Figure 12. The grain sizes were equivalent to those resulting from the hub heat treatment cycle. The rim material exhibited a uniform distribution of relatively fine gamma-prime, with discrete gamma-prime and carbide particles located at the grain boundaries. The hub material exhibited three types of gamma-prime particles, two of which were well dispersed throughout the structure, while the third was more heterogeneously distributed. The coarse gamma-prime was the constituent which remained after the HIP joining operation and the solution treatment, both of which were conducted at temperatures near or slightly below the gamma-prime solvus. The finer gamma-prime was a result of cooling from the solution treatment temperature and the subsequent aging steps. The third type of gamma-prime appeared as remnants of the original dendritic structure associated with the powder particles and evidenced little change as the result of the heat treatment.

The joint between the rim and hub materials exhibited very fine, discrete carbide and gamma-particles. The discontinuous grain boundary morphology appeared to be similar to that of the joint in the hub heat treated material, Figure 11, although the particles were somewhat finer in size. In summary, the combination of microstructures in the rim, hub and joint shown in Figure 12 was also considered suitable for mechanical property testing.

4.1.2.1.4 Mechanical Property Screening Results

The mechanical property screening tests for the HIP'ed cylindrical bars included 480°C (900°F) tensile tests and 760°C (1400°F) stress rupture tests. This testing was conducted in an iterative manner, with processing changes incorporated as the result of the analysis of the screening test data for each iteration.

4.1.2.1.4.1 First Processing Iteration

The first processing iteration for Combination A consisted of the six hour 1265°C (2310°F) vacuum presintering of the Rene' 95 rim material, followed by HIP consolidation with loose Rene' 95 hub powder at 1120°C (2050°F). These processing parameters are listed in Table 3, which also includes the processing parameters utilized for the remaining process iterations for this combination. Analysis of the microstructures resulting from these processing conditions indicated, however, that the HIP consolidation operation did not completely seal the porosity remaining in the rim material after the vacuum presintering operation. For this reason, no mechanical property evaluations were conducted on material of this first processing iteration.

4.1.2.1.4.2 Second Processing Iteration

The second processing iteration changed the HIP consolidation temperature from 1120°C (2050°F) to 1165°C (2125°F). This resulted in complete closure of the porosity remaining in the rim material after the presintering operation. In general, the microstructural responses to both the hub and the rim heat treatments were satisfactory for mechanical property testing. The hub material (loose powder Rene' 95) heat treatment was selected for mechanical property screening studies because it was believed that hub strength may be a limiting factor for this particular combination. The complete listing of the processing parameters and heat treatment for this second process iteration are given in Table 3.

During test specimen preparation for the mechanical property screening trials a problem was encountered during machining of the joint test specimens. A crack was found in the joint area between the rim and hub materials and photomicrographs of this crack are shown in Figure 13. This crack had not been detected during the metallographic examination of as-HIP'ed material nor was it seen during evaluation of the heat treatment response of material removed from the can for heat treat studies. It is therefore likely that the crack formed after the metallographic examination, possibly in salt quenching to 540°C (1000°F) from the 1150°C (2100°F) solution treatment. Although it was not possible to obtain test specimens from the joint

area, the mechanical property response of the large grained (ASTM 0-1) rim material and the finer grained (ASTM 5-6) hub material to the Rene' 95 hub heat treatment was determined. The results are listed in Table 4, which also includes the results of the mechanical property evaluations of the other process iterations discussed below.

The 480°C (900°F) tensile results indicated that the fine grained hub material exhibited tensile strengths of approximately 1380 MPa (200 ksi) and yield strengths of 1140 MPa (165 ksi). The tensile strength was below the program goal. The yield strength of the coarse grained rim material was similar to that of the hub material, but its ultimate strength was approximately 1170 MPa (170 ksi). Published information for Rene' 95 HIP and heat treated according to similar conditions indicates Combination A properties should have a higher tensile strength (1550 MPa (225 ksi)) and somewhat lower yield strength (1110 MPa (161 ksi)) (22). The tensile ductility properties of the fine grained hub material exhibited improved ductility compared to the large grain rim material. The values were, however, below the published values for elongation (15%) and reduction of area (17%) in HIP and heat treated Rene' 95 (22).

Stress rupture tests were conducted on the presintered rim material at 760°C (1400°F)/550 MPa (80 ksi). The average lives of the large grain specimens were approximately 400 hours. This life is almost ten times greater than that anticipated for Rene' 95 processed to a fine grain size. Fine grained material tested at 760°C (1400°F)/690 MPa (100 ksi) exhibited a life of approximately 10 hours, which matches published Rene' 95 data curves. These test results indicated that the presintered Rene' 95 rim material for this combination was easily capable of exceeding the stress rupture program goals but that the hub material tensile properties were not only below the program goal, but also below published values for HIP and heat treated Rene' 95. Metallographic examination indicated that the fracture modes for both the tensile and stress rupture failures were intergranular.

4.1.2.1.4.3 Third Processing Iteration

In the third processing iteration for Combination A the standard Rene' 95 heat treatments were modified in an attempt to improve the ultimate tensile strength and ductility of the hub material. The processing conditions and heat treatment for this third iteration are shown in Table 3. Processing was identical to the second iteration with the exception that an air cool, rather than a salt quench from the solution treatment temperature was used. This type cooling from solution has been shown to improve tensile strength in fine grained Rene' 95 (23). For this iteration, hub material remaining from the second iteration HIP'ed bar was used for re-heat treatment and the preparation of duplicate 480°C (900°F) tensile test specimens. Stress rupture tests on rim material as well as possible joint material evaluations were planned for a third iteration bar to be fabricated pending the results of the two hub tensile screening tests.

The tensile test results for the two specimens are shown in Table 4. There was some improvement in the tensile ductility values, but at a slight loss in both the ultimate and yield strength values. The improved ductility values were, however, still substantially below those reported in the literature for HIP and heat treated Rene' 95 (22). On the basis of these tensile results there was little justification for further testing of the third process iteration material.

4.1.2.1.4.4 Fourth Processing Iteration

The results of the first three processing iterations indicated that the presintered rim material of this combination exhibited potential to exceed the stress rupture program goals, but that the hub material properties were below the tensile strength goal at 480°C (900°F). The use of several heat treatments, including air cooling after solution treatment instead of salt quenching, did not improve the strength. This suggested that hydrogen soluble gas atomized powder might not respond properly to the heat treatments. Accordingly, 9 kg (20 lbs) of -60 mesh production argon atomized powder was obtained from the Udimet Powder Division of Speical Metals for the fourth iteration. The chemical analysis of this powder is listed in Table 2.

The processing parameters used for the fabrication of the HIP can are listed in Table 3. These included the same vacuum presintering conditions used previously as well as the 1165°C (2125°F) HIP consolidation temperature. The heat treatment, however, was different from that used for the previous iterations. This heat treatment reflected the attempt to maximize the solution temperature in order to more completely dissolve the gamma-prime strengthening phase during the solution operation. It was realized that the high solution treatment could result in grain growth, which would be detrimental to strength, but would allow full solution and reprecipitation of fine gamma-prime during aging, as a compensating factor. This heat treatment did result in a slight increase in grain size in the hub material, from ASTM 5-6 to ASTM 4-5. As expected, there was no change in the grain size of the vacuum presintered rim material. In another change the 1018 mild steel can was removed prior to heat treatment to reduce quenching stresses in the joint area in an attempt to eliminate the occurrence of quench cracking in the joint regions.

The results of the mechanical property testing for this iteration are presented in Table 4. Again, severe quench cracking occurred in the joint regions and it was not possible to obtain tensile or stress rupture specimens from joint material. The tensile results for this fourth iteration were poor in comparison to material tested previously both in terms of strength and ductility levels. The average ultimate strength value, for example, was 1145 MPa (166 ksi), compared to the approximate value of 1380 MPa (200 ksi) for material tested in the second iteration. The ductility for the fourth iteration material was also poor in comparison to second iteration material. Elongation ranged from 1.0-1.3%, for example, while that for the second iteration ranged from 6.5-6.7%. These results suggested that the 1175°C (2150°F) solution treatment temperature may have been too high for the HIP'ed loose powder Rene' 95 hub material. Previous studies on HIP'ed Rene' 95 had indicated an increase in elevated temperature yield and ultimate strength with an increase in solution temperature from 1095°C (2000°F) to 1150°C (2100°F) but the tests did not include a 1175°C (2150°F) solution temperature (22).

The processing changes were beneficial to the rim properties as reflected by the improved stress rupture lives and ductility values. The average rupture life of 633 hours was significantly improved over the 398 hour average life of the second iteration material. The ductility values were double those of second iteration material. The rupture lives can be compared to the anticipated 40 hour life of fine grain Rene' 95 under these test conditions (22). The rupture ductilities were also comparable to those obtained for material tested in the 650-705°C (1200-1300°F) temperature range (22).

4.1.2.1.4.5 Fifth Processing Iteration

For the fifth process iteration, efforts were directed towards using production heat treatment techniques to avoid quench cracks in the joint regions. Sun Steel Treating of Farmington Hills, Michigan, was selected to apply production type techniques for the heat treatment of this can. These production procedures have been successfully used for the heat treatment of T-700 and F-404 turbine disks made from Rene' 95 powders without the occurrence of quench cracking. The cylindrical shape was fabricated using the processing parameters listed in Table 3. This included consolidation of vacuum presintered Rene' 95 with loose powder Rene' 95 at Industrial Materials Technology at 1165°C (2125°F). Loose argon atomized powder was used again because it was felt the 1175°C (2150°F) solution treatment in the fourth iteration may have been too high. The consolidated can was heat treated with the standard Rene' 95 heat treatment at a solution temperature of 1150°C (2100°F). Upon completion of the heat treatment, a portion of the HIP can was removed by surface grinding, and revealed severe quench cracking along the joint between the rim and hub materials. A photograph of this can is shown in Figure 14. The quench cracks prevented the evaluation of tensile and stress rupture properties for specimens from the joint area. It was concluded that, because of the extreme sensitivity of the joint areas to quench cracking during heat treatment, further mechanical property evaluations of this process iteration were not warranted.

4.1.2.1.5 Summary

The processing studies for the Combination A materials consistently indicated that the vacuum presintered Rene' 95 rim material exhibited potential to exceed the stress rupture program goals, but that the loose powder Rene' 95 hub material properties were below the tensile strength goal of 1520 MPa (220 ksi) at 480°C (900°F). The best tensile strength value exhibited by the hub material was approximately 1380 MPa (200 ksi). Potentially more serious than this low tensile strength value, however, was the occurrence of quench cracking at the joint between the hub and rim materials. Cracking occurred with air, oil, and salt quenching from the solution temperature. This quench cracking precluded evaluation of tensile and stress rupture specimens machined from the joint location. Because of this inability to produce a sound joint in the heat treated material, further evaluations for this particular combination were not warranted.

4.1.2.2 Combination B (Loose Powder L/C Astroloy Rim - Loose Powder MERL 76 Hub)

4.1.2.2.1 HIP Consolidation Studies

The fabrication of the Combination B HIP can was the simplest of the four combinations investigated in this program because it involved only one consolidation operation, the single HIP consolidation of the loose L/C Astroloy and MERL 76 powders. The HIP consolidation of this combination was conducted at a temperature which has a special relationship to the gamma-prime solvus temperatures of the two alloys. The MERL 76 hub candidate alloy has a solvus of approximately 1195°C (2180°F), whereas the L/C Astroloy rim candidate alloy has a solvus of approximately

1125°C (2060°F). It is generally regarded that HIP below the gamma-prime solvus is beneficial for strength, whereas HIP above the solvus is beneficial for stress rupture properties. Therefore, for this Astroloy-MERL 76 combination, the powder could be consolidated between the two solvus temperatures in order to promote optimization of both the tensile and stress rupture properties.

The preliminary consolidation conditions selected for Combination B were four hours at 1165°C (2125°F) and 105 MPa (15 ksi). The microstructure of this combination is shown in Figure 15. The L/C Astroloy rim material exhibited a fine, recrystallized grain size, approximately ASTM 6. Recrystallized grains and the lack of coarse gamma-prime particles were evidence that the HIP operation was conducted at a temperature above the gamma-prime solvus. The MERL 76 hub material, on the other hand, exhibited a structure which contained very fine grains, approximately ASTM 8-10, and a relatively large proportion of coarse gamma-prime, evidence of a sub-solvus HIP. The L/C Astroloy grain size was somewhat larger than the typical value of ASTM 10, used in single alloy disks, produced by sub-solvus HIP operation. The MERL 76 hub material microstructure was comparable to that published in the literature for as-HIP MERL 76 HIP'ed at 1165°C (2130°F) (24). The interface between the two alloys was irregular, with isolated instances of intermixing between the loose powders during the can filling operation. Outside of the irregularity, there were no unusual features associated with the interface.

4.1.2.2.2 Heat Treatment Operations

The initial heat treatments investigated for the Combination B material are listed as follows:

MERL 76 Hub Material Heat Treatment	L/C Astroloy Rim Material Heat Treatment
1175°C (2145°F)/2 Hours Air Cool + 760°C (1400°F)/8 Hours Air Cool	1115°C (2040°F)/2 Hours Air Cool + 870°C (1600°F)/8 Hours Air Cool + 980°C (1800°F)/4 Hours Air Cool + 650°C (1200°F)/24 Hours Air Cool + 760°C (1400°F)/8 Hours Air Cool

The hub material treatment was designed to develop optimum tensile properties (14) while the rim material treatment was aimed towards the generation of several gamma-prime sizes in order to increase rupture life and ductility (15).

4.1.2.2.2.1 Hub Material Heat Treatment Results

The resulting microstructure of material given the recommended MERL 76 heat treatment is shown in Figure 16. Considerable evidence of incipient melting was observed in the L/C Astroloy and in the grain boundaries of the MERL 76. This melting resulted from the use of an excessively high solution heat treatment temperature.

4.1.2.2.2.2 Rim Material Heat Treatment Results

The resulting microstructures of material given the standard L/C Astroloy rim material heat treatment are shown in Figure 17. The L/C Astroloy exhibited a grain size of ASTM 6, which was unchanged from the as-HIP grain size. There was a generally uniform distribution of intragranular gamma-prime, and a discrete precipitation of gamma-prime particles at the grain boundaries. There was also some evidence of a gamma-prime depleted zone adjacent to the grain boundaries. The MERL 76 hub material exhibited an ASTM 8-10 grain size, also relatively unchanged from the as-HIP grain size. There were two gamma-prime sizes both randomly distributed throughout the structure. The coarse gamma-prime was a result of the sub-solvus HIP and solution treatment temperatures used, and the finer gamma-prime resulted from the subsequent aging treatments. These same general microstructural features were also characteristic of those found in rim heat treated Combination A, Figure 12, which was also given a sub-solvus solution and multi-step aging treatment. Outside of the irregularity resulting from the mixture of the two powder alloys, the joint between the rim and hub materials was quite indistinct, with no precipitated phases or other microstructural features providing a clear delineation between the rim and hub materials. On the basis of these microstructural results the L/C Astroloy heat treatment was selected for mechanical property evaluations.

4.1.2.2.3 Mechanical Property Screening Results

4.1.2.2.3.1 First Processing Iteration

The first processing iteration for Combination B included HIP consolidation at 1165°C (2125°F) followed by the L/C Astroloy heat treatment. These processing parameters are listed in Table 5, which also includes the processing parameters used for subsequent process iterations for this combination. The results of the mechanical property screening tests are listed in Table 6, which also summarizes the results of the mechanical property tests of the other process iterations.

The MERL 76 hub tensile properties listed in Table 6 indicated that the strength levels obtained using the initial processing parameters were below the 1520 MPa (220 ksi) ultimate tensile strength program goal and were also below levels anticipated on the basis of data reported previously for this alloy, Figure 3 (14). Examination of the failed test bar specimens indicated that fracture occurred in an intergranular manner with no unusual features in the microstructure, Figure 18a. A contributing factor to the low strength levels may have been the use of the low solution temperature for this alloy.

It was observed that the joint tensile specimen failed not in the joint region but in the L/C Astroloy rim material. This was not surprising since it was anticipated that the rim alloy would be the weaker of the two alloys. It was important to note, however, that the joint properties were within 90% of the average values for the duplicate hub tests. This reflected the metallographic analysis conducted on as-heat treated material in that the joint between the rim and hub materials was quite indistinct, with no precipitated phases or other microstructural features providing a clear

delineation between the rim and hub materials. Metallographic analysis of the failed joint specimen indicated that fracture occurred preferentially along prior particle boundaries in the L/C Astroloy. An example of this is shown in Figure 18b. These results suggested the use of a lower HIP consolidation temperature in order to minimize the formation of precipitates along the prior particle boundaries. This type processing modification has been shown to be beneficial in minimizing this problem in HIP consolidated superalloy powders (25).

The L/C Astroloy rim stress rupture results obtained at 760°C (1400°F) were also below those reported in the literature for this alloy (15). At these test conditions a minimum life of approximately 45 hours is expected compared to the 22 hour average life obtained during these screening evaluations. Metallographic examination indicated that the fracture mode was predominantly associated with prior particle boundaries. The joint stress rupture specimens did not fail in the joint region but in the MERL 76 hub material. With the exception of the reduction of area, all other stress rupture properties for the joint specimen were within 90% of the average values for the duplicate rim specimens. This reflected the high quality of the joint area of this combination.

4.1.2.2.3.2 Second Processing Iteration

The processing modifications for the second iteration included changes both in the HIP conditions and the heat treatment cycles. The HIP temperature was decreased from 1165°C (2125°F) to 1120°C (2050°F) in an attempt to minimize the formation of prior particle boundary type precipitates in the L/C Astroloy rim material. In addition to this, the heat treatment was changed to reflect the desire to use a higher solution temperature to optimize the MERL 76 mechanical properties. The solution temperature used in the first iteration was considerably below the 1175°C (2145°F) temperature recommended for MERL 76. For the second iteration, a 1165°C (2130°F) temperature was selected in order to avoid the incipient melting observed as a result of the 1175°C (2145°F) treatment, Figure 16, and still achieve the gamma-prime solutioning required for the MERL 76 material. The increase in grain size resulting from this higher solution temperature was also anticipated to be beneficial to the L/C Astroloy stress rupture properties. The entire set of processing parameters used for this second processing iteration are listed in Table 5 and also reflect several additional changes in the heat treatment used for this iteration. A delayed oil quench from solution as well as modified stress relief and stabilization treatments in the range 870-980°C (1600-1800°F) were investigated on the basis of recent results for HIP and heat treated MERL 76 alloy published by Pratt & Whitney Aircraft on their NASA MATE program (26). These types of heat treatments provided an optimum balance of tensile and stress rupture properties up to 730°C (1350°F) for specimens machined from the JT9D first stage turbine disk configuration.

The results of the mechanical property screening tests are listed in Table 6. The lower HIP temperature/higher solution temperature processing changes resulted in an increase in grain size in the MERL 76 hub material, from ASTM 8-10 to ASTM 4-5, but more importantly, resulted in more complete gamma-prime solutioning for subsequent precipitation during the several step aging heat treatment. This resulted in significant increases in both strength and ductility compared to material

for the first processing iteration. The ultimate strength of the hub material increased from an average of 1255 MPa (182 ksi), to approximately 1395 MPa (202 ksi). The yield strength exhibited a similar increase and the ductility was also significantly improved. Although these property levels were below the desired program goal as well as the anticipated levels reported for MERL 76, they did represent a significant improvement compared to the first processing iteration. The properties of the joint specimen were also improved compared to those of the first iteration, with the most significant improvement being exhibited by the yield strength. Failure was observed not in the joint area, but in the L/C Astroloy rim alloy, reflecting the high quality of the joint for this particular processing iteration. With the exception of the elongation values, all of the other joint area tensile properties were within 90% of the average of the MERL 76 hub material.

The processing modifications of this second iteration did not significantly affect the grain size of the L/C Astroloy rim candidate material. The grain size for the second iteration material was ASTM 5-6, compared to ASTM 4-6 for the first iteration material. That the processing changes were beneficial to the stress rupture properties was demonstrated by the fact that the stress rupture life of the L/C Astroloy exhibited an increase in average rupture life, from 22 hours to 48.6 hours. There was, however, a slight decrease in the reduction of area, from an average of 6.8% for the first iteration, to an average of 3.8% for the second iteration. The stress rupture life demonstrated by the second iteration L/C Astroloy material was equivalent to the expected stress rupture life value for this alloy, and indicated that the processing changes accomplished the purpose of improving the rim stress rupture life as well as the purpose of improving the strength of the hub. The joint material specimen for this iteration exhibited approximately the same life as in the first iteration, with a somewhat reduced ductility. This joint specimen did not fail in the joint, but rather in the MERL 76 hub material, indicating that the bond joint between the rim and hub materials was satisfactory.

4.1.2.2.3.3 Third Processing Iteration

The third processing iteration for this combination was directed toward further strength improvements in the hub material. While the second iteration processing resulted in L/C Astroloy rupture life approximately equal to the expected life values at 760°C (1400°F), the resulting MERL 76 hub ultimate tensile strength was still below the 1520 MPa (220 ksi) goal at 480°C (900°F). In order to increase the tensile strength the solution heat treatment was to be followed directly by an oil quench, rather than a delayed oil quench. This was done to impart a faster cooling rate in the heat treated material (see Table 5).

The tensile results shown in Table 6 indicated that the heat treatment modification used for this iteration was not successful in increasing the tensile properties of the MERL 76 hub material. In general, the strength and ductility values for the third iteration were similar to those obtained for the second iteration. The average ultimate strength value was 1370 MPa (199 ksi) compared to the 1395 MPa (202 ksi) value exhibited by material from the second iteration, and remained below the 1520 MPa (220 ksi) ultimate tensile strength program goal. High joint quality was reflected by the fact that ultimate strength and yield strength values, as well as both ductility values were within 90% of the average values of the duplicate hub specimens. Failure was not observed in the joint region, but instead in the L/C Astroloy rim material portion of the test specimen.

The major benefit derived from the use of a direct oil quench as opposed to the delayed quench heat treatment was an increase by approximately 1.5 times, from an average of 48.6 hours rupture life for second iteration material to an average 78.5 hours for the third iteration L/C Astroloy rim material. The anticipated life for L/C Astroloy tested under these conditions is approximately 45 hours. There was however, loss in rupture ductility in terms of both elongation and reduction of area in the three iterations as the rupture lives increased. The rupture life exhibited by the joint test specimen was only 18.4 hours, and failure did not occur in the joint itself, but rather in the MERL 76 hub portion of the specimen. This indicated that the bond between the rim and hub materials was satisfactory. Significantly in all three process iterations the joint stress rupture specimen failed in the MERL 76 hub material at approximately the same rupture life in spite of the fact that the grain size for the MERL 76 in the second and third iterations was larger (ASTM 4-5) than that in the first iteration (ASTM 8-10).

4.1.2.2.4 Summary

For the MERL 76-L/C Astroloy combination the highest average tensile strength value of the MERL 76 hub material at 480°C (900°F) was 1395 MPa (202 ksi), about 10% below the 1520 MPa (220 ksi) ultimate tensile strength program goal. High joint quality was reflected by the fact that ultimate and yield strengths, as well as ductility were within 90% of the averages obtained in the hub specimens and all failures occurred within the L/C Astroloy rim material. The best average stress rupture life exhibited by the L/C Astroloy rim material at 760°C (1400°F)/550 MPa (80 ksi) was 78 hours, which exceeded the 45 hour life expected for this alloy tested under these conditions. The rupture life of the joint test specimen was 18.4 hours, because the failure occurred in the MERL 76 hub portion of the specimen. It was concluded that the overall combination of strength properties as well as stress rupture capability in conjunction with high joint quality represented an attractive level of mechanical properties which justified more extensive characterization in the flat panel configuration.

4.1.2.3 Combination C (Pre-HIP'ed AF-115 Rim - Rene' 95 Hub)

4.1.2.3.1 AF-115 HIP Preconsolidation Operations

The first step in the fabrication of the Combination C dual alloy cylindrical can shape consisted of the HIP preconsolidation of the AF-115 rim powder. The initial HIP preconsolidation of this material was carried out at 1190°C (2175°F) for four hours and 105 MPa (15 ksi) because it has been demonstrated that these HIP conditions produced optimum stress rupture properties at intermediate temperatures, 650-760°C (1200-1400°F) (19). A photomicrograph of the as-HIP'ed material in the present investigation is shown in Figure 19. The material was not fully densified by the HIP treatment. This lack of complete densification suggested a can leak during the consolidation operation. The ASTM 8 grain size achieved by this HIP operation was limited by the powder particle boundaries and thus did not reach the ASTM 5 grain size anticipated in AF-115 for a HIP operation conducted at 1190°C (2175°F). This preconsolidated compact was used for the preparation of the dual alloy cylindrical shape, however, in the anticipation that hot vacuum outgassing and the second HIP operation would completely seal the remaining porosity.

4.1.2.3.2 HIP Consolidation Operations

The AF-115 HIP preconsolidation step was followed by an operation in which the Rene' 95 powder hub material and the AF-115 rim material were HIP'ed together. The objective here was to fully consolidate the hub material, join the rim and hub materials into a single component, and eliminate any residual porosity remaining in the preconsolidated rim material. The initial HIP consolidation operation for Combination C was carried out for four hours at 1120°C (2050°F) and 105 MPa (15 ksi). These consolidation conditions were identical to those used initially for the Combination A Rene' 95-Rene' 95 material. The photomicrographs of the joint region of the Combination C can are shown in Figure 20. Both the preconsolidated AF-115 rim material and the loose powder Rene' 95 hub material exhibited similar ASTM 8 grain sizes. It was further observed that the porosity present in the AF-115 compact after HIP preconsolidation, Figure 19, was completely eliminated by the 1120°C (2050°F) HIP joining operation. The AF-115 structure was typical of a superalloy which has undergone sub-solvus processing, and was characterized by a considerable amount of coarse gamma-prime precipitate throughout the matrix. The Rene' 95 hub material exhibited a structure identical to that shown by Combination A, Figure 9, and was typical of as-HIP Rene' 95. The Rene' 95 alloy also contained a considerable amount of coarse gamma-prime throughout the structure. The interface between the AF-115 and Rene' 95 materials was difficult to distinguish, due to similarity in etching response of the two alloys and the absence of any unusual phases at the interface.

4.1.2.3.3 Heat Treatment Operations

The initial heat treatments investigated for the Combination C material are listed as follows:

Rene' 95 Hub Material Heat Treatment	AF-115 Rim Material Heat Treatment
1150°C (2100°F)/2 Hours, Salt Quench 540°C (1000°F) Air Cool + 870°C (1600°F)/2 Hours Air Cool + 650°C (1200°F)/24 Hours Air Cool	1190°C (2175°F)/2 Hours Air Cool + 760°C (1400°F)/16 Hours Air Cool

The hub material heat treatment was identical to that applied to the loose powder Rene' 95 hub material of Combination A, a solution treatment slightly below the gamma-prime solvus followed by a double age. The recommended heat treatment for AF-115 is a high temperature solution treatment followed by a single age at 760°C (1400°F). It was recognized that the relatively high solution treatment temperature of the AF-115 alloy could result in an adverse TIP response in the microstructure, despite the use of non-argon atomized powder. This was particularly true in view of the possibility that the AF-115 can leaked during the consolidation operation.

4.1.2.3.3.1 Hub Material Heat Treatment Results

The microstructures of material given the standard Rene' 95 heat treatment are shown in Figure 21. The AF-115 rim material exhibited a random distribution of relatively coarse gamma-prime and the as-HIP grain size of ASTM

8 was maintained as a result of the sub-solvus solution treatment temperature. There was little evidence of the presence of precipitated phases within the grain boundaries and the fine gamma-prime which precipitated during the aging treatments was not resolvable by optical metallography. The Rene' 95 hub material exhibited an ASTM 8-10 grain size and a large proportion of relatively coarse gamma-prime, which resulted from the sub-solvus solution and the aging treatments. This gamma-prime was somewhat coarser than the gamma-prime observed in the Rene' 95 hub material of Combination A given the same heat treatment, Figure 11. This difference in gamma-prime morphology was noted in the as-HIP joined condition was well, and reflected the difference in HIP temperatures used for the two consolidations. The lower consolidation temperature, 1120°C (2050°F), used for Combination C resulted in a coarser heat treated gamma-prime size than the higher temperature consolidation, 1165°C (2125°F), used for Combination A. The joint area between the hub and rim materials was relatively indistinct with little evidence of the presence of unusual phase formations. The microstructures of the hub, rim and joint areas of the Combination C can were considered to be suitable for mechanical property testing.

4.1.2.3.3.2 Rim Material Heat Treatment Results

The microstructural response of Combination C to the AF-115 rim material heat treatment is shown in Figure 22. The AF-115 exhibited extensive triple point porosity, typical of the TIP which can result from an improperly sealed HIP can. The grain size was relatively fine and was approximately the same as that of the original preconsolidation operation, in which the porosity in the structure severely restricted the desired grain growth. There was evidence of unsolutioned gamma-prime particles throughout the microstructure. The grain boundary regions were decorated with a high density of very fine gamma-prime and carbide particles.

The Rene' 95 hub material exhibited substantial grain growth, approximately to ASTM 6, as the result of the suprasolvus solution heat treatment. The gamma-prime was distributed as random, isolated, relatively fine particles. The grain boundaries were decorated by a heavy concentration of relatively fine gamma-prime and carbide particles. Isolated instances of porosity near the interface between the AF-115 material suggested some contamination of the Rene' 95 powder by argon trapped in the AF-115 preconsolidated material. Differences in grain size and overall porosity levels were the most distinguishing features for locating the interface regions.

4.1.2.3.4 Mechanical Property Screening Results

4.1.2.3.4.1 First Processing Iteration

The processing parameters for the first iteration of Combination C are listed in Table 7, which also includes the processing parameters used for the subsequent process iterations. The 1190°C (2175°F) HIP preconsolidation of the AF-115 rim material was followed by HIP consolidation with the loose powder Rene' 95 hub material at 1120°C (2050°F). The standard Rene' 95 heat treatment was selected for mechanical property testing to maintain fine grain size in the Rene' 95 material. Because of the argon contamination of the AF-115 portion of the original HIP can, a replacement can was fabricated for mechanical property evaluations. The 1205°C (2200°F)/2 hour TIP test conducted on this can indicated a satisfactory microstructure. Examination of the

microstructure of this material after the application of the Rene' 95 heat treatment indicated a solutioning and precipitation response similar to that described in the previous section for the original can. However, the grain size in the replacement can was ASTM 5-6, which conforms to that reported in the literature for AF-115 powder HIP'ed at 1190°C (2175°F). This increase in grain size was attributed to more complete consolidation.

The results of the mechanical property screening tests are listed in Table 8. The ultimate strength for the loose powder Rene' 95 hub material was below the 1520 MPa (220 ksi) NASA program goal and below the 1530 MPa (222 ksi) reported previously in the literature (27). The yield strength, however, was above the 1100 MPa (160 ksi) level anticipated for Rene' 95 at 480°C (900°F). Comparison of this first iteration data with that presented previously in Table 4 for the Combination A Rene' 95 hub material offered an insight into the effect of grain size and processing on this alloy. The Combination C Rene' 95 material exhibited a fine ASTM 8-10 grain size as the result of the 1120°C (2050°F) HIP consolidation operation and the 1150°C (2100°F) solution treatment. The Combination A grain sizes ranged from ASTM 5-6 all the way up to ASTM 0-1 because of the use of higher temperature HIP (1165°C (2125°F)) or vacuum pre-sinter consolidation temperature (1265°C (2310°F)). In spite of this large variation in grain size, a significant difference was not observed in the tensile strength values until the ASTM 0-1 grain size was reached. This caused a reduction of approximately 15% in ultimate tensile strength and 9% in yield strength compared to the values obtained for the first iteration Combination C material. Grain size variations from ASTM 8-10 to the range ASTM 5-6 resulted in little change in the strength properties. The ductility values were also significantly lower for ASTM 0-1 grain size material. These results indicate that for Rene' 95 the tensile properties are sensitive to processing modifications particularly when grain size variations from the range ASTM 8-10 to the range 0-1 occur.

High joint quality was reflected by the fact that the joint tensile specimens did not fail in the joint region. Failure was observed in the AF-115 rim material at ultimate and yield strength values which were within 90% of the average values of the duplicate hub specimens. The ductility properties of the AF-115 were not as good, however, ranging approximatley 40% below those of the Rene' 95 material.

The results of the 760°C (1400°F) stress rupture tests were disappointing for this processing iteration. The AF-115 rim material exhibited an average rupture life of only 11 hours. This level of rupture life suggested that the AF-115 offered little potential for the rim application of a dual alloy disk component. In addition, this stress rupture level was far below the published values of approximately 400 hours for HIP AF-115 solution heat treated at 1190°C (2175°F) (19). It was also significant to note that the joint stress rupture specimen failed at the interface between the AF-115 and Rene' 95 but at 20.7 hours, almost double that of the AF-115 specimens. A high magnification photomicrograph of this fracture surface is shown in Figure 23a, and indicates an almost entirely flat surface, suggesting that the failure occurred along the joint interface, possibly as a result of continuous types of films or precipitates in this region. Examination of the photomicrograph of Figure 23b, which displays the joint area of the 480°C (900°F) tensile specimen exhibiting 1235 MPa (179 ksi) ultimate tensile strength, did not, however, indicate the presence of any thick or continuous phase. Nonetheless, the appearance of the fracture and the poor property levels exhibited by the joint stress rupture specimen suggested poor joint quality for this processing iteration.

4.1.2.3.4.2 Second Processing Iteration

The modifications for the second processing iteration were directed towards improving the stress rupture properties of the AF-115 rim material. The tensile strength exhibited by the Rene' 95 material was within 15% of the program goal. The AF-115 rim stress rupture properties, however, were very poor in relation to the expected values. It was reasoned that the rim properties could be improved by the use of a higher solution heat treatment temperature while the Rene' 95 hub properties would not be significantly degraded as long as the grain size did not approach ASTM 0-1. Accordingly, a solution heat treatment 1175°C (2150°F) was selected for the second processing iteration, as well as the single step 760°C (1400°F) age recommended for AF-115. The entire set of processing parameters used for this second iteration are listed in Table 7.

The results of the mechanical property screening tests for this iteration are listed in Table 8. As expected, the grain size of the Rene' 95 hub material increased from ASTM 8-10 to ASTM 6 as the result of the higher solution heat treatment temperature. The ultimate tensile strength, however, was similar to that exhibited by the first iteration material. This results was not surprising in view of the results for the Rene' 95 used for Combination A in which an appreciable reduction in ultimate strength was not observed until a grain size of ASTM 0-1 was reached. There was a slight (8%) reduction in yield strength for second iteration material, and this was attributed to the fact that the simple 760°C (1400°F) age and not the two-step age was used for this iteration. There was an appreciable increase in ductility with the heat treatment change for the second iteration. Elongation increased by approximately 60%, while the reduction of area increased by approximately 50%. An improvement in the joint properties was also observed. Similar to the first iteration joint specimen, failure occurred not in the joint itself but rather in the AF-115 material. An improvement in all the tensile properties was observed, with the greatest improvement being noted in the ultimate tensile strength and the ductility properties. This reflected the high joint quality for this processing iteration.

The most significant change in properties between the two iterations, however, was in the stress rupture life of the AF-115 rim material. The rim stress rupture specimens in the first iteration had failed after an average of only 11 hours. The duplicate stress rupture specimens in the second iteration exhibited an average rupture life of 852 hours, reflecting the importance of the higher temperature solution treatment on the rupture properties. An increase in rupture ductility was also observed in these specimens. The joint specimen also exhibited significantly improved stress rupture life, with a failure life of 124.1 hours as well as improved ductility compared to the first iteration joint specimen. Most significant, however was the increased joint quality which caused failure to occur in the Rene' 95 hub material and not in the joint region.

4.1.2.3.4.3 Third Processing Iteration

The results of the first two processing iterations indicated that the strength of the Rene' 95 hub material was below the program goal but that the stress rupture properties of the AF-115 rim material would be well in excess of the rim alloy program requirement. Both the joint tensile and stress rupture test

specimens failed away from the joint in adjacent material, indicating the joint region to be satisfactory in quality. Several changes were made in the third iteration processing sequence, therefore, to increase the strength of the Rene' 95 hub material. This included using argon atomized Rene' 95 powder instead of soluble gas atomized powder for the hub material and using an extended age at 760°C (1400°F), from 16 to 32 hours, as a means of effecting further strength improvements. Hub powder for this iteration came from the same Special Metals heat of argon atomized Rene' 95 used for the fourth processing iteration for the Combiation A Rene' 95 hub alloy. The complete listing of the processing parameters used for the third processing iteration are listed in Table 7.

The results of the mechanical property screening tests for this iteration are listed in Table 8. The ultimate tensile strength suffered reduction from an average of 1410 MPa (203 ksi) to an average of 1305 MPa (189 ksi). The average yield strength, on the other hand, increased from 1100 MPa (160 ksi) to 1205 MPa (175 ksi). This yield strength value was above the 1100 MPa (160 ksi) level anticipated for Rene' 95 at 480°C (900°F). The ductility values for the argon atomized Rene' 95 given the extended age at 760°C (1400°F) were quite poor in comparison to the second iteration material and, in fact, represented the lowest ductilities observed for the Combination C Rene' 95 hub material. The elongation, for example ranged from 2.4-2.5%, compared to values above 4.5% for the other iterations. High joint quality, however, was reflected by the fact that both ultimate and yield strength values as well as the ductility properties were within 90% of the average values of the duplicate hub specimens. The joint tensile specimen failed along the boundary between the hub and rim material.

Comparing the tensile results of the two iterations employing the argon atomized powder (iteration four of Combination A, Table 4 and iteration three of Combination C, Table 8) indicated Combination C processing resulted in superior tensile properties. For Combination A, the 1165°C (2125°F) HIP and 1175°C (2150°F) solution treatment resulted in an ASTM 4-5 grain size. For Combination C, the 1120°C (2050°F) solution treatment resulted in an ASTM 6 grain size. These differences, in combination with the use of different aging cycles, resulted in strength properties approximately 10% lower for the larger grained material compared to the finer grained material, and a reduction of approximatley 50% in ductility. In general, it was observed that the argon atomized Rene' 95 powder exhibited properties inferior to the hydrogen gas atomized powder.

The stress rupture results indicated that the third iteration specimens were inferior to the second iteration material. The rupture lives of the AF-115 specimens were all below 100 hours compared to the 800 plus hour rupture lives exhibited by second iteration AF-115 alloy. In addition to this, the third iteration material evidenced severe notch sensitivity, with both specimens failing in the threaded regions. The joint specimen which failed in the Rene' 95 hub material region also exhibited extremely poor properties, failing in less than one hour with low ductility. Metallographic analysis of the failed joint test specimen indicated an intergranular type of fracture mode with a considerable degree of secondary cracking along grain boundaries propagating from the fracture surface. The microstructure of this fracture region is shown in the photomicrographs of Figure 24.

4.1.2.3.4.4 Summary

The results of the processing studies for the AF-115 - Rene' 95 combination indicated that the optimum strength of the Rene' 95 hub material was approximately 10% below the program goal, but that the stress rupture properties of the AF-115 rim material could be well in excess of the rim alloy program requirement. High joint quality was reflected by the fact that ultimate and yield strength values, as well as both ductility values were within 90% of the average values of the hub specimens. This combination of properties was exhibited by second iteration material which featured hydrogen atomized Rene' 95 hub material HIP consolidated at 1120°C (2050°F), along with AF-115 powder which had been HIP preconsolidated at 1190°C (2175°F). The heat treatment involved a solution at 1175°C (2150°F) and a single age at 760°C (1400°F). It was concluded that the overall balance of strength, stress rupture and joint properties exhibited by the AF-115 - Rene' 95 dual alloy materials represented an attractive combination of properties and warranted more extensive characterization in the flat panel shape configuration.

4.1.2.4 Combination D (Vacuum Sintered PA-101 Rim - MERL 76 Hub)

4.1.2.4.1 Vacuum Presintering Operations

The first step in the fabrication of the Combination D dual alloy cylindrical shape can involved the preconsolidation of the PA-101 rim material. These studies were conducted on small amounts of -60 mesh PA-101 powder loaded into short ceramic boats. The PA-101 vacuum sintering trials were conducted for six hours at 1245°C (2270°F). The 1245°C (2270°F) sintering temperature resulted in a very low degree of density in the sintered material. As shown in the microstructure of Figure 25a for this sintering condition, a considerable degree of interconnected porosity remained after the operation. An increase in sintering temperature to 1260°C (2300°F) resulted in a grain size of ASTM 2-4, a density in excess of 90% and a small amount of incipient melting, as shown in Figure 25b. Reichman (16) has reported an ASTM 4 grain size as a result of vacuum sintering PA-101 powder at 1275°C (2325°F), followed by HIP at 1230°C (2250°F). It was thus observed that the grains of the PA-101 alloy in the present investigation coarsened to a slightly larger size than that reported in the literature for a higher vacuum sintering temperature. The 1260°C (2300°F) vacuum presinter condition was selected for the PA-101 alloy because the grain size was considered satisfactory for rim preconsolidation and it was not desired to increase the degree of incipient melting throughout the structure by going to higher sintering temperatures.

4.1.2.4.2 HIP Consolidation Operations

The vacuum sintering preconsolidation step was followed by an operation in which the MERL 76 powder hub material and the preconsolidated PA-101 rim material were HIP'ed together. The preliminary consolidation conditions for Combination D included four hours at 1165°C (2125°F) and 105 MPa (15 ksi) and were selected to consolidate the MERL 76 hub powder material while maintaining as fine a grain size as possible. Previous results reported by Pratt & Whitney for MERL 76 HIP'ed in the temperature range 1175-1200°C (2150-2195°F) indicated an ASTM grain size in the range 5-10 (26). The 1165°C (2125°F) HIP consolidation was thus selected to produce a grain size on the low side of that range.

The microstructures of the Combination D materials HIP'ed at this condition are shown in Figure 26. The PA-101 exhibited an ASTM 2-4 grain size, which was relatively unchanged from that developed during the vacuum presintering operation. However, there was evidence of substantially more incipient melting than was expected on the basis of the preconsolidation studies. This suggested a certain degree of variability in the response to the sintering operation. No residual porosity from the preconsolidation treatment was present, indicating that the HIP joining conditions were suitable for the closure of any porosity. The MERL 76 hub alloy exhibited a microstructure similar to that of the hub of the first iteration of Combination B, HIP'ed at the identical conditions, Figure 15. The structure contained very fine ASTM 8-10 grains as well as coarse gamma-prime dispersed throughout the matrix, indicative of sub-solvus HIP consolidation. These as-HIP structures indicated the 1165°C (2125°F) HIP temperature was successful in maintaining a fine grain size in the MERL 76 alloy.

The interface between the hub and rim materials was delineated in certain areas by a coarse, almost continuous film-like constituent. This constituent is clearly shown in the 500X magnification photomicrograph of Figure 26. Electron microprobe analyses indicated this region was rich in both oxygen and carbon, with the oxygen primarily associated with aluminum and silicon, while the carbon was associated with hafnium and tantalum. These regions were highly localized and did not represent the interface in general. The analysis of this constituent suggested that it originated as the result of contamination and improper handling of the preconsolidated PA-101 compact. It was not observed at the interface of those portions of the PA-101 compact which had been carefully faced-off and cleaned prior to the HIP joining operation. The occurrence of the contamination emphasized the necessity of careful cleaning and handling of material to be incorporated into dual alloy disks.

4.1.2.4.3 Heat Treatment Operations

The initial heat treatments investigated for the Combination D material are listed as follows:

MERL 76 Hub Material Heat Treatment	PA-101 Rim Material Heat Treatment
1175°C (2145°F)/2 Hours Air Cool + 760°C (1400°F)/8 Hours Air Cool	1175°C (2150°F)/2 Hours Rapid Air Cool + 760°C (1400°F)/8 Hours Air Cool + 675°C (1250°F)/24 Hours Air Cool

The standard heat treatments for MERL 76 and PA-101 are quite similar, with the only differences being slight solution treatment temperature differences, and a 675°C (1250°F) final aging treatment for the PA-101. Since the microstructural response to the two heat treatments was similar in all respects, only the results for the MERL 76 hub heat treatment will be discussed in detail. The resultant microstructures are presented in Figure 27.

The PA-101 alloy exhibited areas of incipient melting throughout the microstructure. The large primary carbides and eutectic gamma-prime colonies were evidence of this melting. Since there was no porosity evident in the microstructure of the PA-101, it was concluded that the melting occurred prior to heat

treatment. The MERL 76 exhibited an increase in grain size from the as-HIP material, from ASTM 8-10 to ASTM 6. There was almost complete solutioning of the gamma-prime, with little evidence of any coarse particles. Some grain boundary liquation was observed adjacent to the junction between the rim and hub materials, and the grain boundaries also contained discrete particle precipitates and indicated that proper surface preparation procedures can result in a high quality joint interface. In summary the observations on the results of the 1175°C (2145°F) solution treatment temperature indicated that the temperature was too high, particularly in view of the partial liquation and grain growth observed in the MERL 76. Therefore, an investigation of a reduced solution treatment temperature was conducted.

The response of this combination to an 1165°C (2125°F) solution treatment was investigated and the resultant microstructures are presented in Figure 28. The PA-101 was relatively unchanged as a result of the change in solution treatment temperature, being characterized predominantly by the incipient melting throughout the microstructure. The MERL 76, however, was characterized by a considerable change in microstructure as a result of the reduced solution treatment temperature. Coarse gamma-prime, similar to that found in the MERL 76 hub of Combination B given the 1115°C (2040°F) solution treatment (Figure 16) was present, although in considerably smaller amounts, indicative of a solution temperature closer to the gamma-prime solvus. The grain size remained at ASTM 8-10, relatively unchanged from the as-HIP grain size. The interface was free of the continuous oxygen-carbon layer observed previously on the improperly prepared PA-101 surface. Examination of the rim, hub and joint locations indicated that the 1165°C (2125°F) temperature represented a satisfactory solution treatment condition. Since the tensile strength goal of this program was expected to be more difficult to meet than the stress rupture goal, initial emphasis was given to attaining high hub strength. Accordingly, the simple 760°C (1400°F) MERL 76 age was applied initially to Combination D material for mechanical property testing.

4.1.2.4.4 Mechanical Property Screening Results

4.1.2.4.4.1 First Processing Iteration

The processing parameters for the first iteration for Combination D are listed in Table 9, which also includes the processing parameters used for subsequent process iterations for this combination. These parameters included the 1260°C (2300°F) vacuum sinter preconsolidation of the PA-101 rim material followed by HIP consolidation with loose powder MERL 76 hub material at 1165°C (2125°F). Heat treatment consisted of a solution treatment at 1165°C (2125°F) followed by a single age at 760°C (1400°F). The results of the mechanical property screening tests are listed in Table 10.

The tensile results for the MERL 76 hub material indicated that the ultimate strength values were below the 1520 MPa (220 ksi) program goal. The joint area was sound and the tensile properties of the joint test specimen were within 90% of the average value of the duplicate hub specimens, but the reduction of area was only approximately one half that of the hub material. Comparison of these tensile results with those presented previously in Table 6 for the Combination B MERL 76 hub

material offered several observations. First, the property levels exhibited by the first iteration of Combination D were equivalent to those of the first iteration of Combination B in spite of the significant differences in heat treatments. Both combinations included the 1165°C (2125°F) HIP consolidation temperature, but Combination B employed a 1115°C (2040°F) solution treatment with a complicated four step aging cycle. Combination D, on the other hand, was given a 1165°C (2125°F) solution treatment with a simple single step age. As shown in Table 6, mechanical property improvements in the MERL 76 were realized only after the use of a lower temperature HIP consolidation in combination with a higher solution treatment, 1165°C (2130°F) instead of 1115°C (2040°F), as well as the more complicated four step age.

Unlike the tensile properties for this processing iteration, the stress rupture properties were quite promising. The PA-101 rim stress rupture results obtained at 760°C (1400°F) were superior to the results reported by several investigators for this alloy (16,18). Test results were reported over the temperature range 650°C (1200°F) to 980°C (1800°F) and although tests were not specifically conducted at 760°C (1400°F), failure lives of approximately 300 hours were predicted at the test temperature and stress level used in the present program. The average rupture life of the duplicate rim tests was 454.3 hours. The rupture values were also comparable to those reported in the literature (16,18). The joint stress rupture properties for this combination were inferior to those of the rim material. Failure was observed in the specimen radius at a fraction of the average rupture life exhibited by the rim material, and the specimen exhibited little ductility. Metallographic analysis indicated that failure occurred in the PA-101 rim material, which indicated that the PA-101 exhibited notch sensitivity. The fracture surface of this joint stress rupture specimen, shown in Figure 29, indicated that the fracture path was predominantly intergranular.

4.1.2.4.4.2 Second Processing Iteration

The processing modifications for the second iteration included changes both in the HIP conditions and the heat treatment cycles. The HIP consolidation temperature was decreased from 1165°C (2125°F) to 1120°C (2050°F) and the solution treatment temperature was raised from 1165°C (2125°F) to 1170°C (2135°F). The HIP conditions were identical to those for the second iteration of the MERL 76 L/C Astroloy Combination B. The higher solution treatment temperature more closely corresponded with that recommended for MERL 76 but was meant to avoid the incipient melting encountered at the higher solution temperatures used previously. The use of the salt quench from solution as opposed to the slower air cooling compromised the PA-101 stress rupture properties in order to improve the MERL 76 tensile strength. This was followed by the aging treatment recommended for PA-101.

The second iteration changed the MERL 76 hub from the fine grained ASTM 8-10 of the first iteration, to a larger ASTM 4-5 grain size. The processing changes improved the MERL 76 ultimate and yield strengths by approximately 15 and 12%, respectively, and the elongation more than doubled. These property levels are within the ranges published for HIP and heat treated MERL 76 and the ultimate strength level is within 96% of the 1520 MPa (220 ksi) program goal. In addition, comparison with the MERL 76 properties presented in Table 6 for Combination B indicates

that this Combination D second iteration material exhibited the highest level of mechanical properties attained for the MERL 76 material. By comparison, however, the joint region properties for this processing sequence were quite poor. Failure occurred in the PA-101 rim material at only 650 MPa (93 ksi), with essentially nil ductility. Metallographic analysis indicated that the fracture path for this specimen was primarily intergranular, but offered little additional explanation for the relatively low tensile properties.

The low level of tensile strength in the PA-101 portion of the joint tensile specimen was also accompanied by poor stress rupture properties in the rim alloy. The stress rupture lives averaged 67 hours compared to the approximate 450 hour average for the first iteration. The ductility values, however, were only slightly degraded compared to those obtained previously. Some degradation in the PA-101 rupture properties had been anticipated on the basis of results reported in the literature comparing air cooling versus salt quenching from solution, but the loss of more than 75% the rupture life capability was much larger than anticipated. Metallographic examination of the failed test bar specimens indicated ASTM grain sizes of 0-1 as well as microstructures fully equivalent to those for the first iteration material, again with fracture paths following along the grain boundaries. The notch sensitivity observed previously in the PA-101 material of the first iteration was not seen in the second iteration material. That the joint area was of high quality was demonstrated by the fact that rupture after 75.9 hours occurred not in the joint itself, but in the MERL 76 hub material. Elongation and reduction of areas, however, were significantly below those for the rim alloy, being approximately 1% as compared to the 3.5% for the PA-101 alloy.

4.1.2.4.4.3 Third Processing Iteration

The processing modifications for the third iteration included changes in the heat treatment cycle. Specifically, an oil quench from the solution heat treatment temperature was employed in combination with the modified stress relief and stabilization treatments in the range 870-980°C (1600-1800°F) recently developed by Pratt & Whitney Aircraft for the MERL 76 alloy (26). These changes were incorporated primarily to increase the strength of the MERL 76 hub material in order to meet the program tensile strength goal. It was also of interest to determine to what extent the more severe oil quench from solution would affect the properties of the PA-101 alloy and the joint region. The entire set of processing parameters for this third iteration are listed in Table 9, and the results of the mechanical proeprty screening tests are listed in Table 10.

The mechanical property results reflected the fact that the the oil quench and heat treatment modifications of the third iteration were not successful in improving the MERL 76 hub material properties. Of more importance, however, was the fact that the oil quench was too severe and resulted in quench cracking along the joint between the MERL 76 and PA-101. Because of this quench cracking, no joint specimens could be prepared for tensile or stress rupture testing. The tensile properties were especially poor in that the MERL 76 exhibited little ductility compared to material tested previously.

The PA-101 stress rupture properties for this third iteration were also poor with respect to material tested previously. The average rupture life of 20.5 hours was significantly below the 454.3 and 67 hour averages exhibited by the first and second iteration material, respectively. In addition, these specimens also exhibited poor ductility properties with less than 0.5% elongation and approximately 1.0% reduction area. Metallographic examination of the failed test specimens indicated that fracture occurred along grain boundaries in a manner similar to that observed previously in test specimens of the first two process iterations. The microstructure of the failed PA-101 test specimen exhibiting 22.7 hours rupture life is shown in Figure 30. The structure is similar to that shown in Figure 29 for a specimen tested during the first iteration.

4.1.2.4.4.4 Summary

The results of the processing studies for the MERL 76-PA-101 combination indicated that a satisfactory level of properties could be achieved in each of the two alloys, but not using the same processing conditions. For the MERL 76, an optimum average ultimate tensile strength of 1460 MPa (212 ksi) was obtained at 480°C (900°F), which was approximately 96% of the program goal. For the particular processing conditions resulting in this tensile strength, however, the PA-101 stress rupture life at 760°C (1400°F) was only approximately 25% of the maximum rupture life exhibited by this alloy. Processing for maximum rupture life, on the other hand, resulted in an ultimate tensile strength of only 1275 MPa (185 ksi) in the MERL 76. These results indicated that a compromise in both the ultimate tensile strength and the stress rupture life would have to be made for this particular combination. In addition to this drawback, there were problems with the joint specimens during the mechanical property screening evaluations. Processing to the highest MERL 76 ultimate tensile strength resulted in extremely poor tensile strength properties in the PA-101 material portion of the joint specimen. Processing to the highest PA-101 stress rupture life resulted in a possible notch sensitive condition in the PA-101 material itself. This was manifested by the poor rupture life of the joint specimen, which failed in the radius of the PA-101 portion of the specimen. Accordingly, no further evaluations of the cylindrical can configuration were undertaken.

4.1.3 Testing of Shapes

This portion of the program was directed towards a more complete evaluation of the most promising combinations of material pairs and heat treatments. Rectangular panel shapes were HIP consolidated for these evaluations.

4.1.3.1 Materials Selection for Testing of Shapes

An analysis was made of the data developed during the processing of the cylindrical shapes. The results of these analyses are presented in Figures 31 and 32. Figure 31 is a bar graph of the optimum tensile results of the mechanical property screening studies at 480°C (900°F). Also shown in this figure is the 1520 MPa (220 ksi) ultimate tensile strength program goal. Figure 32 shows the optimum stress rupture results of the mechanical property screening studies. Attention is called to the fact that the data for the Combination A processing studies were not included in this analysis because of the severe quench cracks which developed during heat treatment and the

attendent inability to evaluate the joint properties. On the other hand, two processing iterations for Combination D were considered because both presented unique mechanical property advantages.

The 480°C (900°F) tensile properties shown in Figure 31 indicate that none of the material combinations met the ultimate tensile strength program goal. Second iteration Combination D material exhibited the highest average ultimate tensile strength at 1470 MPa (213 ksi), which was approximately 96% of the program goal. A serious problem with this processing sequence, however, involved poor tensile properties of the PA-101 portion of the joint specimen. This material exhibited less than half the ultimate tensile strength of the MERL 76 hub material, with nil ductility. Combinations B and C exhibited the next highest ultimate strengths at approximately 1380 MPa (200 ksi), reaching 90% of the program goal. However, the ultimate tensile strengths of the joint specimens for these combinations were above 95% of the values exhibited by the respective hub materials. The first iteration Combination D material displayed the lowest average ultimate strength value, an average of 1275 MPa (185 ksi). The tensile yield strengths of Combination B and C were somewhat similar. Their joint specimens had yield strength values within 90% of the values of the respective hub materials. The tensile ductilities for Combination B and C were approximately 10%, and the joint specimens exhibited values within 90% of those of the hub materials. Overall, the specimens of Combination D had slightly higher tensile ductilities, except for the joint specimens where they were significantly below those of the MERL 76 hub material.

The stress rupture properties at 760°C (1400°F) shown in Figure 32 indicate that two types of behavior prevailed during the mechanical property screening studies. In one type the rupture life exceeded 400 hours (Combination C and the first iteration Combination D). The other type, which included Combination B and the second iteration Combination D material exhibited average rupture lives of less than 100 hours. It was interesting to note that with the exception of the Combination D second iteration, all of the joint specimen rupture lives were below approximately 25% of the average lives of the respective rim materials. The rupture life of the joint specimen of this lower life iteration was equivalent to that of the PA-101 rim material. The rupture ductility for all of the material combinations averaged less than 5% and, like the tensile ductility results, the ductilities of the joint specimens of Combinations B and C were within 90% of the average values of the respective rim materials, while those for the Combination D processing iterations were less than half those of the average values of the PA-101 rim materials.

On the basis of these comparisons between the optimized mechanical properties of the various material combinations, it was concluded that the Combination B third processing iteration and Combination C second processing iteration materials exhibited attractive balances of properties for the more extensive evaluation in the flat panel shape configuration. The processing details for these particular iterations are listed below:

COMBINATION B	COMBINATION C
Rim - Loose Powder L/C Astroloy	Rim - AF-115 HIP'ed at 1190°C (2175°F)/105 MPa/4 Hours
Hub - Loose Powder MERL 76	Hub - Loose Powder Rene' 95
HIP Joining - 1120°C (2050°F)/105 MPa/4 Hours	HIP Joining - 1120°C (2050°F)/105 MPa (15 ksi) 4 Hours
Heat Treatment - 1165°C (2130°F)/2 Hours, Oil Quench + 870°C (1600°F/40 Minutes Air Cool + 980°C (1800°F)/45 Minutes Air Cool + 650°C (1200°F)/24 Hours Air Cool + 760°F (1400°F)/8 Hours Air Cool	Heat Treatment - 1175°C (2150°F)/2 Hours Air Cool + 760°C (1400°F)/16 Hours Air Cool

4.1.3.2 Combination B (Loose Powder L/C Astroloy Rim - Loose Powder MERL 76 Hub) Testing

4.1.3.2.1 Test Panel Fabrication and Heat Treatment

Efforts for the Combination B material involved the preparation of two test panels each measuring approximately 230 mm (9 inches) x 90 mm (3.5 inches) x 25 mm (1 inch) made of 9 mm (3/8 inch) thick welded 1018 mild steel. The test panel configuration is shown schematically in Figure 6b. Can fabrication and HIP processing was conducted at Industrial Materials Technology. The HIP parameters were 1120°C (2050°F) for four hours and 105 MPa (15 ksi). Can loading, outgassing and sealing procedures were similar to those used for the cylindrical shapes. Heat treatments were conducted on a single test panel. Because of the possibility of quench cracking in the test panel, it was examined ultrasonically and by X-radiography subsequent to the 1165°C (2130°F) solution heat treatment. No cracks or other defects were found in the solution treated material and the four step aging treatment was applied. The microstructures resulting from this heat treatment are shown in Figure 33 and include light photomicrographs of the joint area as well as higher magnification scanning electron photomicrographs of the MERL 76 hub material and the L/C Astroloy rim material.

Because of the high solution temperature used the joint between the MERL 76 and the L/C Astroloy was easily identified. A certain degree of powder intermixing was observed and resulted in an uneven boundary between the two alloy powders. There were, however, no indications of continuous precipitated phases or other deleterious microstructural features within this joint region. The L/C Astroloy exhibited a grain size of ASTM 4-8, which was a finer range than its ASTM 4-6 grain size in the cylindrical shape configuration. There were considerable instances of prior particle

boundary precipitation, suggesting a reason for the finer grain size in the flat panel shape configuration. The prior particle boundary precipitates act to inhibit grain growth during the heat treatment operation. The microstructure of the L/C Astroloy reflected the suprasolvus solution heat treatment temperature by a general absence of large gamma-prime precipitates. Rather, the gamma-prime formed fine precipitates in both the matrix and the grain boundaries as the result of the complex aging heat treatments. The MERL 76 hub material exhibited an ASTM grain size range of 8-10, which was considerably finer than the ASTM 4-5 grain size observed in the cylindrical can configuration. Metallographic examination offered no explanation for this change in the MERL 76 grain size. The microstructural features, were characteristic of MERL 76 powder alloy processed under subsolvus HIP and solution heat treatment conditions. There were two gamma-prime sizes in evidence throughout the structure, both randomly distributed throughout the matrix. The coarse gamma-prime was most characteristic of subsolvus HIP and heat treatment processing and contributed most to identifying the joint between the MERL 76 and the L/C Astroloy. The finer gamma-prime, shown in the scanning electron photomicrograph of the MERL 76 hub material in Figure 33, resulted from the subsequent aging treatments. There was little substantial precipitation along the MERL 76 grain boundaries.

4.1.3.2.2 Mechanical Property Screening Results

Mechanical property screening evaluations including 480°C (900°F) tensile and 760°C (1400°F) stress rupture tests were conducted on the heat treated test panel material in order to determine whether the properties compared favorably with the results obtained during the evaluations of the cylindrical can configuration. On the basis of these results more extensive mechanical property evaluations were planned including alternative heat treatment for the second test panel to be selected on the basis of the mechanical property results. The results of the screening tensile and stress rupture mechanical property tests as well as grain size ranges are presented in Table 11 for the Combination B test panel. The results are discussed in the following sections.

4.1.3.2.2.1 Tensile Test Results

The mechanical property characterization of Combination B material in the cylindrical can configuration indicated that the tensile strength values of the MERL 76 hub alloy at 480°C (900°F) averaged 1370 MPa (199 ksi) for material processed according to the optimum processing parameters. Although this was below the 1520 MPa (220 ksi) ultimate tensile strength goal, high joint quality was reflected by the fact that ultimate and yield strength values, as well as both ductility properties were within 90% of the average values of the duplicate hub specimens. As indicated in Table 11, the tensile properties of specimens prepared from the flat test panels were superior to those exhibited by specimens from the cylindrical shapes. Specifically, the ultimate tensile strengths exhibited by the MERL 76 specimens averaged 1540 MPa (223 ksi), well above the 1370 MPa (199 ksi) average value obtained previously, and exceeding the program goal of 1520 MPa (220 ksi). The yield strength values of the test panel material were comparable to those exhibited by the cylindrical can material. High quality in the joint area was also demonstrated by the fact that failures were not observed along the joint, but rather, in the weaker L/C Astroloy away from the joint.

Although lower than the values exhibited by the MERL 76, the tensile strengths of the joint specimens were still higher than any previously obtained from specimens machined from cylindrical shapes. In all cases the strength values were within 90% of those of the average of the duplicate MERL 76 hub specimens. The tensile ductility values for the specimens from the flat plates were also higher than those obtained previously. The MERL 76 elongations, for example, ranged from 18.6-20.7%, compared to the previous range of 11.8-12.4%. The elongations for the joint specimens were also superior to those obtained previously, ranging from 10.8-13.3%, compared to 7% obtained previously.

Metallographic analysis of selected failed test bar specimens indicated generally a mixed intergranular fracture mode in both the MERL 76 hub specimens and in the failed L/C Astroloy portion of the joint specimens. The microstructure at the fracture surface of the MERL 76 specimen exhibiting the 1565 MPa (227 ksi) ultimate tensile strength is shown in Figure 34, while that for the L/C Astroloy portion of the joint specimen exhibiting the 1455 MPa (211 ksi) ultimate tensile strength is shown in Figure 35. There was no evidence of secondary cracking in the MERL 76 alloy nor was there evidence of slip line formation. As shown in Figure 35 for the L/C Astroloy specimen, however, secondary cracking and slip line formation were both evident. The secondary cracking was observed to initiate both along slip lines at the surface of the specimen as well as at prior particle boundaries within the material. The secondary cracks were observed to propagate along the slip bands and the prior particle boundaries.

4.1.3.2.2.2 Stress Rupture Results

The stress rupture evaluation of Combination B material in the cylindrical can configuration indicated that the maximum average rupture life at 760°C (1400°F) for material processed according to the optimized condition was 78 hours, which exceeded the expected life of 45 hours for L/C Astroloy tested under these conditions. As indicated in Table 11, however, the stress rupture properties of the specimens prepared from the flat test panel were inferior to those exhibited by specimens from the cylindrical shapes. The L/C Astroloy rim specimen failed after only 24.9 hours, and exhibited extreme notch sensitivity by the fact that failure occurred in the thread area. That the L/C Astroloy was even inferior to the MERL 76 hub candidate alloy was suggested by the fact that the joint specimen failed not in the joint or the MERL 76, but in the L/C Astroloy. Previous joint stress rupture specimens had failed in the MERL 76 portion of the specimens. The rupture ductility of this joint specimen was also somewhat lower (2.5% elongation versus approximately 3.0% elongation) than previously obtained.

The metallographic examination of failed test bars suggested that the relatively poor stress rupture properties exhibited by the L/C Astroloy were associated with fracture along prior particle boundaries. As shown in Figure 36 for the L/C Astroloy portion of the joint specimen exhibiting 36.7 hours rupture life, extensive secondary cracking away from the fracture surface itself was observed associated with the outlines of prior powder particles. These prior particle boundaries acted both as sites for crack initiation as well as pathways for crack propagation.

4.1.3.2.2.3 Summary

The mechanical properties exhibited by specimens machined from the flat plate panel varied in terms of their relationship to the properties obtained from the cylindrical shape configuration. The tensile properties were superior to those obtained previously, while the stress rupture properties were significantly below those exhibited previously. Extensive prior particle boundary precipitation was primarily responsible for the poor stress rupture properties. Because of this condition there was little likelihood that a modification in the heat treatment would significantly improve the stress rupture properties for the second test panel. Accordingly, no further testing was conducted on the second test panel material.

The screening results did suggest, however, that the MERL 76 hub material candidate of this combination might have promise as both a hub or a rim material. The high level of tensile strength was documented and the fact that the joint stress rupture specimens failed in the L/C Astroloy and not the MERL 76 suggested that the stress rupture life of the MERL 76 would be greater than that exhibited by the L/C Astroloy. Additional testing, therefore was conducted on the MERL 76 portion of this combination.

4.1.3.2.3 MERL 76 Mechanical Property Test Results

The additional testing conducted on the MERL 76 material included duplicate stress rupture tests at 760°C (1400°F)/550 MPa (80 ksi) and duplicate low cycle fatigue tests at 480°C (900°F). The stress rupture conditions were selected to investigate the possibility of using MERL 76 as both a hub and rim material and to determine whether the MERL 76 could provide improved stress rupture capability compared to the L/C Astroloy tested previously. The low cycle fatigue tests were conducted because repeated applications of high stresses in the disk hub areas can give rise to possible low cycle fatigue limitations (5). The results are listed in Table 12.

MERL 76 exhibited little improvement in rupture life capability compared to the L/C Astroloy. The previous maximum rupture life was in a joint specimen which failed in the L/C Astroloy portion of the specimen after 36.7 hours. The 40.5 average rupture life of the MERL 76 showed little promise as a candidate rim material in this particular HIP and heat treated condition.

The low cycle fatigue testing for the MERL 76 alloy included duplicate tests at 480°C (900°F) at a total strain range of 0.7% and a frequency of 20 cycles per minute. As shown in Table 12, the first specimen lasted 69,120 cycles when the test had to be terminated because the specimen stripped the threads of the testing fixture grips. The grips were rethreaded and the duplicate specimen exhibited a life of 137,460 cycles to failure. It was not possible to determine the failure origin for this specimen because arcing occurring during final specimen separation (caused by the direct resistance method employed to heat the specimen) and deposited a recast layer on the fracture surface thus obscuring the details of this surface. Secondary cracks away from the fracture surface, however, indicated crack propagation was transgranular, similar to that reported in the literature for HIP'ed MERL 76 low cycle fatigue specimens

tested at 650°C (1200°F) (29). The failure life for the Combination B specimen, however, was lower than that anticipated for this alloy. In material tested at 649°C (1200°F) and a total strain range of 0.9%, for example, a failure life of approximately 150,000 cycles was observed (29).

4.1.3.3 Combination C (Pre-HIP'ed AF-115 Rim-Rene' 95 Hub) Testing

Can fabrication and HIP processing for the two Combination C test panels was conducted at Industrial Materials Technology. This included HIP preconsolidation of the AF-115 portions of the panels at 1190°C (2175°F) for four hours and 105 MPa (15 ksi). HIP consolidation with the loose powder Rene' 95 hub material was then accomplished at 1120°C (2050°F) at four hours and 105 MPa (15 ksi). Two heat treatment iterations were investigated for these panels, the first involving the 1175°C (2150°F) solution treatment used for the second cylindrical can shape processing iteration and the second a modification evaluated in order to increase the rupture ductility of the AF-115 rim material. For both heat treatment iterations the test panels were examined ultrasonically and by X-radiography subsequent to the solution treatments to insure that no quench cracks had developed during heat treatment. Mechanical property screening evaluations, including 480°C (900°F) tensile and 760°C (1400°F) stress rupture tests, were conducted to determine whether the properties compared favorably with the results obtained during the evaluation of the cylindrical can configuration and whether more extensive mechanical property evaluations should be conducted on the test panels.

4.1.3.3.1 First Heat Treatment Iteration

The first heat treatment iteration was a two hour solution at 1175°C (2150°F) followed by a salt quench to 540°C (1000°F) and a 16 hour age at 760°C (1400°F). The microstructures resulting from this heat treatment are shown in Figure 37 and include light photomicrographs of the joint area as well as higher magnification scanning electron photos of the Rene' 95 hub material and the AF-115 rim material.

The microstructure of the joint area indicated a high quality bond with little evidence of any continuous or otherwise deleterious phases at the joint line. The AF-115 rim alloy exhibited a grain size of ASTM 8, which was considerably smaller than the ASTM 3-5 grain size in the AF-115 portion of the cylindrical can processed with identical conditions. The smaller grain size of the flat panel material compared to the cylindrical can configuration was also observed in the L/C Astroloy-MERL 76 Combination B. The general microstructure of the AF-115 reflected the subsolvus temperature processing conditions. Many relatively large gamma-prime particles were observed, principally within the matrices of the fine grains. Fine gamma-prime particles were also observed throughout the matrix of the alloy, the result of cooling from the solution heat treatment temperature and the 760°C (1400°F) aging treatment. There was little evidence of extensive grain boundary precipitation in the AF-115 alloy. The Rene' 95 hub material exhibited an ASTM 4-8 grain size compared to an ASTM 6 grain size seen previously in the cylindrical can material. The microstructure reflected the suprasolvus processing temperature and displayed a gamma-prime morphology consisting of random, isolated, relatively fine particles. There was little evidence of precipitation along the Rene' 95 grain boundaries.

4.1.3.3.1.1 Mechanical Property Screening Results

The mechanical property screening tests included 480°C (900°F) tensile tests and 760°C (1400°F) stress rupture tests and the results are presented in Table 13.

4.1.3.3.1.1.1 Tensile Test Results

The tensile strength characterization of Combination C material in the cylindrical can configuration indicated that the strength of the Rene' 95 hub material was below the program goal. The best combination of properties indicated an average tensile strength of 1410 MPa (204 ksi). As shown in Table 13, however, the tensile strength results for material machined from the flat test panel indicated an improvement compared to the values exhibited by the cylindrical can material. Also similarly to the results obtained previously, joint quality was high, with failures occurring in the AF-115 material portions of the specimens away from the joint areas. For both the duplicate specimens, the properties (strength values as well as the ductility values) were all within 90% of the values exhibited by the Rene' 95 hub alloy material.

Metallographic examination of failed test bar specimens indicated that the failure mode was a function of the test material. In the Rene' 95 specimens, failure was predominantly transgranular. There was considerable evidence of slip throughout the microstructure and, as shown in the photomicrographs of the Rene' 95 specimen exhibiting the 1495 MPa (217 ksi) ultimate tensile strength in Figure 38, the slip lines were associated with crack initiation at the Rene' 95 surface. In the joint tensile test specimens, where failure occurred in the AF-115 material, fracture paths were primarily intergranular with little evidence of slip. An example of this is shown in the secondary cracking propagating from the main fracture surface in the photomicrographs in Figure 39, for the joint specimen exhibiting the 1440 MPa (209 ksi) ultimate tensile strength.

4.1.3.3.1.1.2 Stress Rupture Results

The AF-115 alloy of Combination C material tested in the cylindrical can configuration exhibited over 800 hours rupture life at 760°C (1400°F), well in excess of the rim alloy program requirement. In addition, while the joint stress rupture specimen exhibited only 124.1 hours rupture life, failure occurred away from the joint in adjacent material, indicating that the joint region was satisfactory in quality. As shown in Table 13, the AF-115 rim material exhibited 522 hours rupture life, while the joint specimen failed after 158.1 hours. Although the AF-115 rupture life was lower than previously, the life showed potential for application in the rim portion of a dual alloy disk. The joint specimen provided improved rupture life capability compared to the cylindrical can material. In this specimen, failure occurred in the Rene' 95 away from the joint area. Metallographic examination revealed that the fracture was entirely intergranular in these specimens. The Rene' 95 microstructure near the fracture surface of the joint specimen is shown in Figure 40. Extensive secondary cracking along grain boundaries can be seen in the Rene' 95 portion of this specimen.

4.1.3.3.1.1.3 Summary

The mechanical properties exhibited by specimens machined from the first heat treatment test panel all compared favorably with the properties obtained from the cylindrical shaped material. The ultimate tensile strength of the Rene' 95 test panel material was slightly improved, and although the stress rupture life of the AF-115 material was lower than obtained previously, the over 500 hour life promised considerable potential for this alloy as a rim material in a dual alloy disk. On the basis of these screening results, more extensive testing was conducted on the first iteration test panel.

4.1.3.3.1.2 Mechanical Property Test Results

The more extensive mechanical property tests results for the Combination C materials tested under the first heat treatment iteration are listed in Table 14 and include stress rupture tests on the Rene' 95 hub and AF-115 candidate materials as well as joint material, tensile tests on the AF-115 rim material, and low cycle fatigue tests on the Rene' 95 hub material.

The mechanical property testing on the AF-115 rim candidate material in this heat treatment condition included stress rupture tests at a number of conditions, was well as tensile tests at 760°C (1400°F). The stress rupture conditions were selected in order to characterize the rupture life response of the AF-115 material in comparison to data available in the literature for HIP and heat treated material (28), and the 760°C (1400°F) tensile tests were conducted in order to provide data which would be useful in designing the joint location for the dual alloy disk. The stress rupture properties at 540°C (1000°F) and 815°C (1500°F) were comparable to those reported in the literature by General Electric for HIP and heat treated AF-115. The life of 127 hours at 650°C (1200°F), however, was significantly lower than the 500 hour life anticipated for this stress rupture condition. Metallographic examination of the failed test bar showed that a large, non-metallic inclusion on the fracture surface contributed to the premature failure. The 760°C (1400°F) ultimate tensile and yield strengths of the AF-115 were in the same range as data available in the literature, while the ductility values were approximately 3-4% below the reported numbers. This low ductility was also characteristic for the stress rupture tests and indicated that heat treatment modifications should be directed at improving the ductility in the AF-115 material.

The Rene' 95 stress rupture life at 650°C (1200°F) was slightly superior to that anticipated for as-HIP and heat treated Rene' 95 from CF6 HPT Rear Shafts produced by General Electric during the NASA MATE program (22). The Rene' 95 material of the present program exhibited an average rupture life of 139.5 hours, compared to the anticipated 70 hours life for these stress rupture conditions. The ductilities in the present study were lower, with elongation, for example, ranging from 1.6-2.5% versus approximately 4% for the MATE material. The quality of the joint specimen was excellent, however, with a rupture life of 425.2 hours for the same test conditions. Failure in this particular specimen occurred in the Rene' 95 portion of the test bar, indicating that the Rene' 95 can offer appreciable rupture resistance in the joint regions.

The Rene' 95 stress rupture life at 650°C (1200°F) was slightly superior to that anticipated for as-HIP and heat treated Rene' 95 from CF6 HPT Rear Shafts produced by General Electric during the NASA MATE program (22). The Rene' 95 material of the present program exhibited an average rupture life of 139.5 hours, compared to the anticipated 70 hours life for these stress rupture conditions. The ductilities in the present study were lower, with elongation, for example, ranging from 1.6-2.5% versus approximately 4% for the MATE material. The quality of the joint specimen was excellent, however, with a rupture life of 425.2 hours for the same test conditions. Failure in this particular specimen occurred in the Rene' 95 portion of the test bar, indicating that the Rene' 95 can offer appreciable rupture resistance in the joint regions.

The Rene' 95 low cycle fatigue results indicated considerable scatter in the data, with failure lives ranging between 45,000-218,000 cycles. This type of scatter has been observed previously in HIP and heat treated Rene' 95 (30,31) and has been attributed to the location, size and nature of the failure origins (31). These can include nonmetallic inclusions, porosity and hollow particles (31). Again the fracture surfaces were obscured by a recast layer, but metallographic analysis indicated that secondary cracking followed transgranular paths, similar to those reported in the literature for HIP Rene' 95 (31).

4.1.3.3.2 Second Heat Treatment Iteration

Work conducted by General Electric on heat treatment variations of as-HIP AF-115 alloy suggested that a hot salt quench from solution to 650°C (1200°F), as opposed to the quench to 540°C (1000°F) used in the present study could result in improved tensile and stress rupture ductility. This alternative quench was applied to the second panel of this combination. Upon completion of the solution heat treatment step, however, it was learned that an error had occurred, and that the solution temperature had been 1205°C (2200°F) instead of 1175°C (2150°F).

The test panel was given the 760°C (1400°F) age and metallographic analysis of the structure indicated that the higher solution temperature did not significantly affect the grain size of the Rene' 95, but that the grain size for the AF-115 increased from ASTM 8 to ASTM 4-7, with only a small number of the ASTM 7 grains evident throughout the structure. The microstructures resulting from this heat treatment are shown in Figure 41 and include light photomicrographs of the joint area as well as higher magnification scanning electron photos of the Rene' 95 hub material and the AF-115 rim material. Comparison with Figure 37 which displays the microstructures of this material after the first heat treatment indicates little change in the joint region or the Rene' 95 material, but a significant change in the AF-115. As before, the joint between the Rene' 95 and AF-115 was of high quality with little indication of continuous types of precipitates and the Rene' 95 displayed a microstructure typical of material heat treated above the gamma-prime solvus. The AF-115 alloy in Figure 41, unlike that in Figure 37 had a gamma-prime morphology consisting of random, isolated, relatively fine particles characteristic of heat treatment above the gamma-prime solvus, as opposed to the numerous larger particles apparent in subsolvus heat treated material shown in Figure 37. Another, more subtle, change in the microstructure of the second iteration material was the presence of greater amounts of grain boundary precipitates in both the Rene' 95 and the AF-115 than seen in the first heat treatment iteration material.

4.1.3.3.2.1 Mechanical Property Screening Results

Mechanical property screening tests including 480°C (900°F) stress rupture tests were conducted on material of the second heat treatment iteration to determine if the higher solution heat treatment temperature would result in property degradation, particularly in the Rene' 95 hub portion of the test panel. The results of these second iteration screening tests are shown in Table 15.

4.1.3.3.2.1.1 Tensile Test Results

The tensile results indicated that the higher solution temperature in the second heat treatment iteration did not significantly affect the tensile properties. The ultimate and yield strength values for the Rene' 95 hub material specimens for both the first and second heat treatment iterations differed by less than 5% while the tensile ductilities were almost identical. The joint specimens for the second iteration exhibited high quality, with failures occurring in the AF-115 rim material well away from the joint location. The major difference between the two heat treatments for the AF-115 was a loss of approximately 7 percent of the ultimate tensile strength due to the higher solution heat treatment temperature. Metallographic analysis of the failed test specimens indicated little change in fracture mode for the Rene' 95 material between the two iteration materials. Transgranular fracture with considerable evidence of slip formation prevailed. The AF-115, on the other hand, exhibited a change in fracture mode, from an intergranular type shown in Figure 39 for first iteration heat treatment material, to the mixed mode type shown in Figure 42 showing the presence of considerable slip line formation.

4.1.3.3.2.1.2 Stress Rupture Results

The stress rupture results indicated that the AF-115 specimens and the joint specimens for the second heat treatment iteration were superior to those of the first iteration in rupture life. The duplicate specimens averaged 717 hours life compared to the 522 hour life of the first iteration material. It was significant to note that the rupture ductility remained unchanged as the result of the heat treatment. The joint stress rupture specimens averaged 255 hours life exceeding the 158 hour life of first iteration material. This 255 hour life was the highest average exhibited for a joint stress rupture specimen for this combination. In both instances failure was observed in the Rene' 95 portion of the specimen indicating that the higher solution heat treatment resulted in an improvement in the stress rupture capability of the Rene' 95 portion of the joint specimen. Metallographic analysis of the failed test bar specimens indicated an intergranular fracture mode in both the AF-115 and the Rene' 95 portion of the joint specimens, similar to the results for the first iteration heat treatment.

4.1.3.3.2.1.3 Summary

The mechanical properties exhibited by specimens machined from the second heat treatment test panel all compared favorably with those of the first test panel. There was less than a 10 percent difference between the strength values for the two heat treatment iterations and the ductility values were

identical. The stress rupture lives of second iteration material were clearly superior to those of the first iteration. On the basis of these screening results, more extensive testing was conducted on the second iteration material.

4.1.3.3.2.2 Mechanical Property Test Results

The more extensive mechanical property test results for the Rene' 95 AF-115 materials tested under the second heat treatment iteration are listed in Table 16 and included the same tensile, stress rupture and low cycle fatigue tests as those conducted on the first heat treatment iteration material. (Compare with Table 14).

The AF-115 stress rupture results indicated that the higher temperature solution heat treatment was beneficial to rupture life over the entire range of test temperatures. The most significant improvement, however, was observed at the 540°C (1000°F) and 650°C (1200°F) temperatures, in which nearly an order of magnitude increase in rupture life was observed. There was also a slight increase in rupture ductility for the second heat treatment material. The results of the 760°C (1400°F) tensile tests conducted on the AF-115 rim candidate material indicated that an improvement was obtained in all the tensile properties as a result of employing the second heat treatment. The ultimate tensile and yield strength values increased by approximately 3%, while more significant ductility improvements were obtained including a doubling of the elongation and a 20% increase in reduction of area. With the increase in ductility properties compared to first heat treatment iteration material, the tensile properties exhibited by the AF-115 with the higher solution temperature were comparable to those available in the literature for HIP and heat treated AF-115 (28).

While beneficial to the AF-115 alloy, the higher solution heat treatment temperature of the second heat treat iteration was not beneficial to the Rene' 95 hub candidate material. Tests conducted both on the Rene' 95 and the joint material at 650°C (1200°F) indicated a significant decrease in rupture life with the second heat treatment. Previously, Rene' 95 heat treated with the 1175°C (2150°F) solution heat treatment exhibited an average rupture life of 139.5 hours compared to an anticipated 70 hours life reported for HIP and heat treated material (22). With the 1205°C (2200°F) solution treatment, however, a maximum life of only 41.6 hours was obtained in one of two duplicate specimens, while the second exhibited a thread failure. The joint stress rupture specimen was also affected, with failure occurring in the Rene' 95 portion of the specimen at 22.9 hours of life.

The duplicate Rene' 95 480°C (900°F) low cycle fatigue tests conducted at 0.7% total strain range indicated the same degree of scatter as observed with the first iteration material. The failure lives for the second heat treatment iteration ranged from 38,000-112,000 cycles compared to the range of 45,000-218,000 cycles for first iteration material. Examination of the failed test bars indicated that the recast layer type of fracture surface was observed on the specimen which failed after approximately 112,000 cycles. A different type of fracture surface was observed, however, with the specimen exhibiting approximately 38,000 cycles failure life. As shown in Figure 43, this failure was prematurely initiated at the location of the thermocouple weld outside of the hot zone of the specimen.

4.2 Disk Shape Study

The Disk Shape Study was conducted on selected pairs of material combinations in order to evaluate the quality of the joint region and to identify potential problems associated with the more complicated disk configuration. A simulated version of the T-700 disk sonic shape was used as the disk shape demonstrator of the dual alloy process concept. Disks were fabricated from Combination A (sintered Rene' 95 rim/loose powder Rene' 95 hub), Combination B (loose powder L/C Astroloy rim/loose powder MERL 76 hub), and Combination C (HIP AF-115 rim/loose powder Rene' 95 hub) as representative of those combinations with the greatest potential for dual alloy processing. The disks were sectioned to reveal the circumference of the joint between the hub and rim materials.

The T-700 sonic shape HIP can used for the disk shape study was fabricated at the Sterling Forest Laboratory of the International Nickel Company. The can was fabricated from IN-744 (Fe-26Cr-6.5Ni-0.5Ti) sheet initially 1.6 mm (1/16 inch) in thickness. IN-744 is a two-phase (austenite/ferrite) alloy capable of being superplastically deformed once it has been worked and heat treated to a typically 0.5 micron fine grain size. The T-700 can was superplastically deformed by inflating argon gas between two welded circular sheets in a heated assembly, consisting of upper and lower mold halves. A complete T-700 HIP can and a can sectioned to show the HIP cavity are presented in Figure 44. For Combinations A and C, where pre-sintered or pre-HIP'ed rims were required for the dual alloy disk, the T-700 can was sectioned along its horizontal plane to allow positioning of the rim before the final HIP operation.

4.2.1 Combination A (Vacuum Sintered Rene' 95 Rim - Rene' 95 Hub)

4.2.1.1 Rim Pre-Sintering

Rim pre-sintering operations were directed towards the consolidation of the Rene' 95 powder into a ring shape without encountering tearing as a result of the shrinkage occurring during sintering. Ring molds were prepared from Thermo-Sil castable silica molding material. The initial vacuum pre-sinter operation was conducted at 1245°C (2275°F), instead of the 1265°C (2310°F) temperature used for the simple shape study to minimize the possibility of tearing in the consolidated product. A sintered ring is shown in Figure 45a. This ring exhibited an overall shrinkage of 15% in its dimensions as a result of the sintering operation. Examination of the ring indicated no tearing during the consolidation operation. As shown in the photomicrograph of Figure 45b the grain size of the sintered Rene' 95 was ASTM 4-5, which was finer than the desired ASTM 1-2 for rim material and resulted from the sintering temperature.

Subsequently a grain growth heat treatment was evaluated to achieve a larger grain size (ASTM 1-2) in the rim material, while minimizing the possibility of tearing in the compact during the sinter consolidation operation. The result of post-sintering the ring material in vacuum for six hours at 1265°C (2310°F) is shown in Figure 46; a satisfactory grain growth to ASTM 1-2 had been achieved. The areas of porosity evident throughout the microstructure suggested the presence of gases entrapped within the powder particles. As demonstrated in the Simple Shape Study, this porosity can be sealed during the subsequent HIP consolidation with the hub powder. After the second sinter operation the ring exhibited 6% shrinkage; the total shrinkage in its dimensions for both operations amounted to 21%.

4.2.1.2 HIP Consolidation

Subsequent to the grain growth heat treatment studies for the sintered Rene' 95, the ring component was prepared for HIP consolidation with the Rene' 95 hub powder in the T-700 can. The entire surface of the sintered and heat treated ring was first grit blasted to remove oxide scale formation, then its internal surface was ground to a 50 rms finish. The ring was next ultrasonically degreased with acetone, washed in methyl alcohol and distilled water. These procedures were similar to those used for the cylindrical components of the simple shape study. The ring was then positioned within the rim portion of the lower half of the T-700 can as shown in the photograph in Figure 47. The two halves of the can were then welded together and the entire assembly leak checked. The hub portion of the can was loaded by the procedure described previously for the preparation of the cylindrical HIP cans. The can was leak checked prior to shipment to Industrial Materials Technology for HIP consolidation. This consolidation operation used the following parameters: 4 hours/1165°C (2125°F)/105 MPa (15 ksi).

4.2.1.3 Evaluation

Upon completion of the HIP consolidation operation evaluations were conducted on the disk which included X-ray and zyglo penetrant inspections. The X-ray inspections failed to locate the presence of cracks or other defects at the joint between the sintered Rene' 95 rim material and the loose powder Rene' 95 hub material. No other defects were identified throughout the body of this disk. Upon completion of the X-ray inspection the disk was sectioned in half along its horizontal plane. Zyglo penetrant analysis of both sectioned halves indicated that the joint areas were free of defect indications as were the other regions within this component. Particular attention was paid in this analysis to the rim portion of the disk for indications which could be related to residual porosity from the sintering operation. No such indications were observed on either half.

Both portions of the sectioned disk were etched with Kalling's etch to highlight macrostructural features on the machined surfaces. A photograph of one of the sectioned components is shown in Figure 48. The joint between the sintered Rene' 95 rim region and the loose powder Rene' 95 hub region can easily be located in this photograph. The high quality of the joint in this region is reflected by the fact that consolidation of the rim and hub materials was accomplished without joint cracking during the HIP operation. A dimensional analysis of the sectioned surface indicated that the rim portion of the disk experienced no additional shrinkage during the HIP consolidation operation. Consolidation of the loose powder Rene' 95 hub, however, resulted in approximately 15% shrinkage of the thickness dimensions as a result of the HIP operation.

The activities directed towards the sintered Rene' 95 rim-loose powder Rene' 95 hub disk component successfully demonstrated the feasibility of this approach for the fabrication of a complex shape. Of particular importance here was the fact that HIP consolidation of a circular component comprising a single alloy, but processed in two different ways in two different regions, was accomplished without cracking along the joint between the two materials. It was appreciated, however, that the eventual applicability of this approach is dependent upon (1) maintaining high cleanliness on the surface of the pre-sintered portion of the disk which will be bonded to the loose powder and (2) a suppression of quench cracking such as experienced during the heat treatment of the simple cylindrical shapes of Rene' 95.

4.2.2 Combination B (Loose Powder L/C Astroloy Rim-Loose Powder MERL 76 Hub)

The Combination B study included an evaluation of the effects of powder mixing because of the possibility that a certain amount of mixing of hub and rim alloy powders could occur in certain areas of the dual alloy disk.

4.2.2.1 T-700 Disk Shape Study

4.2.2.1.1 HIP Consolidation

The study of the dynamics of centrifugal powder filling was performed using a clear block of lucite into which a T-700 configuration had been machined. This block is shown in Figure 49. The preliminary studies were directed towards determining the powder distribution (rim versus hub) as a function of rotational speed. Rotational speeds up to 2000 rpm created a powder distribution as shown schematically in Figure 50a for powder filling through the top of the block. The collection of powder thrown against the side of the bottom portion of the T-700 hub configuration was not significantly reduced by the application of higher rotational speeds. Studies were then directed towards the use of a flared isertion rod, the use of which is shown schematically in Figure 50b, which would direct powder away from the hub depression during can filling operations. This method was not completely successful in eliminating the collection of a certain amount of rim alloy powders in the hub depression. It was recognized that potential mixing of rim and hub alloy powders in areas such as these in the dual alloy disk represented possible processing defects which could significantly alter the mechanical property response of the material. Because of the possibility of this intermixing, part of the effort for Combination B included a characterization of the mechanical property response of the mixed powders. The results of this study are discussed in Section 4.2.2.2 - Defect Characterization.

The T-700 disk shape was filled centrifugally using the flared insertion rod shown in Figure 50b to minimize the accumulation of rim alloy powder in the hub depression area of the disk shape. For the rim portion of the disk, 2 Kg (4 lbs.) of -60 mesh L/C Astroloy powder was poured down the fill tube while the disk was rotating at 5000 rpm. This amount of powder had been observed to accomplish complete filling of the rim portion of the machined lucite block. The hub portion of the disk was then loaded with 2 Kg (4 lbs) of -60 mesh MERL 76 powder through the fill tube while the disk was rotating at 5000 rpm. The flared insertion rod was not used for the hub powder filling operation. Outgassing and can sealing were accomplished using the same procedures as described previously for the preparation of the cylindrical HIP cans. The disk was leak checked prior to shipment to Industrial Materials Technology where HIP consolidation was accomplished using the following parameters: 4 hours/1120^{o}C (2050^{o}F)/105 MPa (15 ksi).

4.2.2.1.2 Evaluation

X-ray and zyglo penetrant inspections were conducted on the HIP'ed disk after completion of the consolidation operation. The X-ray examination did not indicate the presence of obvious defects throughout the structure of this component. During this evaluation, however, it was observed that there was no definitive boundary between the L/C Astroloy rim portion of this disk and the MERL 76

hub portion. This suggested that significant mixing of the two powders had probably occurred during the fabrication operation. Upon completion of the X-ray inspection the disk was sectioned in half along its horizontal plane. The two halves were then sectioned in half again along their vertical planes. Zyglo penetrant analyses of these sections indicated that they were free of defect indications along all of the machined surfaces.

The machined surfaces of sections were etched with Kalling's etch to highlight the macrostructural features on these surfaces. Photographs showing the typical macrostructures on both the horizontal and vertical planes are shown in Figure 51. The absence of a precise, circular line of definition between the rim and hub areas, as well as the considerable amounts of intermixing between the powders implied appreciable turbulence during the can filling operation. It also seems likely that some intermixing occurred during handling and transportation of the sealed can prior to HIP consolidation. There was considerable shape distortion accompanying the HIP operation which rendered meaningful dimensional analysis and shrinkage evaluations for this fabrication process impossible.

In summary, the effort directed towards the fabrication of a complex disk shape component from two different loose powders in a single HIP consolidation operation was not successful. The primary problem was the inability to control the boundary location between the two powders which resulted in intermixing. While it is appreciated that this single step manufacturing process offers the greatest payoff in terms of fabrication economics, attention must be focused on the proper location of the boundary between the two different powders.

4.2.2.2 Defect Characterization

4.2.2.2.1 Specimen Preparation

Specimen preparation efforts for the defect characterization study included the manufacture of two cylindrical HIP cans identical in configuration to those used previously in the Simple Shape Study of the Task I - Process Evaluation. Powder for this portion of the program was provided by NASA and consisted of -100 mesh argon atomized MERL 76 and L/C Astroloy powders produced by Universal Cyclops. The chemical compositions of these powders are listed in Table 17. For comparison purposes, one can was prepared according to the normal Combination B processing sequence in which one half the can was first filled with one of the alloys, and the remainder with the other alloy. The second can contained the "defect" powders, that is powders blended to the maximum HIP can preparation and consolidation were conducted at Industrial Materials Technology according to HIP processing and heat treatment procedures used for the Combination B flat panel test material:

HIP Consolidation: 4 Hours/1120°C (2050°F)/105 MPa (15 ksi)

Heat Treatment: 1165°C (2130°F)/1 Hours Direct Oil Quench
+ 870°C (1600°F)/40 minutes Air Cool
+ 980°C (1800°F)/45 minutes Air Cool
+ 650°C (1200°F)/24 Hours Air Cool
+ 760°C (1400°F)/8 Hours Air Cool

4.2.2.2.2 Mechanical Property Evaluations

Results of mechanical property evaluations, including 480°C (900°F) tensile and 760°C (1400°F) stress rupture tests, on these materials are listed in Table 18. The tensile results indicated that the MERL 76-L/C Astroloy powder blend was superior to either of the two alloys themselves. The powder blend exhibited an average ultimate strength of approximately 1440 MPa (209 ksi). By comparison, the MERL 76 and the L/C Astroloy (failure in the joint area specimens occurred in the L/C Astroloy portion of the specimens) both exhibited an average ultimate strength of approximately 1275 MPa (185 ksi). The powder blend exhibited a similar degree of superiority in yield strength as well as ductility properties. Metallographic analysis of the failed tensile bars indicated that the fracture paths in the powder blend were primarily transgranular but also included portions of prior particle boundaries. An example of a typical fracture surface is shown in the photomicrographs of Figure 52. The MERL 76 portion of the structure is characterized by fine grain size and the presence of large gamma-prime particles in the high magnification photomicrograph of Figure 52b. Considerable evidence of slip formation was also observed in the L/C Astroloy material. It was also noted that the powder blend was not completely homogeneous, but was characterized by large segregated areas of predominately single alloy composition. Typical fracture surfaces of the MERL 76 and L/C Astroloy (from the joint specimen) are shown in Figure 53. Extensive void formation is evident in the MERL 76 microstructure shown in Figure 53a, while extensive prior particle boundary formation is evident in the L/C Astroloy microstructure shown in Figure 53b. These defects were not present to the same degree in the microstructure of the powder blend, Figure 52.

The stress rupture results also indicated that the powder blend was superior to either the L/C Astroloy or the MERL 76 (failure of the joint specimen occurred in the MERL 76 portion of the specimen). The rupture life of the powder blend was double that of the L/C Astroloy and approximately five times that of the MERL 76. The rupture ductilities were also clearly superior. Metallographic analysis indicated that the fracture paths in the powder blend specimens were primarily intergranular and followed grain boundaries both in the L/C Astroloy portions and the MERL 76 portions of the specimens. Examples of this intergranular cracking are shown in Figure 54. Intergranular cracking provided a common fracture path in the MERL 76 alloy (from the joint specimen), Figure 55a, and prior particle boundaries were the common fracture paths in the L/C Astroloy, Figure 55b. The particular area shown in Figure 55b was taken from the L/C Astroloy specimen exhibiting thread failure and indicates that a prior particle boundary was intimately associated with the fracture surface.

In summary, the mixing of the MERL 76 and L/C Astroloy powders did not result in degradation of the tensile and stress rupture properties. To the contrary, the powder blend resulted in improvements in both strength, rupture life and ductility compared to the individual alloy powders. This suggested that any powder mixing resulting from the HIP can loading of a dual alloy disk may not necessarily represent a major defect in terms of mechanical property response. This should be qualified, because with powders of other compositions, the contrary may be the case.

4.2.3 Combination C (HIP AF-115 Rim-Rene' 95 Hub)

The Combination C assembly was performed at the Udimet Powder Division, Special Metals Corporation, of Ann Arbor, Michigan. Fabrication of the T-700 shape involved a two step operation, including HIP consolidation of the AF-115 rim, followed by the consolidation of this rim with the Rene' 95 hub powder.

4.2.3.1 Rim Pre-Consolidation

The rim pre-consolidation effort was directed towards the fabrication of an AF-115 ring shape for the simulated T-700 disk configuration. This ring shape was made from a T-700 container from which a 100 mm (4 inch) diameter hole was cut in the center portion. A 100 mm (4 inch) diameter, 6 mm (0.250 inch) thick wall steel pipe was used for the center sleeve in order to restrict shrinkage of the inner dimension of the ring during the HIP consolidation operation. The ring container was filled in air with AF-115 alloy powder using a top fill tube and cold vacuum outgassed. The pressure level on this container was less than 8.0×10^{-5} torr before the final sealing operation. HIP consolidation was conducted at Cameron Metal Powder Systems, Brighton, Michigan, using the following parameters: 4 hours/1190°C (2175°F)/105 MPa (15 ksi). Upon completion of the HIP operation the container was stripped from the consolidated powder by chemical etching. A dimensional analysis of this ring indicated an overall shrinkage of approximately 14% in its dimensions as a result of this HIP consolidation operation. A photograph of this AF-115 ring shape chemically stripped of its container is shown in Figure 56. The circular attachment on the upper portion of the ring is a the remnant of removed the fill tube.

4.2.3.2 HIP Consolidation

Subsequent to the consolidation of the AF-115 ring, the inner diameter of the AF-115 rim was ground and polished to a 50 rms finish to remove the layer of reaction products developed during the container etching process and to promote better bonding during HIP'ing with the Rene' 95 hub alloy powder. The ring was then positioned within the rim portion of the lower half of the T-700 disk as shown in the photograph in Figure 57. The two halves of the disk were then welded together for final filling of the hub alloy powder. The hub portion of the disk was filled with Rene' 95 powder and cold vacuum outgassed to a pressure level of less than 1×10^{-5} torr before the final sealing operation. HIP consolidation was performed by Fiber Materials, Inc. of Hazelton, Pennsylvania, using the parameters of 4 hours/1120°C (2050°F)/105 MPa (15 ksi). A photograph of the dual alloy T-700 disk in the as-HIP'ed condition is shown in Figure 58. The remnant of the fill tube for the AF-115 rim portion of the disk can be seen in the upper left portion of the T-700 disk.

4.2.3.3 Evaluation

The evaluation of the T-700 disk included X-ray and zyglo penetrant inspections. The X-ray inspections revealed no crack like or other defect indications along the joint between the HIP'ed AF-115 rim material and the loose powder Rene' 95 hub materials nor any defects throughout the body of the disk. Subsequent to the X-ray inspection the disk was sectioned in half along its horizontal plane. Zyglo penetrant analysis of both sectioned halves showed no defect indications.

Both portions of the sectioned disk were etched with Kalling's etch to highlight macrostructural features on the machined surfaces. A photograph of one of these sections is shown in Figure 59. The joint between the HIP'ed AF-115 rim region and the loose powder Rene' 95 hub region can easily be located in this photograph. The absence of cracking in this joint region reflected the high quality achieved during the HIP consolidation operation. A dimensional analysis of the sectioned surface indicated that the AF-115 portion of the disk experienced no additional shrinkage during the second HIP consolidation operation. Consolidation of the loose powder Rene' 95 hub, however, resulted in approximately a 15% shrinkage of the thickness dimensions as a result of this second HIP operation.

In summary, the effort directed towards the pre-HIP'ed AF-115 rim-loose Rene' 95 powder hub disk component successfully demonstrated feasibility of this approach for the manufacture of a complex shape. Of significance here was the fact that HIP consolidation of a circular component comprising two different alloys was accomplished without cracking along the joint between the two alloys. It was realized, however, that the eventual applicability of this process is dependent upon maintaining high cleanliness on the surface of the pre-HIP'ed AF-115 to be bonded to the loose Rene' 95 powder.

4.3 Materials Selection for Task II

The materials selection for the Task II disk evaluation involved an analysis of all of the data developed during the testing of the Combinations B and C rectangular panel shapes. Particular attention was paid to the 480°C (900°F) tensile data for hub candidate materials and the stress rupture data over the range from 540-815°C (1000-1500°F) for rim candidate materials. These analyses are presented in Figures 60 and 61.

The 480°C (900°F) tensile properties shown in Figure 60 indicate that the MERL 76 rim material of Combination B exhibited the highest average ultimate tensile strength at 1540 MPa (223 ksi) and also met the program goal of 1520 MPa (220 ksi). This material also exhibited the highest ductility values. High joint quality was reflected in this material by the fact that the average ultimate tensile strength for joint specimens was 1430 MPa (207 ksi), which was within 90% of the value for the MERL 76. By comparison, the ultimate tensile strengths of the Rene' 95 specimens from the two Combination C panels were both inferior to the MERL 76 specimens, yet within 95% of the program goal. The effect of solution treatment temperature was evident in this Rene' 95 material, with the material treated at 1175°C (2150°F) exhibiting superior average ultimate tensile strength compared to material treated at 1205°C (2200°F). The joint quality was also high in the Combination C material, with joint specimen ultimate tensile strength values for both solution heat treatments well in excess of 90% of the Rene' 95 material. The ductility values for the Rene' 95 specimens were comparable but were inferior to the MERL 76, with elongation, for example, at approximately one half that exhibited by the MERL 76. In summary, the tensile results indicated that the MERL 76 hub candidate alloy exhibited ultimate tensile strength capability exceeding the program goal as well as the highest ductility values of the hub candidate materials. Although the Rene' 95 specimens exhibited inferior tensile strength and ductility values compared to the MERL 76, it was observed that their strength was within 95% of the program goal.

The stress rupture properties shown in Figure 61 indicate that the AF-115 rim alloy of Combination C exceeded the program goal in both of the solution heat treatment conditions. Superior rupture life capability was exhibited by material which had been solution treated at 1205°C (2200°F). By comparison, rupture lives of the L/C Astroloy rim material and MERL 76 hub material of Combination B both indicated little potential to meet the program goals. The L/C Astroloy or MERL 76 rupture capability was significantly inferior to that of the AF-115 as illustrated by the 760°C (1400°F) test results in which the rupture lives for the Combiantion B materials did not exceed 45 hours, while the values of the AF-115 were all above 500 hours.

On the basis of these comparisons between the tensile and stress rupture properties of the plate material it was concluded that the AF-115 rim-Rene' 95 hub material combination exhibited the best overall balance of properties for the Task II disk evaluation. The tensile properties were quite close to the program goal, while the rupture properties exceeded the program requirement. While the L/C Astroloy rim-MERL 76 hub alloy combination exhibited tensile strength capability which exceeded the program goal, the rupture properties indicated little potential to meet the program requirements.

5.0 TASK II - SUB-SCALE DISK EVALUATION

This task accomplished the scale-up of the AF-115 rim-Rene' 95 hub material combination to a larger disk configuration for more complete evaluations. The work included the fabrication of a CFM-56 prototype disk and mechanical property and microstructural analyses.

5.1 Disk Fabrication

Fabrication of the CFM-56 disk took place at the Udimet Powder Division, Special Metals Corporation, of Ann Arbor, Michigan. A schematic diagram of this disk configuration is shown in Figure 62. In conformance with the Task I Process Evaluation study the fabrication of this component involved a two step operation, HIP consolidation of the AF-115 rim, followed by the HIP joining of this rim with the Rene' 95 hub powder. Argon atomized powders of -140 mesh size fraction were used for this disk and their compositions are listed in Table 19. The argon atomization process was selected for Task II instead of the hydrogen process used in Task I because of the availability of sufficient quantities of the AF-115 and Rene' 95 powders. The specified maximum size fraction was reduced from the -60 mesh used in Task I to -140 mesh in order to minimize thermally induced porosity in the consolidated product.

5.1.1 Rim Pre-Consolidation

The AF-115 ring shape was made from a CFM-56 container from which a 250 mm (10 inch) diameter hole was cut in the center portion. A 250 mm (10 inch) diameter, 6 mm (0.250 inch) thick sheet of stainless steel was formed into a ring and welded as the center sleeve of the CFM-56 container. The ring container was filled in air with AF-115 alloy powder using a side fill tube and cold vacuum outgassed. The pressure level on this container was less than 8.0×10^{-5} torr before the final sealing operation. HIP consolidation at Cameron Metal Powder Systems, Brighton, Michigan, used parameters of 4 hours/1190°C (2175°F)/105 MPa (15 ksi). A photograph of this AF-115 ring shape chemically stripped of its container is shown in Figure 63. The circular appearing attachment on the portion of the ring nearest the scale is a remnant of the fill tube sectioned from the ring.

5.1.2 HIP Consolidation

Upon completion of the consolidation of the AF-115 ring, preparation was made for the HIP consolidation of this shape with the Rene' 95 hub powder in the CFM-56 can. The inner diameter of the AF-115 ring was ground and polished to a 50 rms finish to insure removal of the layer of reaction products developed during the chemical etching process and to improve the bond quality during HIP'ing with the Rene' 95 hub alloy powder. Final containerization was made difficult because of the fact that the stainless steel sleeve had not restricted the shrinkage of the diameter of the AF-115 ring. The outer diameter of the ring was much smaller than the final container can, and the ridges of the rim did not fit into the ridges of the final container. To accomodate the smaller rim into this container, 3 mm (0.125 inch) diameter stainless steel tubes were used to position the outer diameter of the AF-115 rim to avoid shifting after final can sealing. A photograph

of this ring "spoked" into position for final HIP consolidation is shown in Figure 64a. Because the part sat too high in the final container because of its poor fit in the ridges, a band of stainless steel sheet was fabricated for the outer can diameter. Top and bottom portions of the CFM-56 can were then welded to this band to complete the can fabrication. The final configuration is shown in Figure 64b.

The hub portion of the disk was side filled with Rene' 95 powder and cold vacuum outgassed to a pressure level of less than 1 x 10^{-5} torr before the final sealing operation. HIP consolidation was conducted at Fiber Materials Inc. of Hazelton, Pennsylvania, using the parameters of 5 hours/1120°C (2050°F)/105 MPa (15 ksi). The longer HIP cycle (5 versus 4 hours) was required to allow for the lower thermal conductivity of the alumina bubbles used to fixture this part in the autoclave. A photograph of this dual alloy CFM-56 disk in the as-HIP'ed condition is shown in Figure 65.

5.1.3 Quality Evaluation

Evaluations conducted on the CFM-56 disk included zyglo penetrant inspection and metallographic examination. The disk was sectioned in half and then one of the half sections was quartered. Zyglo penetrant analysis of the sectioned pieces indicated that the prepared joint areas were free of defect indications. The zyglo analysis did, however, reveal the presence of a crack between the middle of the outer edge of the AF-115 rim and the inner portion of the HIP can. An example of this crack is shown in Figure 66 (arrow) for one of the quarter sections etched with Kalling's etch to highlight the macrostructural features on the machined surfaces. The crack was associated with a sharp ridge on the outside surface of the AF-115 rim, indicating that such discontinuities must be avoided to insure crack-free HIP consolidation. Note also in this figure that the Rene' 95 powder completely surrounds the AF-115 pre-HIP'ed rim, almost as if the AF-115 were inserted in the Rene' 95. This resulted from the need to modify the CFM-56 can configuration to accomodate the AF-115 rim shape and Rene' 95 powder was needed to fill all the space in the container.

Metallographic analysis indicated a significant difference in the as-HIP'ed grain sizes of the AF-115 and Rene' 95 alloys. A light photomicrograph showing the typical joint structure is shown in Figure 67. The grain size for the AF-115 alloy ranged from ASTM 6-8 while that for the Rene' 95 ranged from ASTM 8-10. It was also observed that the grains in the AF-115 adjacent to the Rene' 95 were somewhat larger in size than those farther away from the joint. The AF-115 grains in the joint region were generally ASTM 6 in size while those away from the joint ranged from ASTM 6-8. This suggested that some deformation may have occurred in this region during the Rene' 95 consolidation operation. Examination of the joint area did not indicate the presence of potentially harmful phases. A TIP test during which material sectioned from the disk was exposed at 1205°C (2200°F) for 2 hours produced little evidence of porosity in the microstructure.

5.2 Disk Evaluation

5.2.1 Heat Treatment Verification

The heat treatment verification was conducted to determine whether the heat treatment developed in Task I for the flat panel shapes was appropriate for the CFM-56 disk or whether adjustments would be required (for section size change effects, for

example). One quarter section was shipped to General Metal Heat Treating of Cleveland, Ohio, and given the following heat treatment: 1205°C (2200°F)/2 hours salt quench to 650°C (1200°F) + 760°C (1400°F)/16 hours air cool. Solutioning at 1205°C (2200°F) provided superior rupture life and ductility compared to solutioning at 1175°C (2150°F), Figure 61.

5.2.1.1 Microstructural Evaluation

The typical heat treated microstructure of this quarter section in the center of the AF-115-Rene' 95 joint in the hub area is shown in Figure 68. Comparison with the as-HIP'ed microstructure, Figure 67, indicated that grain growth occurred in both alloys as a result of this heat treatment. The AF-115 grain size increased from ASTM 6-8 to ASTM 4-6. The Rene' 95 grain size increased from ASTM 8-9 to ASTM 6-7. The microstructure of both alloys reflected the suprasolvus solution heat treatment temperature, and displayed a gamma-prime morphology consisting of random, isolated, relatively fine particles. There were considerably more of these particles in the Rene' 95 than the AF-115. The AF-115 alloy also displayed considerable evidence of triple point incipient melting in the form of as-cast type eutectic at the grain boundary triple points. There was some concern over the effects of this triple point melting on the mechanical property performance of this alloy. It was also observed that there no longer were grain size differences between the areas adjacent to the joint and those areas farther away from the joint. In the 100X magnification photomicrograph in Figure 68 the interface between the AF-115 and Rene' 95 alloys was delineated by some type of phase or precipitate. In the 500X photomicrograph these areas were revealed as isolated locations of triple point incipient melting in the AF-115 alloy.

Comparison of the microstructure in Figure 68 with that in Figure 41 for the flat plate test panel given the identical heat treatment indicated that, with the exception of the incipient melting in the AF-115, there was considerable similarity in the structure. The grain sizes were relatively similar as were the gamma-prime morphologies for both alloys. This different response to incipient melting in the AF-115 could be accounted for by subtle differences in chemistry between the heats of powder used for the two components.

Of greater concern than the incipient melting in the AF-115 was a quench crack condition which was observed upon zyglo examination of the heat treated disk quarter section. A schematic diagram showing the extent of this cracking is shown in Figure 69. The dotted line in the diagram outlines the AF-115 portion of the dual alloy disl. The cracking was associated primarily with the AF-115-Rene' 95 interface as well as with sharp corners in the AF-115 shape geometry. It was observed that the joint cracking was limited to that portion of the AF-115 surface which had not been specially prepared for the HIP consolidation with the Rene' 95 hub powder. This cracking emphasizes the need for maximum cleanliness in the mating surfaces to insure a high quality bond. In addition to the interface cracking, cracking was also observed in the AF-115 portion of the quarter section. Part of this cracking was observed to extend from the interface between the two alloys, but cracking was also located within the AF-115. These cracks followed intergranular paths. It is suspected that quenching stresses associated with the large mass of the CFM-56 rim portion of the disk may have been partially responsible for the cracking within the AF-115.

5.2.1.2 Mechanical Property Evaluation

Mechanical property evaluations were conducted on specimens machined from the AF-115 and Rene' 95 regions of the disk section closest to the AF-115 prepared surface. These tests included 480°C (900°F) tensile tests for the Rene' 95 alloy and 760°C (1400°F) stress rupture tests for the AF-115 alloy. The stress rupture tests employed a stress level of 620 MPa (90 ksi) instead of the 550 MPa (80 ksi) level used previously in order to shorten test time from the over 500 hour lives experienced at the lower stress level. The results of these tests are listed in Table 20.

Comparison of these results with those presented previously in Table 15 for flat plate specimens with the identical heat treatment indicated that the tensile results for the CFM-56 specimens compared favorably with those from the flat plate test panel. On the average, the CFM-56 specimens exhibited an 8% improvement in ultimate tensile strength (coming within 99% of the program goal), a three fold improvement in tensile elongation, a 27% improvement in tensile reduction of area, but a 7% reduction in yield strength compared to the flat panel test specimens. In terms of the stress rupture results, comparison with the flat panel properties of Table 15 also indicate that the CFM-56 specimens compared favorably with those from the flat panel. On a Larson-Miller plot the rupture lives at the two different stress levels would indicate comparable life capability while the CFM-56 specimens exhibited more than double the rupture ductility of the flat panel specimens. Metallographic evaluation of the failed Rene' 95 showed predominantly transgranular fractures while the AF-115 stress rupture specimen exhibited an intergranular type fracture mode. These results were similar to those observed for the failed flat panel test specimens.

5.2.1.3 Summary

Heat treatment verification studies were conducted on a quarter section of the CFM-56 disk using the optimum heat treatment resulting from the Task I effort with the flat plate test panels. The results indicated that the Rene' 95 tensile and AF-115 stress rupture properties were in general superior to those of the flat plate test panel. In spite of this, however, several observations made during these evaluations suggested that this heat treatment be modified in a second iteration. First, the AF-115 portion of the quarter section exhibited grain boundary triple point melting. While apparently of little consequence to the stress rupture performance of the alloy, there was concern that this type of structure might have a degrading effect upon the low cycle fatigue evaluations planned for the more extensive testing of the remainder of the disk. The second factor concerned the extensive quench cracking observed in the quarter section after heat treatment. Both of these observations suggested that a reduction in the solution heat treatment temperature might be beneficial to the quality of the CFM-56 disk. It was anticipated that reducing the solution temperature would (1) eliminate the occurrence of incipient melting in the AF-115 and (2) reduce the quenching stresses by reducing the thermal gradient in the heat treated disk. Accordingly, the second iteration solution heat treatment temperature for the subsequent testing was reduced from 1205°C (2200°F) to 1190°C (2175°F).

5.2.2 Mechanical Property Testing

Extensive mechanical property tests were conducted on a half section of the CFM-56 disk material heat treated according to the second iteration heat treatment. These evaluations included tensile, stress/creep rupture and low cycle fatigue tests and were conducted under conditions typically used to characterize disk materials.

5.2.2.1 Disk Heat Treatment

The heat treatment, performed by General Metal Heat Treating of Cleveland, Ohio, consisted of 1190°C (2175°F)/2 hours salt quench to 650°C (1200°F) + 760°C (1400°F)/16 hours air cool. The typical heat treated microstructure of this half section in the center of the AF-115-Rene' 95 joint in the hub area is shown in Figure 70. Lowering the solution heat treatment temperature from 1205°C (2200°F) to 1190°C (2175°F) resulted in changes in the microstructure of the half section compared to that of the quarter section given the first iteration heat treatment, Figure 68. The Rene' 95 alloy exhibited an ASTM 6-8 grain size compared to an ASTM 6-7 grain size. The microstructure was still characteristic of a suprasolvus heat treatment; the gamma-prime morphology consisted of random, isolated, relatively fine particles, and was relatively unchanged from the structure appearing in the first iteration material in Figure 68.

The microstructure of the AF-115 alloy, however, was significantly different. Not only was the triple point melting completely eliminated, but the structure was indicative of a sub-solvus heat treatment. Only partial solutioning of the gamma-prime occurred as a result of this treatment and numerous large primary gamma-prime particles were present throughout the matrix of the AF-115 shown in Figure 70. The grain size of this material was generally similar to that displayed by the as-HIP'ed structure.

The joint interface was characterized by an almost linear array of fine particles which appeared to be partially recessed into the Rene' 95 alloy. Electron microprobe analysis identified these particles as aluminum/titanium rich oxides. It was significant to note that these particles were not observed in the joint area of the quarter section described previously in Figure 67 for the as-HIP'ed microstructure or in Figure 68 for the first heat treatment iteration. This suggested a possible variability in the quality of the surface preparation of the AF-115 prior to HIP with the Rene' 95.

While the lower solution temperature of the second heat treatment iteration suppressed the triple point melting in the AF-115, it was not successful in eliminating the quench cracking. The quench cracks were observed during zyglo examination of the heat treated section and a schematic diagram showing the extent of this cracking is shown in Figure 71. Again, the dotted line in the diagram outlines the AF-115 portion of the dual alloy disk. In general, the cracking was as extensive as had been observed previously with the first heat treatment iteration, Figure 69. These cracks were associated either with the AF-115-Rene' 95 interface or with sharp corners in the AF-115 geometry. Cracks were also seen within the Rene' 95 and AF-115 portions of the disk but these always appeared to result from propagation from the interfaces between the two alloys.

5.2.2.2 Tensile Test Results

The results of tensile tests, conducted upon AF-115, Rene' 95 and joint material specimens over a wide temperature range, are listed in Table 21. Plots of the average tensile strength as well as average tensile ductility data are shown in Figures 72 and 73, respectively. Included in this plot for comparison purposes are data available in the literature for HIP and heat treated Rene' 95 (22) and AF-115 (28). The Rene' 95 data was generated by General Electric under the NASA MATE program on specimens machined from the CF6-50 HPT Rear Shaft HIP'ed at 1120°C (2050°F) and solution treated at the same temperature. The CF6-50 ASTM 8 grain size was thus finer and the gamma-prime morphology more characteristic of a partially solutioned structure than that of the Rene' 95 shown in Figure 70. The AF-115 data was generated by General Electric under an Air Force sponsored program on specimens HIP'ed at 1190°C (2175°F) and solution treated at the same temperature (28). The resulting microstructures were thus generally equivalent to those for the AF-115 portion of the CFM-56 disk shown in Figure 70.

Rene' 95 tensile tests were conducted over the temperature range from room temperature to 675°C (1250°F). Compared to the first iteration heat treatment, lowering the solution heat treatment temperature resulted in a loss of approximately 6% in the ultimate tensile strength and about one half the elongation. The yield strength and reduction of area were unaffected by the change. At this particular ultimate strength level the Rene' 95 hub material was within 92% of the program goal of 1520 MPa (220 ksi). Compared to material tested from the CF6-50 shaft over this temperature range, the CFM-56 material exhibited approximately 5-10% less ultimate tensile strength and 5% less yield strength. The CFM-56 ductility was below that of the CF6-50 material from room temperature to 480°C (900°F) but was superior at higher temperatures.

AF-115 tensile tests were conducted over the temperature range from 480°C (900°F) to 760°C (1400°F). Comparison of the data with that available for AF-115 in the literature indicated that the CFM-56 exhibited superior ultimate tensile strength at 480°C (900°F) but inferior ultimate strength at higher temperatures and approximately 5-10% less yield strength over the range of temperatures tested. In terms of ductility, the CFM-56 material was superior at temperatures of 480-650°C (900-1200°F) and comparable at 760°C (1400°F).

A comparison of the CFM-56 Rene' 95 and AF-115 data for comparable test temperatures indicated that the AF-115 ultimate strength was superior at 480°C (900°F) (to the point of being within 98% of the program goal) and comparable at 650°C (1200°F). The yield strengths were comparable and the ductility values indicated AF-115 was superior over the test temperature range. The failures were predominantly transgranular for both alloys as shown in Figure 74 for materials tested at 650°C (1200°F).

Duplicate joint tensile tests were conducted at 650°C (1200°F). Failure occurred in the Rene' 95 portion of the specimen. The ultimate strength was within 85% of the Rene' 95 when tested separately and the ductilities were particularly poor, with average elongation being 2.4% compared to the 8.9%. An example of the type of failure is shown in Figure 75. While evidence of transgranular secondary cracking can

be seen on this fracture surface, the primary fracture path appears almost linear and is recessed into the Rene' 95 away from the AF-115 interface. This suggested that the fracture in these specimens was associated with a linear array of oxide particles observed previously in the Rene' 95 near the joint area of the heat treated microstructure shown in Figure 70.

5.2.2.3 Stress/Creep Rupture Results

Stress/creep rupture tests of Rene' 95, AF-115 and joint material specimens were conducted over a wide variety of conditions and the results of these tests are listed in Table 22. A Larson-Miller plot of the average stress rupture life results for the Rene' 95, AF-115 and joint material specimens is shown in Figure 76. Also included in this plot for comparison purposes are the data available for HIP and heat treated Rene' 95 (22) and AF-115 (28). The processing history of these materials was described previously in Section 5.2.2.2 for the tensile test results. A Larson-Miller plot of the average time to 0.2% creep results for the AF-115 specimens is shown in Figure 77 along with data available in the literature for HIP and heat treated AF-115.

The Rene' 95 stress rupture tests were conducted over the temperature range from 595°C (1100°F) to 705°C (1300°F) and included combination notch-smooth type tests as well as the regular smooth stress rupture tests. The combination notch-smooth stress rupture tests were conducted at 595°C (1100°F) and 650°C (1200°F). The fact that all failures were observed in the smooth portions of the specimens indicated the absence of notch-brittleness at these test conditions. The Larson-Miller plot of the average Rene' 95 life values shown in Figure 76 indicate that this alloy would exhibit an approximate rupture life of 150 hours at 675°C (1250°F) and 925 MPa (134 ksi) and could not meet a rim material rupture life goal of 300 hours. Comparison of the data for the fine grain CF6-50 shaft specimens (22) indicates that the larger grained CFM-56 material exhibited superior rupture life capability by approximately 10 times at the lower temperatures but only comparable capability at the 705°C (1300°F) test temperature. Examination of the failed stress rupture bars indicated a predominantly transgranular fracture mode over the entire range of test temperatures. A typical example of this type of cracking is shown in Figure 78a for a Rene' 95 specimen tested at 650°C (1200°F). A secondary crack is shown in these photomicrographs propagating from the primary fracture surface. This type of fracture mode was different from that exhibited by the Rene' 95 area of joint stress rupture specimens tested at 760°C (1400°F) during the Task I evaluation. As shown in Figure 40, the Rene' 95 exhibited an intergranular type fracture mode at the higher temperature.

The AF-115 rupture tests were conducted over the temperature range from 650°C (1200°F) to 815°C (1500°F) and included combination notch-smooth stress rupture tests, regular smooth stress rupture tests as well as creep rupture tests. Like the Rene' 95, the AF-115 exhibited an absence of notch brittleness. The notch-smooth specimens, tested at 650°C (1200°F) and 760°C (1400°F), all failed in the smooth section of the test specimen. These results indicate that the program goal involving the absence of a notch brittle condition in the rim material was met. The lower solution heat treatment temperature in the second iteration resulted in a slight loss in rupture life capability with little significant effect on the rupture ductility. On the basis of the 760°C

(1400°F)/690 MPa (100 ksi) tests conducted on the second iteration material, an anticipated life of 100 hours could be expected at the 620 MPa (90 ksi) stress level which compares to an average stress rupture life of 403 hours for first iteration material. The Larson-Miller plot of the average AF-115 life values shown in Figure 76 indicates that this material could exceed the 300 hour rim material rupture life program goal at 675°C (1250°F) and 925 MPa (134 ksi). The data presented in Figure 76 suggest that the AF-115 portion of the disk would exhibit an approximate rupture life of 500 hours under these test conditions. Comparison of the data available in the literature (28) for HIP and heat treated AF-115 indicated that the average rupture life for the CFM-56 material was comparable at the 760°C (1400°F) and 815°C (1500°F) test temperatures, while approximately 75% lower at the 650°C (1200°F) test temperature. Comparison of the creep data indicated that the CFM-56 material was inferior to AF-115 HIP processed and heat treated with identical parameters (28). The average time to 0.2% creep for the AF-115 portion of the CFM-56 disk is plotted in Figure 77 compared to the data in the literature for this alloy. The results for the CFM-56 are approximately 70% below the published data at 760°C (1400°F) and 815 °C (1500°F) and approximately 90% below the published data at 650°C (1200°F). Examination of the failed stress rupture bars indicated that the fracture mode for the AF-115 was a function of the test temperature. At 650°C (1200°F) the fracture mode was predominantly transgranular, while at 760°C (1400°F) and 815°C (1500°F) the fracture mode was intergranular. An example of the transgranular type cracking is shown in Figure 78b for an AF-115 specimen tested at 650°C (1200°F). Note the secondary cracks propagating from the primary fracture surface.

A comparison of the AF-115 and Rene' 95 rupture data for the comparable 650°C (1200°F) rupture test condition indicated that the AF-115 alloy exhibited approximately 5 times the rupture life capability of Rene' 95. The rupture ductility values, however, were comparable for both alloys at this temperature. The Rene' 95 tests conducted at 705°C (1300°F) and the AF-115 tests conducted at 760°C (1400°F) suggest that the rupture life trend would continue at the higher test temperatures.

Duplicate joint stress rupture tests were conducted at 650°C (1200°F). The results indicated that the average rupture life (47.8 hours) and elongation (3.2%) of the joint specimens were fully equivalent to the average life (49.1 hours) and elongation (3.6%) for the Rene' 95 rupture specimens. The comparison was made with Rene' 95 because it was the weaker of the alloys tested separately at 650°C (1200°F). The average elongation of the joint specimens (5.7%), however, was lower than the average for the Rene' 95 (7.9%). Examination of the failed test bar specimens revealed that failure occurred in the Rene' 95 portion of the specimens and an example of the type of failure is shown in Figure 79. Similar to the tensile fracture shown in Figure 75 the primary fracture path for the stress rupture specimen appears almost linear and is recessed into the Rene' 95 alloy away from the AF-115 interface. Again, this type of fracture surface was associated with the linear array of oxide particles observed in the Rene' 95 near the joint area. It was significant to note that in spite of the presence of these particles the stress rupture life of the joint specimens was fully equivalent to that of the Rene' 95 specimens.

5.2.2.4 Low Cycle Fatigue Tests

Low cycle fatigue tests were conducted upon AF-115 specimens at 650°C (1200°F) and Rene' 95 specimens at 480°C (900°F). In order to eliminate the problems experienced previously including (1) the re-cast layer on the fracture surface caused by arcing from the direct resistance heating method used for these tests and (2) the fracture initiation at the thermocouple weld shown in Figure 43, the low cycle fatigue testing was conducted by Mar-Test Inc. of Cincinnati, Ohio. An induction heating system was used for these tests instead of direct resistance heating and it was anticipated that this change would eliminate the previously mentioned problems. In addition to this change, the specimen diameter was increased from 6mm (0.250 inch) to 8 mm (0.312 inch) in order to increase the relative volume of material tested and also increase the probability of the presence of defects in these alloys. The tests were conducted with completely reversed loading at total strain ranges of 0.85 and 0.7% and the results are listed in Table 23.

The Rene' 95 results indicated that the specimen tested at the 0.7% total strain range level exhibited a life of 142,846 cycles with failure occurring in the threaded portion of the specimen. The failure life was within the range of values obtained during previous low cycle fatigue testing of this alloy in spite of the thread failure and was also within the scatter range of fatigue results reported in the literature for this alloy (30,31). The specimen tested at the 0.85% strain range level exhibited a life of 24,966 cycles, again comparable to that presented in the literature for this alloy (30,31). This specimen failed within the gage section and an analysis of the fracture surface indicated a sub-surface fracture initiation. This fracture site is shown in Figure 80. Fracture originated at the area indicated by the arrow in Figure 80a and analysis of this region failed to indicate the presence of any foreign particles in this region. Metallographic analysis indicated that fracture propagated in a transgranular type mode.

The 0.7% strain range test of the AF-115 specimen was terminated after 305,508 cycles because of excessive machine time. Data available in the literature predicted a fatigue life of approximatley 10,000 cycles at this strain range level and temperature for a AF-115 which had been HIP and heat treated at conditions similar to those for the CFM-56 disk, but where the low cycle fatigue tests were conducted with zero-tension loading as opposed to the completely reversed loading of the CFM-56 material (32). The specimen tested at the 0.85% total strain range level exhibited a failure life of 44,318 cycles, compared to a published life of 5,000 cycles at this strain range. This specimen failed within the gage section and an analysis of the fracture surface indicated a sub-surface fracture initiation. This fracture site is shown in Figure 81. Fracture originated at the area indicated by the arrow in Figure 81a and analysis of this region indicated the presence of hafnium-rich oxides. Analysis of the large particles on the outside surface of the specimen indicated that these were regions of contamination which occurred after the fatigue test and had nothing to do with the fracture process. Metallographic analysis indicated that fracture propagated in a transgranular type mode.

5.2.2.5 Summary

The mechanical property studies conducted on the CFM-56 disk material heat treated to the lower solution temperature of the second iteration indicated that the lower solution treatment was not beneficial to either alloy. The Rene' 95 exhibited slightly lower ultimate strength (within 92% of the program goal) and elongation while the AF-115 exhibited lower rupture life capability. (The AF-115 did, however, meet the rupture life goal.) Analysis of the Rene' 95 and AF-115 results with those reported in the literature for these two alloys indicated the comparisons varied as a function of the test type. For the Rene' 95, the tensile strength values were generally less than those reported in the literature, with ductility being lower than the published values at the lower test temperatures and higher at the elevated temperatures. The Rene' 95 stress rupture and low cycle fatigue results were comparable or superior to those available in the literature. For the AF-115, the tensile values were a function of test temperature with superior results at the lower temperature and inferior properties at the higher temperatures. The AF-115 stress rupture results were comparable while the low cycle fatigue results were superior to those reported in the literature. Joint material evaluations included tensile and stress rupture tests and the results indicated that in spite of a linear array of oxide particles adjacent to the joint the tensile properties were within 85% of the weaker of the two materials (Rene' 95) and the stress rupture properties were equivalent to those of the weaker of the two materials (Rene' 95).

A comparison of the Rene' 95 and AF-115 results for comparable test conditions indicated that the AF-115 was superior in terms of tensile properties as well as stress rupture properties. At the 480^{o}C (900^{o}F) test temperature used for much of the screening evaluations of this program, the AF-115 exhibited an average ultimate tensile strength of 1505 MPa (218 ksi), within approximately 98% of the program goal of 1520 MPa (220 ksi) at this temperature. By comparison, the Rene' 95 exhibited an average ultimate strength of 1410 MPa (204 ksi). At the 650^{o}C (1200^{o}F) stress rupture test temperature, the AF-115 exhibited five times the rupture life capability of Rene' 95. In terms of component design, then, the tensile results would suggest using AF-115 for the portion of the disk expected to experience temperatures of 480^{o}C (900^{o}F) or higher. The stress rupture results would suggest using the AF-115 for the portion of the disk expected to experience temperatures of 650^{o}C (1200^{o}F) or higher.

6.0 SUMMARY OF RESULTS

The objective of this program was the development and evaluation of techniques for the preparation, joining and heat-treatment of two materials for use in the production of dual alloy disks. The results of the program are presented below:

1. Feasibility was demonstrated for the preparation of dual alloy disk components with the following parameters:

   Rim Alloy - AF-115 HIP consolidated at 1190°C (2175°F)/4 Hours/105 MPa (15 ksi).

   Hub Alloy - Loose Rene' 95 powder.

   HIP Consolidation - 1120°C (2050°F)/5 Hours/105 MPa (15 ksi)

   Heat Treatment - 1190°C (2175°F)/2 Hours Salt Quench to 650°C (1200°F) plus 760°C (1400°F)/16 Hours.

2. Mechanical property levels achieved in a prototype CFM-56 disk relative to program goals:

   - Hub alloy 480°C (900°F) average ultimate tensile strength of 1410 MPa (204 ksi) compared to program goal of 1520 MPa (220 ksi).
   - Rim alloy rupture life capability of 500 hours at 675°C (1250°F)/925 MPa (134 ksi) compared to program goal of 300 hours.
   - Joint tensile properties within 85% and joint stress rupture properties equivalent to weaker of two materials (Rene' 95) compared to program goal to be within 90% of the weaker of the two materials.
   - Absence of notch sensitivity in either the rim or hub material.
   - 480°C (900°F) Rene' 95 and 650°C (1200°F) AF-115 low cycle fatigue properties equivalent to those available in the literature for HIP and heat treated material.

3. Major problems encountered during the course of the manufacture of the CFM-56 disk included quench cracking during heat treatment and joint cleanliness. There was a relationship between these two problems. While quench cracking was observed near sharp corners or other discontinuities, it was also associated with those portions of the alloy interfaces which had not been specifically prepared for the HIP consolidation operation. Quench cracking was not observed in areas surface ground and cleaned in preparation for HIP.

7.0 CONCLUDING REMARKS

In addition to the feasibility demonstration for the preparation of a component made from two different materials, the combination of tensile, stress rupture and low cycle fatigue properties exhibited by the AF-115/Rene' 95 CFM-56 disk indicated considerable potential for dual alloy disk applications. Although the present investigation included the evaluation of only a limited number of HIP consolidation and heat treatment operations the range of properties exhibited by the dual alloy component was greater than can be achieved by the use of a single material. Analysis of the results of this program suggested specific areas in which further improvements could be achieved in both the quality and performance of the dual alloy product as well as in the process economics.

In terms of quality, major emphasis should be directed towards maintaining a high level of joint cleanliness of the dual alloy materials. This can be accomplished by careful preparation of all surfaces of pre-consolidated material anticipated to come into contact with loose powder during subsequent consolidation. Failure to do so may result in the quench cracking situation observed after heat treatment of the CFM-56 disk in which cracks were associated primarily with the AF-115/Rene' 95 interface which had not been specifically prepared for the bonding operation.

In terms of mechanical property performance, the results indicated that in certain instances the second heat treatment employed for the CFM-56 disk resulted in property levels below those published in the literature for the specific alloys. During the heat treatment verification portion of the program, however, Rene' 95 tensile and AF-115 stress rupture properties exceeded those obtained during the more extensive mechanical property evaluations conducted on material with the second heat treatment. This suggested that performance could be improved through a more thorough evaluation of the effects of heat treatment on the material.

In terms of process economics, it is anticipated that improvements can be achieved through either process or alloy modifications. Process modifications would include changing from the double HIP operation used for the CFM-56 disk to a single HIP operation employing loose powders of both alloy compositions. This change, however, would require re-definition of an optimum HIP consolidation temperature for both the AF-115 and Rene' 95 as well as an evaluation of the effect of this change upon the heat treatment response of the alloys. The change would also require solution of the powder mixing problems encountered during the manufacture of the prototype T-700 shapes from the loose powder MERL 76-L/C Astroloy combination. This might be accomplished by using a thin vacuum sintered separator made from a mixture of both alloys to prevent powder intermixing during the canning operation.

Process economics can also be affected by the choice of alloys. The Rene' 95 used for the hub portion of the CFM-56 disk contained 8% cobalt while the AF-115 rim contained 15% cobalt. Results presented at a recent NASA workshop on strategic materials suggested that while cobalt is necessary for elevated temperature creep rupture capability, it apparently has little effect upon tensile properties (33). These results suggest that process economics could be improved by the use of a modified cobalt alloy for the hub portion of the disk, where creep rupture capability is not as critical as tensile strength. The alloy with the normal cobalt content would then be used for the rim portion of the disk, where creep rupture capability is important.

8.0 REFERENCES

1. Committee on Implementation of Cost Saving Recommendations for Aerospace Construction, "Aerospace Cost Savings - Implications for NASA and the Industry," National Materials Advisory Board Report NMAB-326, (1975).

2. Freche, J. C., Waters, W. J., and Ashbrook, R. L., "Method of Forming Articles of Manufacture From Superalloy Powders," U.S. Patent 3,775, 101, November 27, 1973.

3. Freche, J. C. and Ault, G. M., "Progress in Advanced High Temperature Materials Technology," Superalloys: Metallurgy and Manufacture, B. H. Kear, et al, eds., Claitors Publishing Division, Baton Rouge, La., September 1976.

4. Peterson, G. P., "Trends in the Application of Advanced Powder Metallurgy in the Aerospace Industry," Advanced Fabrication Techniques in Powder Metallurgy and Their Economic Implications, AGARD-CP-200, Ottawa, Canada, 1976.

5. Alver, A. S. and Wong, J. K. "Improved Turbine Disk Design to Increase Reliability of Aircraft Jet Engines," NASA-CR-134985, NASA Contract NAS 3-18558, October 1975.

6. Bartos, J. L. and Mathur, P. S., "Development of Hot Isostatically Pressed (As-HIP) Powder Metallurgy Rene' 95 Hardware," Superalloys: Metallurgy and Manufacture, B. H. Kear, et al, eds., Claitors Publishing Division, Baton Rouge, La., September 1976.

7. Kent, W. B, "Development of an Extra High Strength Powder Metallurgy Nickel Base Superalloy," NASA CR-135131, NASA Contract NAS 3-16795, January 1977.

8. Evans, D. J., "Manufacture of Low Cost P/M Astroloy Turbine Disks," Advanced Fabrication Techniques in Powder Metallurgy and Their Economic Implications, AGARD-CP-200, Ottawa, Canada, 1976.

9. Vishnevsky, C., "Bi-Casting of Gas Turbine Components," TRW Technical Memorandum TM-4776, February 1975.

10. Helmink, R. C., "Casting of Dual Property Turbine Wheels for Small Gas Turbine Engines," TRW Inc. Report ER-8029F, prepared under Williams Research Contract No. 102036, January 1981.

11. Schwerts, J. H., Rizzo, F. J., and Chandhok, "Dual-Property Integral Turbine Wheel for Small Engines," AFML Report IR-269-7 (III), February 1980, Crucible Research Center.

12. Ewing, B. A., "A Solid-to-Solid HIP-Bond Processing Concept for the Manufacture of Dual-Property Turbine Wheels for Small Gas Turbines," Superalloys 1980, Proceedings of the Fourth International Symposium on Superalloys, 1980, American Society for Metals.

13. Carlson, D. M., "P/M AF-115 Dual Property Disk Process Development," Superalloys 1980, Proceedings of the Fourth International Symposium on Superalloys, 1980, American Society for Metals.

14. Blackburn, M. J. and Sprague, R. A., "Production of Components by Isostatic Pressing of Nickel Base Superalloy Powders," Metals Technology, August 1977.

15. NASA-MATE Industry-Government Review, Pratt & Whitney Aircraft, NASA Contract NAS3-20072, February 23-24, 1977.

16. Reichman, S. H., "Low Cost P/M Superalloy Applications to Present and Future Turbines," The International Journal of Powder Metallurgy and Powder Technology, October 1975.

17. Bartos, J. L. and Mathur, P. S., "Development of Hot Isostatically Pressed Rene' 95 Turbine Parts," United States Army USAAMRDC-Technical Report 76-30, Contract Number DAAJ02-73-C-0106, Phase II, July 1976.

18. Fiedler, L. J., and Rizzo, F. J., "Manufacturing Methods for Superalloy Powder Production and Consolidation," AFML Report IR-271-3 (II), Contract F33615-73-C-5040, February 1974.

19. Bartos, J. L., "Development of a Very High Strength Disk Alloy for 1400^{o}F Service," AFML Report TR-74-187, Contract F33615-72-C-1797, November 1974.

20. Coyne, J. E., "Microstructural Control in Titanium and Nickel-Base Forgings: An Overview," Metals Technology, June 1977.

21. Brown, E. E., Boettner, R. C., et. al., "MINIGRAIN^{R} Processing of Nickel Base Alloys," Superalloys-Processing, MCIC-72-10, Battelle Columbus, September 1972.

22. Pfouts, W. R., et al, "Powder Metallurgy Rene' 95 Rotating Turbine Engine Parts," NASA CR-159802, June 1979, General Electric Company.

23. Bartos, J. L., "Review of Superalloy Powder Metallurgy Processing for Aircraft Gas Turbine Application," MiCon 78: Optimization of Processing, Properties, and Service Performance Through Microstructural Control, ASTM STP 672, ASTM, 1979.

24. Evans, D. J., and Malley, D. R., "Manufacturing Process for Production of Near Net Shapes by Hot Isostatic Pressing of Superalloy Powder," AFWAL IR 186-7T (VI), February 1979, Pratt & Whitney Aircraft, Government Products Division.

25. Gessinger, G. H., and Bomford, M. J., "Powder Metallurgy of Superalloys," International Metallurgical Reviews, Review No. 181, 1974.

26. Evans, D. J., "HIP Manufacture of High Strength Turbine Components," NASA-MATE Industry-Government Review, NAS3-20072, March 29, 1979, Pratt & Whitney Aircraft, Commercial Products Division.

27. Arnold, D. B., Mosier, J. S., and Harrison, R. W., NASA-MATE Program. Eleventh Quarterly Engineering Report, NAS3-20074, Report No. R78AEG-64, 1 September - 30 November 1978, General Electric Company.

28. Redden, T. K., "Advanced Superalloy Dual-Property Turbine Disk," First Interim Technical Report, Contract F33615-77-C-5253, April 1978, General Electric Company.

29. Cowles, B. A., Warren, J. R., and Hanke, F. K., "Evaluation of the Cyclic Behavior of Aircraft Turbine Disk Alloys," NASA CR-165123, August 1980, Pratt & Whitney Aircraft Group, Government Products Division.

30. Personal Communication, R. A. Sprague, General Electric Company, August 1981.

31. Shahani, V., and Popp, H. G., "Evaluation of Cyclic Behavior of Aircraft Turbine Disk Alloys," NASA CR-159433, June 1978, General Electric Company.

32. Conway, J. B., and Stentz, R. H., "High Temperature Low Cycle Fatigue Data for Three High Strength Nickel-Base Superalloys," AFWAL-TR-80-4077, June 1980, Martest, Inc.

33. NASA COSAM Workshop on Effects of Cobalt in High Temperature Superalloys, held at NASA Lewis Research Center, July 2, 1981.

Table 1

Compositions of Candidate Alloys for Dual Alloy Disks (Weight Percent)

I. Rim Alloy Candidates

Alloy	Ni	Cr	Co	Mo	W	Ta	Cb	Al	Ti	Fe	Mn	Si	C	B	Zr	Hf	Nb
Rene' 95	Bal.	14.0	8.0	3.5	3.5	-	3.5	3.5	2.5	-	-	-	0.15	.010	0.05	-	-
L/C Astroloy	Bal.	15.0	17.0	5.0	.025	-	-	4.0	3.5	0.25	.08	0.10	0.04	.025	.03	0	0
PA-101	Bal.	12.48	9.19	1.90	3.92	3.95	0.10	3.43	4.04	0.17	0.10	0.02	0.17	0.16	0.12	0.90	-
AF-115	Bal.	10.7	15.0	2.8	5.9	-	2.7	3.8	3.9	-	-	-	0.05	.02	0.05	0.75	-

II. Hub Alloy Candidates

Rene' 95	Bal.	14.0	8.0	3.5	3.5	-	3.5	3.5	2.5	-	-	-	0.15	.010	0.05	-	-
MERL 76	Bal.	12.4	18.5	3.2	-	-	-	4.97	4.32	-	-	-	.022	.020	.06	0.75	1.75

Table 2

Chemical Analyses (Weight Percent) of Ingots and Atomized Powders[1]

Alloy	Ingot Source	Heat Number	Cr	Co	Mo	W	Ta	Cb	Al	Ti	C	B	Zr	Hf	O_2[3]	N_2[3]	Ni
Rene' 95		Aim	14.0	8.0	3.5	3.5		3.5	3.5	2.5	.08	.01	.05				Bal.
	Special-Metals	9-5055	13.0	8.4	3.55	3.45		3.56	3.69	2.62	.06	.012	.04				Bal.
		Powder	12.46	8.11	3.38	3.71		3.21	3.41	2.48	.071	.07	.05		124	9	Bal.
	Special-Metals	9-6370[2]	12.83	7.82	3.42	3.54		3.44	3.63	2.52	.069	.04	.04		71	22	Bal.
L/C Astroloy		Aim	15.0	17.0	5.0				4.0	3.5	.04	.025	.03				Bal.
	Howmet	19987570	14.79	16.42	4.91				3.95	3.46	.03	.016	.05				Bal.
		Powder	14.51	16.48	4.81				3.86	3.53	.04	.019	.06		100	5	Bal.
PA-101		Aim	12.0	9.0	2.0	4.0	4.0		3.5	4.0	.15	.01	.01	.90			Bal.
	Cannon-Muskegon	B-5046	12.4	8.78	4.38	4.43	4.43		3.51	4.02	.077	.015	.068	.78			Bal.
		Powder	12.3	8.61	1.95	3.95	3.81		3.45	3.88	.09	.016	.07	.82	122	6	Bal.
AF-115		Aim	10.5	15.0	3.0	5.9		1.7	3.8	3.9	.05	.02	.05	0.75			Bal
	Special-Metals	7-11387	10.9	15.0	2.8	5.65		1.72	3.78	3.67	.05	.002	.05	0.7			Bal.
		Powder	10.3	14.67	2.94	5.43		1.48	3.45	3.78	.06	.003	.06	0.75	115	10	Bal.
MERL 76		Aim	12.5	18.5	3.0			1.5	4.9	4.2	.02	.02	.06	0.75			Bal.
	Howmet	1167543	12.68	18.29	3.27			.45[4]	4.94	4.35	.03	.019	.06	0[4]			Bal.
		Powder	12.42	18.40	2.89			1.63	4.8	4.42	.04	.03	.07	0.82	121	7	Bal.

(1) Except where indicated all powders were hydrogen gas atomized.
(2) Argon atomized heat.
(3) Analysis in ppm
(4) Ladle additions were made prior to atomization to increase the element content to desired level.

Table 3

Parameters Used for Combination A (Vacuum Sintered Rene' 95 Rim - Rene' 95 Hub) Processing Iterations

Process Iteration	Vacuum Pre-sinter	HIP Consolidation	Heat Treatment[2]
1	6 Hrs/1265°C (2310°F)	4 Hrs/1120°C (2050°F)/ 105 MPa (15 Ksi)	No heat treatment tested.
2	6 Hrs/1265°C (2310°F)	4 Hrs/1165°C (2125°F)/ 105 MPa (15 Ksi)	1150°C (2100°F)/2 Hours Salt Quench to 540°C (1000°F) + 870°C (1600°F)/1 Hour + 650°C (1200°F)/24 Hours
3	6 Hrs/1265°C (2310°F)	4 Hrs/1165°C (2125°F)/ 105 MPa (15 Ksi)	1150°C (2100°F)/2 Hours, Air Cool + 870°C (1600°F)/1 Hour + 650°C (1200°F)/24 Hours
4[1]	6 Hrs/1265°C (2310°F)	4 Hrs/1165°C (2125°F)/ 105 MPa (15 (Ksi)	1175°C (2150°F)/2 Hours + 870°C (1600°F)/1 Hour + 650°C (1200°F)/24 Hours
5[1]	6 Hrs/1265°C (2310°F)	4 Hrs/1165°C (2125°F)/ 105 MPa (15 ksi)	Same as Iteration 2, done at Sun Steel Heat Treat

(1) Argon atomized Rene' 95 powder used for hub materials for this iteration.

(2) Unless otherwise noted, heat treatment involved air cooling from temperature.

Table 4

Mechanical Property Screening Test Data for Combination A (Vacuum Sintered Rene' 95 Rim - Rene' 95 Hub) Cylindrical Test Bar Material

$480^{o}C$ ($900^{o}F$) Tensile Test Results

Process Iteration	Test Material	Grain Size	Ultimate Tensile Strength MPa	Ksi	0.2% Yield Strength MPa	Ksi	% Elongation	% R.A.	Comments
NASA Program Goal		1520	220						
			No tensile tests were conducted because of porous rim material						
2	Hub	5-6	1380	200	1160	168	6.7	7.9	
	Hub	5-6	1380	200	1150	167	6.5	6.8	
	Rim	0-1	1165	169	1110	161	1.3	3.1	
	Rim	0-1	1205	175	1110	161	4.7	3.6	
	Joint	(1)							
3	Hub	5-6	1350	196	1100	160	7.1	10.2	
	Hub	5-6	1360	197	1110	161	7.3	10.5	
4	Hub	4-5	1195	173	1140	165	1.3	3.7	
	Hub	4-5	1095	159	1035	150	1.0	2.9	
	Joint	(1)							

$760^{o}C$ ($1400^{o}F$)/550 MPa (80 Ksi) Stress Rupture Results

			Rupture Life (Hours)	% Elongation	% Reduction Area	Comments
1			No stress rupture tets were conducted because of porous rim material			
2	Rim	0-1	418.6	1.8	1.8	
	Rim	0-1	377.5	1.3	1.4	
	Hub	5-6	9.5	0.9	0.9	690 MPa (100 Ksi) stress was used.
	Hub	5-6	0.5	0.8	0.0	Test failed in fillet radius.
	Joint	(1)				
3			No stress rupture test conducted in third process iteration			
4	Rim	0-1	730.0	2.1	1.9	
	Rim	0-1	536.5	3.0	3.5	
	Joint	(1)				

(1) Severe quench cracking in joint area - no test specimens available.

Table 5

Parameters Used for Combination B (Loose Powder L/C Astroloy Rim - Loose Powder MERL 76 Hub) Processing Iterations

Process Iteration	HIP Consolidation	Heat Treatment(1)
1	4 Hours/1165°C (2125°F)/105 MPa (15Ksi)	1115°C (2040°F)/2 Hours + 870°C (1600°F)/8 Hours + 980°C (1800°F)/4 Hours + 650°C (1200°F)/24 Hours + 760°C (1400°F)/8 hours
2	4 Hours/ 1120°C (2050°F)/105 MPa (15 Ksi)	1165°C (2140°F)/2 Hours, 15 Second Delay - Oil Quench + 870°C (1600°F)/40 Minutes + 980°C (1800°F)/45 Mintes + 650°C (1200°F)/24 Hours + 760°C (1400°F)/8 Hours
3	4 Hours/1120°C (2050°F)/105 MPa (15 Ksi)	1165°C (2130°F)/2 Hours, Direct Oil Quench + 870°C (1600°F)/40 Minutes + 980°C (1800°F)/45 Minutes + 650°C (1200°F)/24 Hours + 760°C (1400°F)/8 Hours

(1) Unless otherwise noted, heat treatment involved air cooling from temperature.

Table 6

Mechanical Property Screening Test Data for Combination B (Loose Powder L/C Astroloy Rim - Loose Powder MERL 76 Hub) Cylindrical Test Bar Material

Process Iteration	Test Material	Grain Size	Ultimate Strength MPa	Ultimate Strength Ksi	0.2% Yield Strength MPa	0.2% Yield Strength Ksi	% Elongation	% Reduction Area	Comments
NASA Program Goal			1520	220					
1	Hub	8-10	1235	179	925	134	7.2	11.1	
	Hub	8-10	1270	184	1000	145	4.3	13.1	
	Joint	4-10	1205	175	910	132	9.2	14.4	Failed in rim material.
2	Hub	4-5	1420	206	1095	159	12.4	13.9	
	Hub	4-5	1365	198	1100	160	11.8	12.6	
	Joint	4-6	1250	181	1040	151	7.0	15.7	Failed in rim material.
3	Hub	4-5	1370	199	1055	153	13.1	10.9	
	Hub	4-5	1365	198	1035	150	12.7	9.9	
	Joint	4-6	1310	190	1020	148	10.9	9.7	Failed in rim material.

$760^{o}C$ ($1400^{o}F$)/550 MPa (80 Ksi) Stress Rupture Results

Process Iteration	Test Material	Grain Size	Rupture Life (Hours)	% Elongation	% Reduction Area	Comments
1	Rim	4-6	18.0	3.0	6.8	
	Rim	4-6	26.5	3.8	6.8	
	Joint	4-10	21.3	3.8	2.9	Failed in hub material.
2	Rim	5-6	58.8	3.2	4.0	
	Rim	5-6	36.4	2.8	3.5	
	Joint	4-6	28.8	1.1	1.7	Failed in hub material.
3	Rim	5-6	86.5	0.3	0.9	
	Rim	5-6	70.4	0.3	1.7	
	Joint	4-6	18.4	0.2	1.0	Failed in hub material.

Table 7

Parameters Used for Combination C (Pre-HIP'ed AF-115 Rim - Rene' 95 Hub) Processing Iterations

Process Iteration	AF-115 HIP Pre-Consolidation	HIP Consolidation	Heat Treatment[2]
1	4 Hrs/1190°C (2175°F)/ 105 MPa (15 Ksi)	4 Hrs/1120°C (2050°F)/ 105 MPa (15 Ksi)	1150°C (2100°F)/2 Hours Salt Quench to 540°C (1000°F) + 870°C (1600°F)/1 Hour + 650°C (1200°F)/24 Hours
2	4 Hrs/1190°C (2175°F)/ 105 MPa (15 Ksi)	4 Hrs/1120°C (2050°F)/ 105 MPa (15 Ksi)	1175°C (2150°F)/2 Hours Salt Quench to 540°C (1000°F) + 760°C (1400°F)/16 Hours
3[1]	4 Hrs/1190°C (2175°F)/ 105 MPs (15 Ksi)	4 Hrs/1120°C (2050°F)/ 105 MPa (15 Ksi)	1175°C (2150°F)/2 Hours Salt Quench to 532°C (1000°F) + 760°C (1400°F)/32 Hours

(1) Argon atomized Rene' 95 powder used for hub material in this iteration.
(2) Unless otherwise noted, heat treatment involved air cooling from temperature.

Table 8

Mechanical Property Screening Test Data for Combination C (Pre-HIP'ed AF-115 Rim - Rene' 95 Hub) Cylindrical Test Bar Material

$480^{o}C$ ($900^{o}F$) Tensile Rest Results

Process Iteration	Test Material	Grain Size	Ultimate Strength MPa	Ultimate Strength Ksi	0.2% Yield Strength MPa	0.2% Yield Strength Ksi	% Elongation	% Reduction Area	Comments
NASA Program Goal			1520	220					
1	Hub	8-10	1385	201	1185	172	5.5	7.5	
	Hub	8-10	1380	200	1195	173	4.5	6.7	
	Joint	5-10	1235	179	1130	164	3.1	3.9	Failed in rim material.
2	Hub	6	1340	194	1055	153	8.4	11.5	
	Hub	6	1470	213	1150	167	7.8	10.0	
	Joint	3-6	1345	195	1110	161	11.0	14.4	Failed in rim material.
3	Hub	6	1310	190	1225	178	2.5	6.1	
	Hub	6	1295	188	1195	173	2.4	6.0	
	Joint	3-6	1305	189	1170	170	4.1	6.1	Failed at joint interface.

$760^{o}C$ ($1400^{o}F$)/550 MPa (80 Ksi) Stress Rupture Results

			Rupture Life (Hours)	% Elongation	% Reduction Area	Comments
1	Rim	5-6	9.5	1.2	2.1	
	Rim	5-6	13.0	1.0	1.0	
	Joint	5-10	20.7	0.7	0.6	Failed at joint interface.
2	Rim	3-5	859.8	3.4	3.7	
	Rim	3-5	844.0	2.6	3.1	
	Joint	3-6	124.1	2.3	3.5	Failed in hub material.
3	Rim	3-5	80.4	Thread Failure		
	Rim	3-5	79.3	Thread Failure		
	Joint	3-6	0.3	0.3	1.0	Failed at joint interface.

Table 9

Parameters Used for Combination D (Vacuum Sintered PA-101 Rim - MERL 76 Hub) Processing Iterations

Process Iteration	Vacuum Pre-Sinter	HIP Consolidation	Heat Treatment[1]
1	6 Hrs/1260°F (2300°F)	4 Hrs/1165°C (2125°F)/ 105 MPa (15 Ksi)	1165°C (2125°F)/1 Hour Air Cool + 760°C (1400°F)/8 Hours
2	6 Hrs/1260°C (2300°F)	4 Hrs/1120°C (2050°F)/ 105 MPa (15 Ksi)	1170°C (2135°F)/2 Hours Salt Quench to 540°C (1000°F) + 760°C (1400°F)/8 Hours + 675°C (1250°F)/24 Hours
3	6 Hrs/1260°C (2300°F)	4 Hrs/1120°C (2050°F)/ 105 MPa (15 Ksi)	1170°C (2135°F)/2 Hours Oil Quench + 870°C (1600°F)/40 Minutes + 980°C (1800°F)/45 Minutes + 650°C (1200°F)/24 Hours + 760°C (1400°F)/16 Hours

(1) Unless otherwise noted, heat treatment involved air cooling from temperature.

Table 10

Mechanical Property Screening Test Data for Combination D (Vacuum Sintered PA-101 Rim - MERL 76 Hub) Cylindrical Test Bar Material

480°C (900°) Tensile Test Results

Process Iteration	Test Material	Grain Size	Ultimate Strength MPa	Ultimate Strength Ksi	0.2% Yield Strength MPa	0.2% Yield Strength Ksi	% Elongation	% Reduction Area	Comments
NASA Program Goal			1520	220					
1	Hub	8-10	1330	193	1015	147	7.6	18.0	
	Hub	8-10	1215	176	1015	147	3.2	12.1	
	Joint	0-10	1140	165	985	143	4.9	6.2	Failed in rim material.
2	Hub	4-5	1475	214	1145	166	12.8	13.6	
	Hub	4-5	1460	212	1130	164	12.6	12.9	
	Joint	0-5	640	93	NA	NA	0	0	Failed in rim material.
3	Hub	4-5	985	143	985	143	0.7	0.6	
	Hub	4-5	970	141	970	141	1.0	0.8	
	Joint	0-5	(1)						

760°C (1400°F)/550 MPa (80 Ksi) Stress Rupture Results

Process Iteration	Test Material	Grain Size	Rupture Life (Hours)	% Elongation	% Reduction Area	Comments
1	Rim	0-1	340.1	5.3	5.0	
	Rim	0-1	568.5	3.6	3.9	
	Joint	0-10	10.1	0.9	0.5	Failed in rim material at radius.
2	Rim	0-1	20.1	3.2	3.4	
	Rim	0-1	113.6	3.8	3.8	
	Joint	0-5	75.9	1.1	1.3	Failed in hub material.
3	Rim	0-1	22.7	0.3	1.0	
	Rim	0-1	18.3	0.3	0.9	
	Joint	0-5	(1)			

(1) Severe quench cracking in joint area - no test specimens available.

Table 11

Mechanical Property Screening Test Data for Combination B (Loose Powder L/C Astroloy Rim - MERL 76 Hub) Flat Panel Test Material

480°C (900°F) Tensile Test Results

Test Material	Grain Size	Ultimate Strength MPa	Ksi	0.2% Yield Strength MPa	Ksi	% Elongation	% Reduction Area	Comments
NASA Program Goal		1520	220					
Hub	8-10	1565	227	1060	154	20.7	19.6	
Hub	8-10	1510	219	1040	151	18.6	17.8	
Joint	4-10	1455	211	1050	152	13.3	14.5	Failed in rim material
Joint	4-10	1400	203	1015	147	10.8	11.6	Failed in rim material

760°C (1400°F) 550 MPa (80 Ksi) Stress Rupture Results

		Rupture Life (Hours)	% Elongation	% Reduction Area	Comments
Rim	4-8	24.9	0.7	0.6	Thread failure
Joint	4-10	36.7	2.5	2.5	Failure in rim material

Test Panel Parameters — HIP Consolidation - 4 Hours/1120°C (2050°F)/105 MPa (15 Ksi)
Heat Treatment
+ 1165°C (2130°F)/2 Hours Direct Oil Quench
+ 870°C (1600°F)/40 Minutes
+ 980°C (1800°F)/45 Minutes
+ 650°C (1200°F)/24 Hours
+ 760°C (1400°F)/8 Hours

Unless otherwise noted, heat treatment involved air cooling from temperature.

Table 12

Mechanical Property Data for Combination B
Loose Powder L/C Astroloy Rim - Loose Powder MERL 76 Hub)
Flat Panel Test Material

760°C (1400°F) 550 MPa (80 Ksi) Stress Rupture Results

Test Material	Rupture Life (Hours)	% Elongation	% Reduction Area
Hub	37.7	4.2	4.2
Hub	43.3	4.0	3.6

480°C (900°F) Low Cycle Fatigue Results

	Total Strain Range (%)	Cycles To Failure
Hub	0.7	69, 120(1)
Hub	0.7	137, 460

(1) Test interrupted without failure when test specimen stripped threads in gripping fixture.

Test Panel Processing Parameters

HIP Consolidation - 4 Hrs/1120°C (2050°F)/ 105 MPa (15 Ksi)

Heat Treatment - 1165°C (2130°F)/2 Hours Direct Oil Quench
+ 870°C (1600°F)/40 Minutes
+ 980°C (1800°F)/45 Minutes
+ 650°C (1200°F)/24 Hours
+ 760°C (1400°F)/8 Hours

Unless otherwise noted, heat treatment involved air cooling from temperature.

Table 13

Mechanical Property Screening Test Data for First Iteration Combination C (Pre-HIP'ed AF-115 Rim - Rene' 95 Hub) Flat Panel Test Material

$480^{o}C$ ($900^{o}F$) Tensile Test Results

Test Material	Grain Size	Ultimate Strength MPa	Ultimate Strength Ksi	0.2% Yield Strength MPa	0.2% Yield Strength Ksi	% Elongation	% Reduction Area	Comments
NASA Program Goal		1520	220					
Hub	4-8	1495	217	1100	160	9.1	12.1	
Hub	4-8	1470	213	1080	157	8.6	10.3	
Joint	4-8	1440	209	1130	164	8.3	10.3	Failed in rim material
Joint	4-8	1380	200	1060	154	8.0	10.9	Failed in rim material

$760^{o}C$ ($1400^{o}F$) 550 MPa (80 Ksi) Stress Rupture Results

		Rupture Life (Hours)	% Elongation	% Reduction Area	Comments
Rim	8	522.0	2.4	3.8	
Joint	4-8	158.0	2.0	5.0	Failed in hum material

Test Panel Processing Parameters:
HIP Pre-Consolidation - 4 Hours/$1190^{o}C$ ($2175^{o}F$)/105 MPa (15 Ksi)
HIP Consolidation - 4 Hours/$1120^{o}C$ ($2050^{o}F$)/105 MPa (15 Ksi)
Heat Treatment - $1175^{o}C$ ($2150^{o}F$)/2 Hours Salt Quench to $540^{o}C$ ($1000^{o}F$)
- + $760^{o}C$ ($1400^{o}F$)/16 Hours Air Cool

Table 14

Mechanical Property Data for First Iteration Combination C (Pre-HIP'ed AF-115 Rim - Rene' 95 Hub) Flat Panel Test Material

760°C (1400°F) Tensile Test Results

Test Material	Ultimate Strength MPa	Ultimate Strength Ksi	0.2% Yield Strength MPa	0.2% Yield Strength Ksi	% Elongation	% Reduction Area
Hub	1170	170	1015	147	3.4	6.8
Rim	1145	166	995	144	5.0	8.0

Stress Rupture Results

Test Material	Test Temperature °C	Test Temperature °F	Stress Level MPa	Stress Level Ksi	Rupture Life (Hours)	% Elongation	% Reduction Area	Comments
Hub	650	1200	1035	150	148.0	1.6	2.7	
Hub	650	1200	1035	150	130.9	2.5	3.7	
Joint	650	1200	1035	150	425.2	1.5	4.4	Failed in hub material
Rim	540	1000	1170	170	282.3	3.6	4.7	
Rim	650	1200	1035	170	127.0	1.0	3.7	
Rim	815	1500	415	60	121.0	1.7	2.5	

480°C (900°F) Low Cycle Fatigue Results

	Total Strain Range (%)	Cycle to Failure
Hub	0.7	45,480
Hub	0.7	217,740

Test Panel Processing Parameters:

HIP Pre-Consolidation - 4 Hours/1190°C (2175°F)/105 MPa (15 Ksi)
HIP Consolidation - 4 Hours/1120°C (2050°F)/105 MPa (15 Ksi)
Heat Treatment - 1175°C (2150°F)/2 Hours Salt Quench to 540°C (1000°F)
- + 760°C (1400°F)/16 Hours Air Cool

Table 15

Mechanical Property Screening Test Data for Second Iteration Combination C (Pre-HIP'ed AF-115 Rim - Rene' 95 Hub) Flat Panel Test Material

480°C (900°F) Tensile Test Results

Test Material	Grain Size	Ultimate Strength MPa	Ultimate Strength Ksi	0.2% Yield Strength MPa	0.2% Yield Strength Ksi	% Elongation	% Reduction Area	Comments
NASA Program Goal		1520	220					
Hub	4-8	1455	211	1150	167	8.7	12.1	
Hub	4-8	1440	209	1150	167	9.6	10.8	
Joint	4-8	1325	192	1145	166	7.4	11.5	Failed in rim material
Joint	4-8	1315	191	1140	165	8.8	10.9	Failed in rim material

760°C (1400°F) 550 MPa (80 Ksi) Stress Rupture Tests

		Rupture Life (Hours)	% Elongation	% Reduction Area	
Rim	4-7	787.4	2.2	4.3	
Rim	4-7	646.5	3.0	4.7	
Joint	4-8	284.2	3.6	5.5	Failed in hub material
Joint	4-8	226.5	4.0	6.1	Failed in hub material

Test Panel Processing Parameters:
HIP Pre-Consolidation - 4 Hours/1190°C (2175°F)/105 MPa (15 Ksi)
HIP Consolidation - 4 Hours/1120°C (2050°F)/105 MPa (15 Ksi)
Heat Treatment - 1205°C (2200°F)/2 Hours Salt Quench to 650°C (1200°F) + 760°C (1400°F)/16 Hours Air Cool

Table 16

Mechanical Property Data for Second Iteration Combination C (Pre-HIP'ed AF-115 Rim - Rene' 95 Hub) Flat Panel Test Material

760°C (1400°F) Tensile Test Results

Test Material	Ultimate Strength MPa	Ultimate Strength Ksi	0.2% Yield Strength MPa	0.2% Yield Strength Ksi	% Elongation	% Reduction Area
Rim	1200	174	1040	151	7.9	9.1
Rim	1185	172	1025	149	6.0	8.5

Stress Rupture Results

Test Material	Test Temperature °C	Test Temperature °F	Stress Level MPa	Stress Level Ksi	Rupture Life (Hours)	% Elongation	% Reduction Area	Comments
Hub	650	1200	1035	150	7.9	0	0	Thread failure
Hub	650	1200	1035	150	41.6	5.3	4.0	
Joint	650	1200	1035	150	22.9	8.6	4.3	Failed in hub material
Rim	540	1000	1170	170	296.8	4.8	6.4	
Rim	650	1200	1035	150	462.5	4.0	5.1	
Rim	815	1500	415	60	419.2	3.9	4.3	

480°C (900°F) Low Cycle Fatigue Results

	Total Strain Range (%)	Cycles to Failure
Hub	0.7	37,620
Hub	0.7	111,960

Test Panel Processing Parameters:

HIP Pre-Consolidation - 4 Hours/1190°C (2175°F)/105 MPa (15 Ksi)
HIP Consolidation - 4 Hours/1120°C (2050°F)/105 MPa (15 Ksi)
Heat Treatment - 1205°C (2200°F)/2 Hours Salt Quench to 650°C (1200°F) + 760°C (1400°F)/16 Hours Aor Cool

Table 17

Chemical Analyses (Weight Percent) of Powders Used for Defect Characterization Study[1]

Alloy	Heat Number	Cr	Co	Mo	W	Cb	Al	Ti	C	B	Zr	Hf	O_2[2]	N_2[2]	Ni
L/C	Aim	15.0	17.0	5.0			4.0	3.5	.04	.025	.03				Bal.
Astroloy	KR486	14.99	17.09	5.00			4.05	3.45	.047	.028	.01		81	20	Bal.
MERL 76	Aim	12.5	18.5	3.0		1.5	4.9	4.2	.02	.02	.06	0.75			Bal.
	K512	11.95	18.11	3.04		1.45	5.13	4.16	.028	.018	.06	0.43	72	20	Bal.

(1) Powder argon atomized at Universal Cyclops.
(2) Analysis in ppm.

Table 18

Mechanical Property Results for Loose Powder MERL 76/L/C Astroloy Defect Study

480°C (900°F) Tensile Results

Test Material	Ultimate Strength MPa	Ultimate Strength Ksi	0.25 Yield Strength MPa	0.25 Yield Strength Ksi	% Elongation	% Reduction Area	Comments
MERL 76 (Hub)	1290	187	1015	147	6.4	9.7	
	1250	181	1000	145	5.1	8.8	
Joint Area	1305	189	1035	150	7.3	8.5	Failed in L/C Astroloy
	1275	185	995	144	6.5	7.7	Failed in L/C Astroloy
MERL 76/Astroloy Blend	1450	210	1080	157	11.8	10.9	
	1430	207	1070	155	10.9	8.9	

760°C 1400°F)/550 MPa (80 Ksi) Stress Rupture Results

Test Material	Rupture Life (Hours)	% Elongation	% Reduction Area	Comments
L/C Astroloy (Rim)	2.8	0.2	0.6	Thread Failure
	21.9	2.5	1.9	
Joint Area	6.1	1.4	0.6	Failed In MERL 76
	10.7	2.1	1.5	Failed in MERL 76
MERL 76/Astroloy Blend	59.8	4.7	1.8	
	46.5	5.0	2.9	

Heat Treatment: 1165°C (2130°F)/2 Hours Direct Oil Quench + 870°C (1600°F)/40 Minutes + 980°C (1800°F)/45 Minutes + 650°C (1200°F)/24 Hours + 760°C (1400°F)/16 Hours

Unless otherwise noted, heat treatment involved air cool from temperature.

HIP Consolidation: 4 Hours/1120°C (2050°F)/105 MPa (15 Ksi)

Table 19

Chemical Analysis of Powders Used for CFM-56 Disk[1]

Alloy	Source	Master Blend	Cr	Co	Mo	W	Cb	Al	Ti	C	B	Zr	Hf	O_2(2)	N_2(2)	Ni
AF-115		Aim	10.5	15.0	3.0	5.9	1.7	3.8	3.9	.05	.02	.05	0.75			Bal.
	Special Metals	80052	10.78	15.12	2.74	5.85	1.77	3.72	3.7	.042	.02	.055	0.68	83	15	Bal.
Rene' 95		Aim	14.0	8.0	3.5	3.5	3.5	3.5	2.5	.08	.01	.05				Bal.
	Special Metals	80050	12.79	8.08	3.44	3.45	3.45	3.45	2.39	.06	.01	.043		70	38	Bal.

(1) Analyses in Weight Percent
(2) Analysis in ppm

Table 20

Mechanical Property Results for CFM-56 Disk for First Heat Treatment Iteration(1)

480°C (900°F) Tensile Test Results

Test Material	Grain Size	Ultimate Strength MPa	Ultimate Strength Ksi	0.2% Yield Strength MPa	0.2% Yield Strength Ksi	% Elongation	% Reduction in Area
NASA Program Goal		1520	220				
Rene' 95 Hub	6-7	1520	220	1075	156	25.0	13.7
Rene' 95 Hub	6-7	1490	216	1070	155	25.7	15.6

760°F 1400°F)/620 MPa (90 Ksi) Stress Rupture Tests

		Rupture Life (Hours)	% Elongation	% Reduction Area
AF-115 Rim	4-6	434.7	9.2	11.4
AF-115 Rim	4-6	371.6	10.0	9.5

(1) Heat Treatment: 1205°C (2200°F)/2 Hours Salt Quench to 650°C (1200°F) + 760°C (1400°F)/16 Hours Air Cool

Table 21

Tensile Test Results for CFM-56 Disk for Second Heat Treatment Iteration[1]

Test Material	Grain Size	Test Temperature °C	Test Temperature °F	Ultimate Strength MPa	Ultimate Strength Ksi	0.2% Y.S. MPa	0.2% Y.S. Ksi	% Elongation	% R.A.	Comments
Rene' 95 Hub	6-8	Room Temperature		1520	220	1130	164	11.6	13.4	
Rene' 95 Hub	6-8	Room Temperature		1490	216	1140	165	10.9	12.8	
Rene' 95 Hub	6-8	480	900	1415	205	1075	156	9.0	12.8	
Rene' 95 Hub	6-8	480	900	1410	204	1055	153	8.8	10.7	
Rene' 95 Hub	6-8	650	1200	1385	201	1060	154	14.6	17.9	
Rene' 95 Hub	6-8	650	1200	1370	199	1035	150	17.3	19.4	
Rene' 95 Hub	6-8	675	1250	1315	191	1005	146	21.5	23.0	
Rene' 95 Hub	6-8	675	1250	1275	185	970	141	20.8	19.7	
AF-115 Rim	6-8	480	900	1510	219	1060	154	21.9	25.4	
AF-115 Rim	6-8	480	900	1490	216	1070	155	19.8	17.8	
AF-115 Rim	6-8	650	1200	1400	203	1025	149	24.4	23.0	
AF-115 Rim	6-8	650	1200	1385	201	1025	149	23.6	21.8	
AF-115 Rim	6-8	760	1400	1100	160	1015	147	12.0	13.5	
AF-115 Rim	6-8	760	1400	985	143	965	140	4.4	6.1	
Joint	6-8	650	1200	1185	172	1005	146	2.6	2.6	Rene' 95 Failure
Joint	6-8	650	1200	1180	171	1035	150	2.2	4.6	Rene' 95 Failure

(1) Heat Treatment: 1190°C (2175°F)/2 Hours Salt Quench to 650°C (1200°F) + 760°C (1400°F)/16 Hours Air Cool.

Table 22

Creep/Stress Rupture Test Results for CFM-56 Disk for Second Heat Treatment Iteration[1]

Test Material	Grain Size	Test Type	Test Temperature °C	Test Temperature °F	Stress Level MPa	Stress Level Ksi	Rupture Life (hrs.)	Time to 0.1% Creep (hours)	Time to 0.2% Creep (hours)	% El.	% R.A.	Comments
Rene' 95 Hub	6-8	Notch/	595	1100	1170	170	708.7			1.3	8.2	Smooth Failure
Rene' 95 Hub	6-8	Smooth Rupture	595	1100	1170	170	674.6			3.5	7.8	Smooth Failure
Rene' 95 Hub	6-8	Notch/	650	1200	1035	150	64.8			3.7	8.8	Smooth Failure
Rene' 95 Hub	6-8	Smooth Rupture	650	1200	1035	150	50.4			2.9	7.5	Smooth Failure
Rene' 95 Hub	6-8	Rupture	650	1200	1035	150	35.3			4.4	7.2	
		Rupture	650	1200	1035	150	45.9			3.5	8.1	
Rene' 95 Hub	6-8	Rupture	705	1300	830	120	104.3			4.9	10.4	
		Rupture	705	1300	830	120	86.7			5.0	8.9	
AF-115	6-8	Notch/	650	1200	1035	150	215.9			4.4	6.6	Smooth Failure
AF-115	6-8	Smooth Rupture	650	1200	1035	150	187.6			5.8	7.0	Smooth Failure
AF-115 Rim	6-8	Notch/	760	1400	690	100	89.5			7.0	9.8	Smooth Failure
AF-115 Rim	6-8	Smooth Rupture	760	1400	690	100	70.6			8.1	9.0	Smooth Failure
AF-115 Rim	6-8	Creep	650	1200	1035	150	257.9	0.25	0.5	4.7	7.8	
AF-115 Rim	6-8	Creep	650	1200	1035	150	243.6	0.45	0.7	4.0	8.0	
AF-115 Rim	6-8	Creep	760	1400	690	100	92.7	1	3.3	9.0	15.3	
AF-115 Rim	6-8	Creep	760	1400	690	100	80.5	1.8	2.6	10.0	14.1	
AF-115 Rim	6-8	Creep	815	1500	515	75	35.2	0.2	1.2	5.6	14.1	
AF-115 Rim	6-8	Creep	815	1500	515	75	29.7	0.2	1.1	4.8	13.9	
Joint	6-8	Rupture	650	1200	1035	150	44.1			2.9	5.3	Rene' 95
Joint	6-8	Rupture	650	1200	1035	150	51.5			3.5	6.0	Rene' 95

(1) Heat Treatment: 1190°C (2175°F)/2 Hours Salt Quench to 650°C (1200°F) + 760°C (1400°F)/16 Hours Air Cool.

Table 23

Low Cycle Fatigue Results for CFM-56 Disk for Second Heat Treatment Iteration[1]

Test Material	Grain Size	Test Temperature (°C)	Test Temperature (°F)	A	t	N_f	Comment
Rene' 95 Hub	6-8	480	900		0.7	142,846	Thread Failure
Rene' 95 Hub	6-8	480	900		0.85	24,966	
AF-115 Rim	6-8	650	1200		0.7	305,508	Test Terminated
AF-115 Rim	6-8	650	1200		0.85	44,318	

(1) Heat Treatment: 1190°C (2175°F)/2 Hours Salt Quench to 650°C (1200°F) + 760°C (1400°F)/16 Hours Air Cool

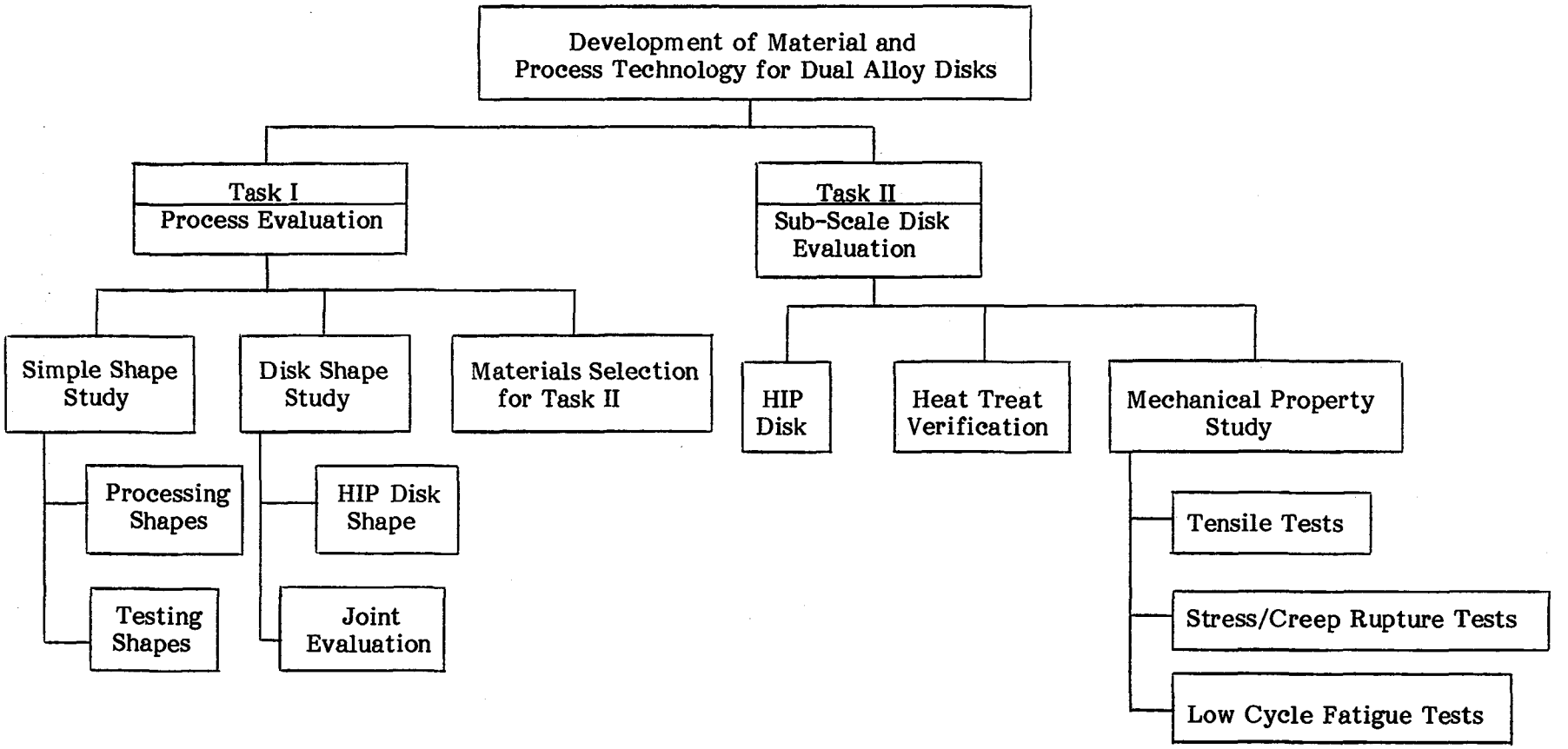

Figure 1. Program Work Breakdown Structure.

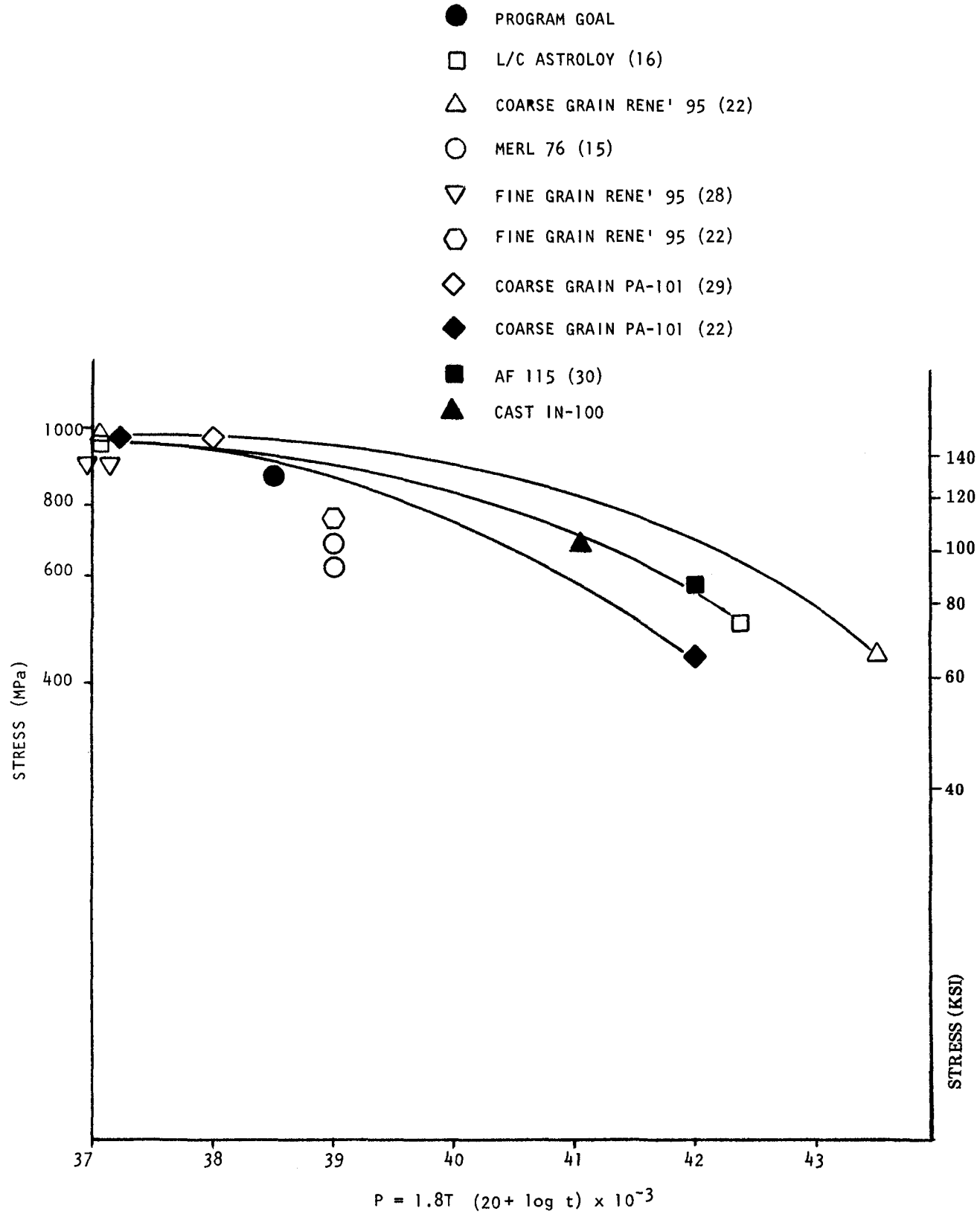

Figure 2. Larson-Miller Parameter Plot of Stress Rupture Properties of Candidate Rim Alloys. Data Presented for P/M Heat Treated Alloys.

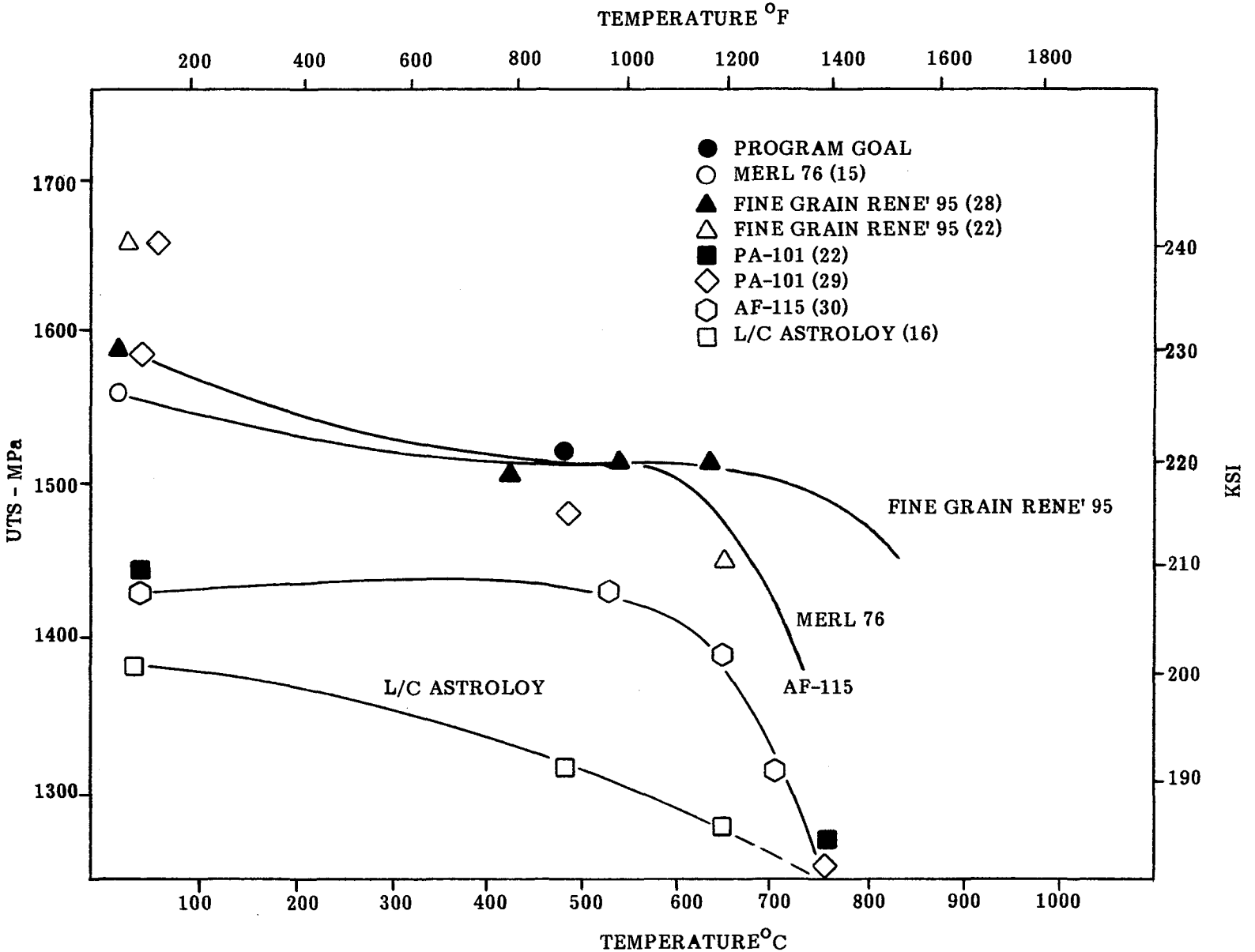

Figure 3. Plot of Ultimate Tensile Strength Versus Temperature for Candidate Hub Alloys. Data Presented for P/M Heat Treated Alloys.

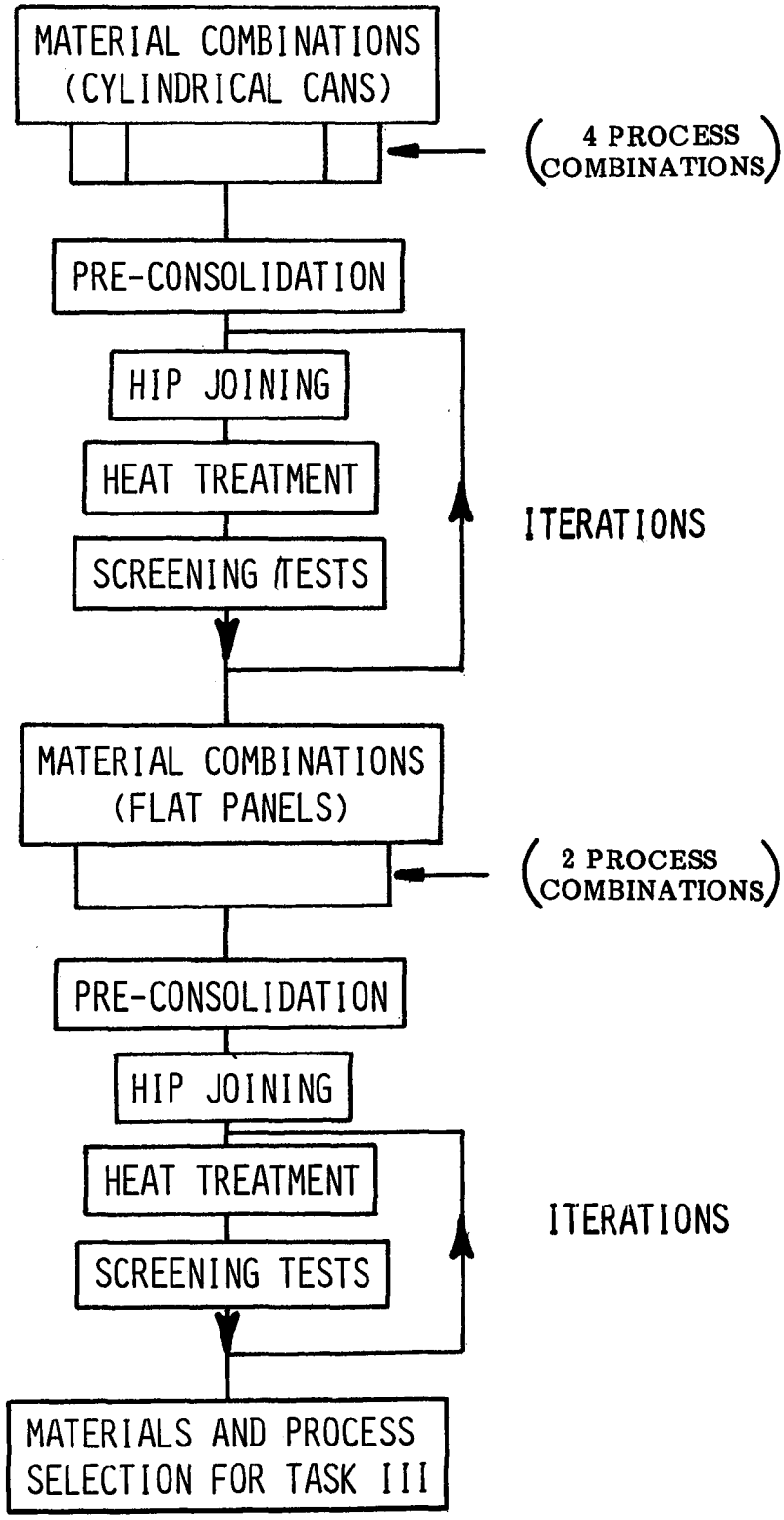

Figure 4. Flow Diagram Describing Activities Conducted During Simple Shape Study.

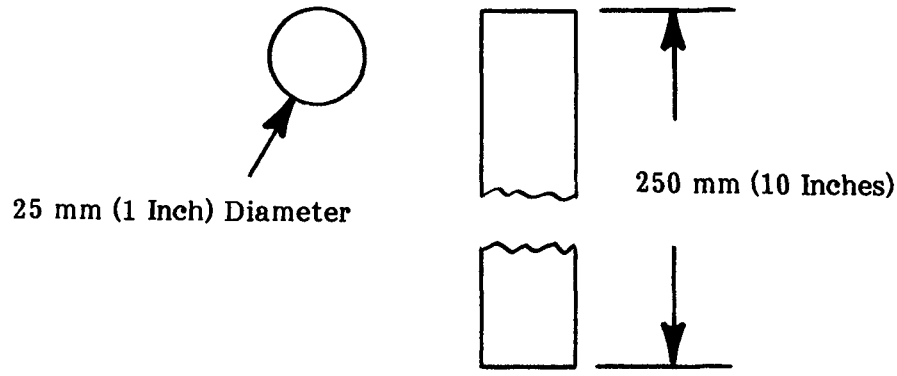

(a) Cylindrical Shape

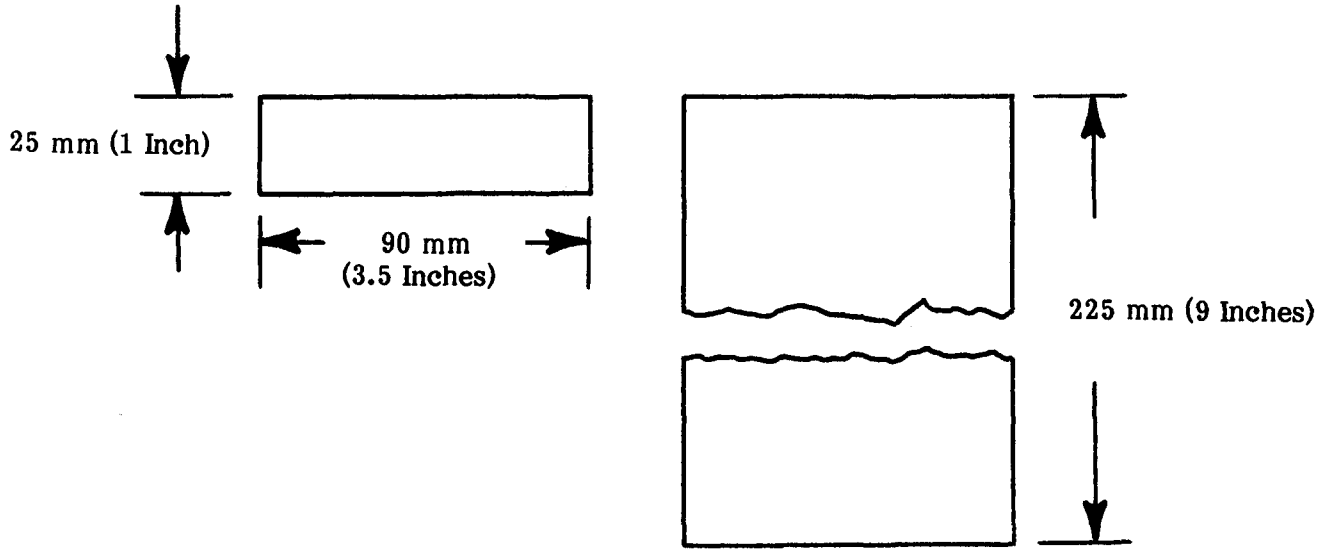

(b) Flat Panel Shape

Figure 5. Schematic Diagram of (a) Cylindrical Shape and (b) Flat Panel Shape Used for the Simple Shape Study.

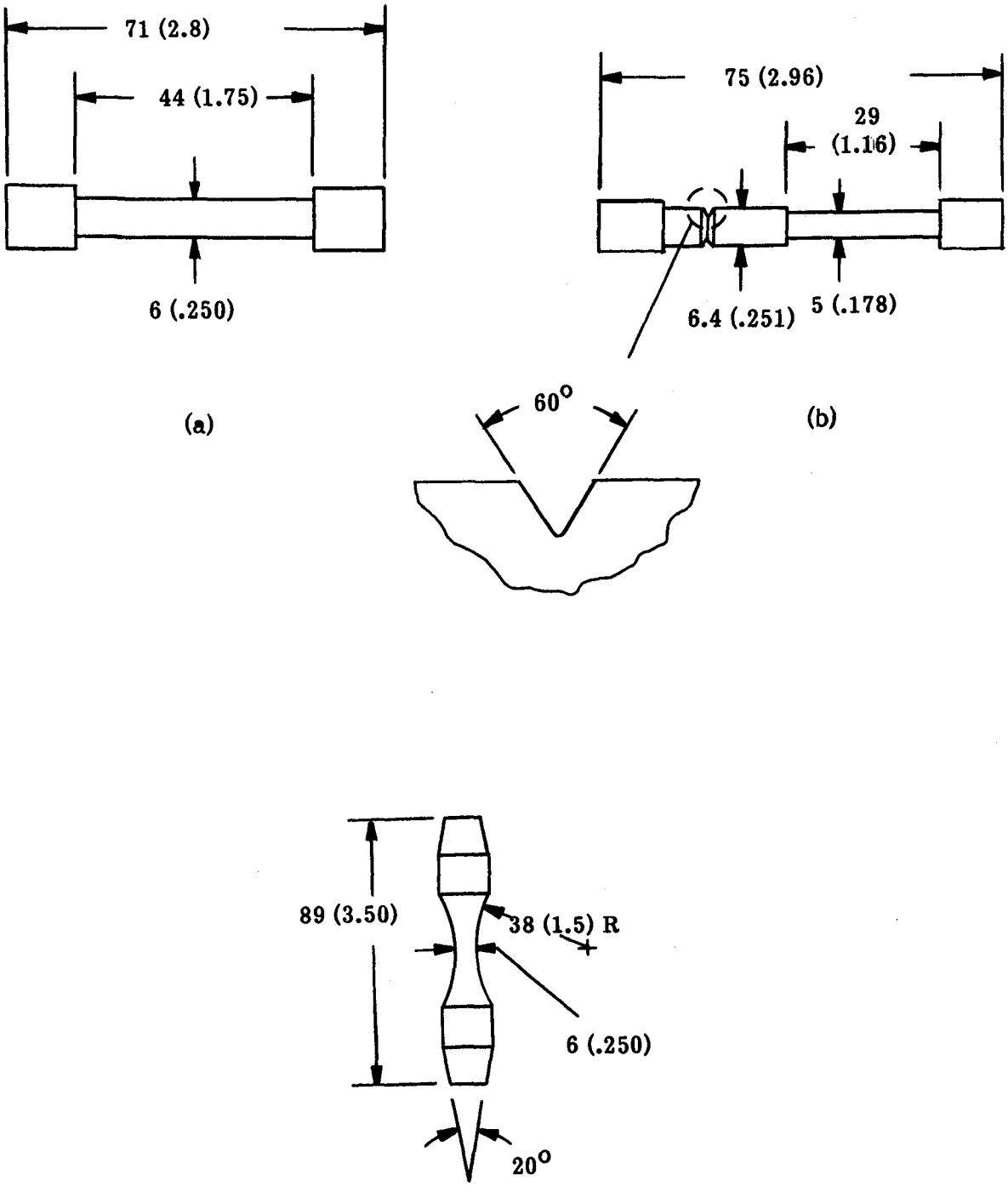

Figure 6. Schematic Diagram of (a) Tensile/Stress Rupture, (b) Combination Notch-Smooth Stress Rupture, and (c) Low Cycle Fatigue Test Specimen Configurations.

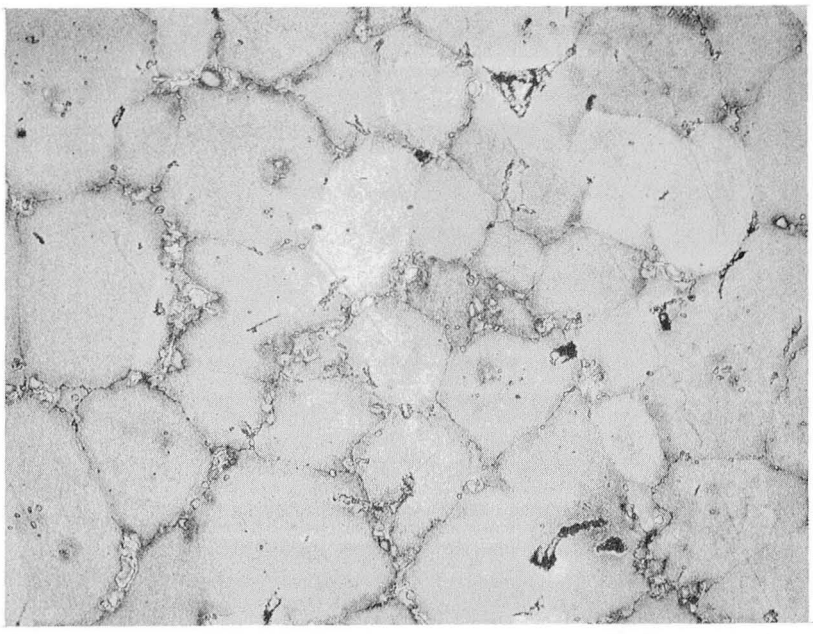

a) 1300°C (2375°F) Sintering Temperature
Grain Size ASTM #1

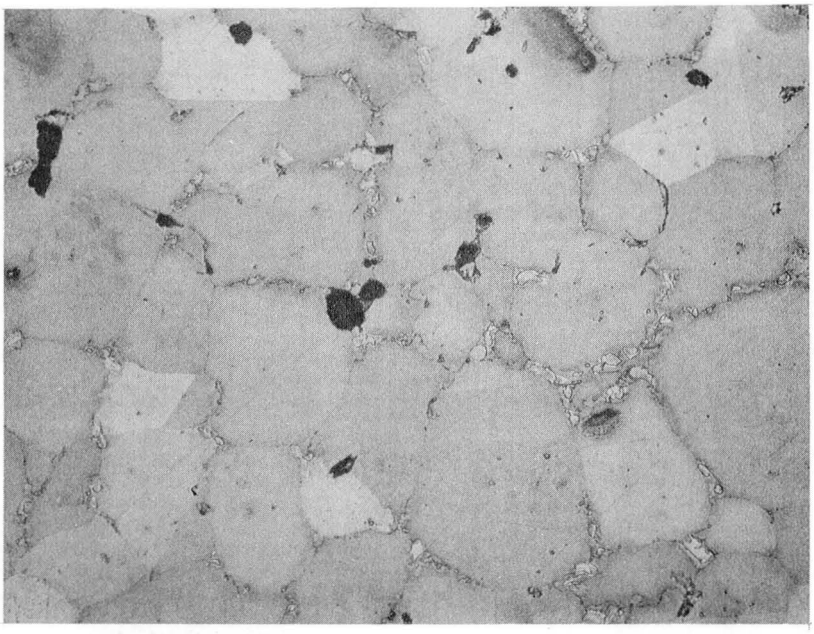

b) 1265°C (2310°F) Sintering Temperature
Grain Size ASTM # 1 to 2.

Figure 7. Light Photomicrographs of Rene' 95 Vacuum Sintered at Various Temperatures for Six Hours. Note Porosity and Incipient Melting. Magnification 100X.

Figure 8. Photograph of Typical HIP Consolidated Cylindrically Shaped Can. Scale in Inches.

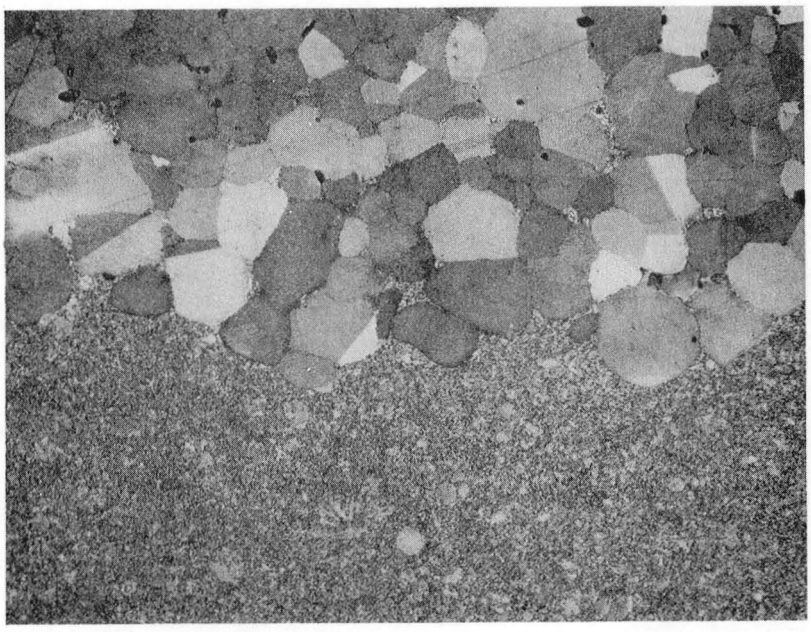

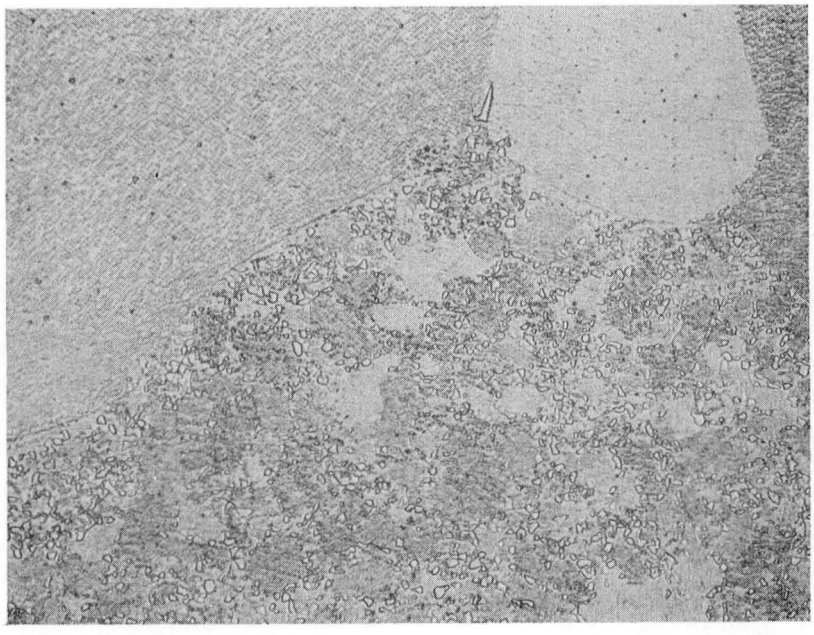

Figure 9. Light Photomicrographs of Microstructure of Joint Region of Combination A Material HIP Joined for Four Hours at 1120°C (2050°F)/105 MPa (15 ksi).

a) Combination A, HIP'ed at 1120°C (2050°F)/103 MPa (15 ksi)/4 Hours Plus 1163°C (2125°F)/137 MPa (20 ksi)/4 Hours.

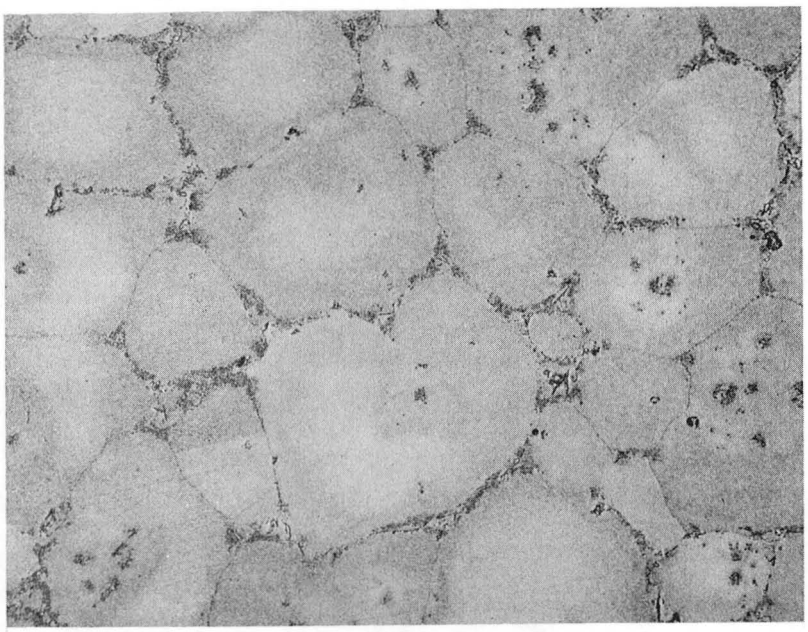

b) Vacuum Presintered Rene' 95 HIP'ed at 1143°C (2090°F)/137 MPa (20 ksi)/4 Hours.

Figure 10. Light Photomicrographs of Microstructure of Various Combination A Materials HIP'ed at Two Conditions at NASA, Magnification, 100X.

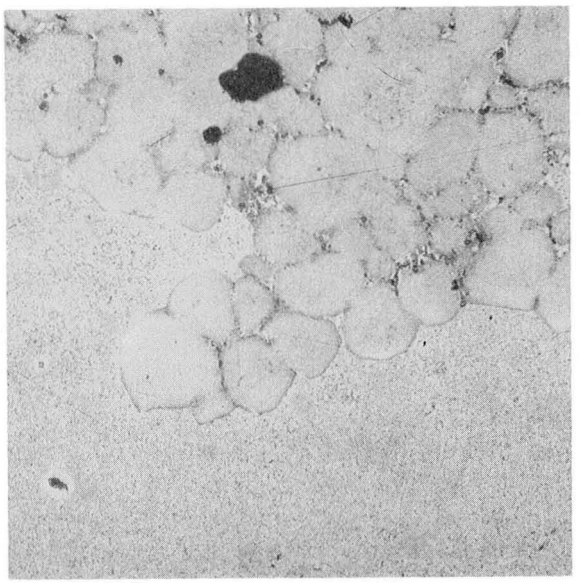

a) Joint, 50X

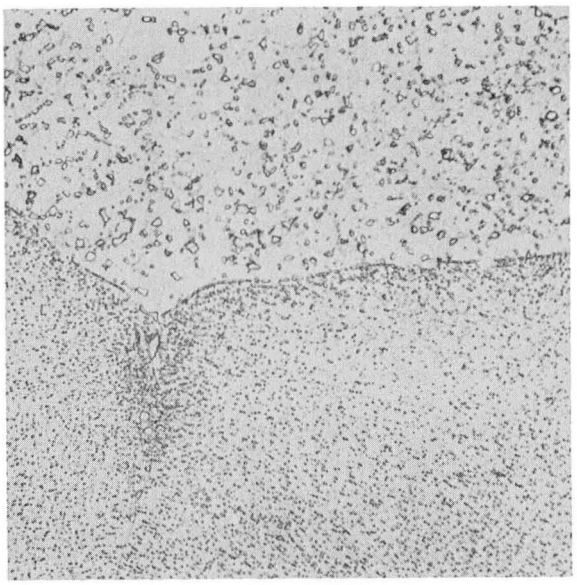

b) Joint, 500X

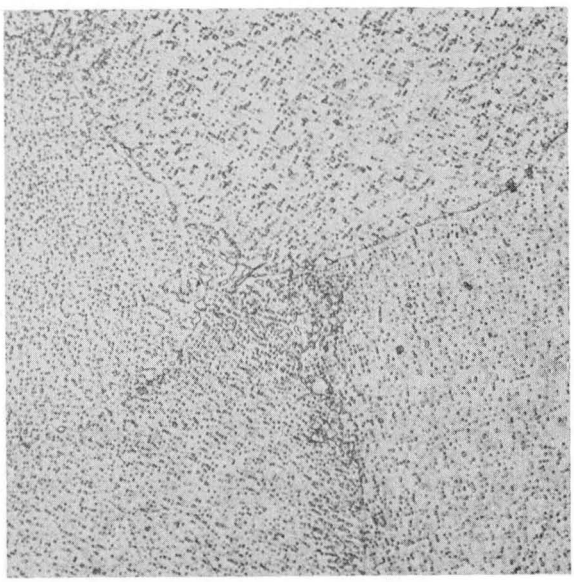

c) Rim, Vacuum Presintered
Rene' 95, 500X

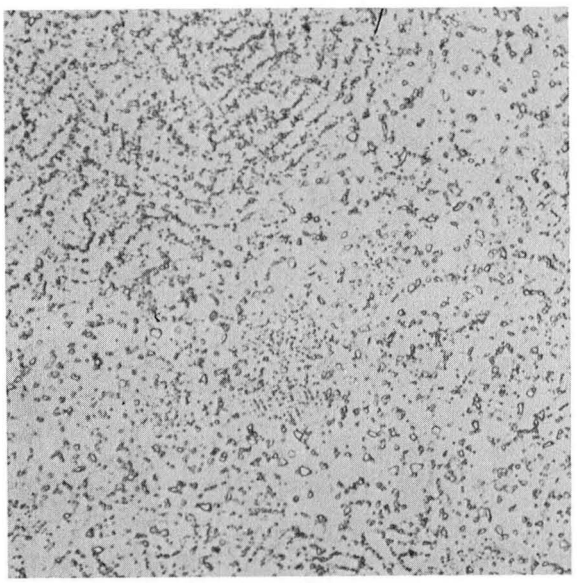

d) Hub, Loose Powder
Rene' 95, 500X

Figure 11. Light Photomicrographs of Microstructure of Combination A with Hub (Standard Rene' 95) Heat Treatment.
1150°C (2100°F)/2 Hours Salt Quench to 540°C (1000°F)
+ 870°C (1600°F)/1 Hour+ 650°C (1200°F)/24 Hours.

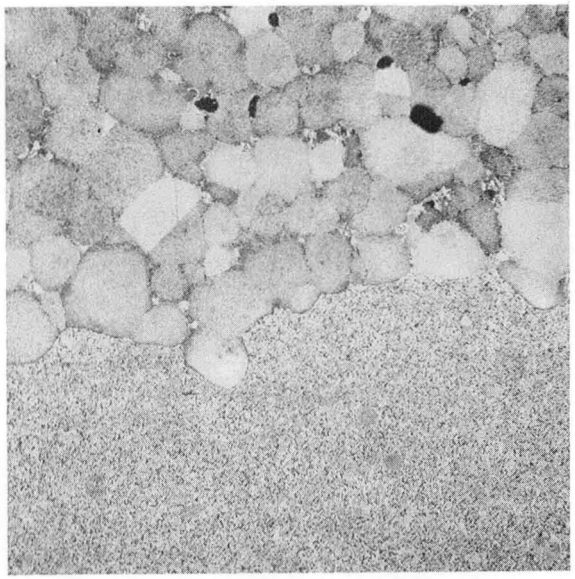

a) Joint, 50X

b) Joint, 500X

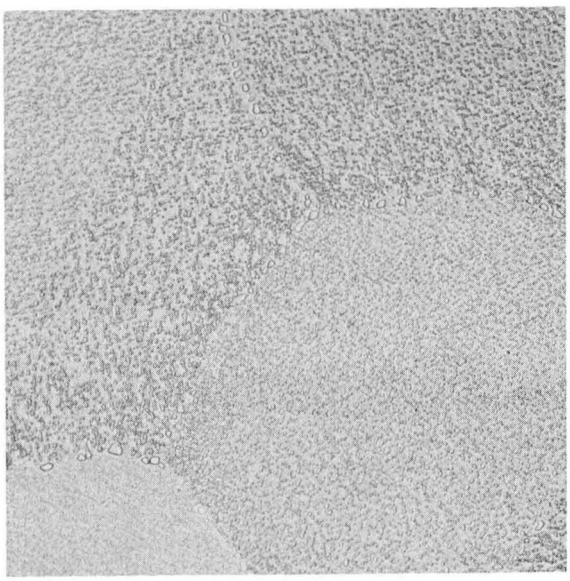

c) Rim, Vacuum Presintered
Rene' 95, 500X

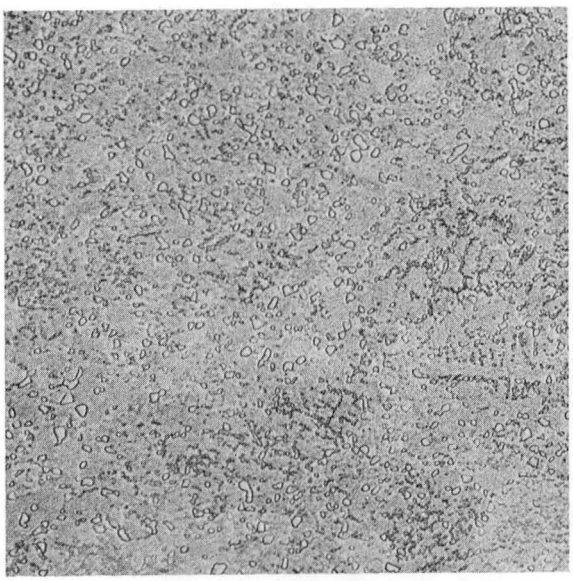

d) Hub, Loose Powder
Rene' 95, 500X

Figure 12. Light Photomicrographs of Microstructures of Combination A with Rim Heat Treatment.
1150°C (2100°F)/2 Hours Salt Quench to 540°C (1000°F)
+ 870°C (1600°F)/8 Hours + 1040°C (1900°F)/4 Hours
+ 650°C (1200°F)/24 Hours + 760°C(1400°F)/8 Hours

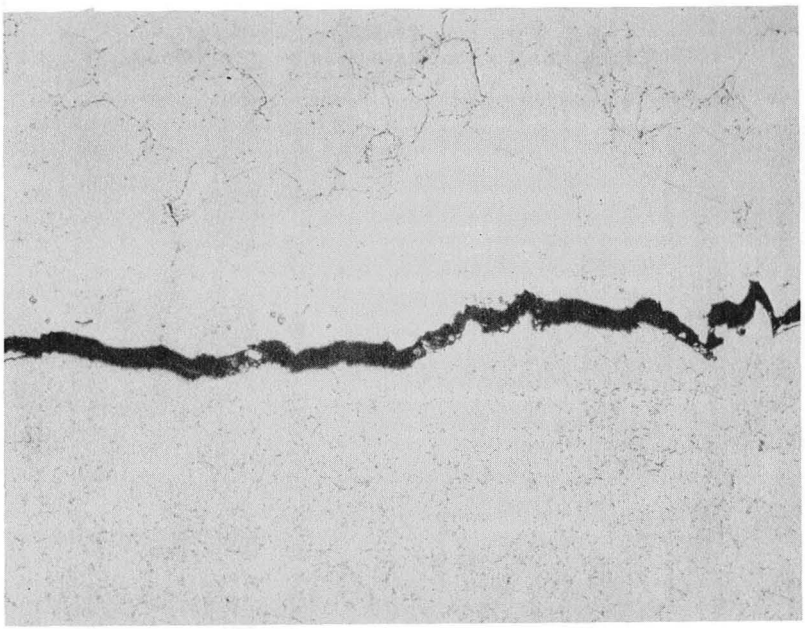

a) 100X

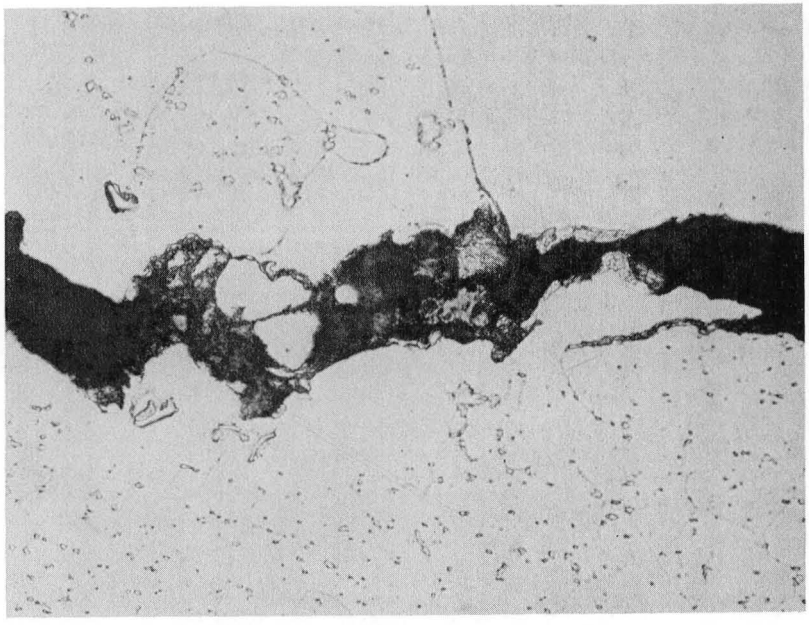

b) 500X

Figure 13. Light Photomicrographs of Crack Located in Joint Area of Combination A with Hub (Standard Rene' 95) Heat Treatment.
1150°C (2100°F)/2 Hours Salt Quench to 540°C (1000°F)
+ 870°C (1600°F)/1 Hour + 650°C (1200°F)/24 Hours

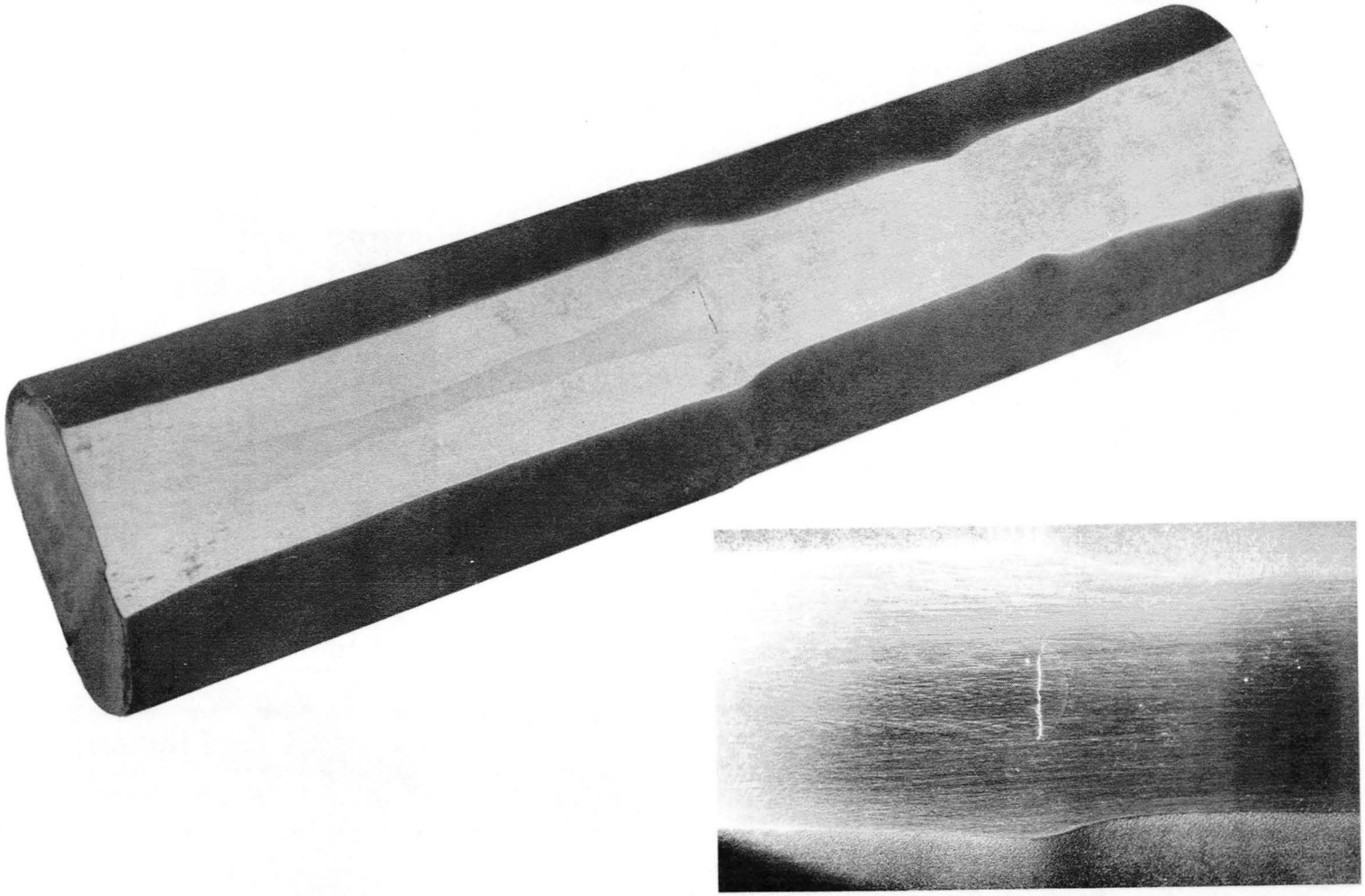

Figure 14. Photograph of Heat Treated Combination A HIP Can Showing a Quench Crack Near the Joint Between the Rim/Hub Candidate Alloys.

50X

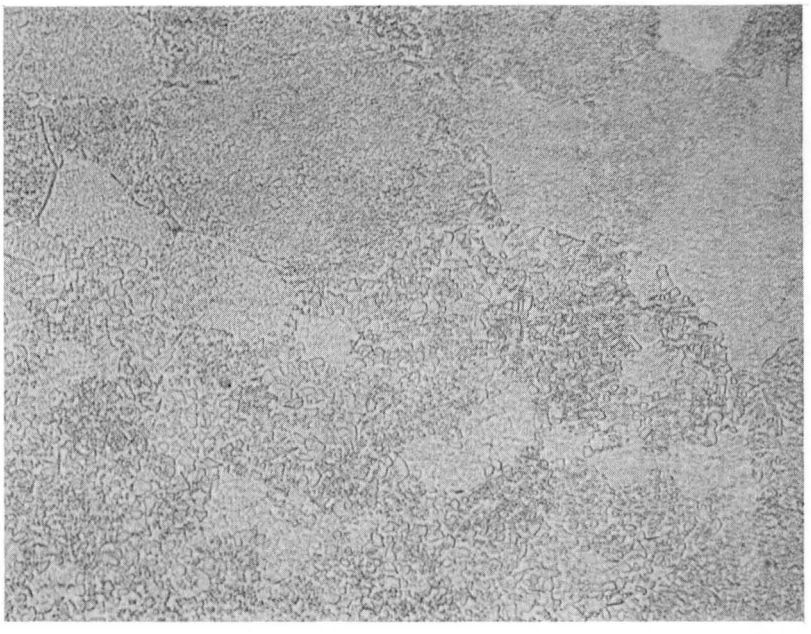

500X

Figure 15. Light Photomicrographs of Microstructure of Combination B, Loose Powder L/C Astroloy Rim, Loose Powder MERL 76 Hub, HIP Joined at 1165°C (2125°F).

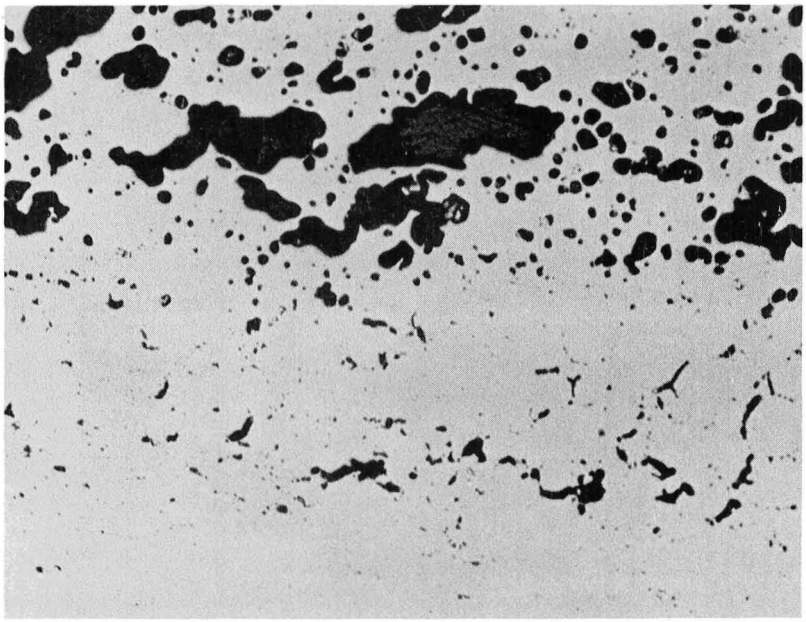

Figure 16. Light Photomicrograph of Structure of Combination B with Hub (Standard MERL 76) Heat Treatment. 1175°C (2145°F)/2 Hours + 760°C (1400°F)/8 Hours. Note Incipient Melting in Both Materials. Magnification, 50X.

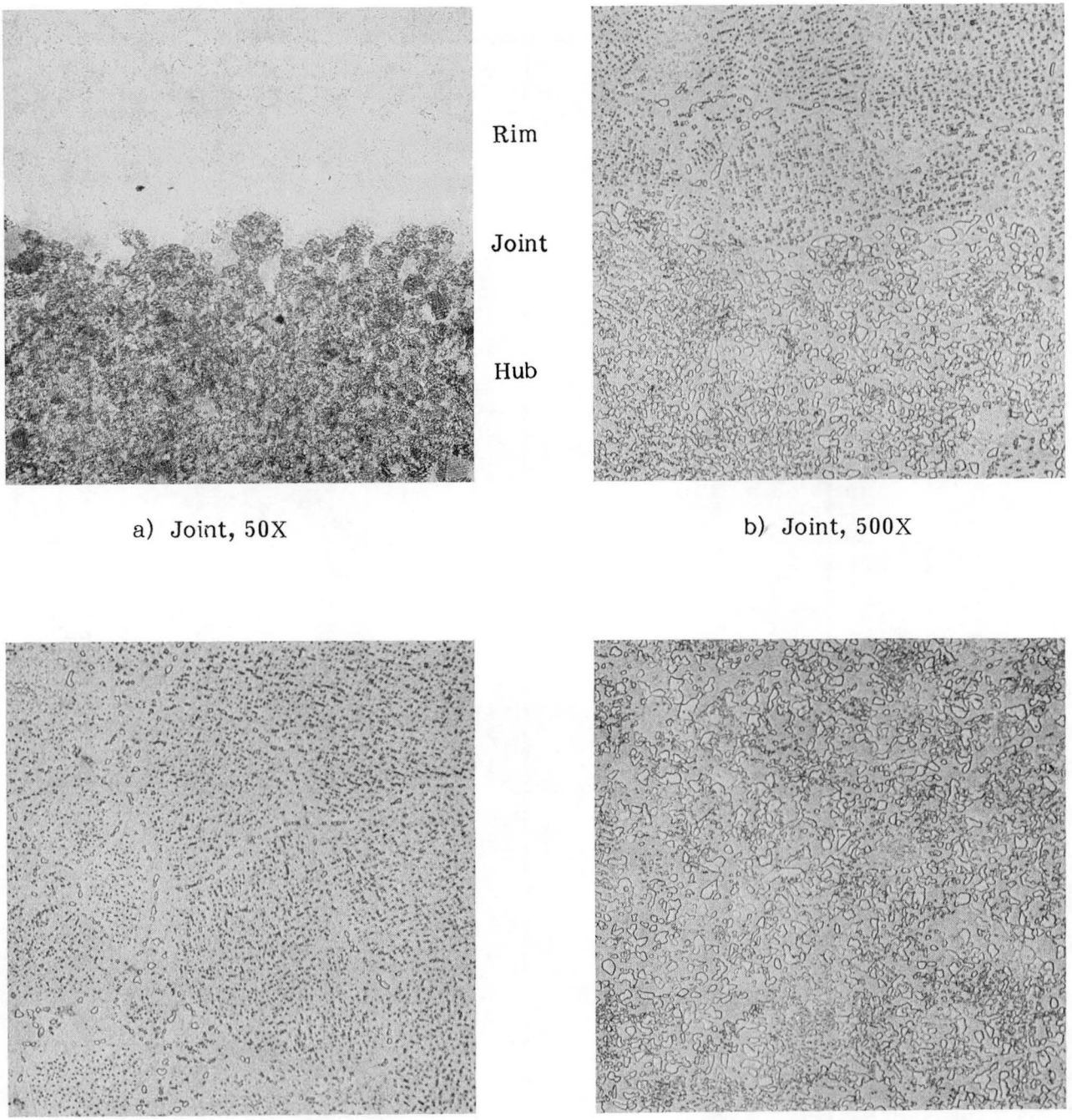

a) Joint, 50X

b) Joint, 500X

c) Rim, Loose Powder Astroloy, 500X

d) Hub, Loose Powder MERL 76, 500X

Figure 17. Light Photomicrographs of Structure of Combination B with Rim (Standard L/C Astroloy) Heat Treatment. 1115°C (2040°F)/2 Hours + 870°C (1600°F)/8 Hours + 980°C (1800°F)/4 Hours + 650°C (1200°F)/24 Hours + 760°C (1400°F)/8 Hours

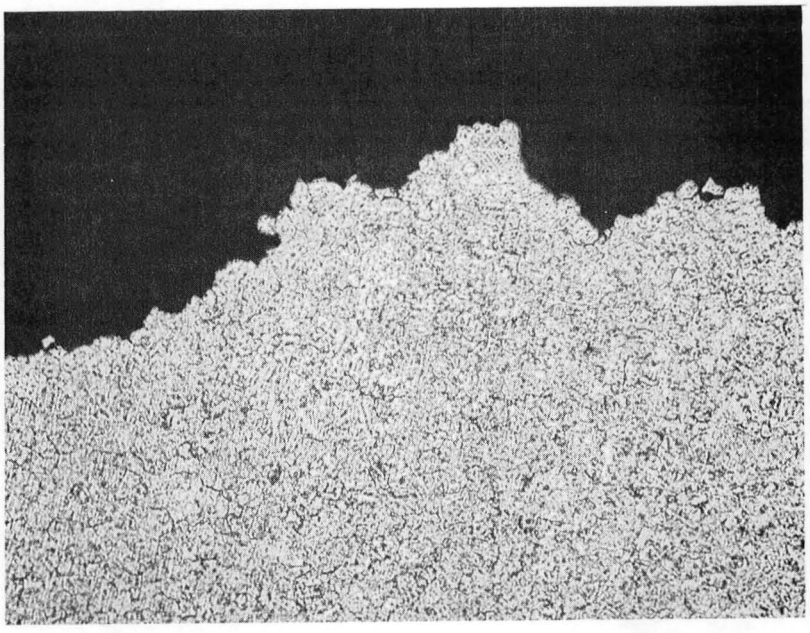

(a)

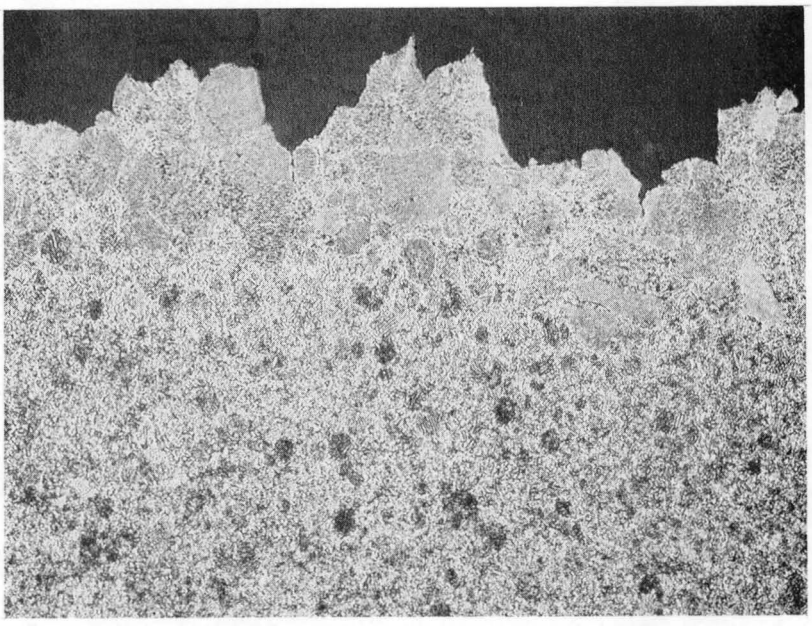

(b)

Figure 18. Light Photomicrographs of Microstructures of (a) MERL 76 Tensile Specimen Exhibiting Ultimate Tensile Strength of 1235 MPa (179 ksi) at 480°C (900°F) and (b) MERL 76 L/C Astroloy Joint Stress Rupture Specimen Exhibiting 21.3 Hours Rupture Life at 760°C (1400°F)/550 MPa (80 ksi). Magnification 100X.

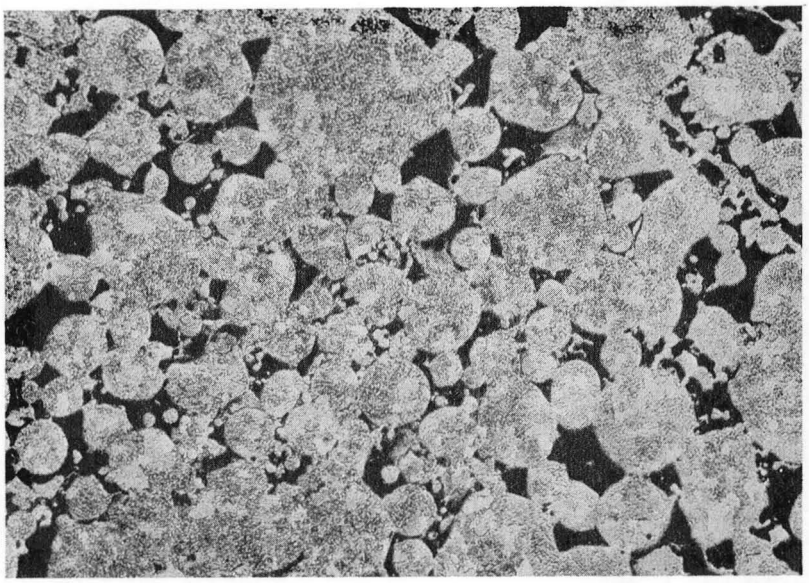

Figure 19. Light Photomicrograph of Microstructure of AF-115 Powder HIP Consolidated at 1190°C (2175°F) for Four Hours and 105 MPa (15 ksi). Note Porosity and Fine Grain Size. Magnification,100X.

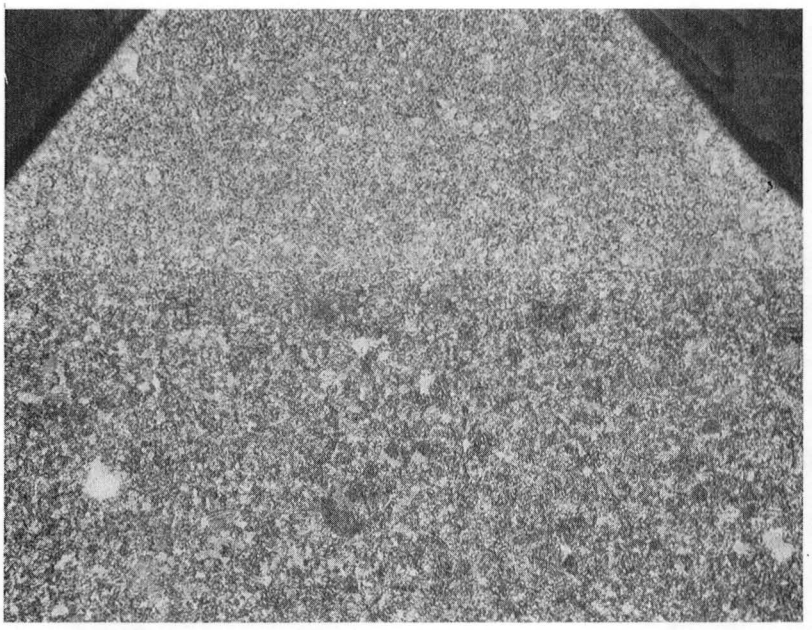

50X

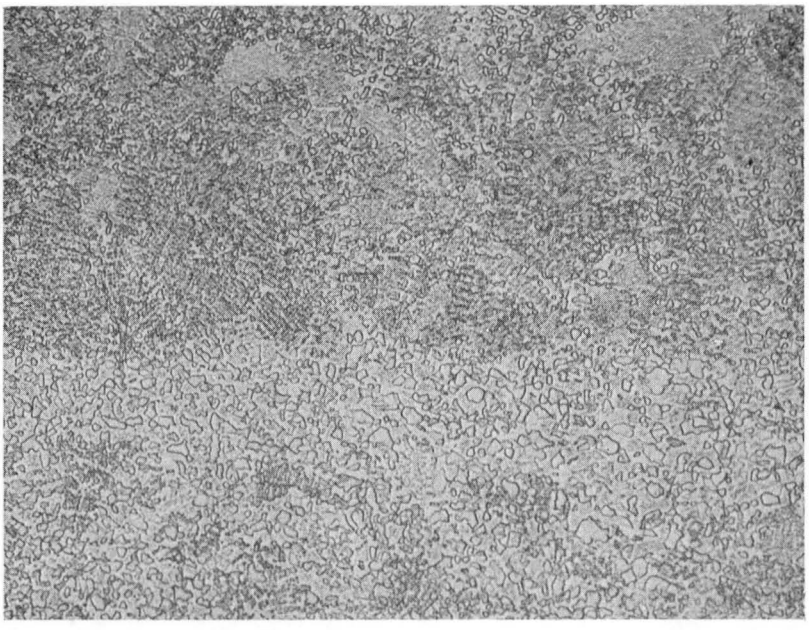

500X

Figure 20. Light Photomicrographs of Microstructure of Combination C, HIP Consolidated AF-115 Rim, Loose Powder Rene' 95 Hub, HIP Joined at 1120°C (2050°F) for Four Hours and 105 MPa (15 ksi).

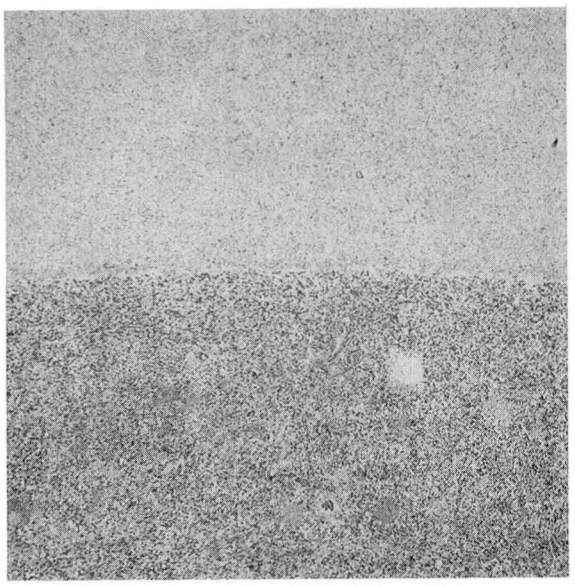

a) Joint, 50X

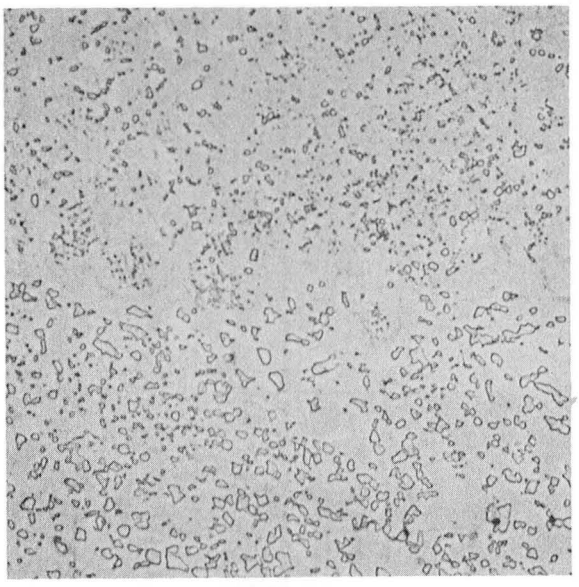

b) Joint, 500X

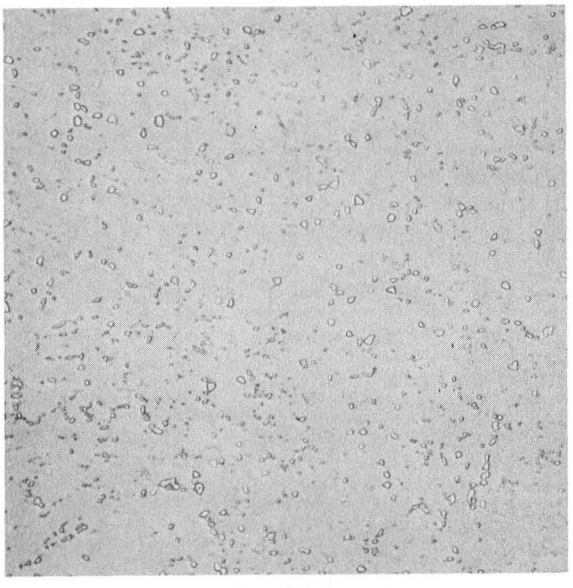

c) Rim HIP'ed AF-115, 500X

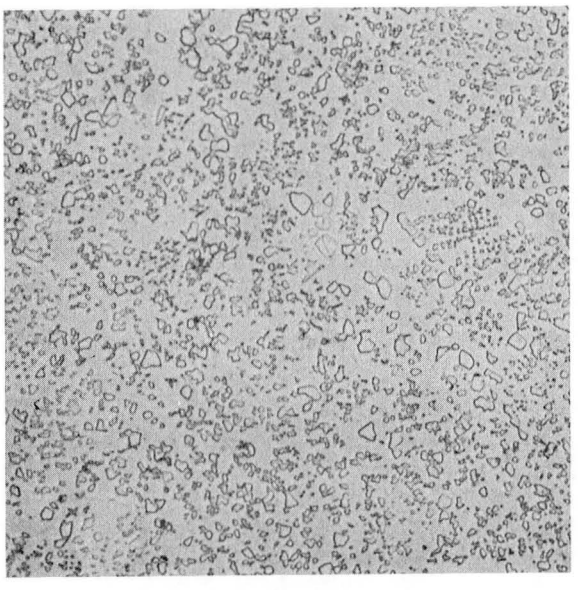

d) Hub, Loose Powder Rene 95, 500X

Figure 21. Light Photomicrographs of Microstructure of Combination C with Hub (Standard Rene' 95) Heat Treatment.
1150°C (2100°F)/2 Hours Salt Quench to 540°C (1000°F)
+ 870°C (1600°F)/1 Hour + 650°C (1200°F)/24 Hours

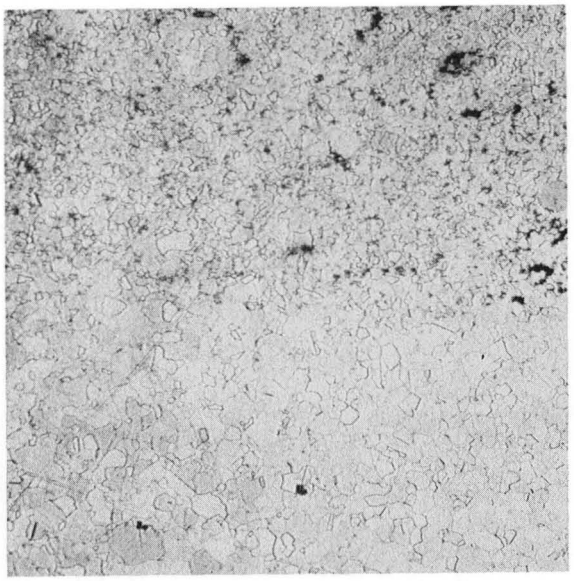

Rim

Joint

Hub

a) Joint, 50X

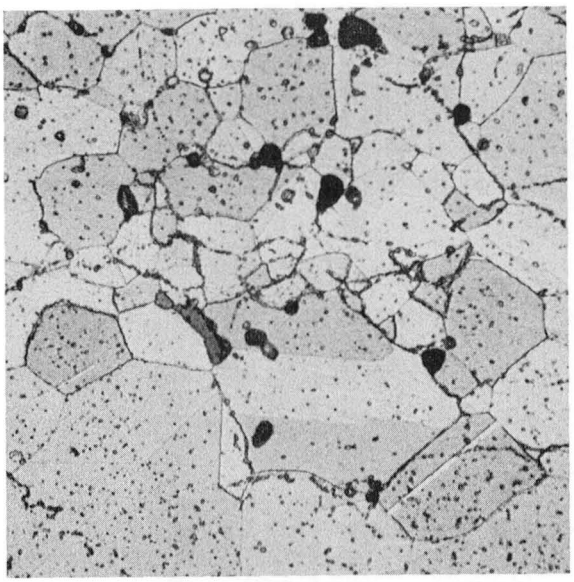

b) Joint, 500X

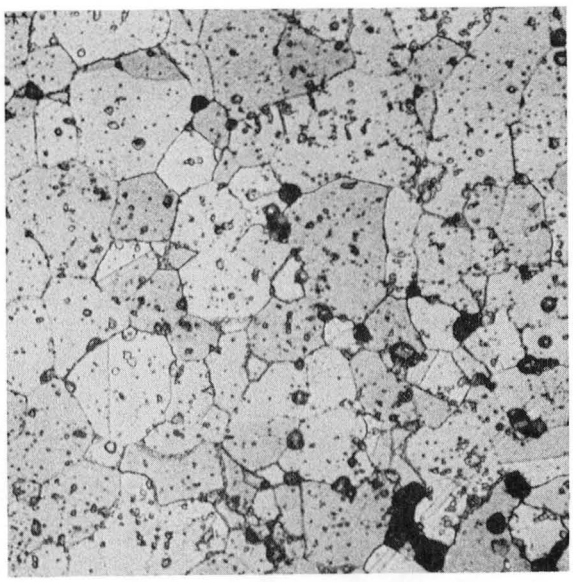

c) Rim, HIP'ed AF-115, 500X

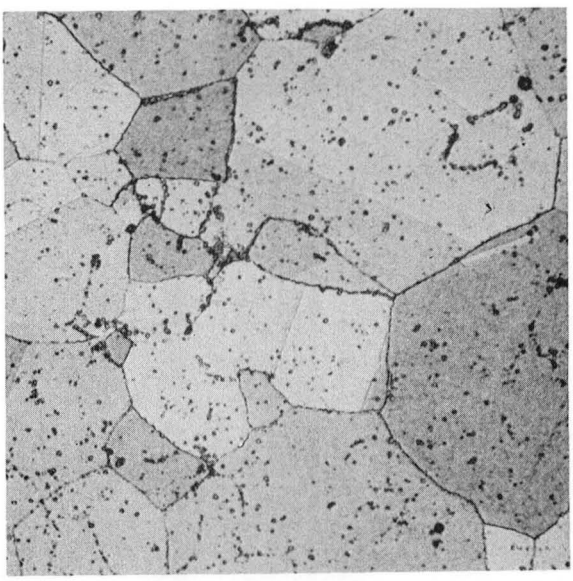

d) Hub, Loose Powder Rene' 95, 500X

Figure 22. Light Photomicrographs of Microstructure of Combination C with Rim (Standard AF-115) Heat Treatment. 1190°C (2175°F)/2 Hours + 760°C (1400°F)/16 Hours. Note Porosity in Rim Material.

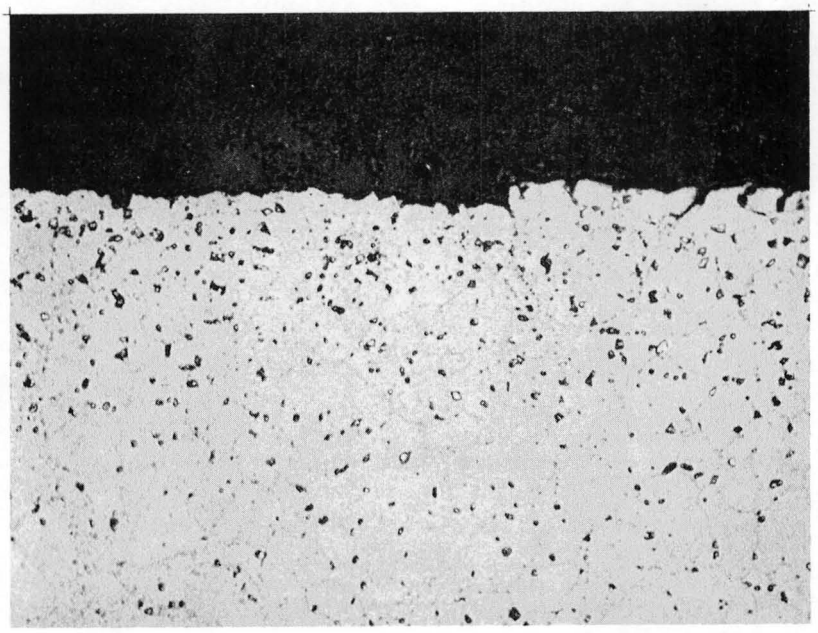

a) Fracture Surface of Joint Specimen Exhibiting 20.7 Hours Rupture Life at 760°C (1400°F)/550 MPa (80 ksi). Note Failure Along Joint Interface.

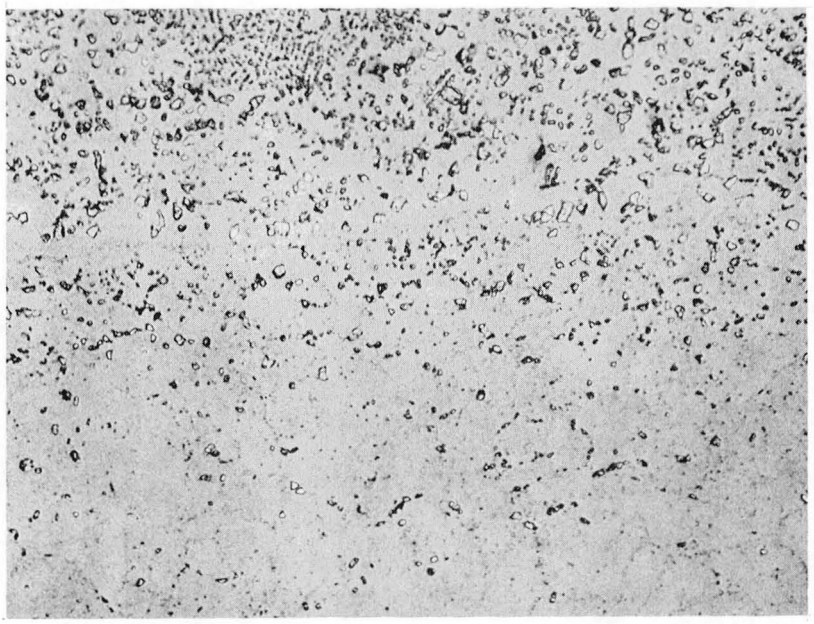

b) Joint Region of Specimen Exhibiting 1235 MPa (179 ksi) Ultimate Tensile Strength at 480°C (900°F). AF-115 Material is in Upper Portion of Photomicrograph.

Figure 23. Light Photomicrographs of Microstructures of First Iteration Combination C Failed Joint Test Specimens. Magnification, 500X.

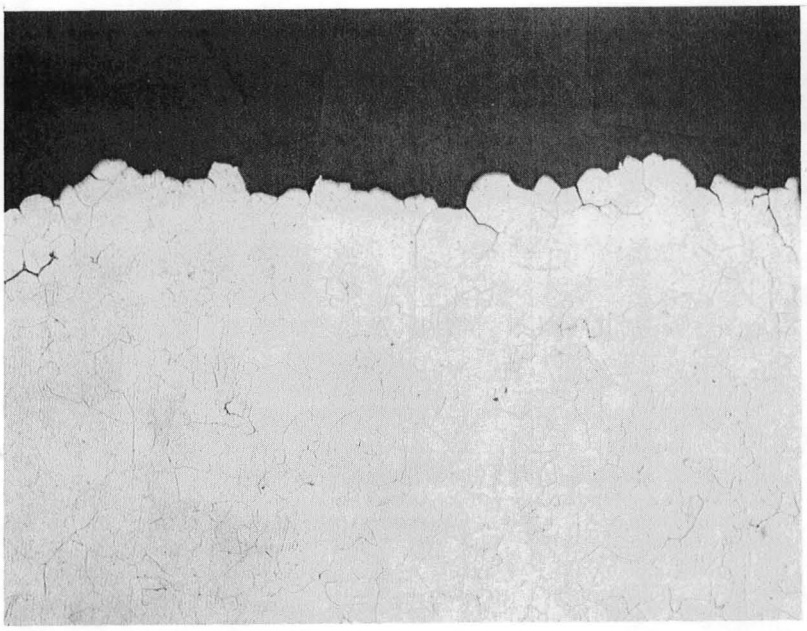

(a) 100X

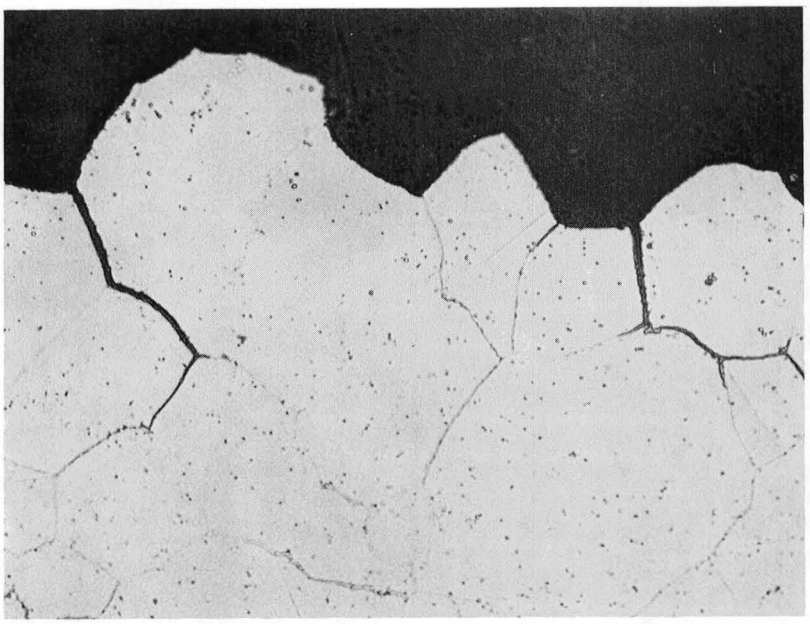

(b) 500X

Figure 24. Light Photomicrographs of Third Iteration Combination C Failed Joint Stress Rupture Specimen Exhibiting 124.1 Hours Rupture Life at 760°C (1400°F)/550 MPa (80 ksi).

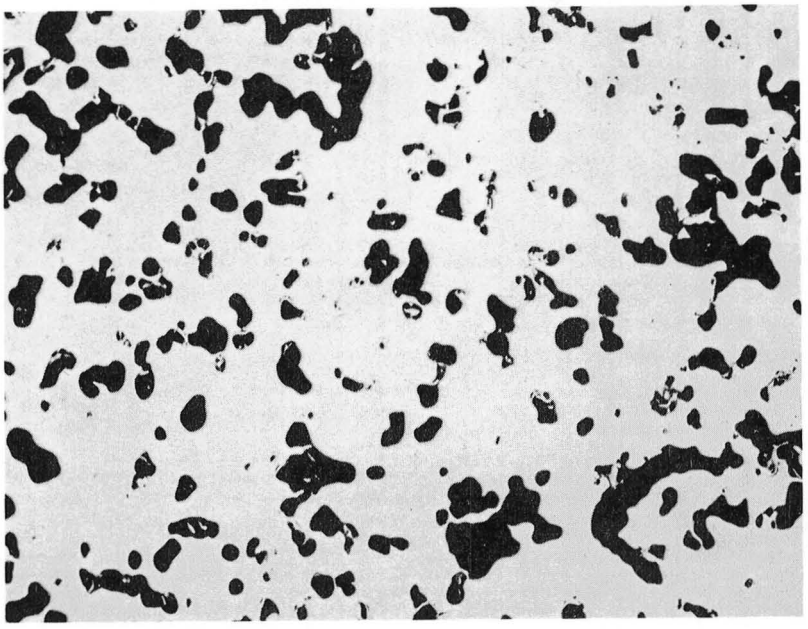

a) 1245°C (2270°F) Sintering Temperature.

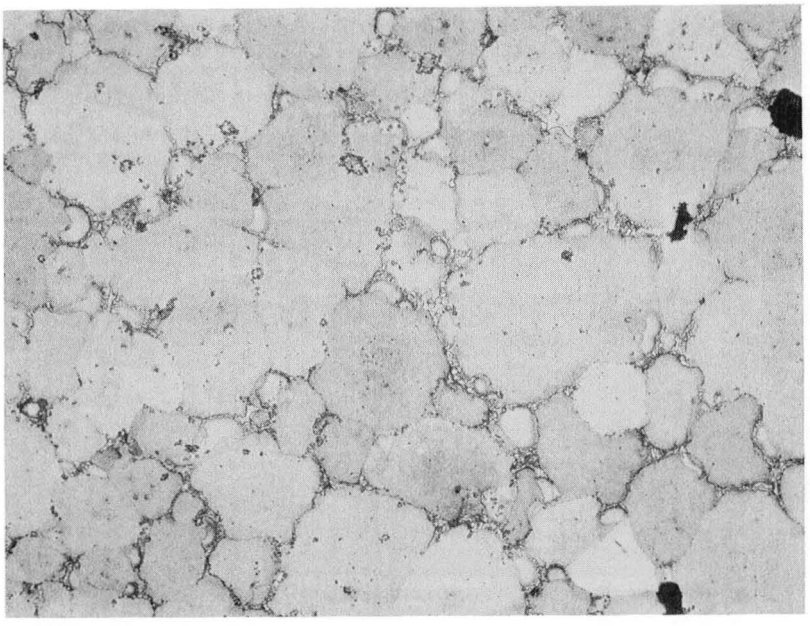

b) 1260°C (2300°F) Sintering Temperature.

Figure 25. Light Photomicrographs of Microstructures of PA-101 Powder Vacuum Sintered for Six Hours at 1245°C (2270°F) and 1260°C (2300°F). Magnification, 100X.

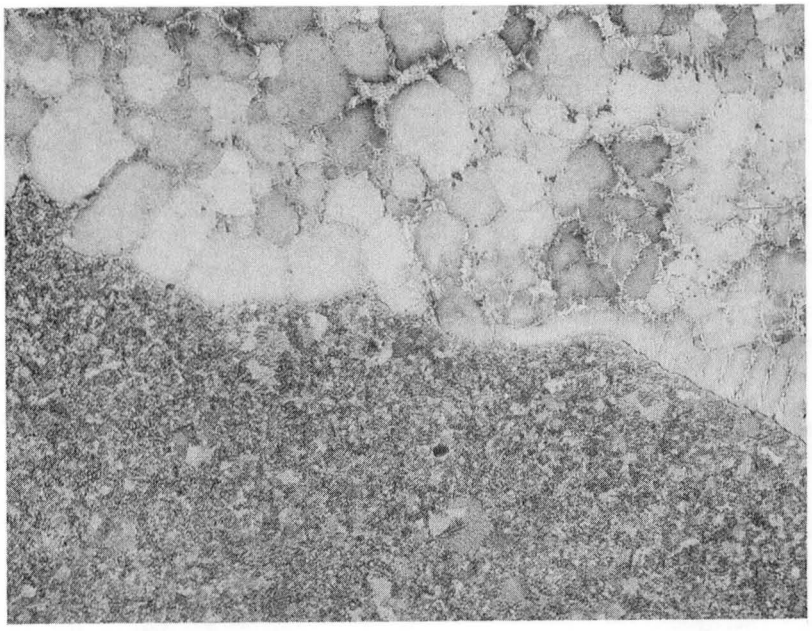

50X

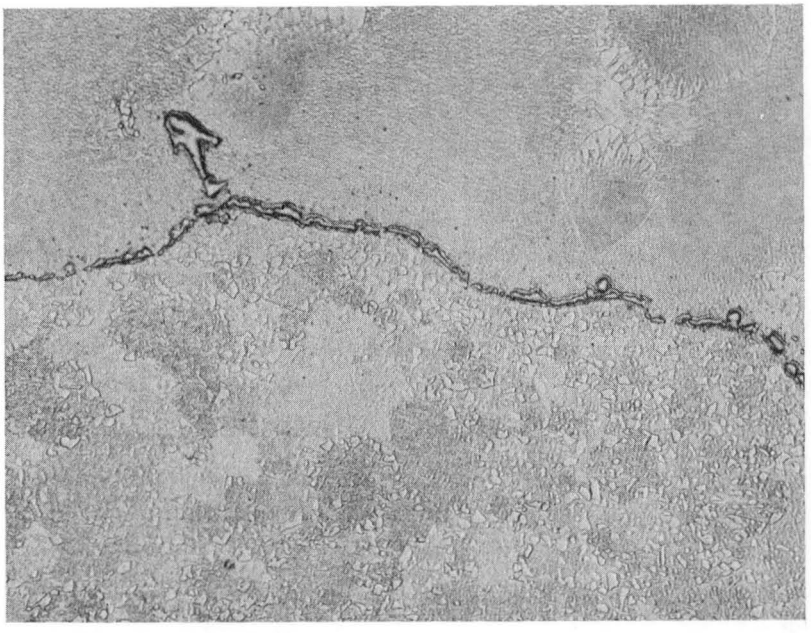

500X

Figure 26. Light Photomicrographs of Microstructures of Combination D, Vacuum Sintered PA-101 Rim, Loose Powder MERL 76 Hub, HIP Joined at 1165°C (2125°F).

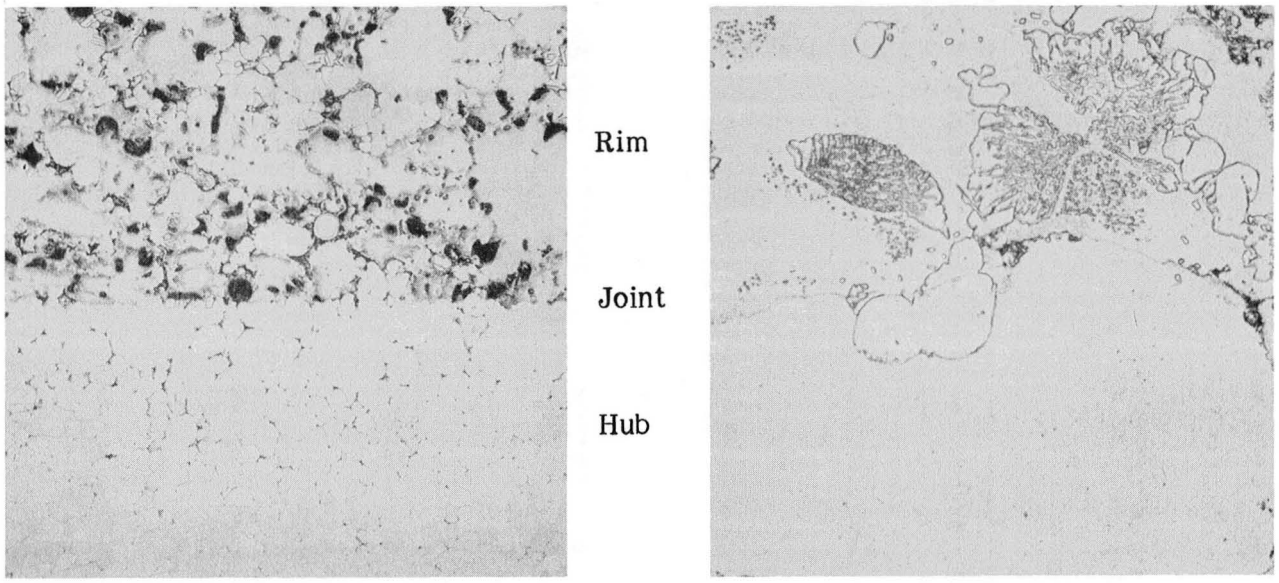

a) Joint, 50X

b) Joint, 500X

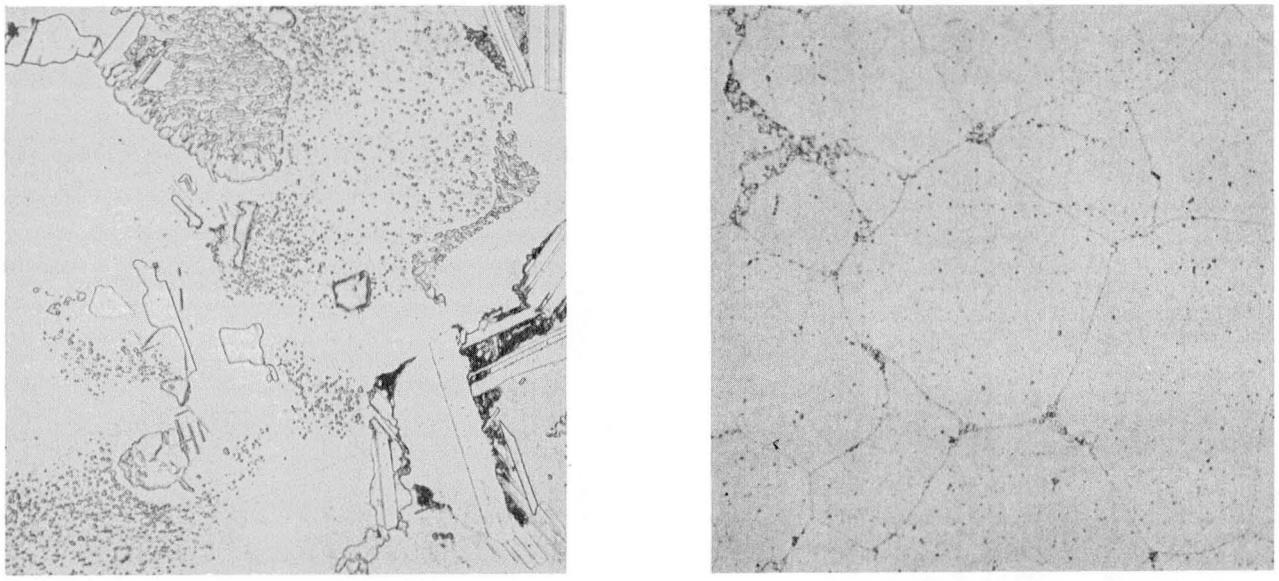

c) Rim, Vacuum Presintered PA101, 500X

d) Hub, Loose Powder MERL 76, 500X

Figure 27. Light Photomicrographs of Microstructure of Combination D with Hub (Standard MERL 76) Heat Treatment. 1175°C (2145°F)/2 Hours + 760°C (1400°F)/8 Hours. Note Incipient Melting in PA-101 Rim, and Grain Boundary Liquation of MERL 76 Hub Adjacent to Joint.

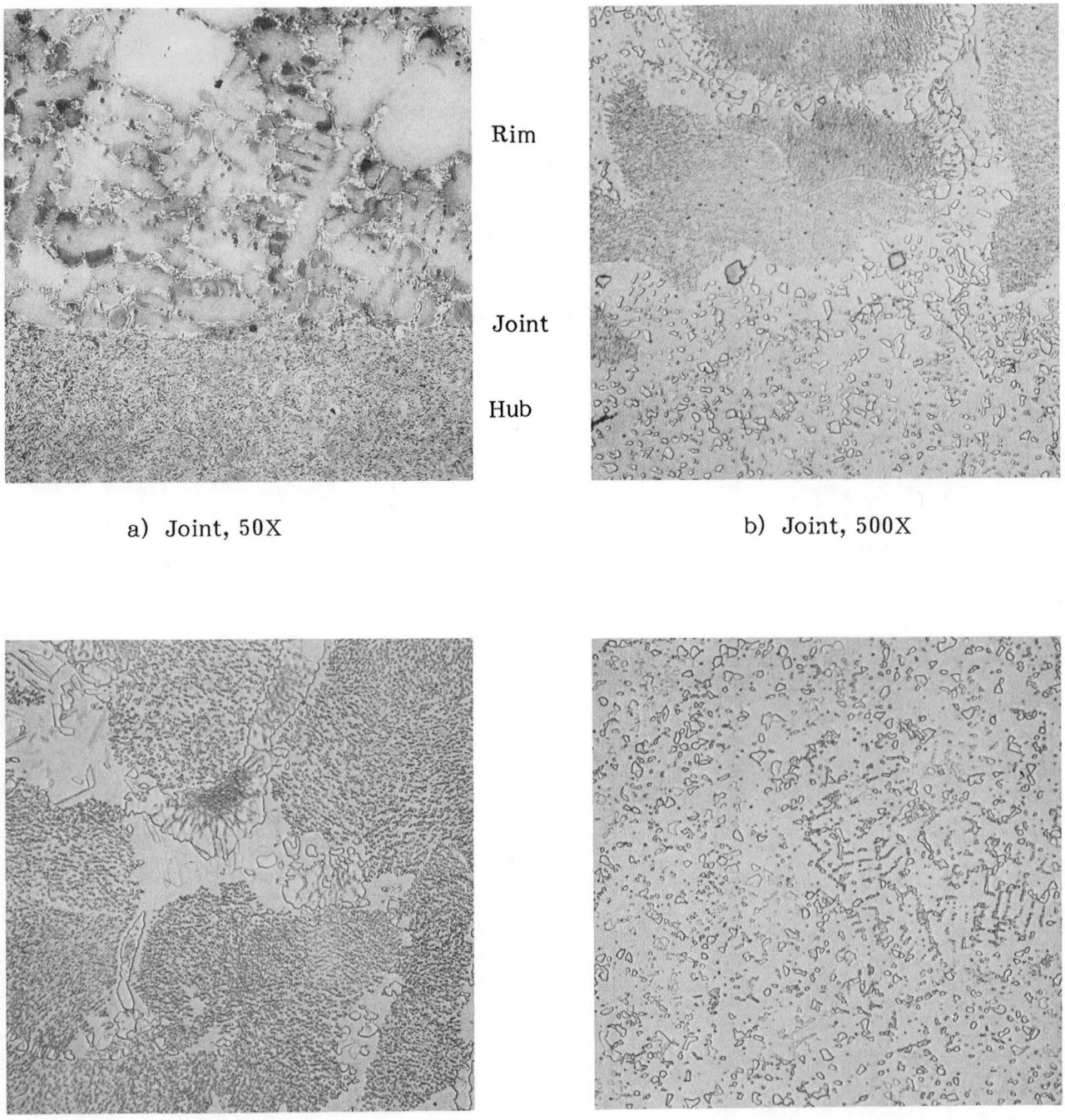

a) Joint, 50X

b) Joint, 500X

c) Rim, Vacuum Presintered PA101, 500X

d) Hub, Loose Powder MERL 76, 500X

Figure 28. Light Photomicrographs of Microstructure of Combination D Solution Treated at 1165°C (2125°F)/1 Hour Air Cool. Note Lack of Grain Boundary Liquation and the Presence of Coarse Gamma-Prime in MERL 76 Hub Material.

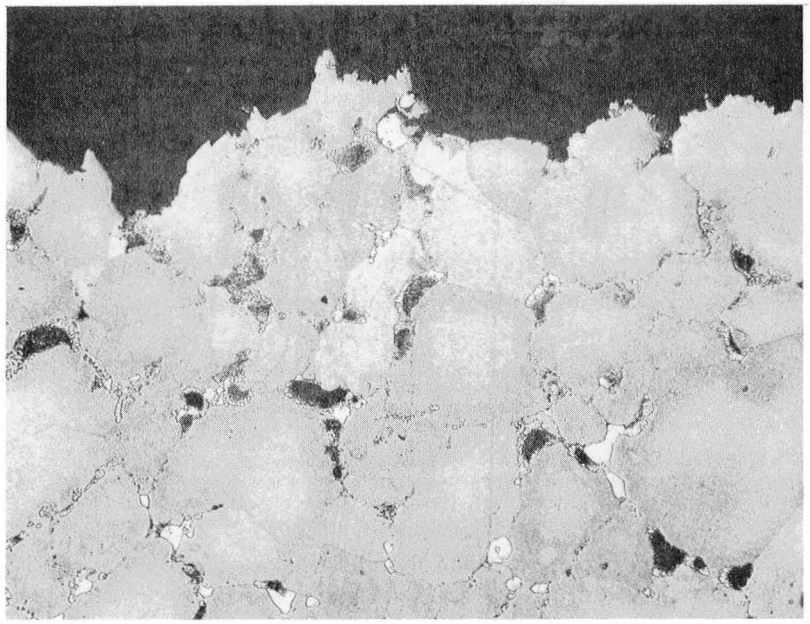

(a) 100X

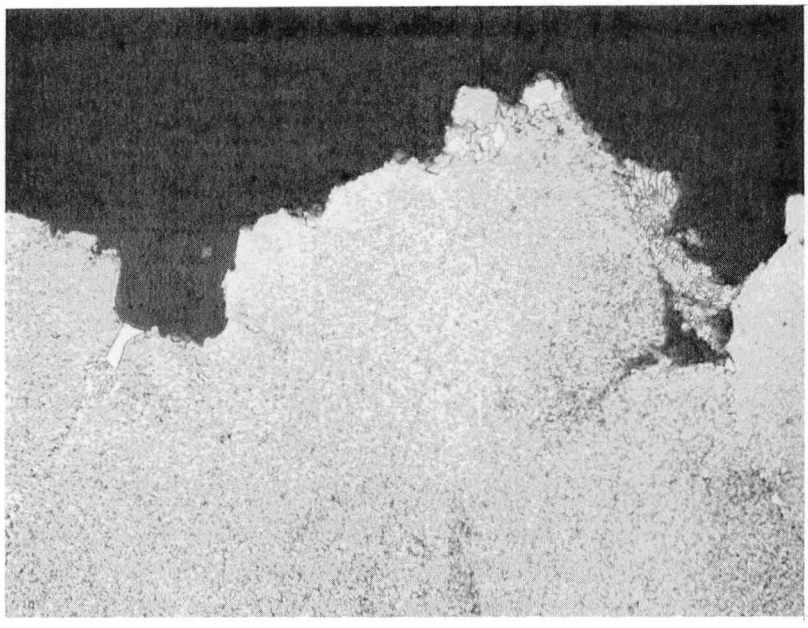

(b) 500X

Figure 29. Light Photomicrographs of Microstructure of First Iteration Combination D Failed Joint Stress Rupture Specimen Exhibiting 10 Hours Rupture Life at 760°C (1400°F)/550 MPa (80 ksi).

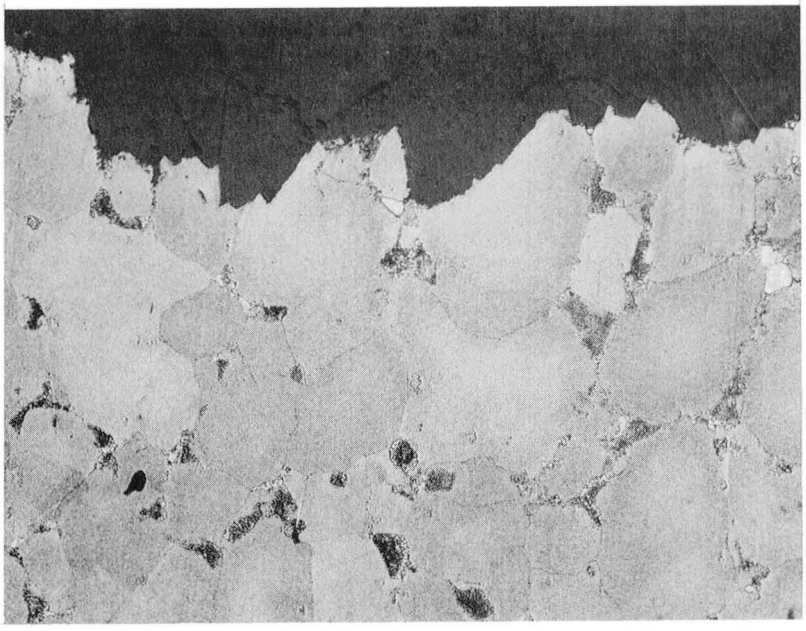

(a) 100X

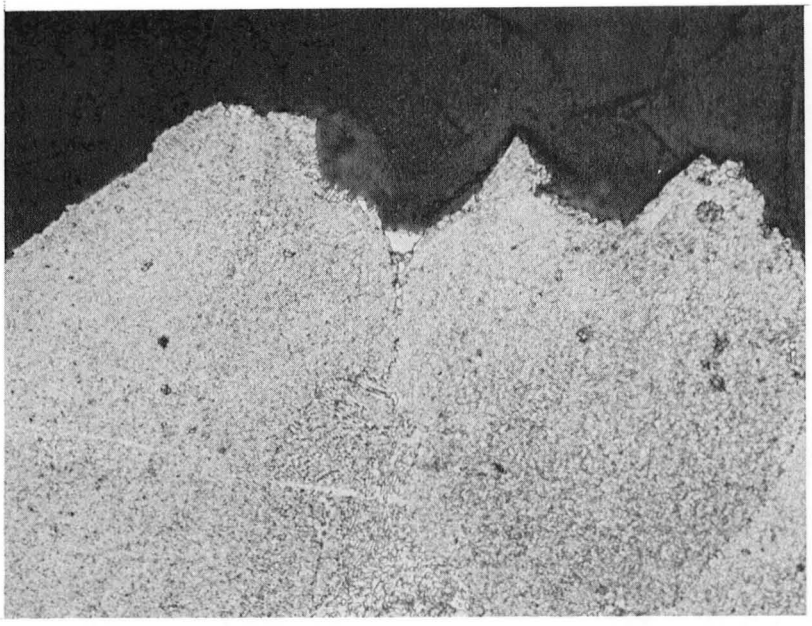

(b) 500X

Figure 30. Light Photomicrographs of Microstructure of Third Iteration Combination D Failed Joint Stress Rupture Specimen Exhibiting 22.7 Hours Life at 760°C (1400°F)/550 MPa (80 ksi).

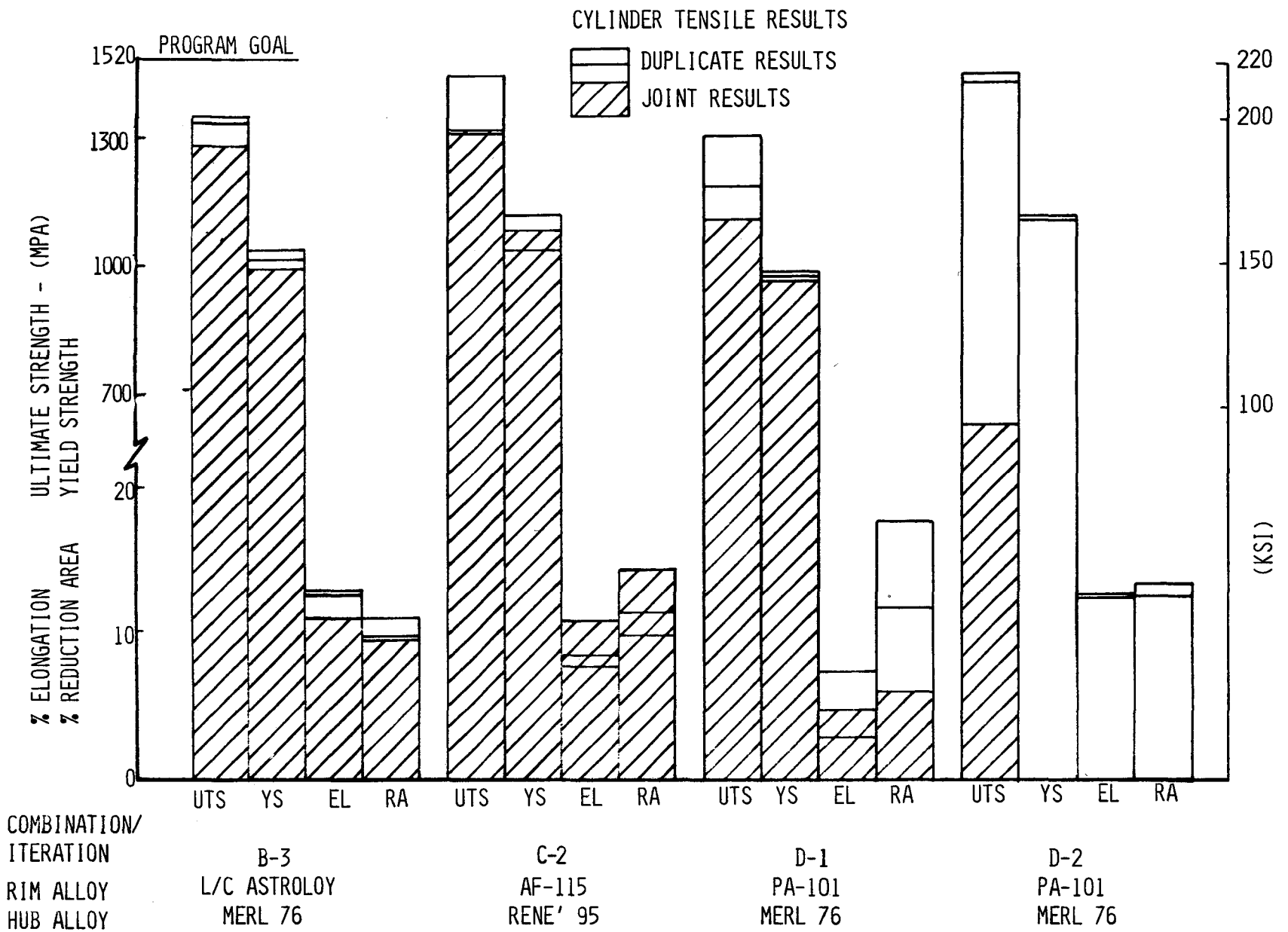

Figure 31. Plot of Optimum 480°C(900°F) Tensile Results for Specimens Machined From Cylinder Shapes.

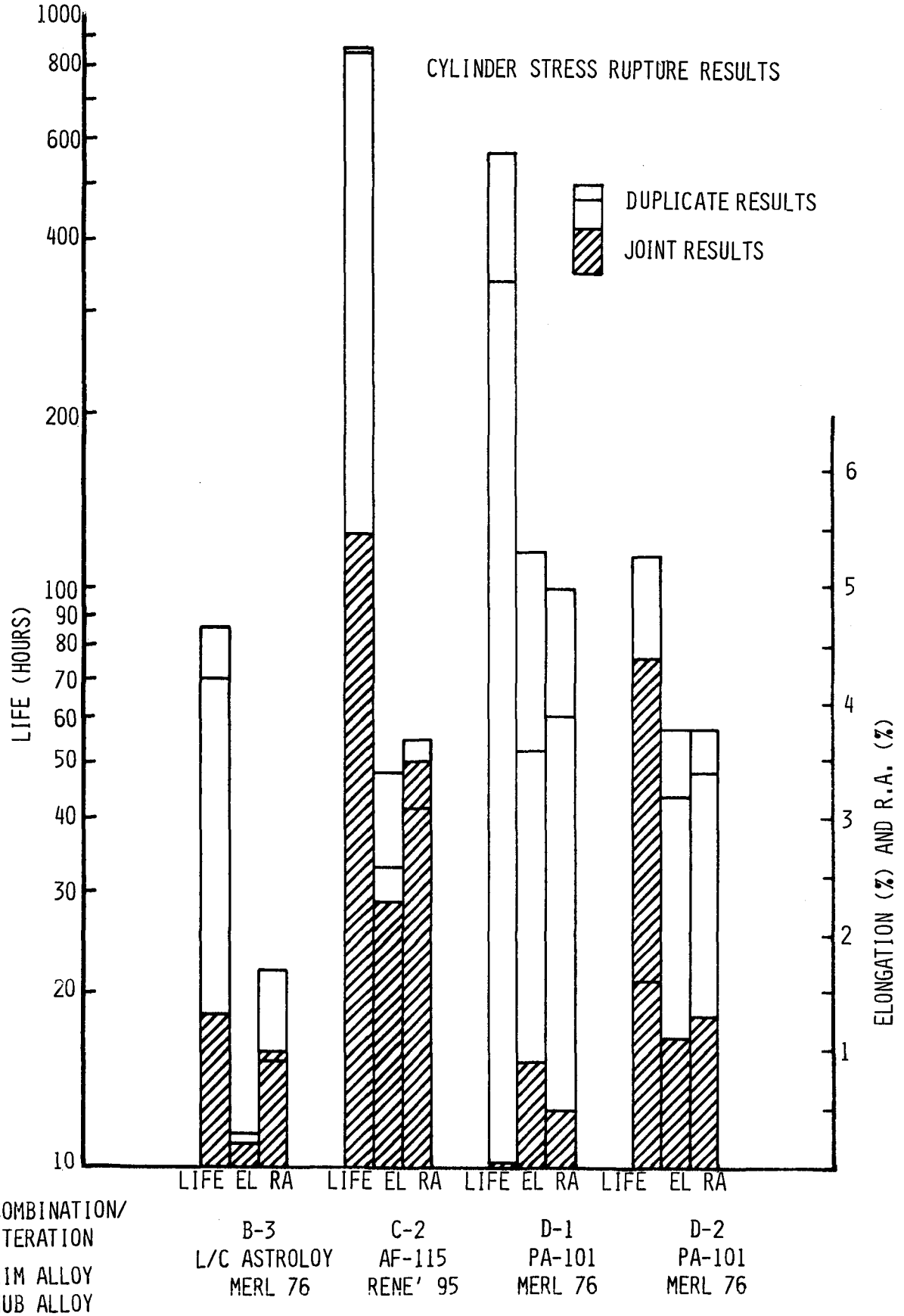

Figure 32. Plot of Optimum 760°C (1400°F)/550 MPa (80 ksi) Stress Rupture Results for Specimens Machined From Cylinder Shapes.

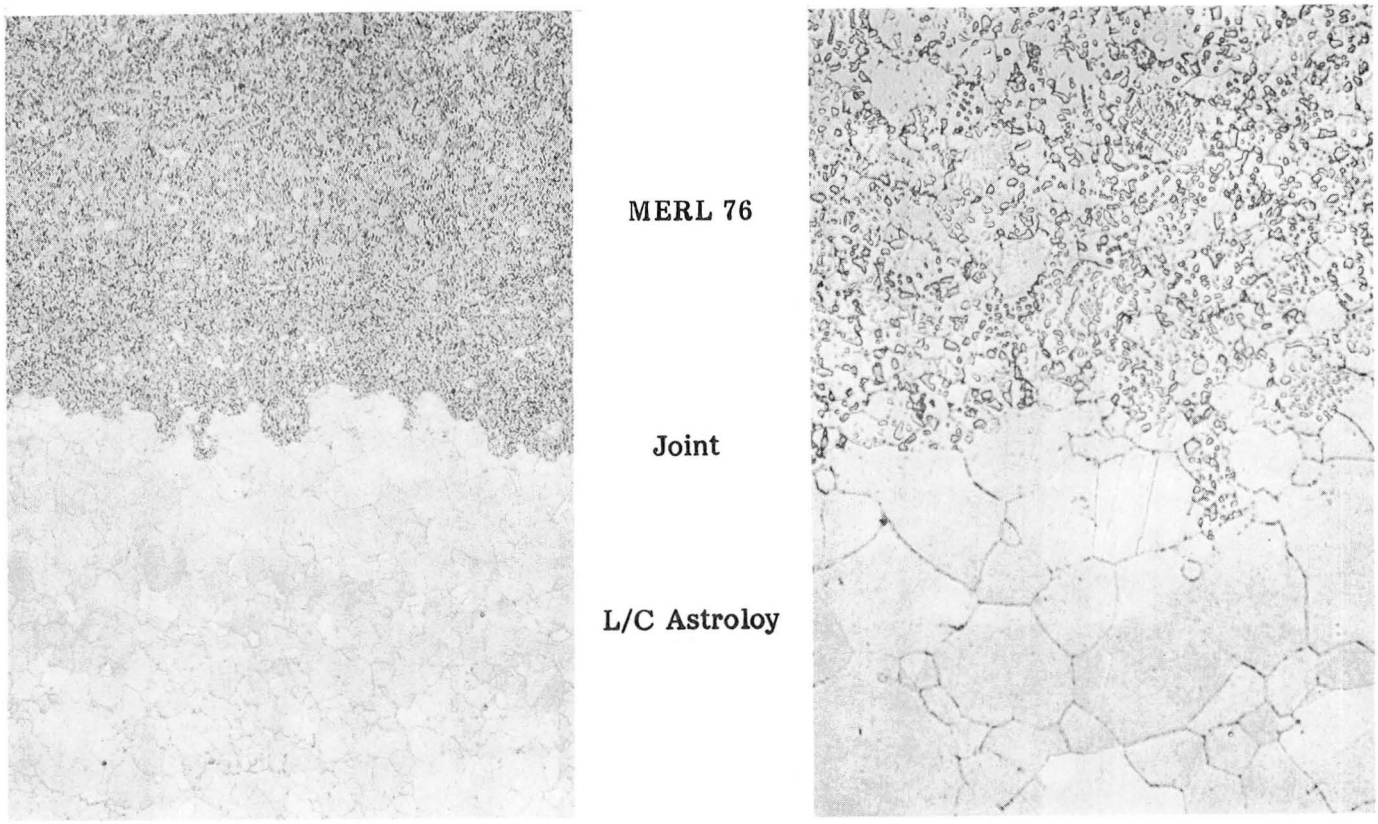

(a) 100X

(b) 500X

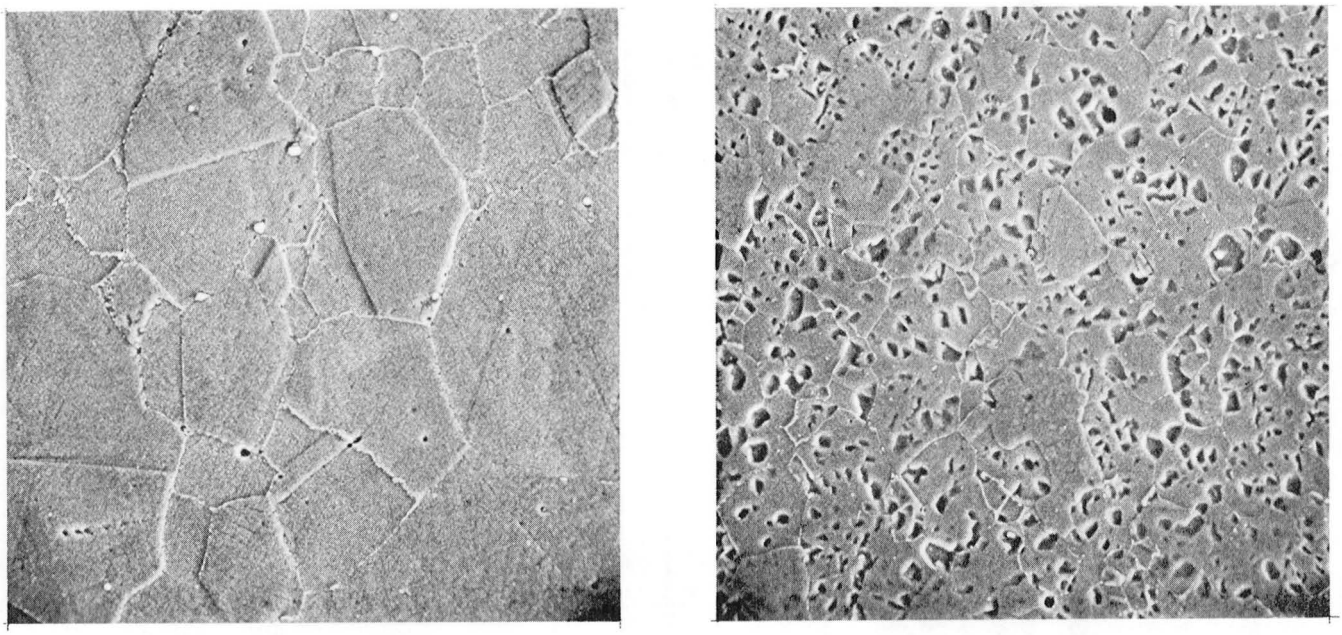

(c) L/C Astroloy - 1000X

(d) MERL 76 - 1000X

Figure 33. Photomicrographs of Heat Treated Microstructure of Combination B Flat Panel Shape After 1170°C (2130°F)/2 Hours Oil Quench +870°C (1600°F)/40 Minutes + 980°C (1800°F)/45 Minutes + 650°C (1200°F)/24 Hours + 760°C (1400°F)/8 Hours.

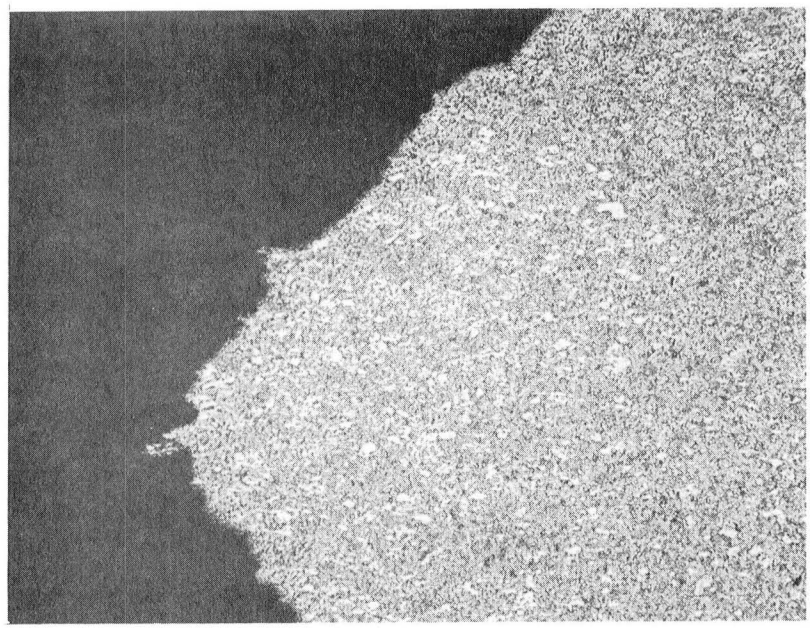

(a) 100X

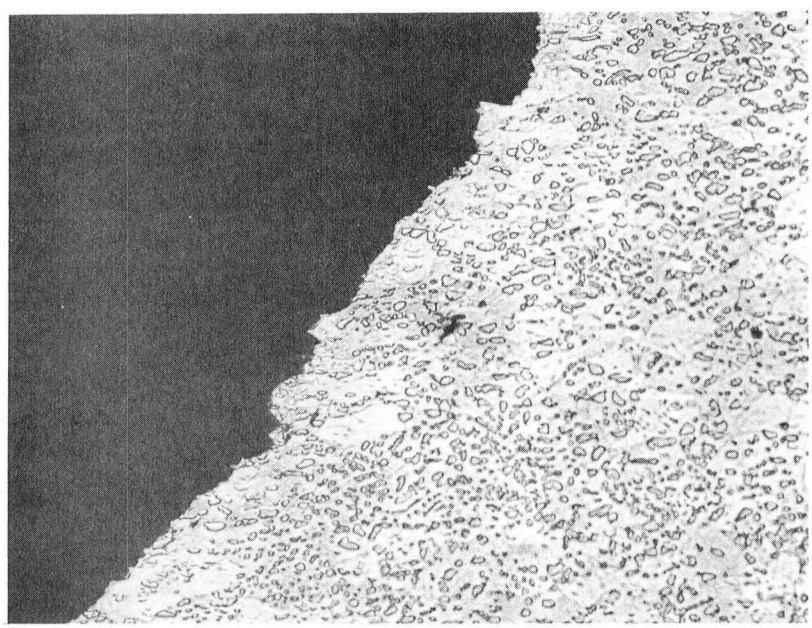

(b) 500X

Figure 34. Light Photomicrographs of Microstructure of MERL 76 Tensile Specimen Exhibiting Ultimate Tensile Strength of 1565 MPa (227 ksi) at 480°C (900°F).

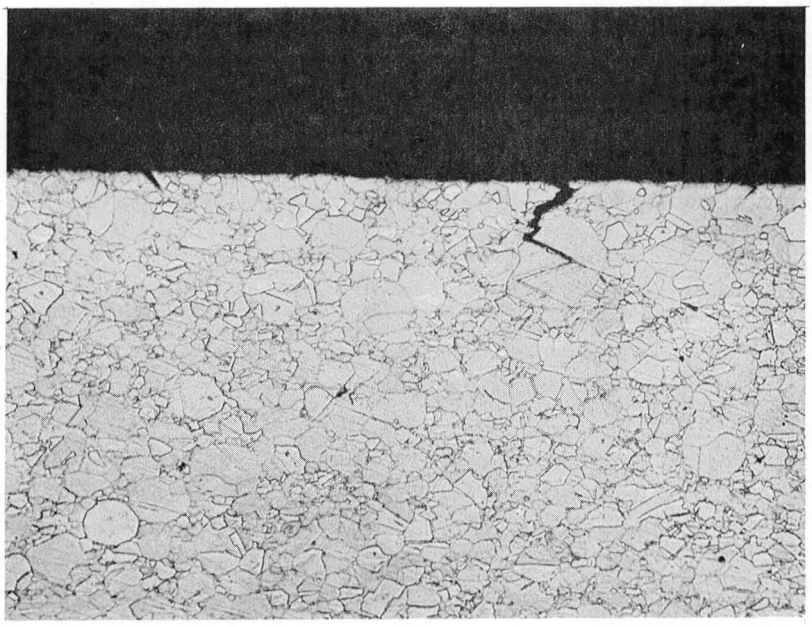

(a) 100X

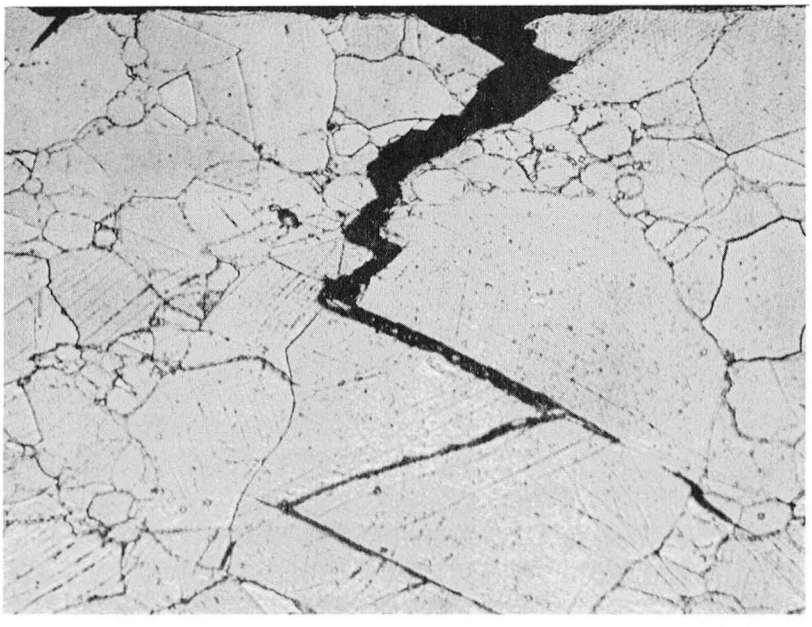

(b) 500X

Figure 35. Light Photomicrographs of Microstructure of L/C Astroloy Tensile Specimen Exhibiting Ultimate Tensile Strength of 1455 MPa (211 ksi) at 480°C (900°F).

(a) 100X

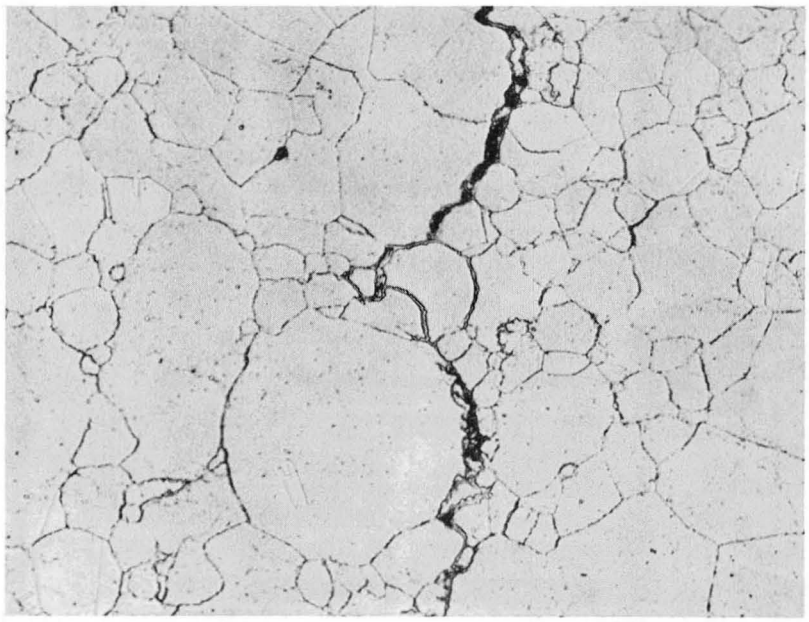

(b) 500X

Figure 36. Light Photomicrographs of Microstructure of MERL 76 L/C Astroloy Joint Stress Rupture Specimen Exhibiting 36.7 Hours Rupture Life at 760°C (1400°F)/550 MPa (80 ksi).

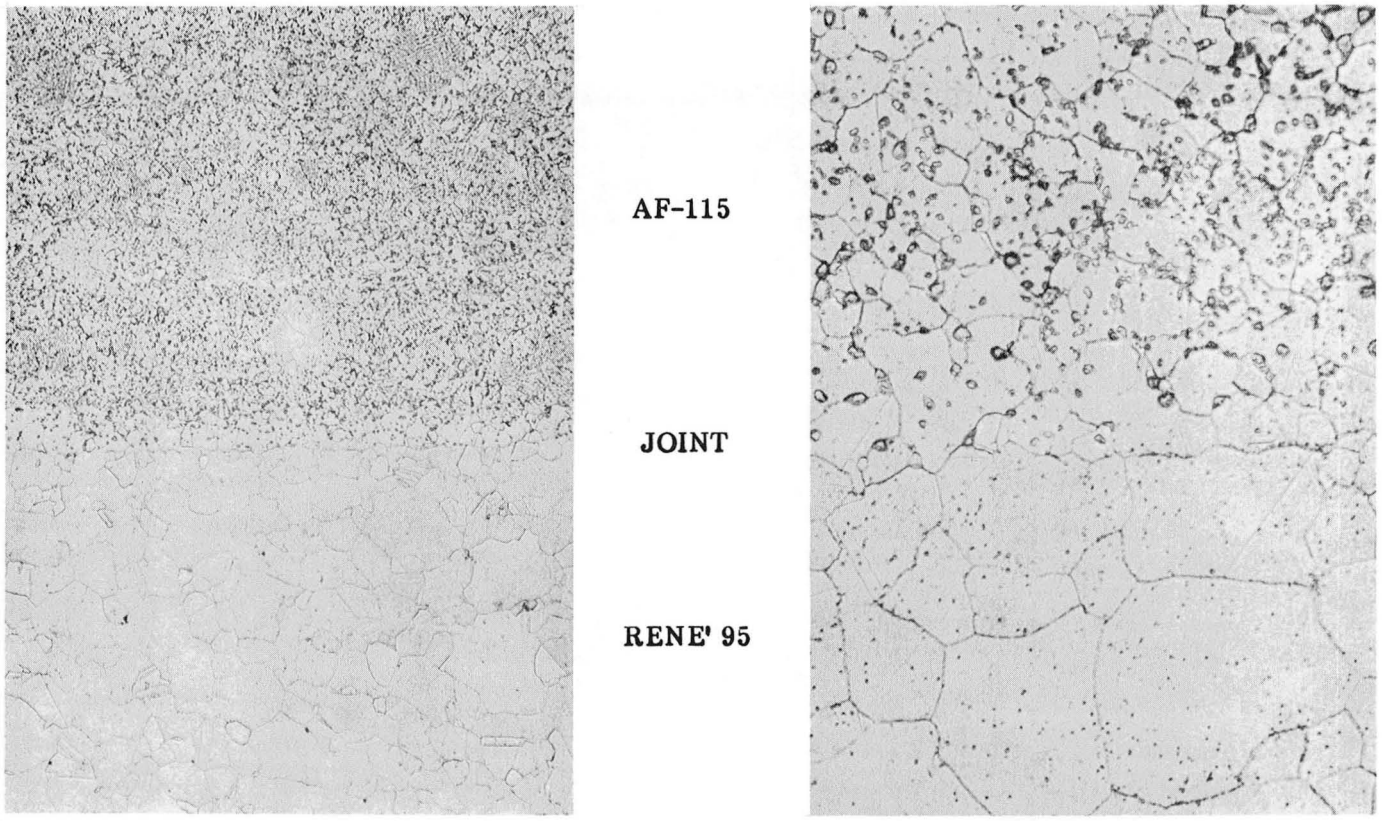

(a) 100X

(b) 500X

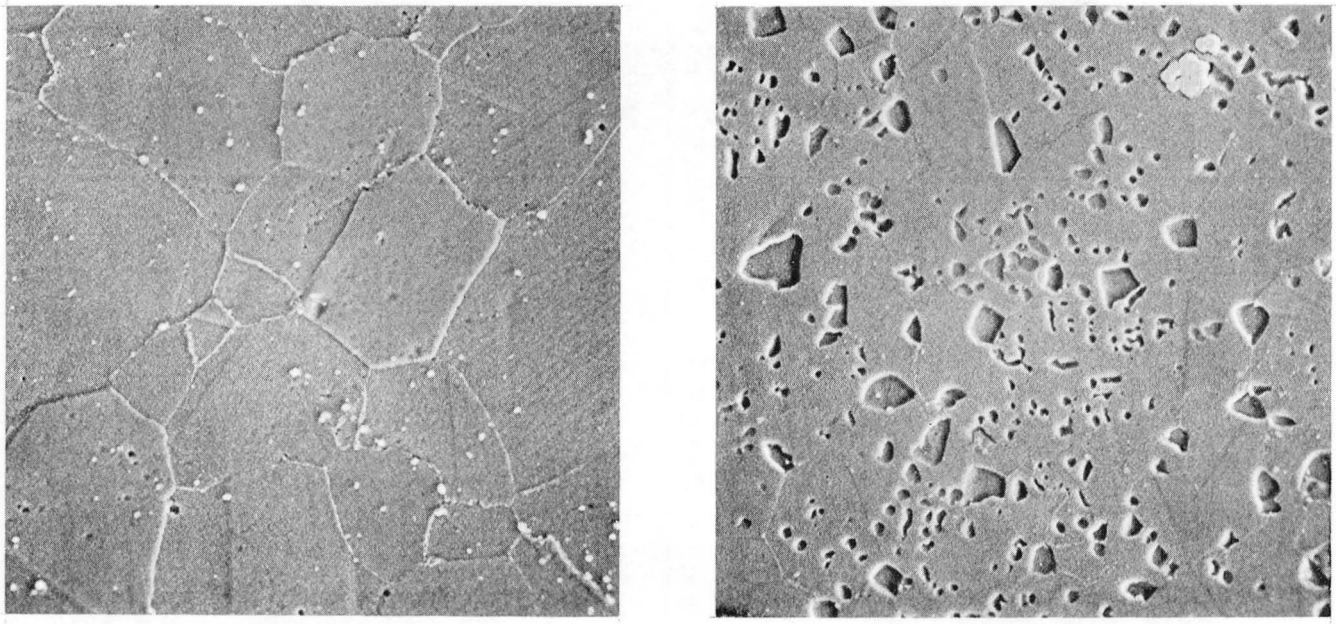

(c) Rene' 95, 1000X

(d) AF-115, 1000X

Figure 37. Photomicrographs of Heat Treated Microstructure of Combination C Flat Panel Shape After First Iteration Heat Treatment. 1175°C (2150°F)/2 Hours Salt Quench to 540°C (1000°F) + 760°C (1400°F)/16 Hours

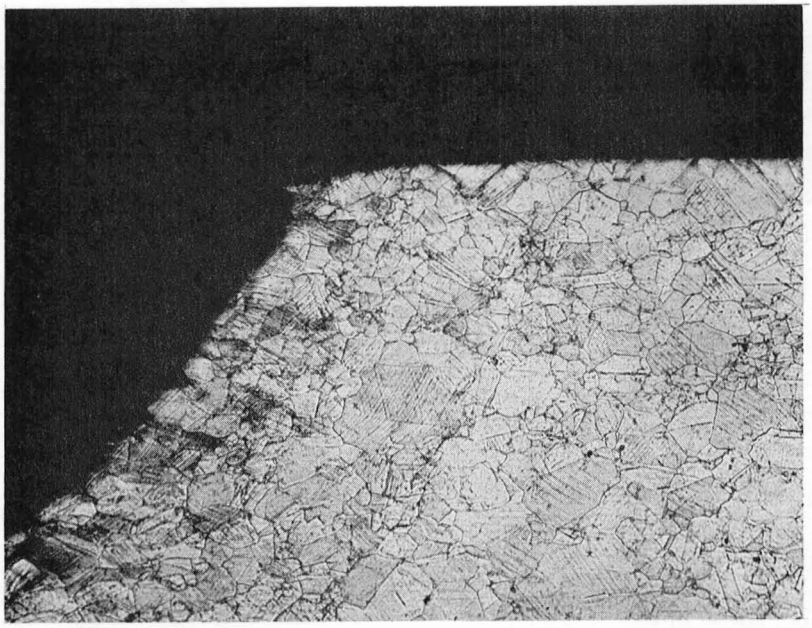

(a) 100X

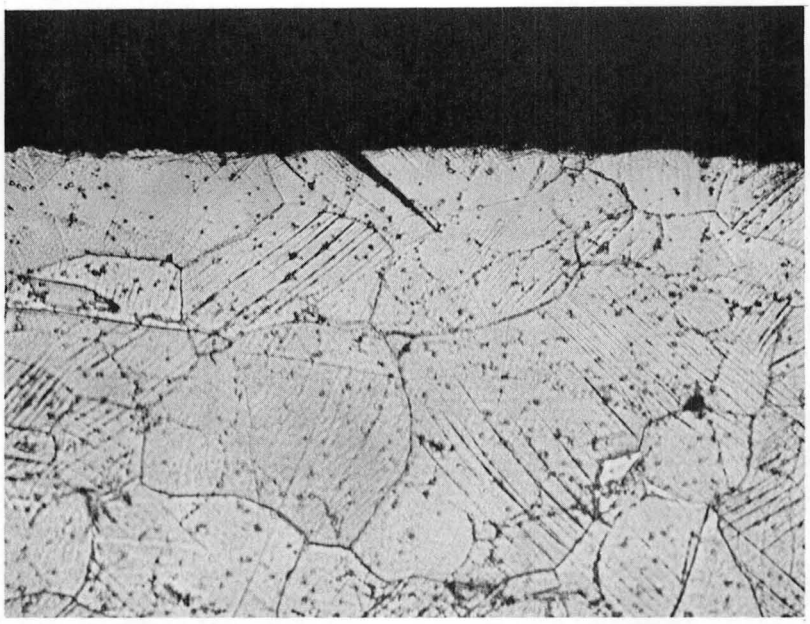

(b) 500X

Figure 38. Light Photomicrographs of Microstructure of Rene' 95 Tensile Specimen Exhibiting Ultimate Tensile Strength of 1495 MPa (217 ksi) at 480°C (900°F).

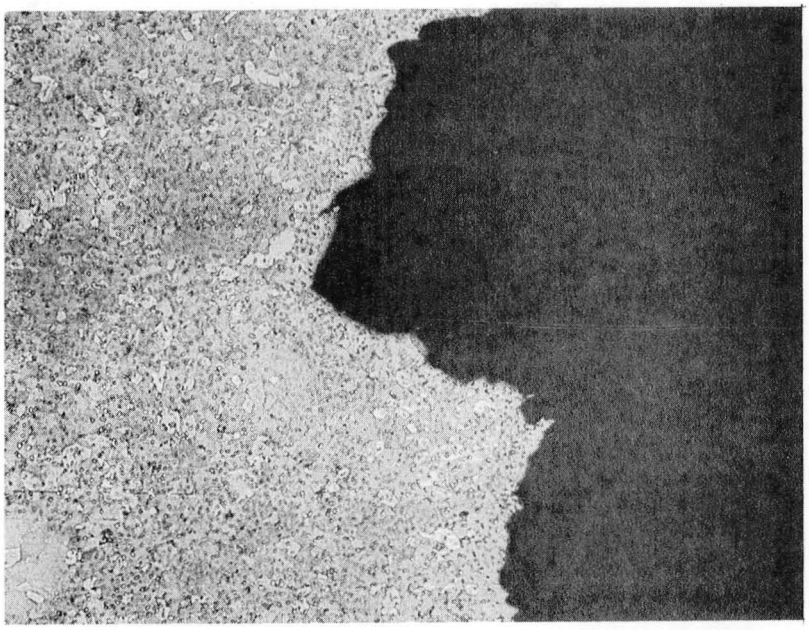

(a) 100X

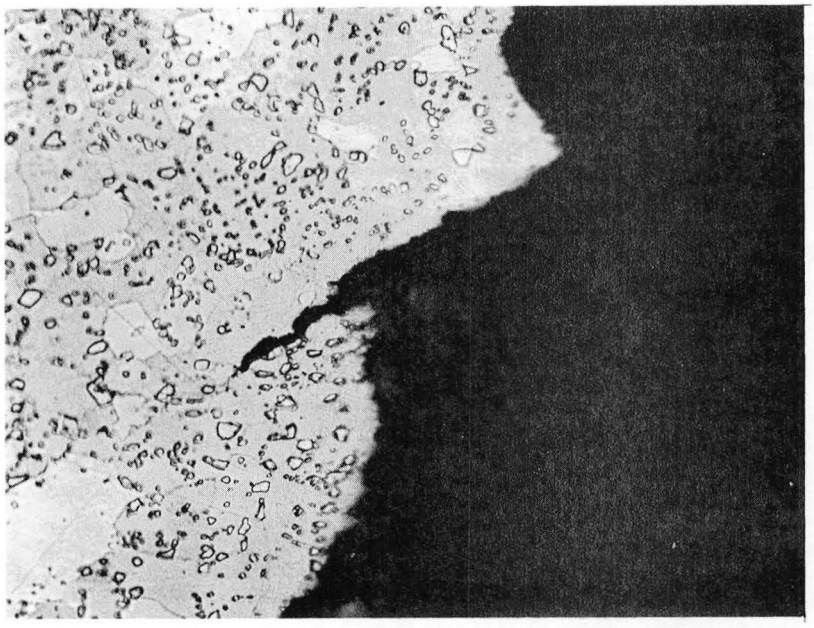

(b) 500X

Figure 39. Light Photomicrographs of Microstructure of Rene' 95/AF-115 Joint Tensile Specimen Exhibiting Ultimate Tensile Strength of 1440 MPa (209 ksi) at 480°C (900°F).

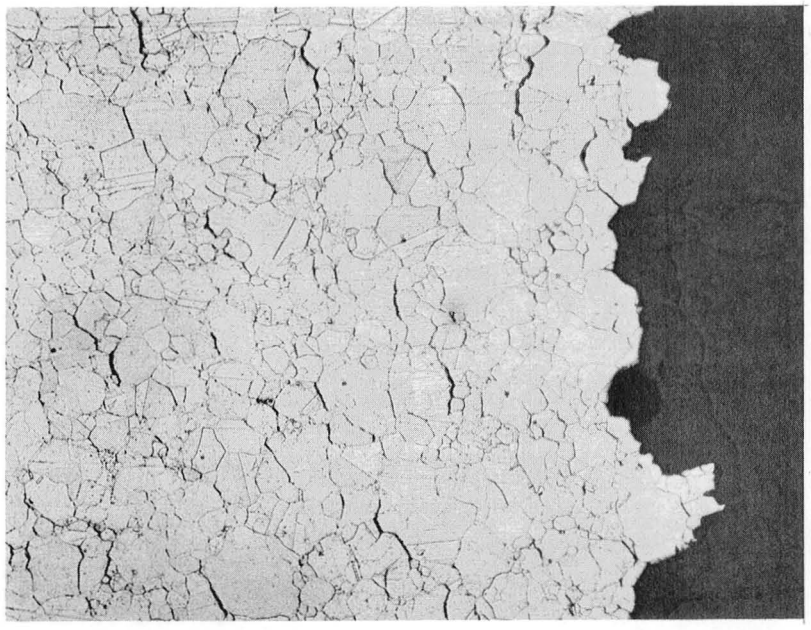

(a) 100X

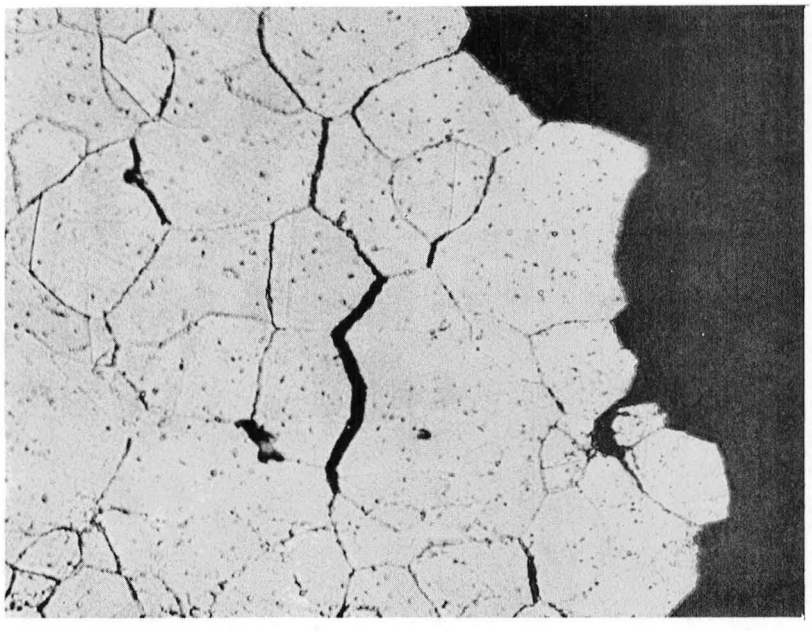

(b) 500X

Figure 40. Light Photomicrographs of Microstructure of Rene' 95-AF-115 Joint Stress Rupture Specimen Exhibiting 158.1 Hours Rupture Life at 760°C (1400°F)/550 MPa (80 ksi). Failure Occurred in the Rene' 95 Portion of the Specimen.

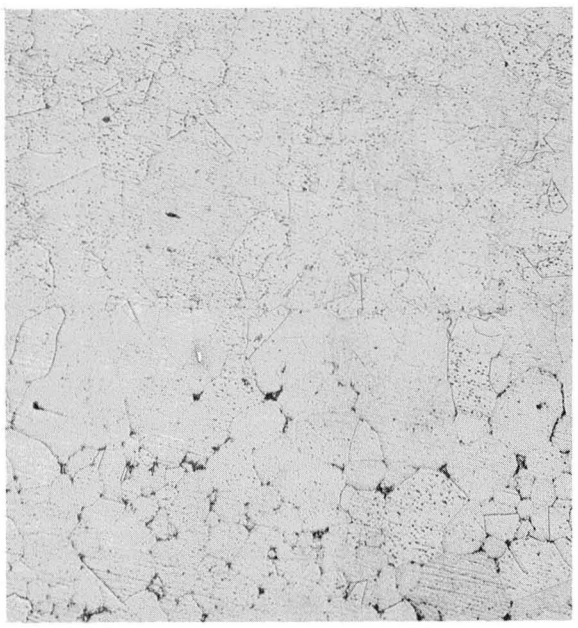

Rene' 95

Joint

AF-115

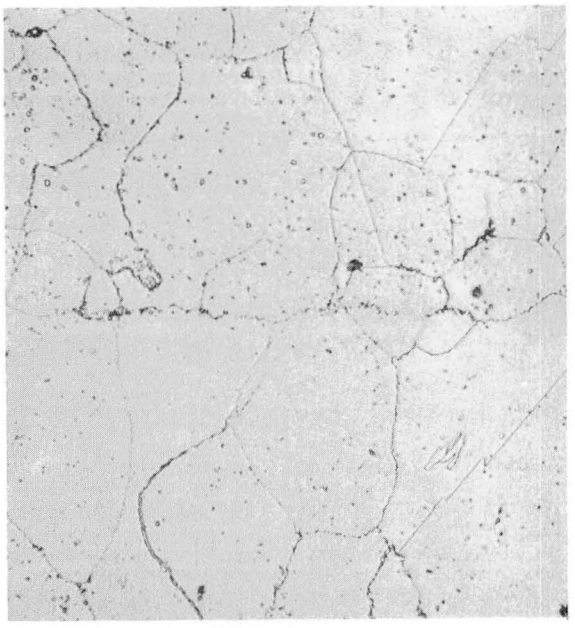

(a) 100X

(b) 500X

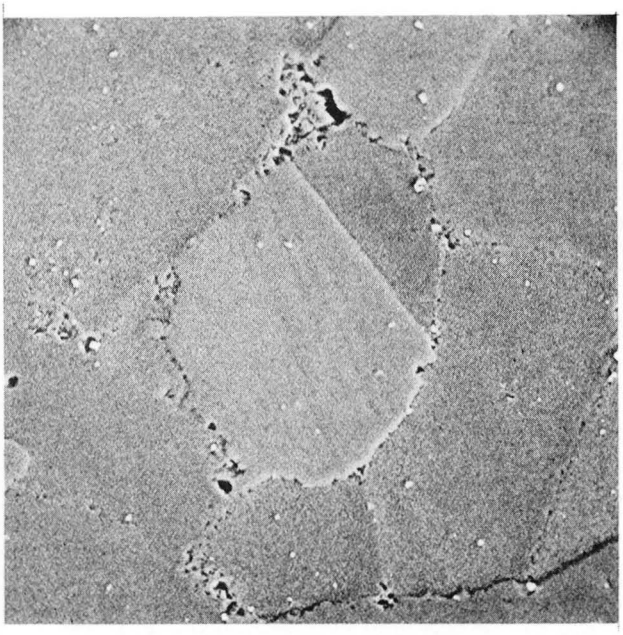

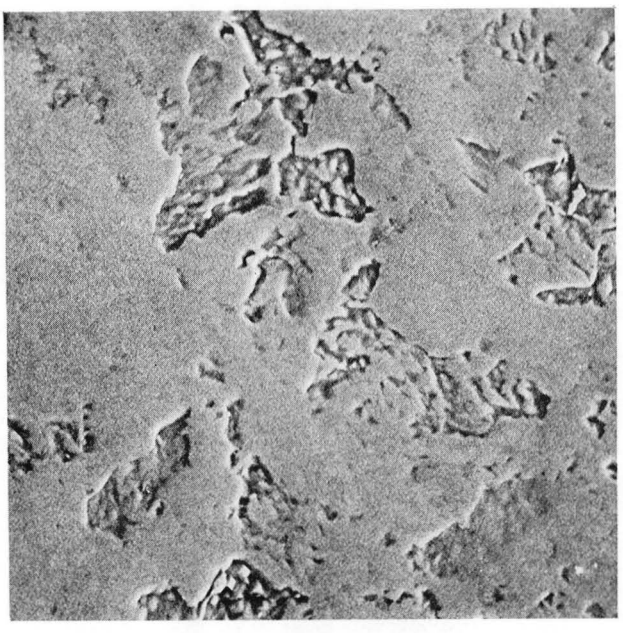

(c) Rene' 95, 1000X

(d) AF-115, 1000X

Figure 41. Photomicrographs of Heat Treated Microstructure of Combination C Flat Panel Shape After Second Iteration Heat Treatment: 1205°C (2200°F)/2 Hours Salt Quench to 650°C (1200°F) + 760°C (1400°F)/16 Hours.

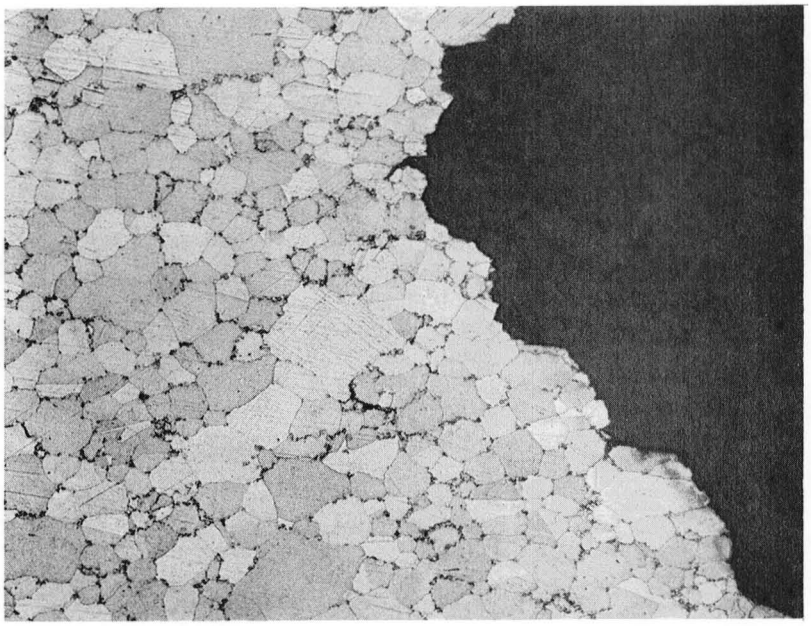

(a) 100X

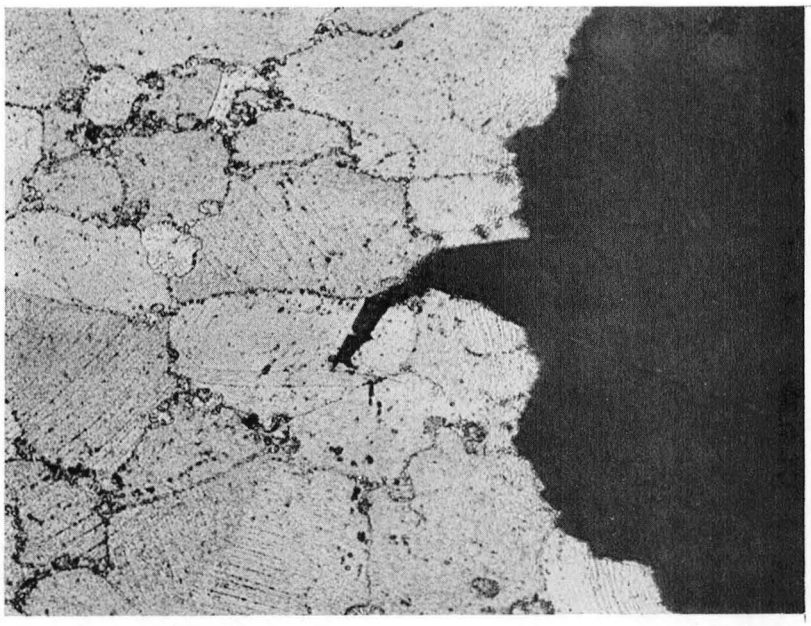

(b) 500X

Figure 42. Light Photomicrographs of Microstructure of Rene' 95 AF-115 Joint Tensile Specimen Exhibiting Ultimate Tensile Strength of 1325 MPa (190 ksi) at 480°C (900°F). The Failure Occurred in the AF-115 Portion of the Specimen.

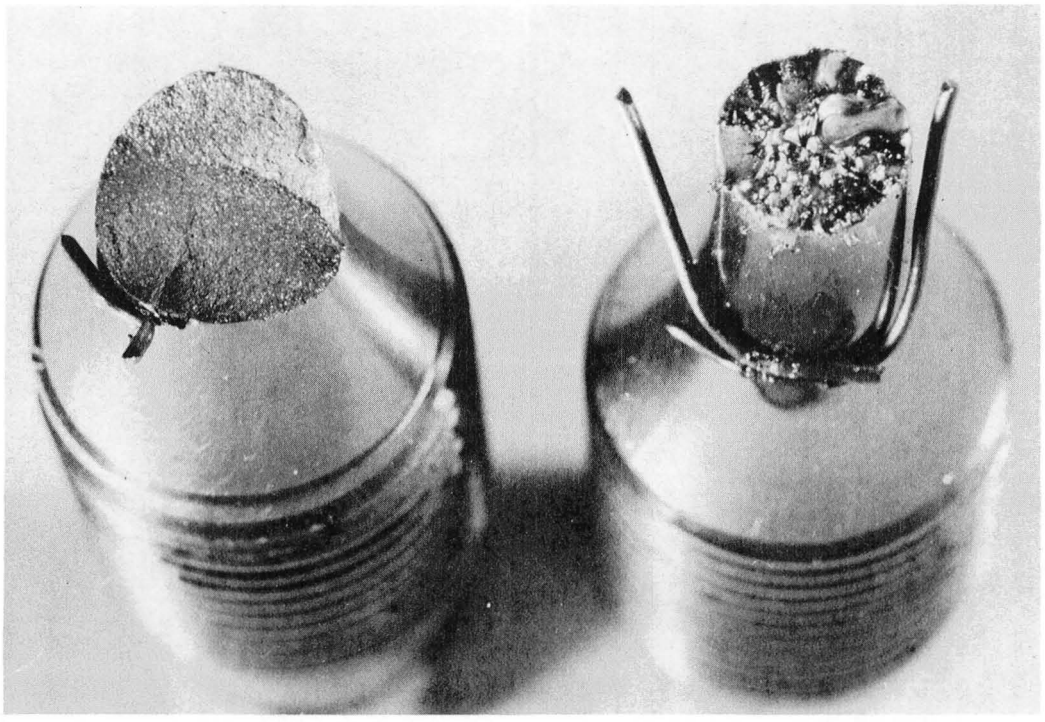

Figure 43. Photograph of Fracture Surfaces of Rene' 95 Low Cycle Fatigue Test Specimens Showing (Left) Fracture Initiation at Thermocouple Weld and (Right) Recast Layer on Fracture Surface.

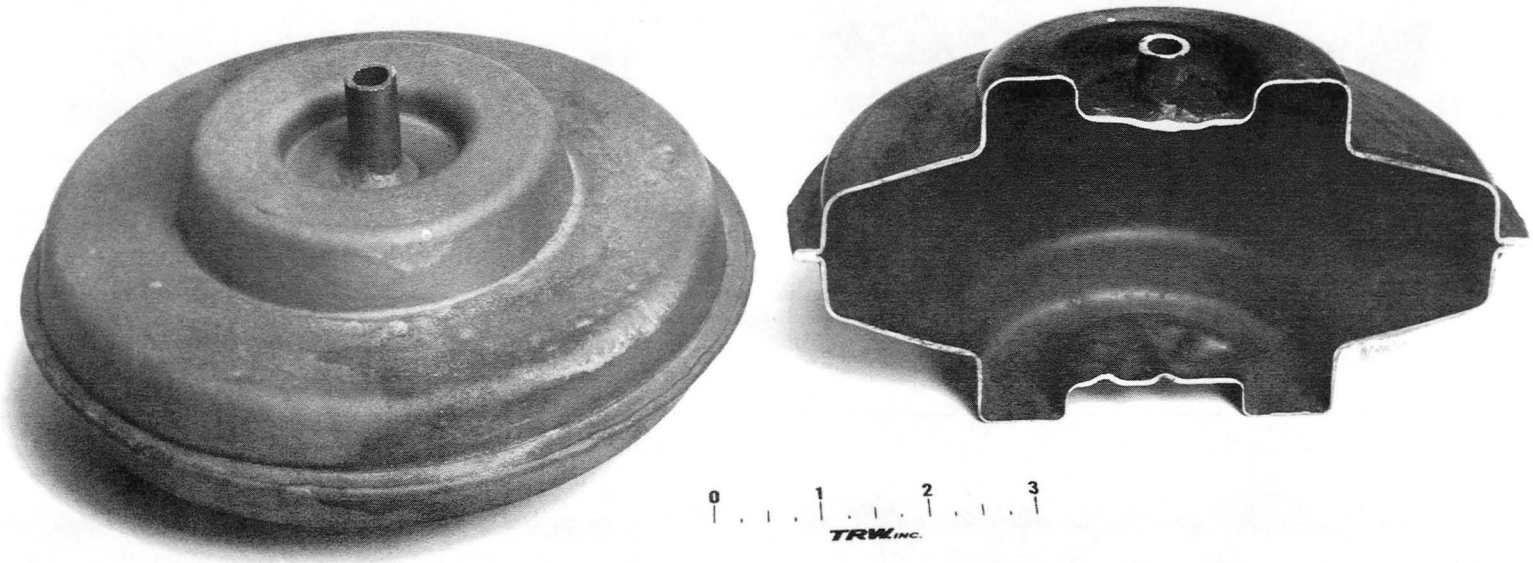

Figure 44. Left - Complete T-700 HIP Can.
Right - T-700 HIP Can Sectioned to Reveal the HIP Cavity.

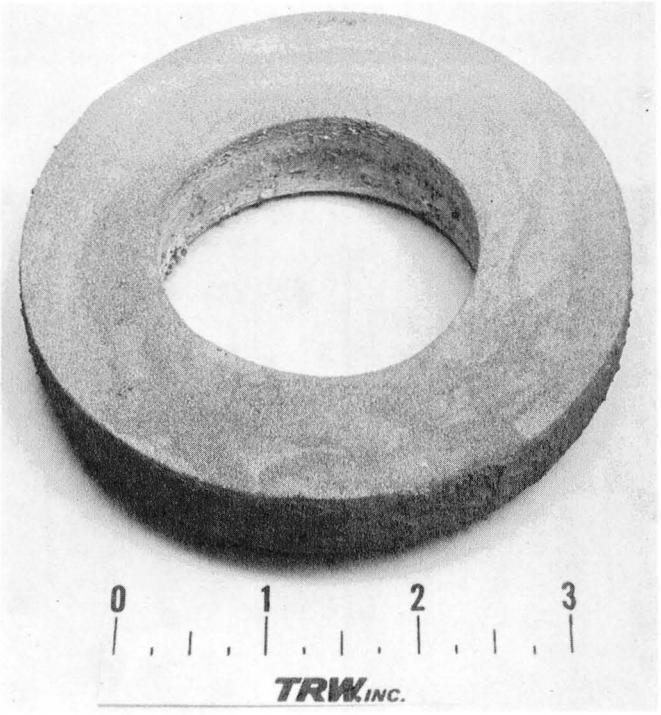

(a) Pre-sintered Ring

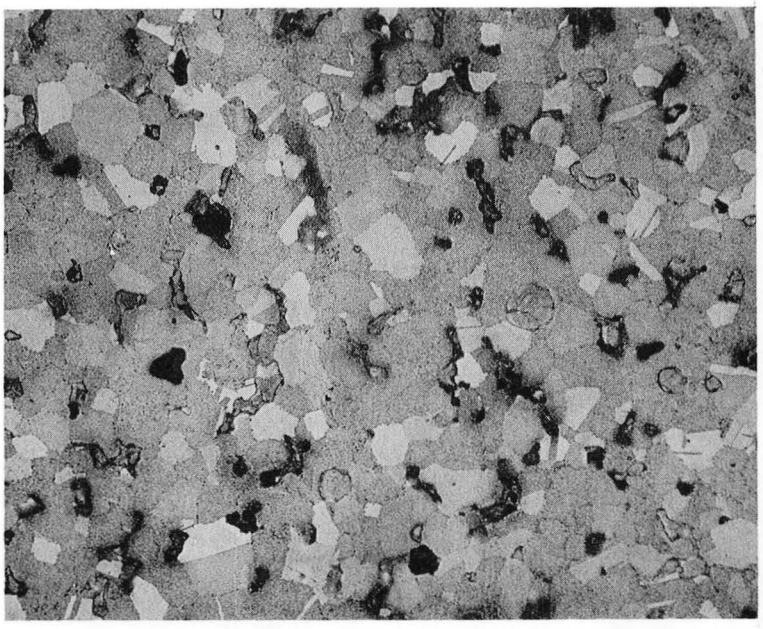

(b) As-sintered Microstructure, 100X Magnification

Figure 45. Photograph (a) and Photomicrograph (b) of Vacuum Pre-Sintered Ring of Rene' 95 Rim Material Sintered for Six Hours at 1245°C (2275°F).

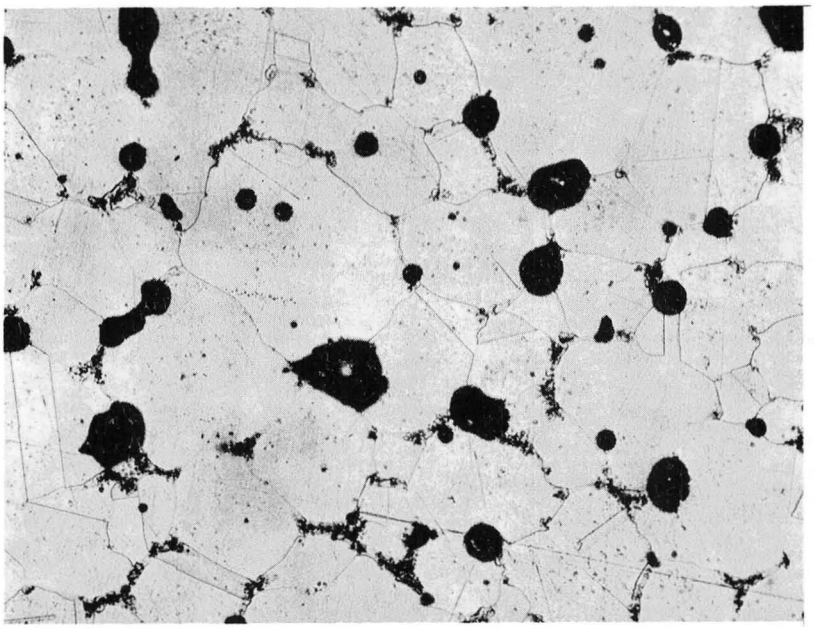

Figure 46. Photomicrograph of Pre-Sintered Rene' 95 Ring After Additional Heat Treatment for 6 Hours at 1265°C (2310°F). Magnification, 100X.

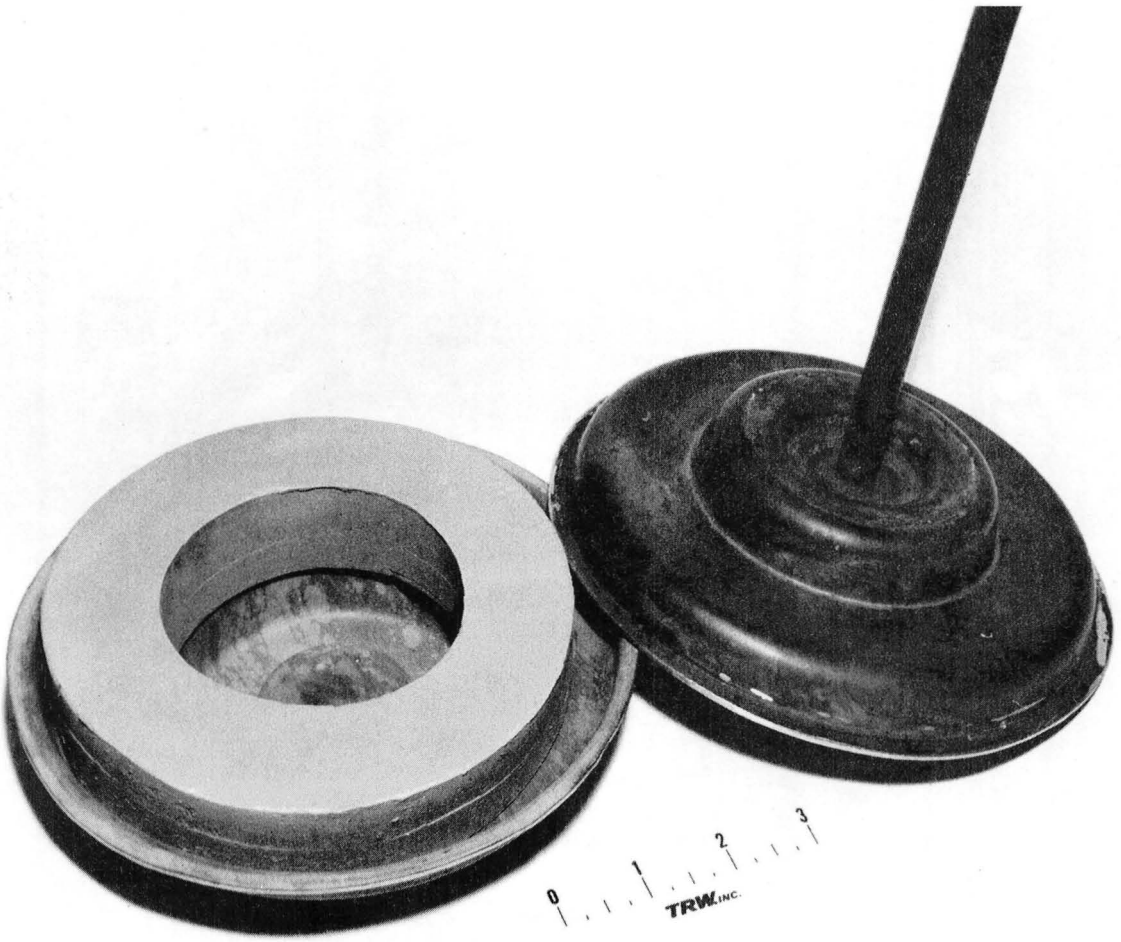

Figure 47. Photograph of Combination A T-700 Disk with Pre-Sintered Rene' 95 Rim Inserted Just Prior to Final Can Sealing. Scale in Inches.

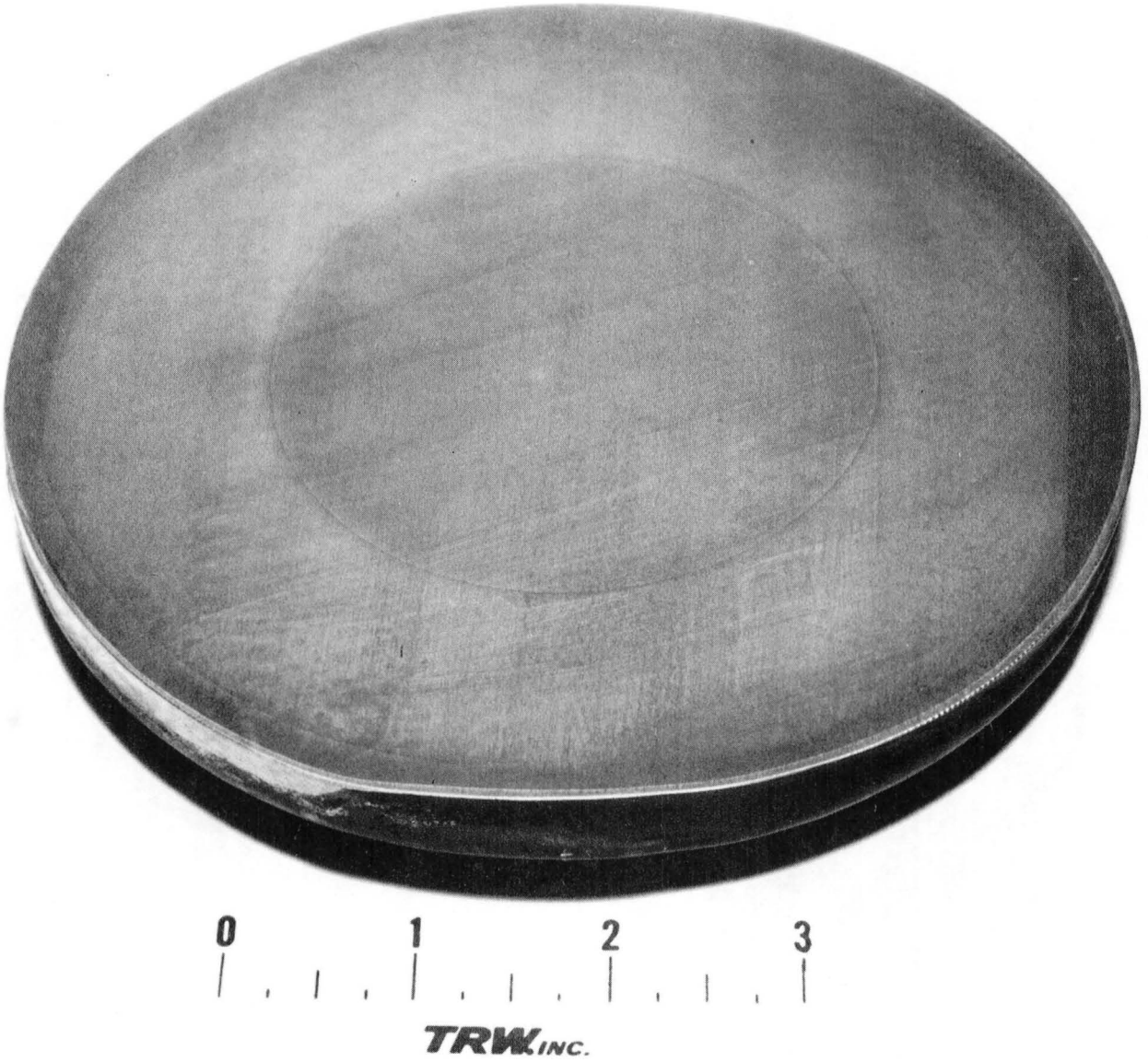

Figure 48. Photograph of Cross Section of Combination A T-700 Disk Sectioned in Half Along the Horizontal Plane. Scale in Inches.

Top

Bottom

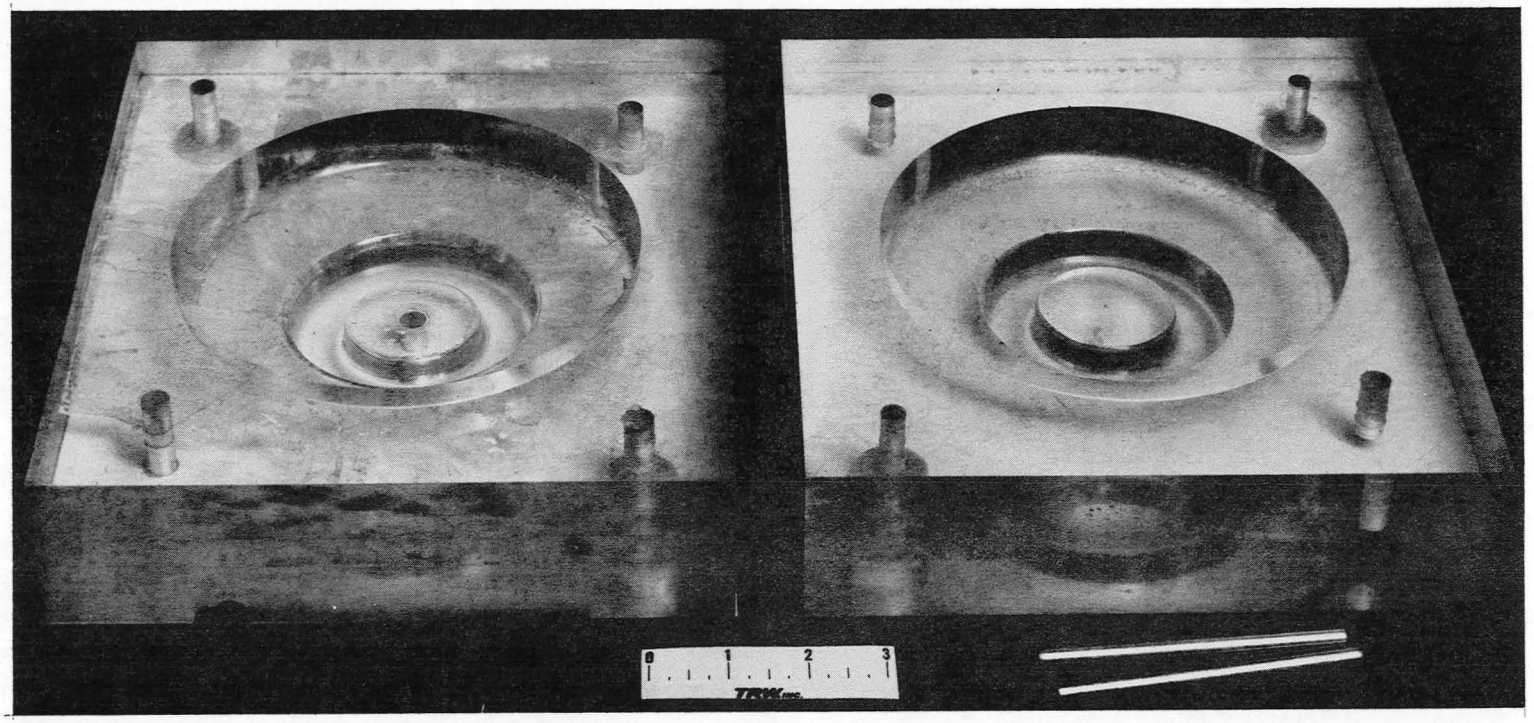

Figure 49. Photograph of Lucite Block Containing Machined Configuration of T-700 Turbine Disk. Scale in Inches.

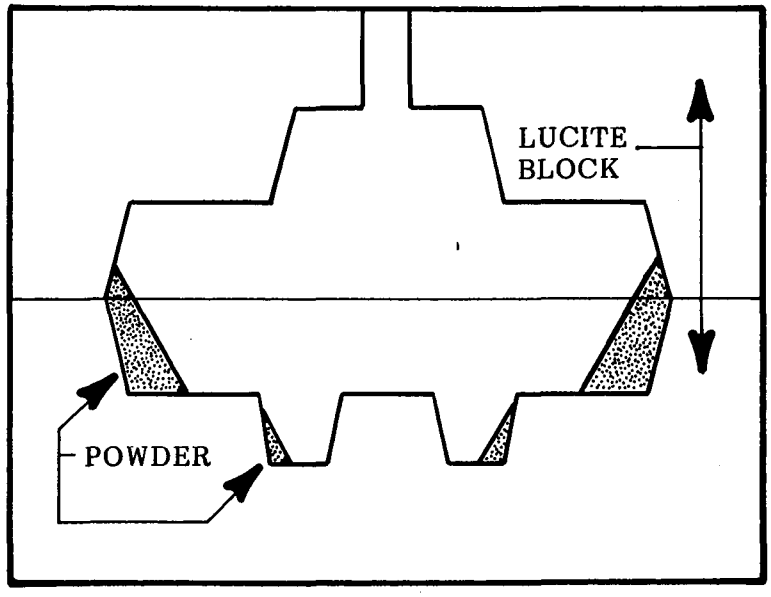

(a) Powder Distribution During Filling

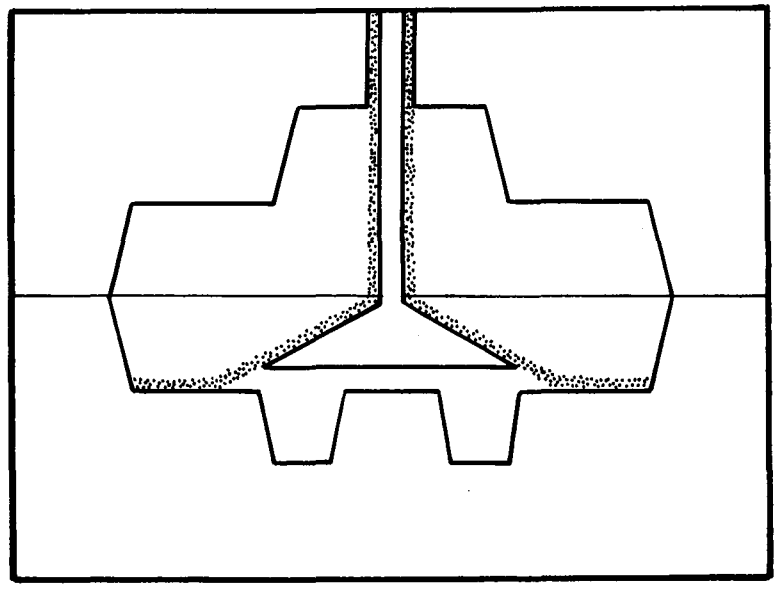

(b) Use of Flared Insertion Tube

Figure 50. Schematic Illustration of (a) Powder Distribution During Centrifugal Powder Filling and (b) Use of Flared Insertion Rod to Prevent Powder Filling in Hub Portion of Disk.

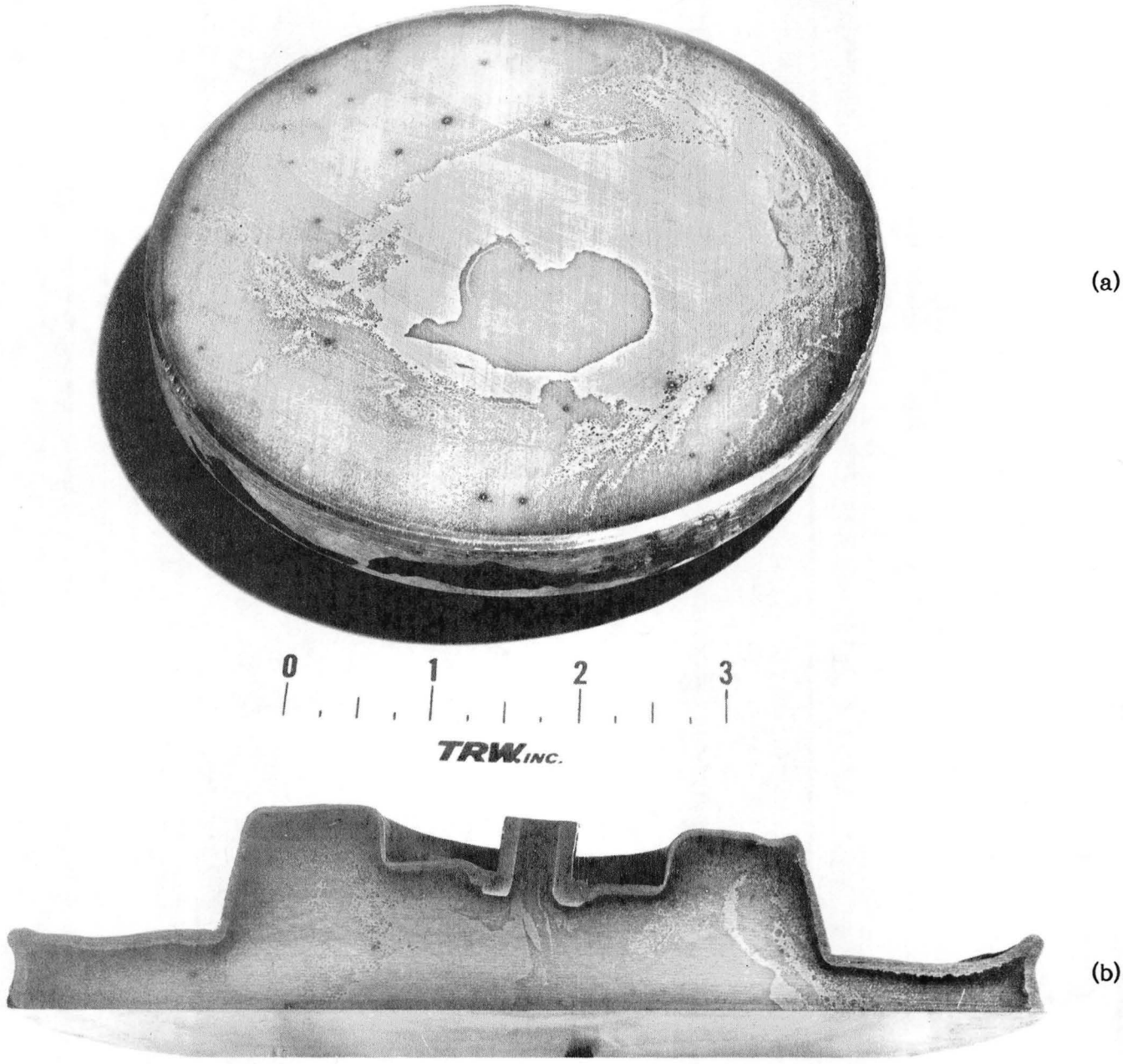

Figure 51. Photographs of Cross Sections of Combination B T-700 Disk Sectioned in Half Along (a) the Horizontal Plane and (b) the Vertical Plane. Scale in Inches.

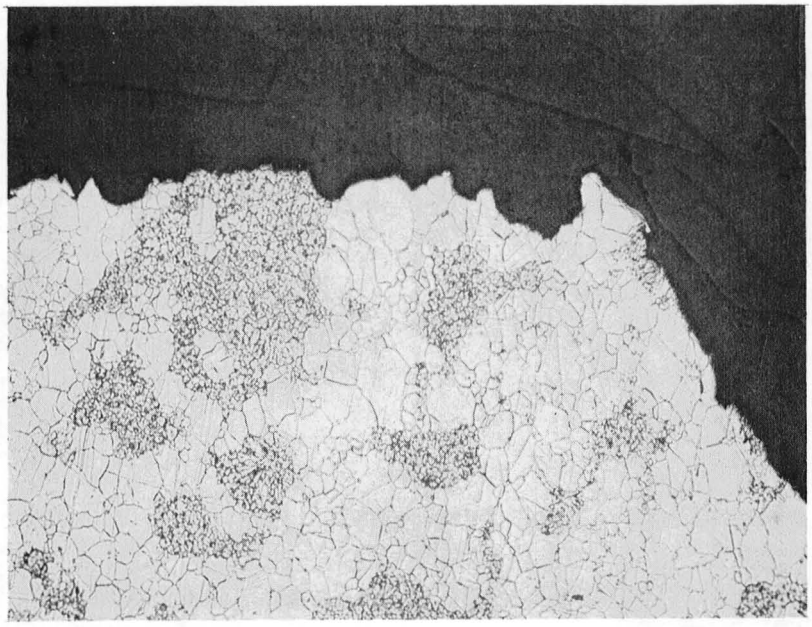

(a) 100X

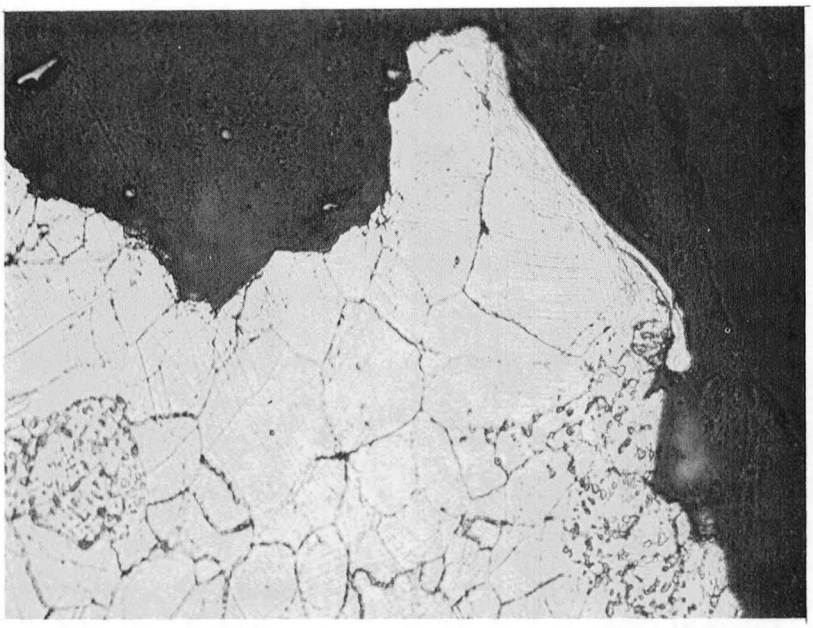

(b) 500X

Figure 52. Light Photomicrographs of Typical Fracture Surface of MERL 76/L/C Astroloy Powder Blend 480°C (900°F) Tensile Specimen.

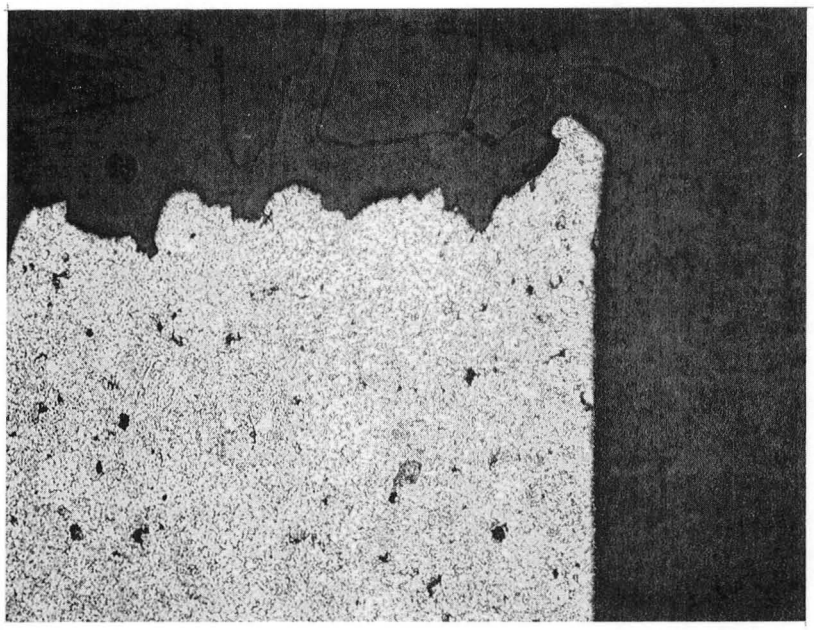

(a)

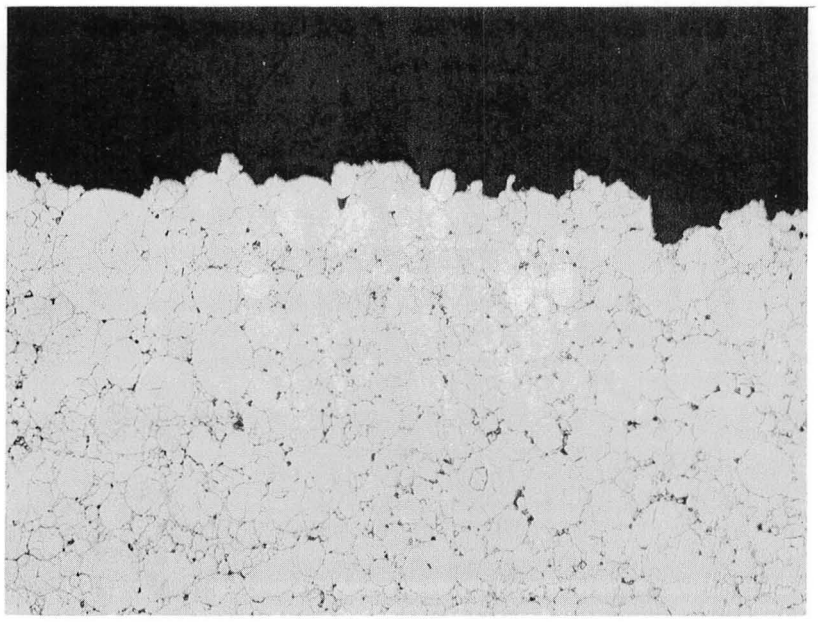

(b)

Figure 53. Light Photomicrographs of Typical Fracture Surfaces of (a) MERL 76 Tensile Specimen and (b) L/C Astroloy Portion of Joint Tensile Specimen tested at 480°C (900°F). Magnification 100X.

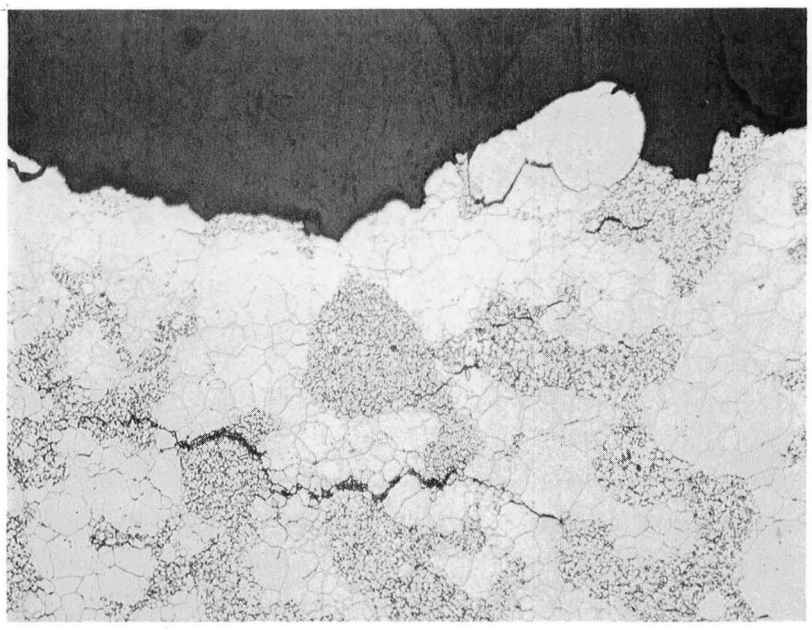

(a) 100X

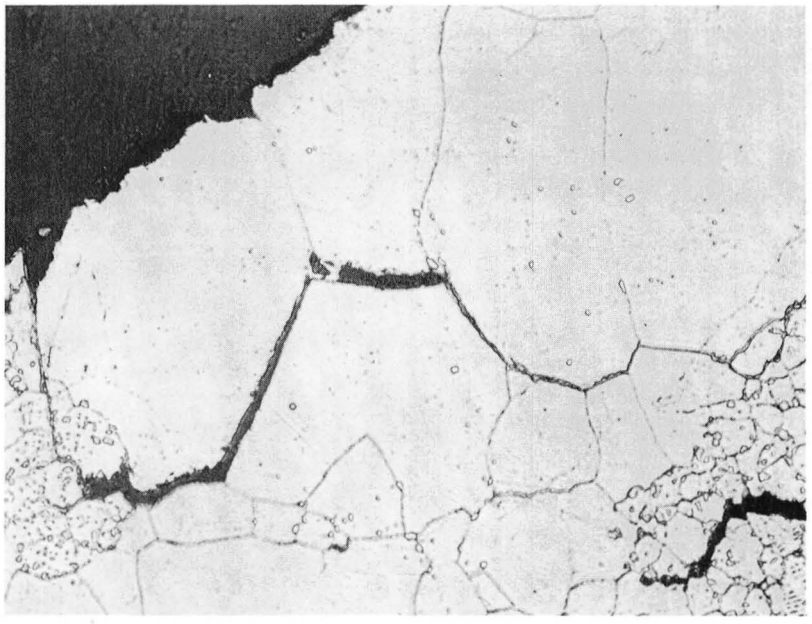

(b) 500X

Figure 54. Light Photomicrographs of Typical Fracture Surface of MERL 76/L/C Astroloy Powder Blend 760°C (1400°F)/550 MPa (80 ksi) Stress Rupture Specimen.

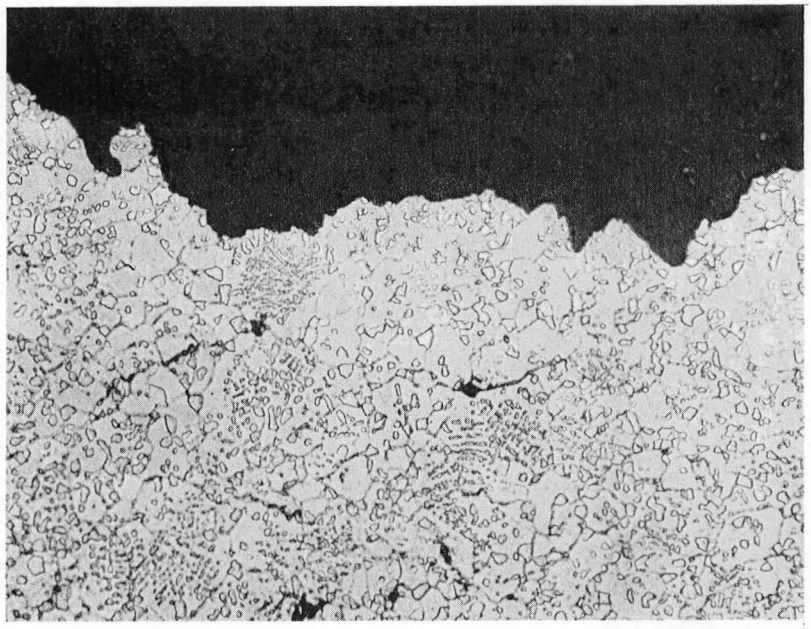

(a) 500X

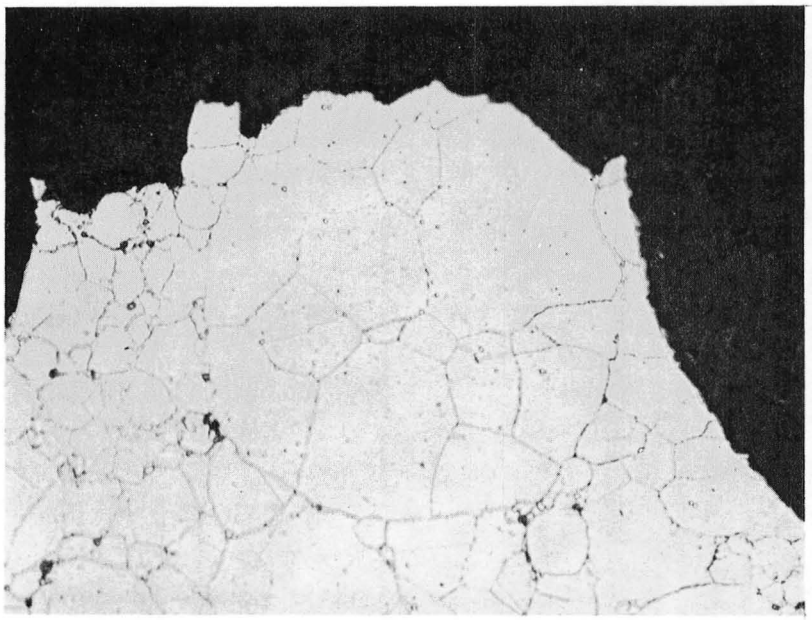

(b) 500X

Figure 55. Light Photomicrographs of Typical Fracture Surfaces of (a) MERL 76 Portion of Joint Stress Rupture Specimen and (b) L/C Astroloy Stress Rupture Specimen, Tested at 760°C (1400°F)/550 MPa (80 ksi).

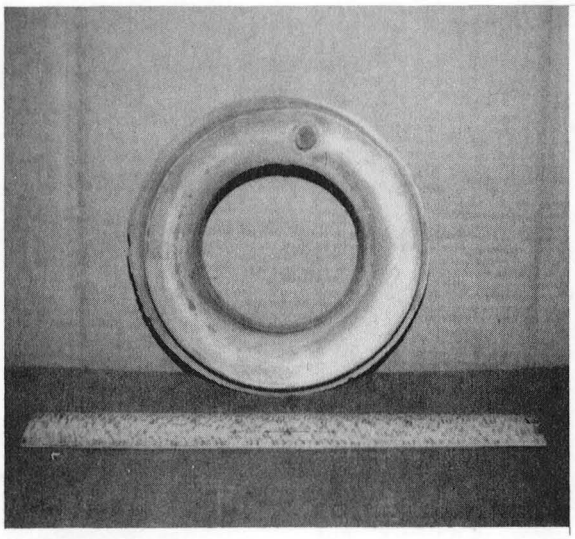

Figure 56. Photograph of AF-115 Ring Shape for T-700 Disk Chemically Stripped of its Container.

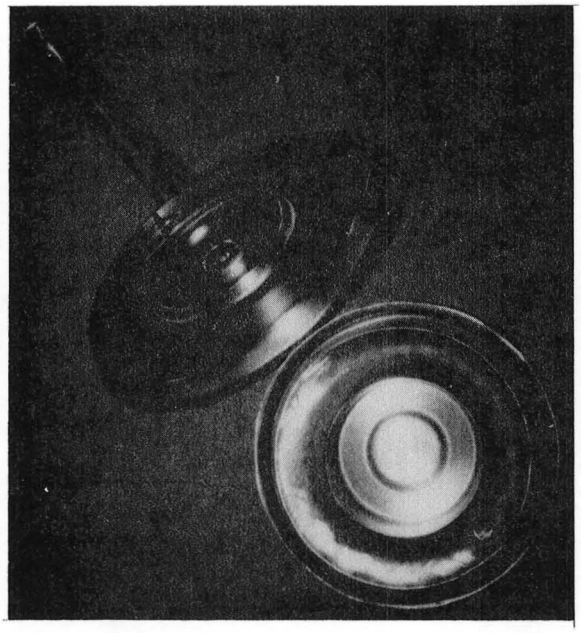

Figure 57. Photograph of Combination C T-700 Disk with HIP'ed AF-115 Rim Inserted Prior to Final Can Sealing.

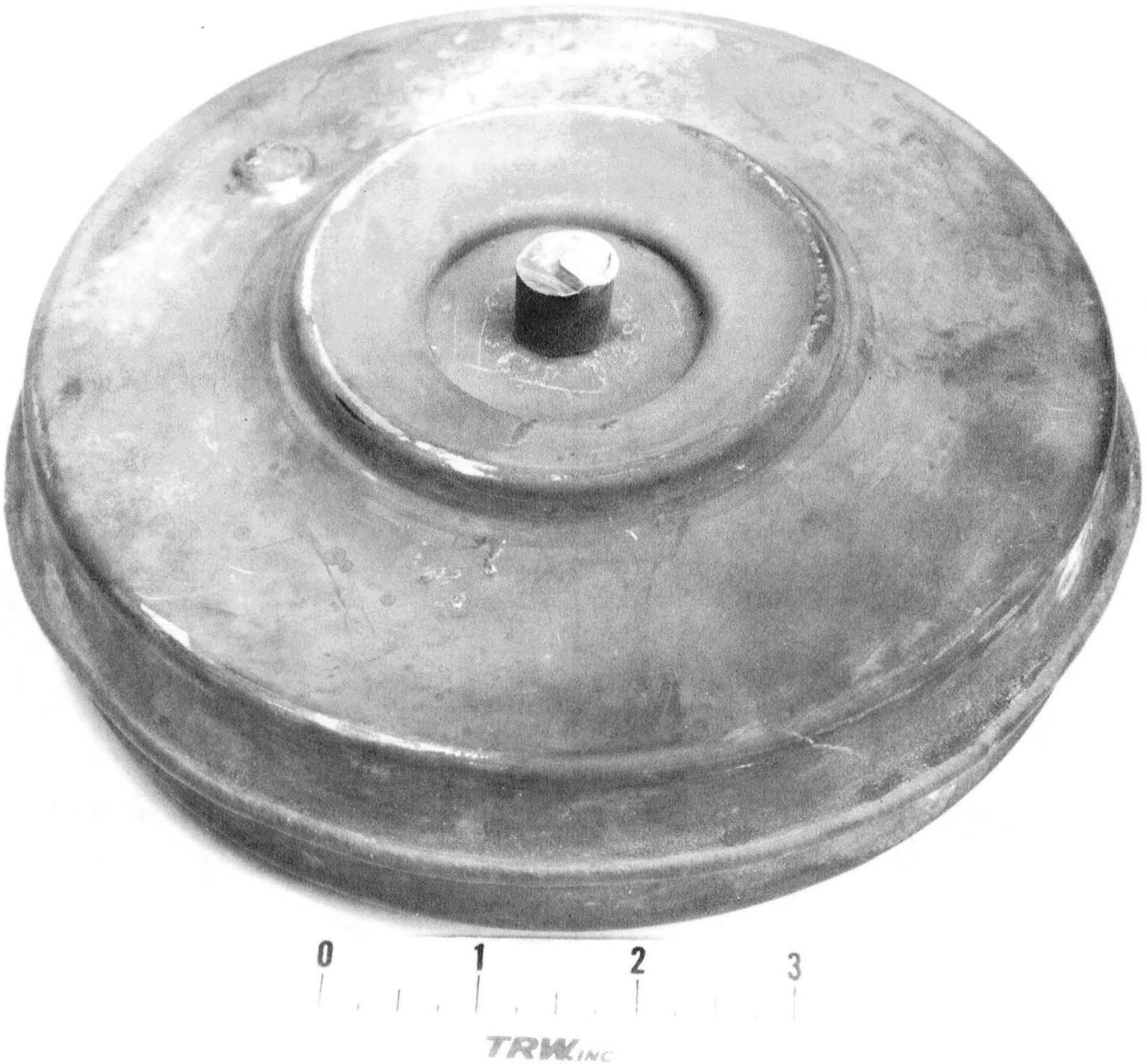

Figure 58. Photograph of Combination C T-700 Disk in the as-HIP Condition. Scale in Inches.

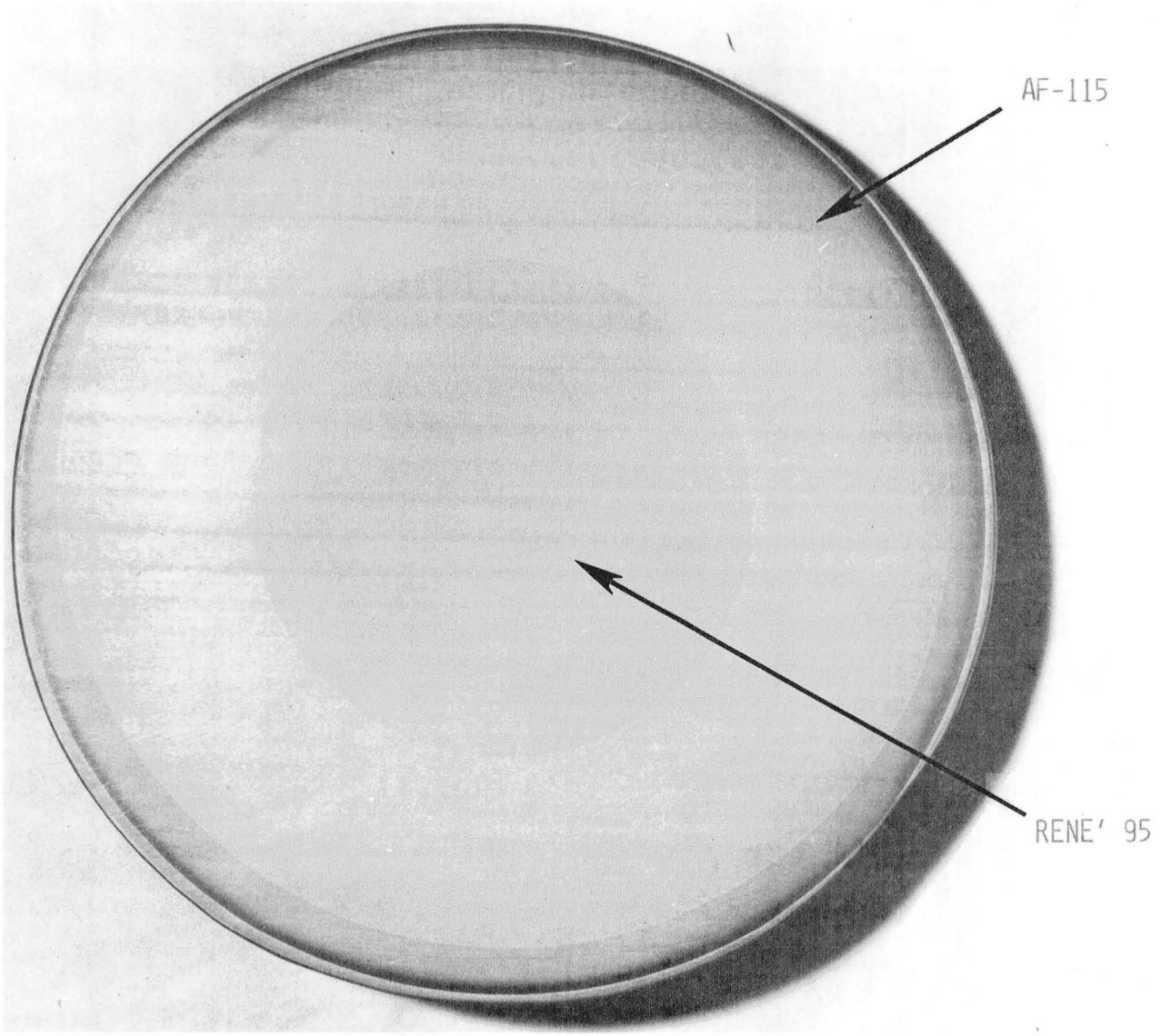

Figure 59. Photograph of Cross Section of Combination C T-700 Disk Sectioned in Half Along the Horizontal Plane.

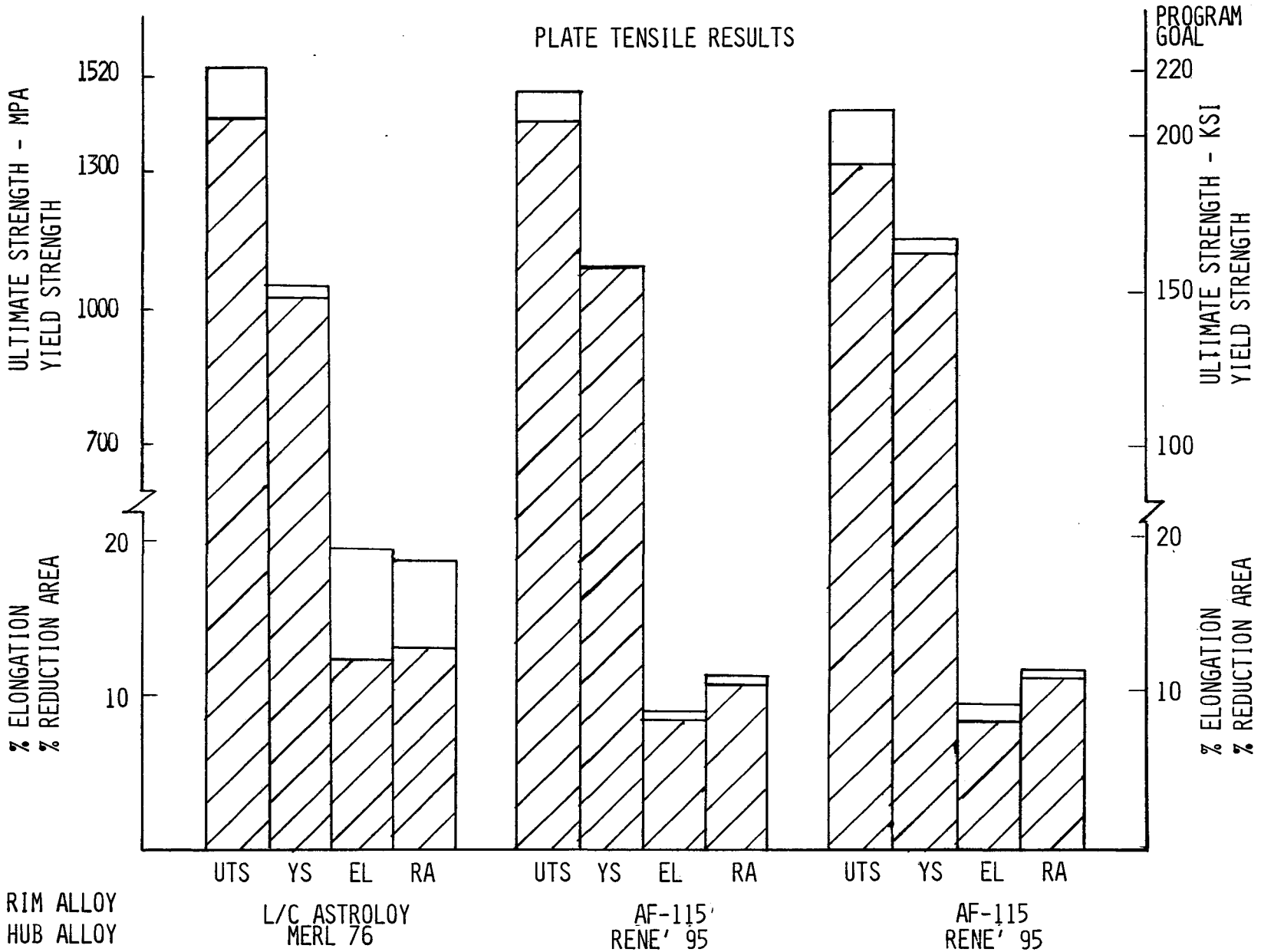

Figure 60. Results of 480°C (900°F) Tensile Tests on Hub Alloy Specimens Machined From Flat Plate Test Panels.

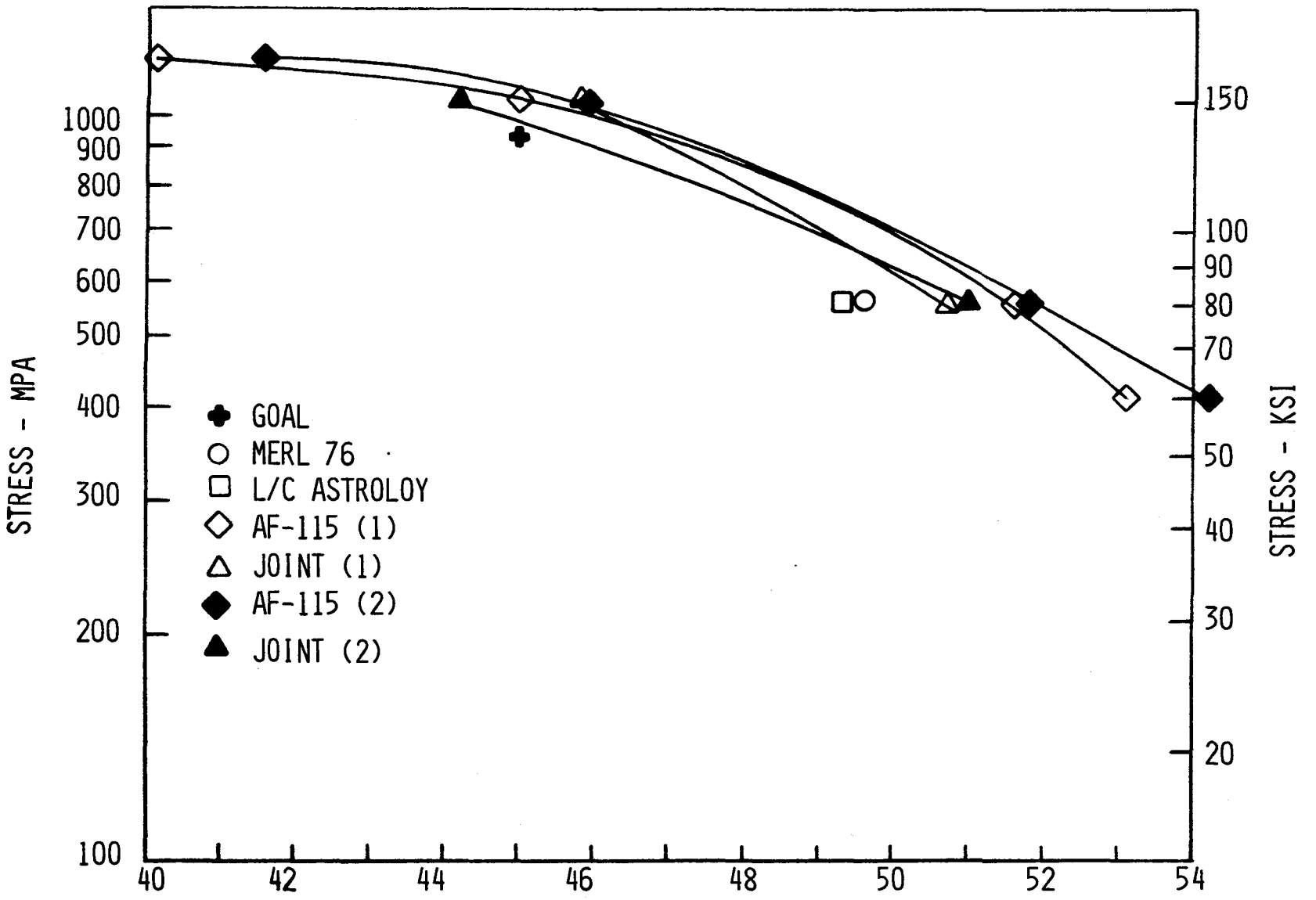

$P = 1.8T\,(25 + \text{Log } t) \times 10^{-3}$ (T in ^{o}K, t in hours)

Figure 61. Larson-Miller Plot of Stress Rupture Results for Specimens Machined From Flat Plate Test Panels (Parentheses Indicate Heat Treat Iterations).

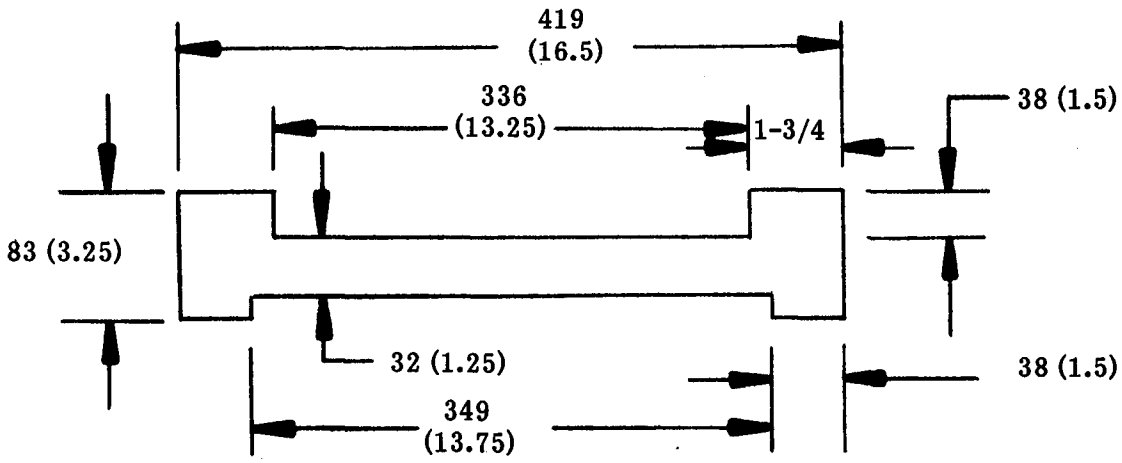

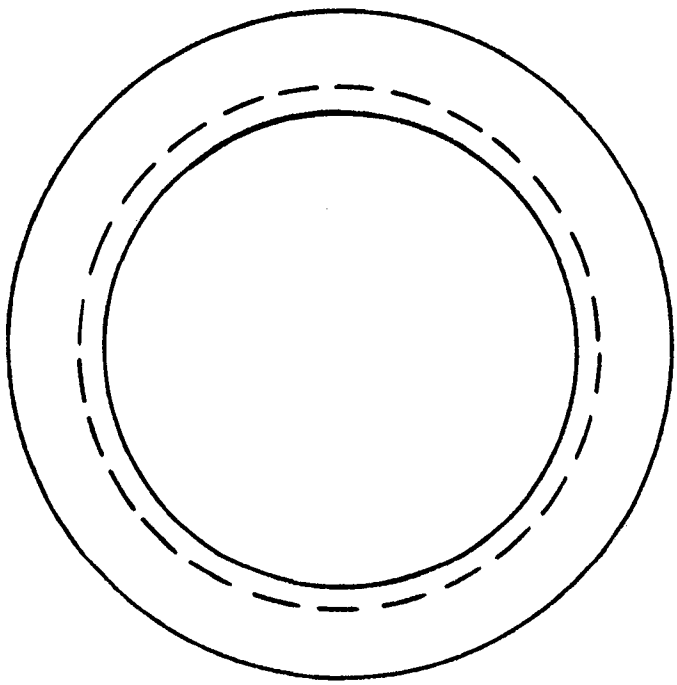

Figure 62. Schematic Diagram of CFM 56 5/8 Disk Used for Task II Sub-Scale Disk Evaluation. Dimensions in mm (Inches).

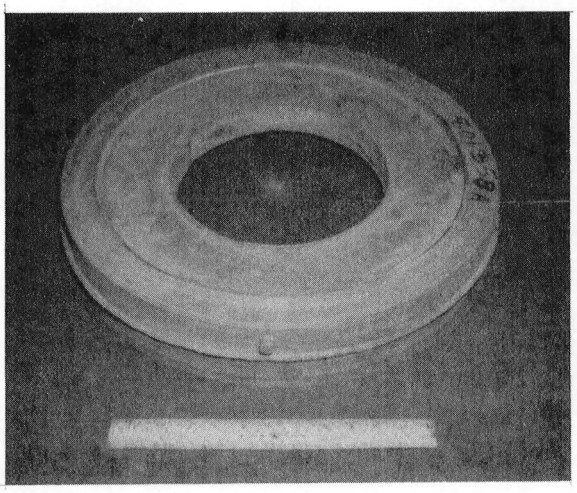

Figure 63. Photograph of Pre-HIP'ed AF-115 Rim Portion of CFM-56 Disk After Chemical Stripping of HIP Container. Scale in Inches.

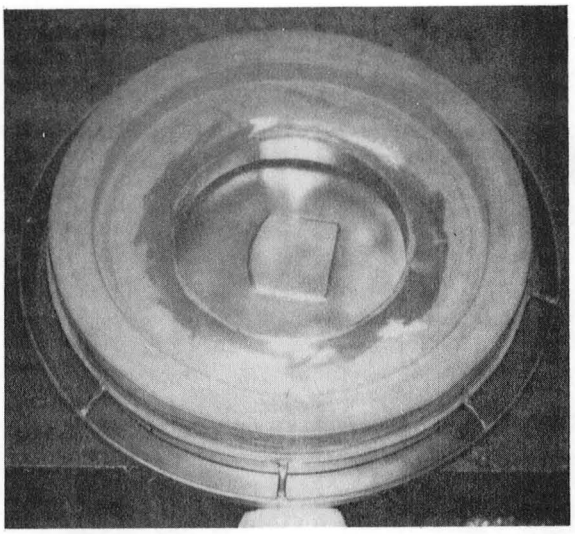

(a)

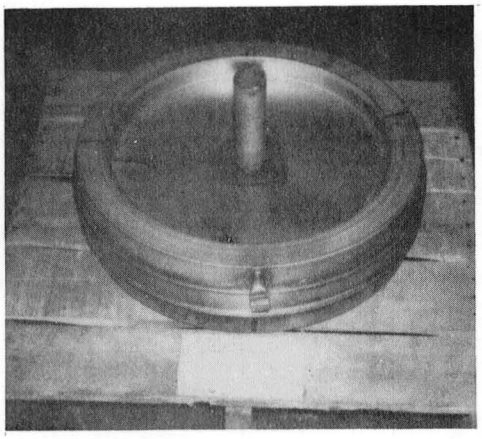

(b)

Figure 64. Photograph of (a) AF-115 Rim Portion of CFM-56 Disk in Position for Final HIP Consolidation and (b) CFM-56 Can Ready for HIP Consolidation.

Figure 65. Photograph of CFM-56 Disk in as-HIP'ed Condition. Scale in Inches.

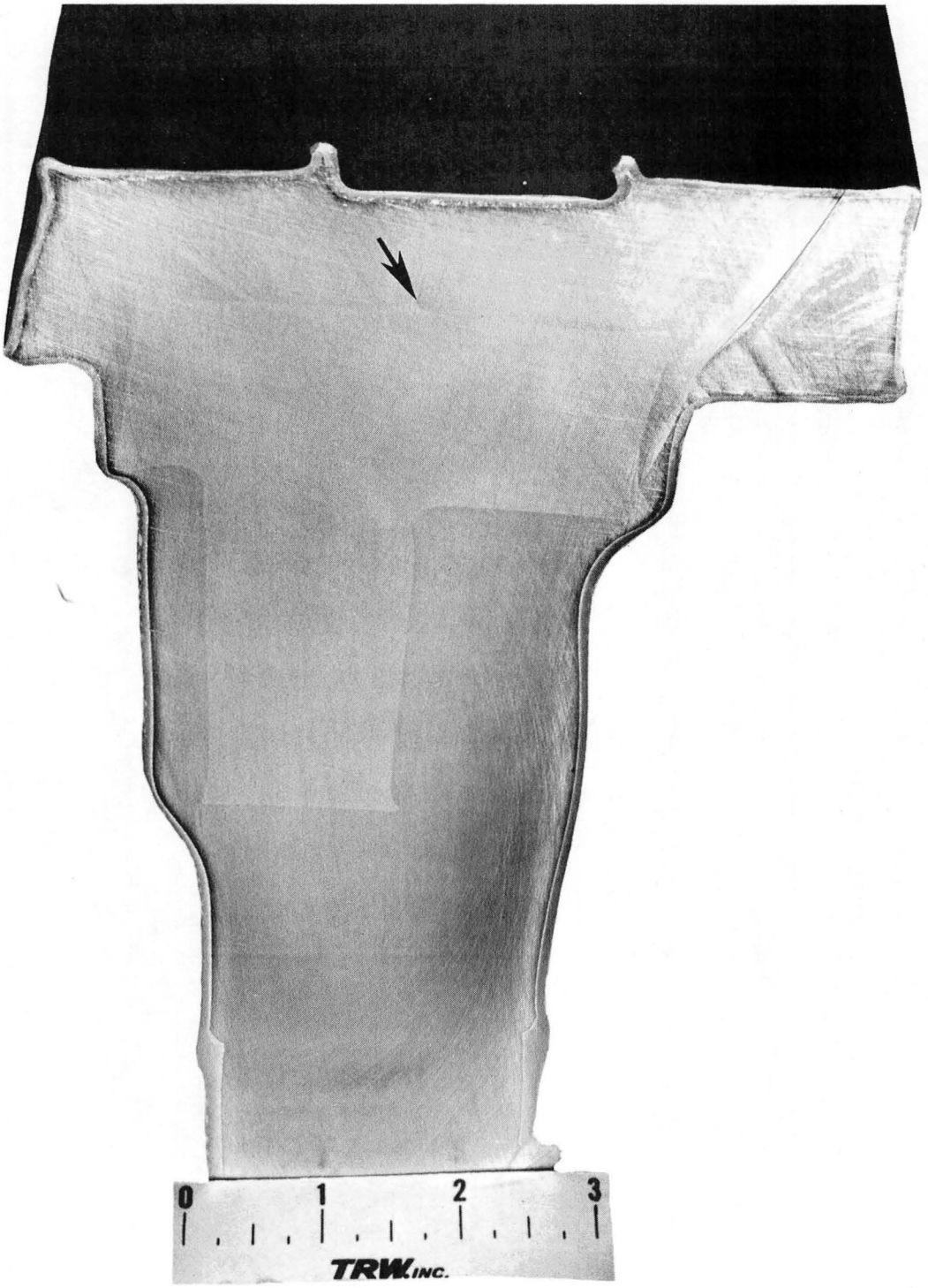

Figure 66. Photograph of Quarter Section of CFM-56 Disk in as-HIP'ed Condition Showing Crack (Arrow) Between Edge of AF-115 Rim and Inside of HIP Can. Scale in Inches.

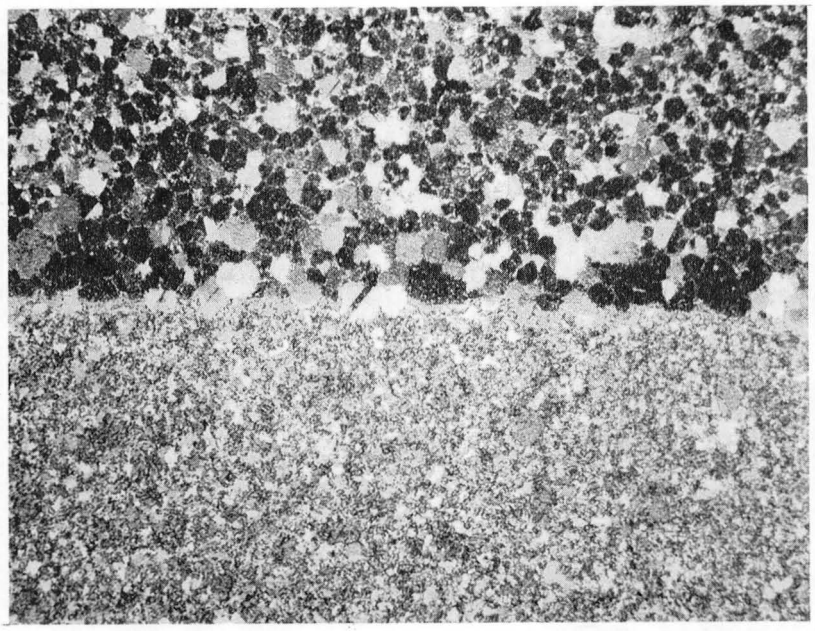

Figure 67. Light Photomicrograph of As-Hip'ed Microstructure in Joint Region of CFM-56 Disk. 100X Magnification.

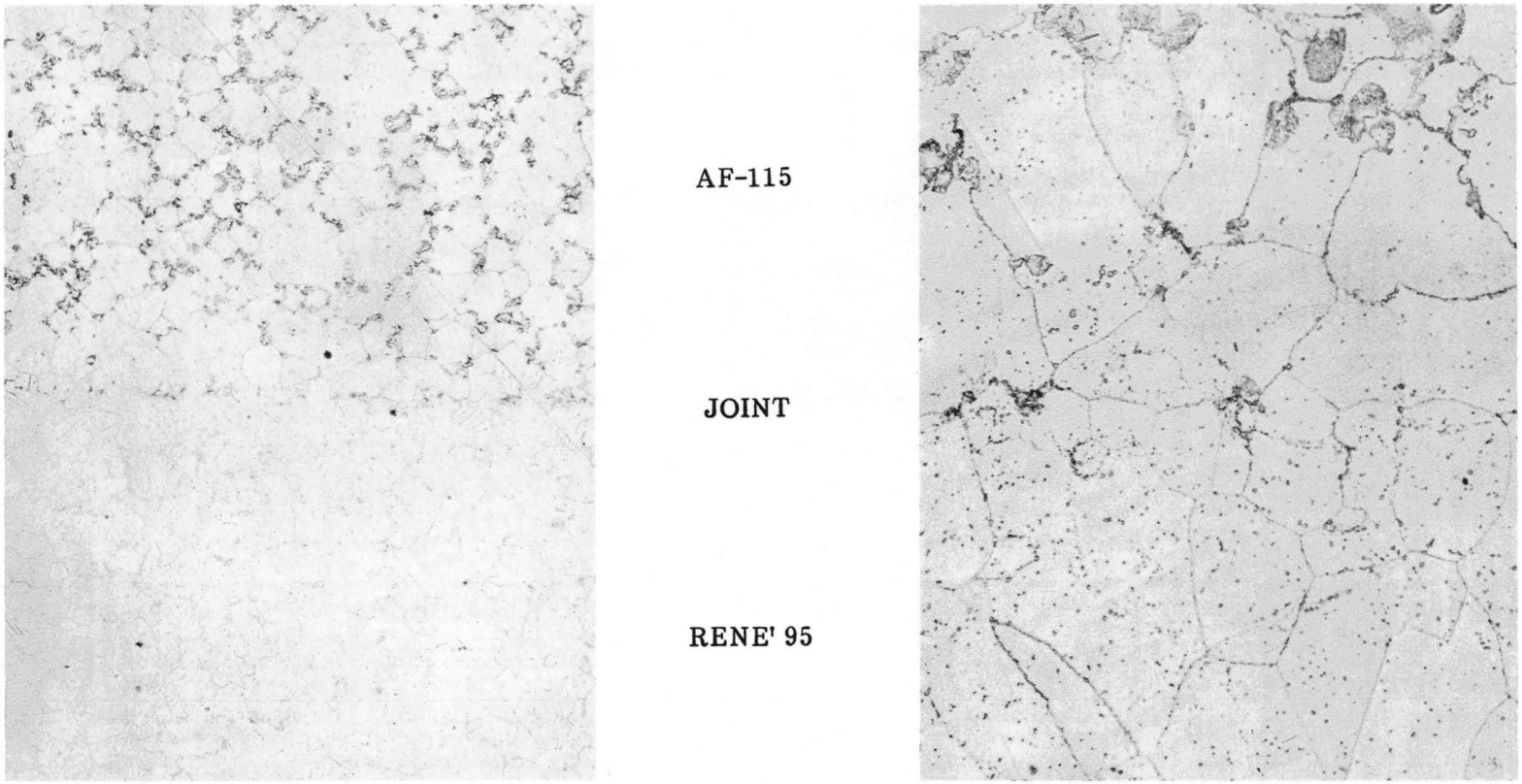

Figure 68. Light Photomicrographs of Microstructure in Joint Region of CFM-56 Disk After First Heat Treatment Iteration: 1205°C (2200°F)/2 Hours Salt Quench to 650°C (1200°F) + 760°C (1400°F)/16 Hours Air Cool.

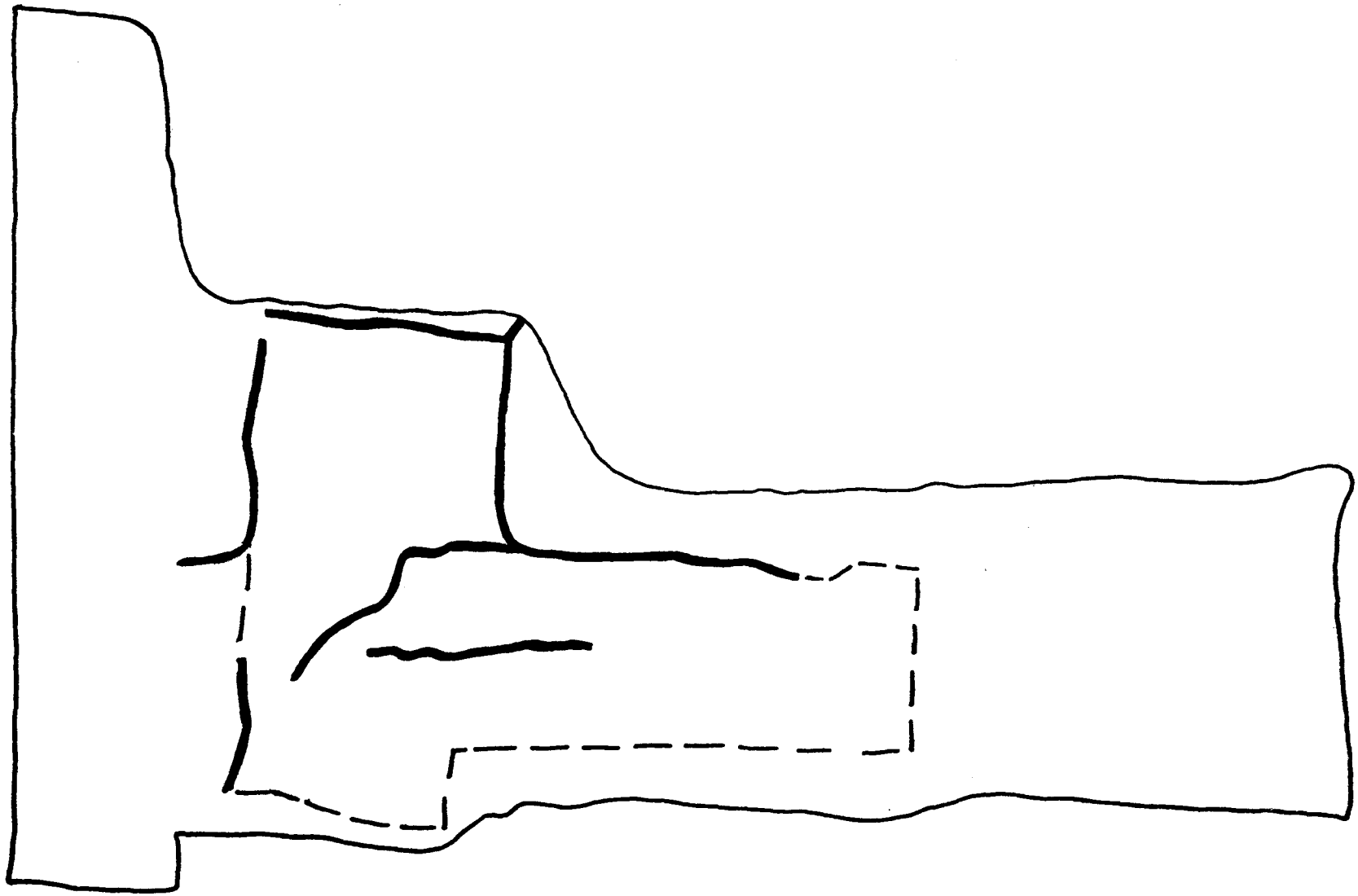

Figure 69. Schematic Diagram of Quarter Section of CFM-56 Disk Showing Zyglo Crack Patterns After First Heat Treatment Iteration.

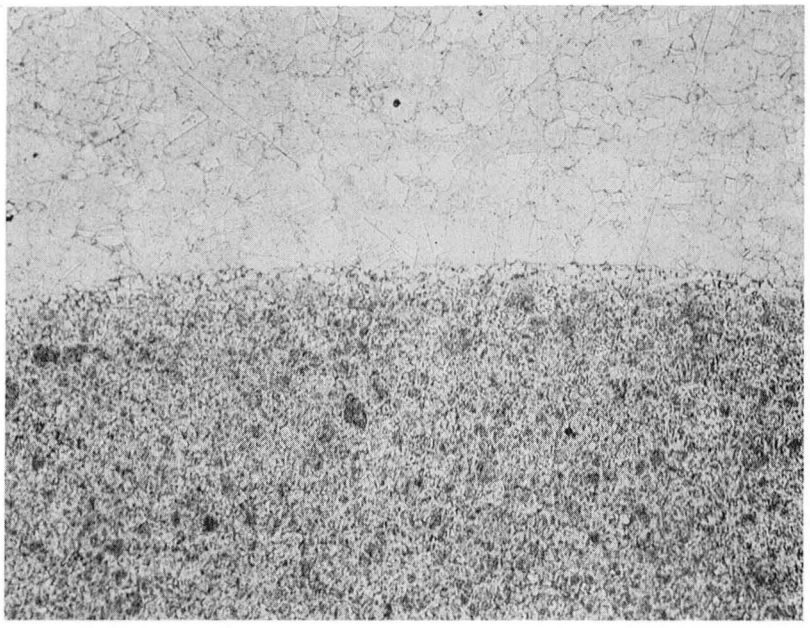

100X

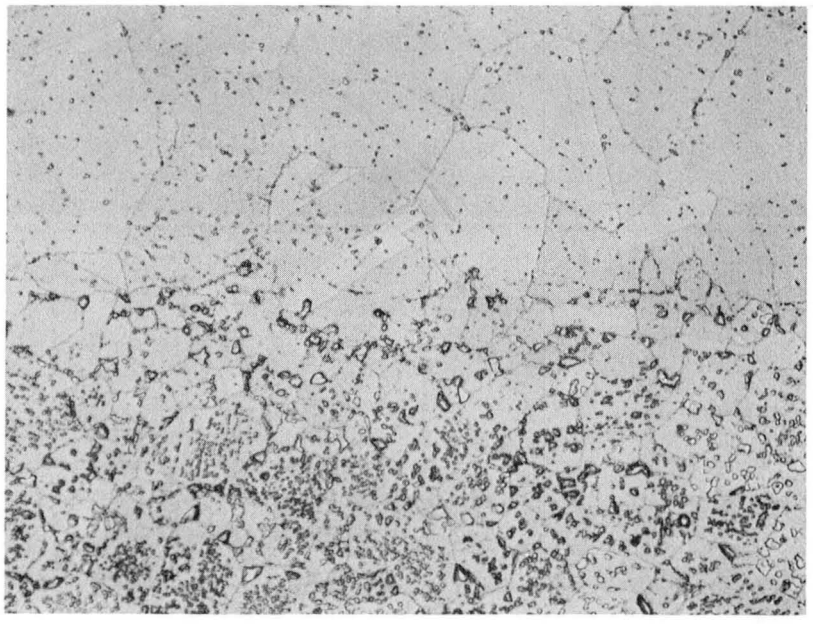

500X

Figure 70. Light Photomicrographs of Microstructure in Joint Region of CFM-56 Disk After Second Heat Treatment Iteration: 1190°C (2175°F)/2 Hours Salt Quench to 650°C (1200°F) + 760°C (1400°F)/16 Hours Air Cool.

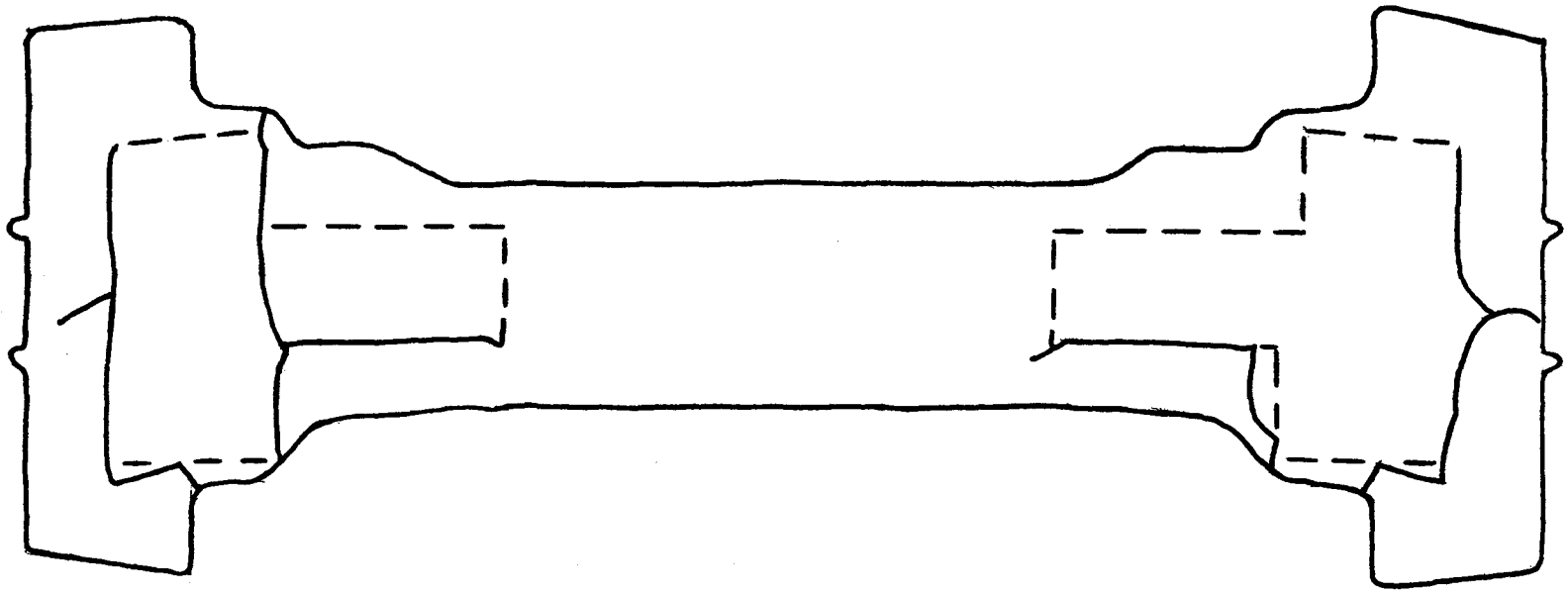

Figure 71. Schematic Diagram of Half Section of CFM-56 Disk Showing Zyglo Crack Patterns After Second Heat Treatment Iteration.

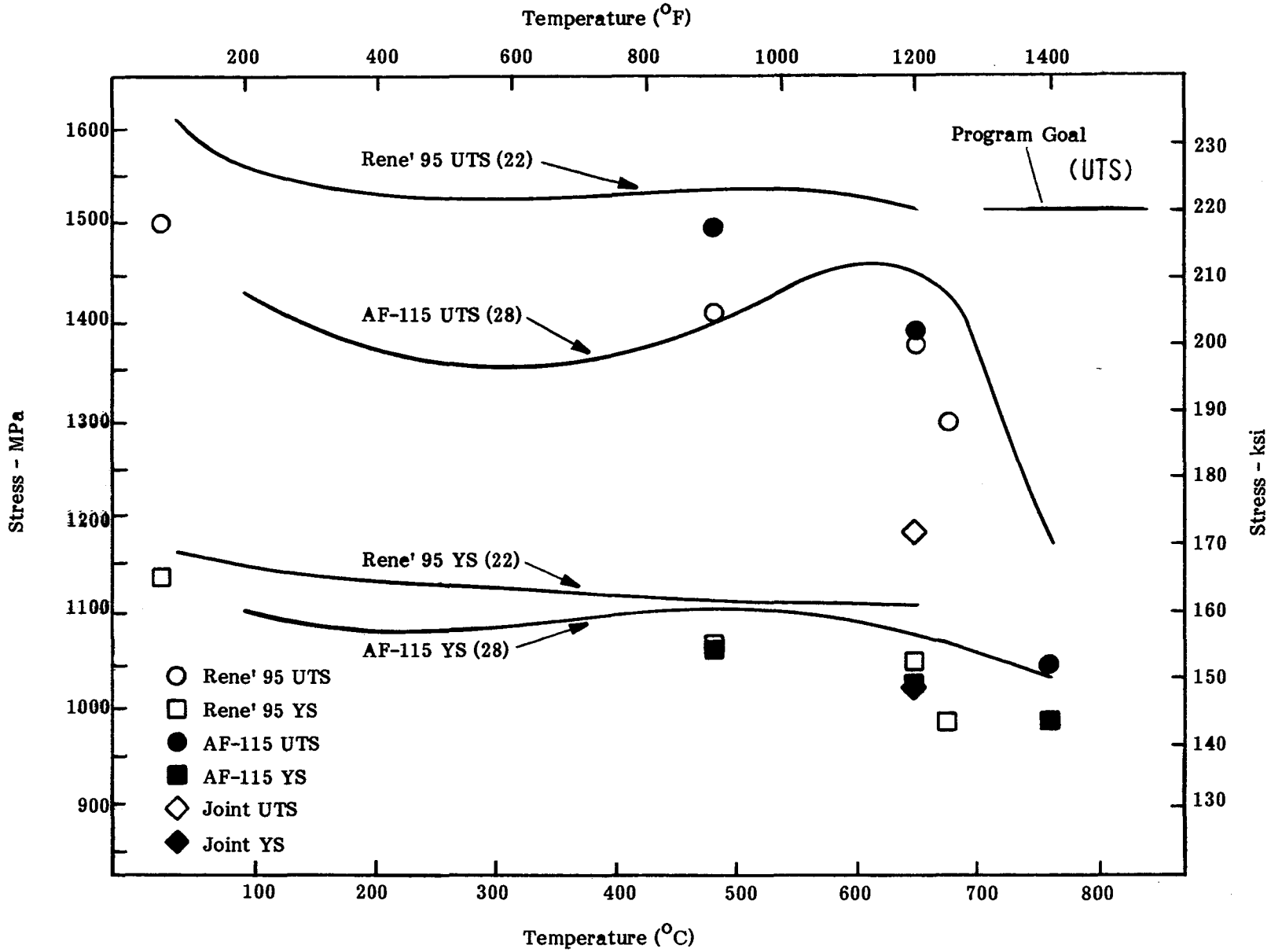

Figure 72. Plot of Average Tensile Strength Results for Specimens Machined From CFM-56 Disk Compared to Data Available for HIP'ed Rene' 95 (22) and AF-115 (28).

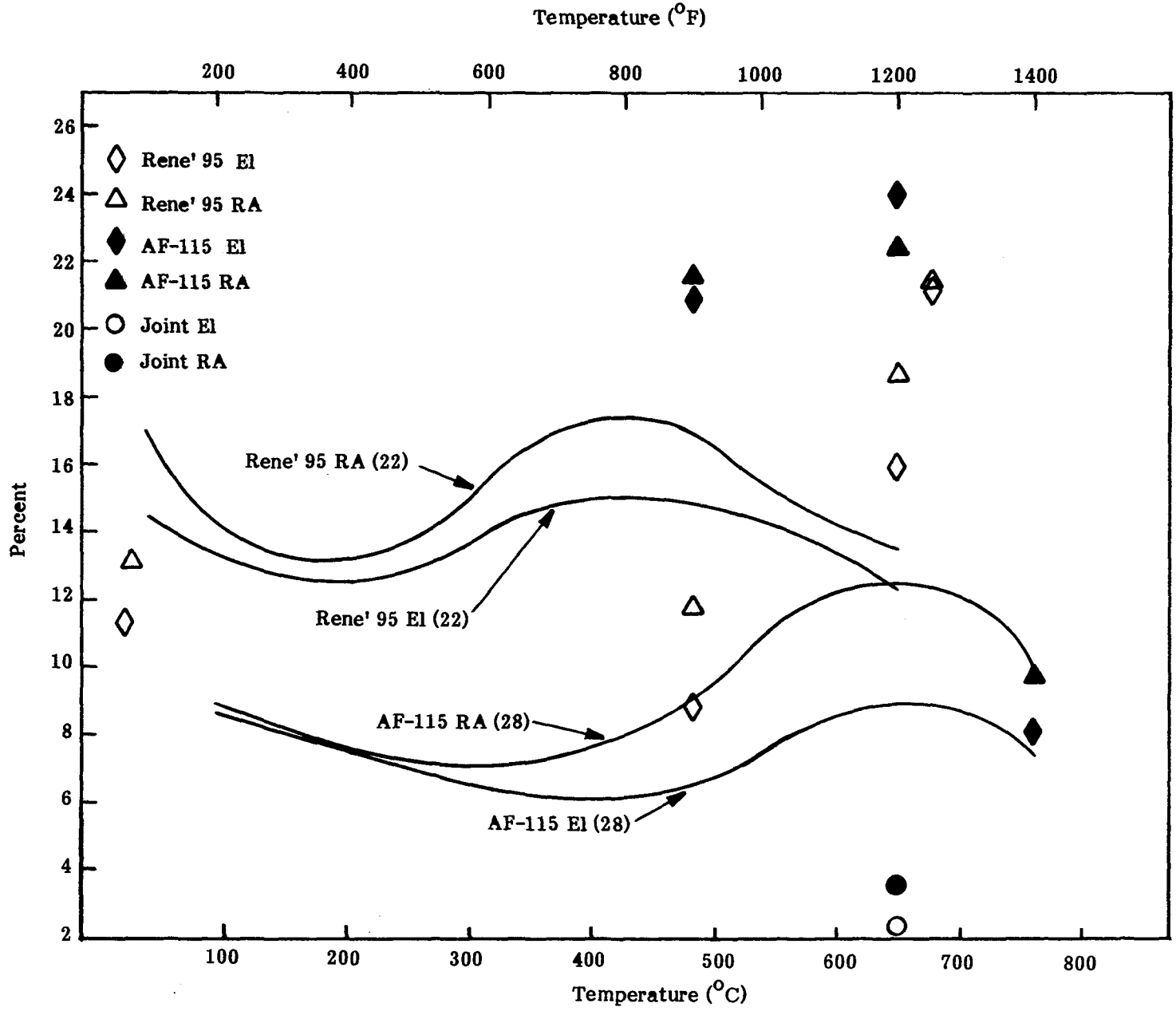

Figure 73. Plot of Average Tensile Ductility Results for Specimens Machined From CFM-56 Disk Compared to Data Available for HIP'ed Rene' 95 (22) and AF-115 (28).

(a) Rene' 95, 100X

(b) Rene' 95, 500X

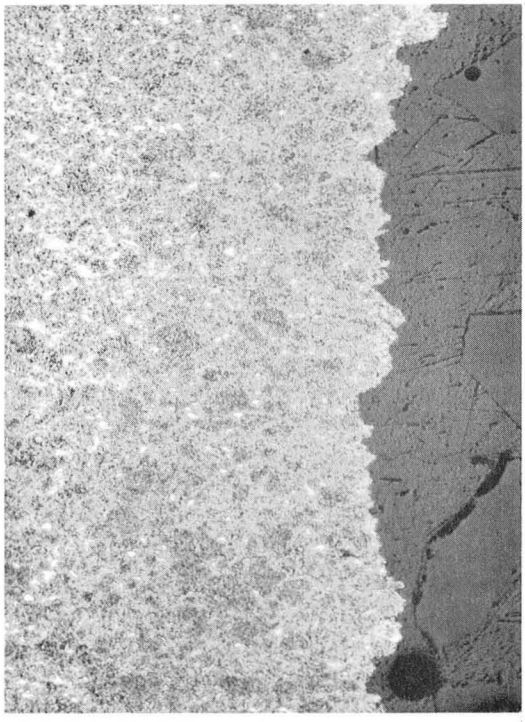

(c) AF-115, 100X

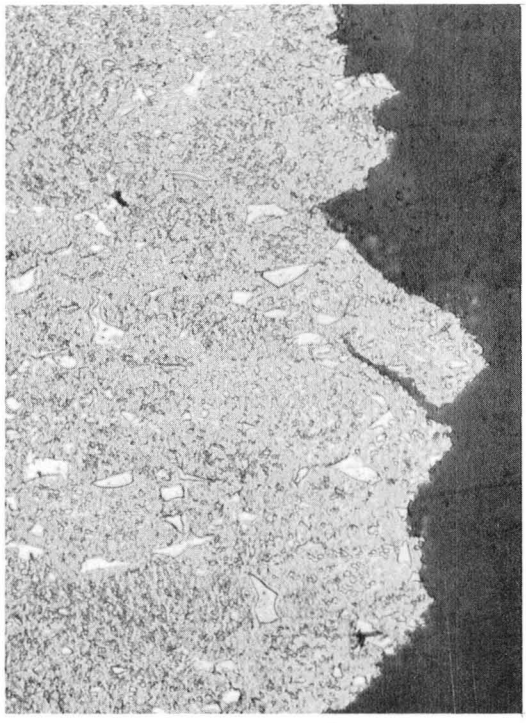

(d) AF-115, 500X

Figure 74. Light Photomicrographs of Typical Fracture Surfaces of Rene' 95 and AF-115 Tensile Specimens from CFM-56 Disk Tested at 650°C (1200°F).

1913-0

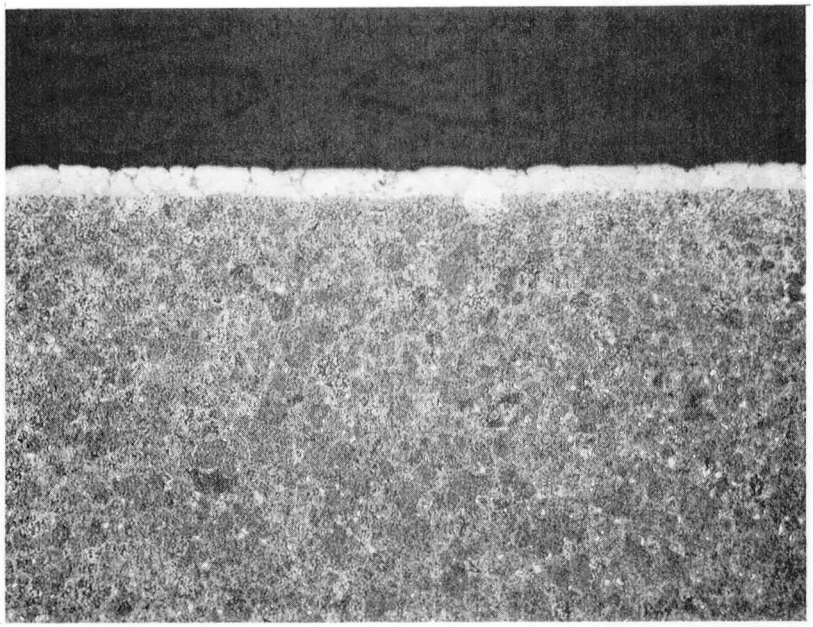

(a) 100X

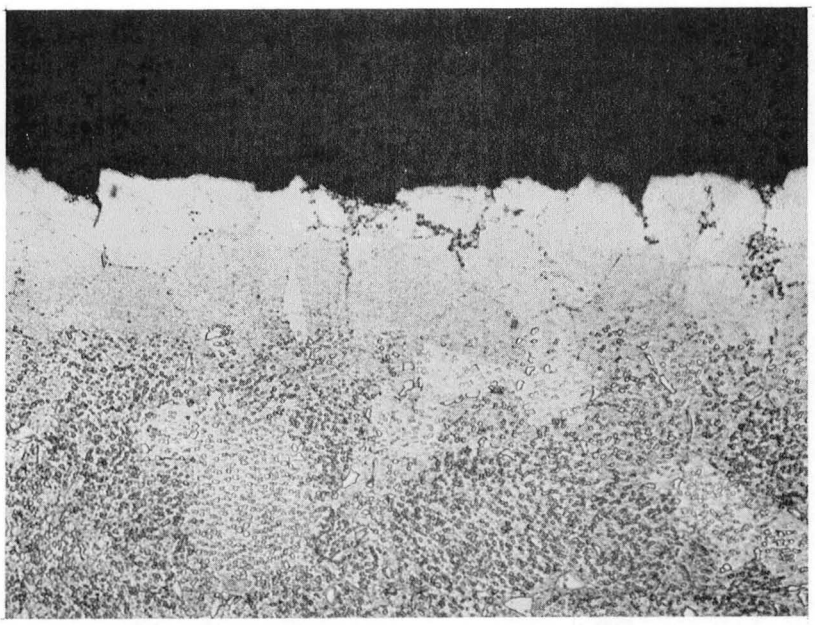

(b) 500X

Figure 75. Light Photomicrographs of Typical Fracture Surface of Joint Tensile Test Specimen From CFM-56 Disk Tested at 650°C (1200°F).

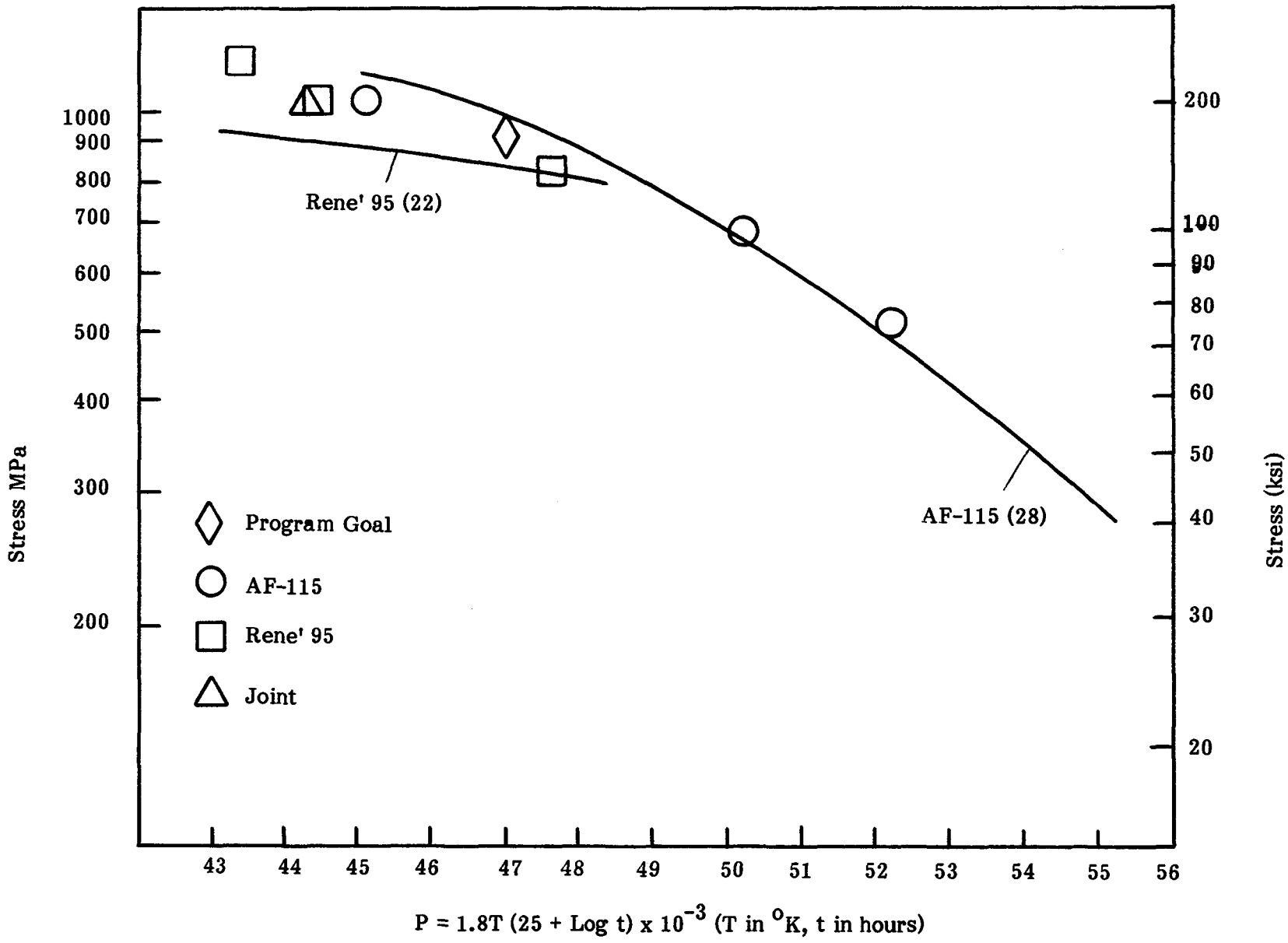

Figure 76. Larson-Miller Plot of Average Stress Rupture Life Results for Specimens Machined From CFM-56 Disk Compared to Data Available for HIP'ed Rene' 95 (22) and AF-115 (28).

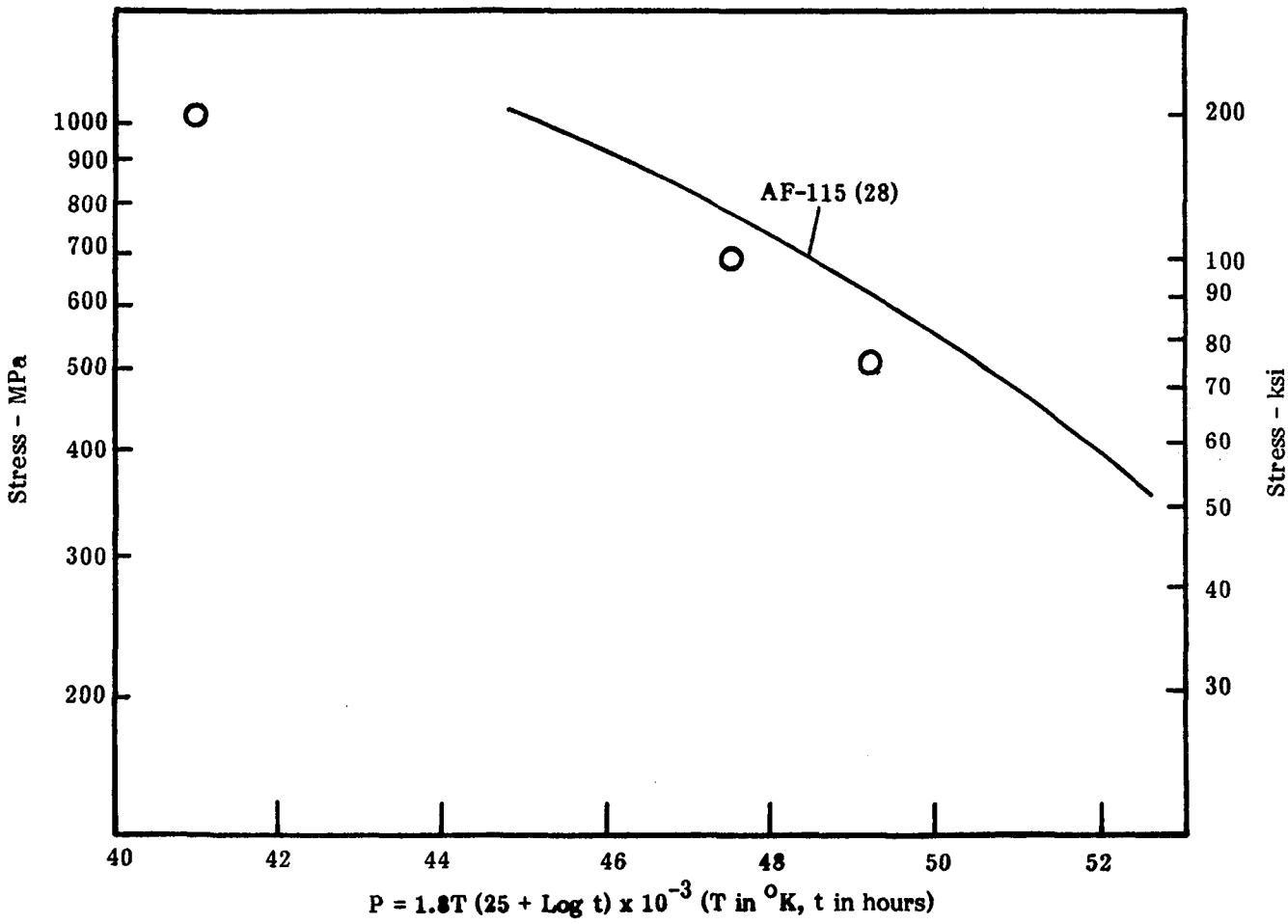

Figure 77. Larson-Miller Plot of Average Time to 0.2% Creep Results for AF-115 Specimens Machined From CFM-56 Disk Compared to Data Available for HIP'ed AF-115 (28).

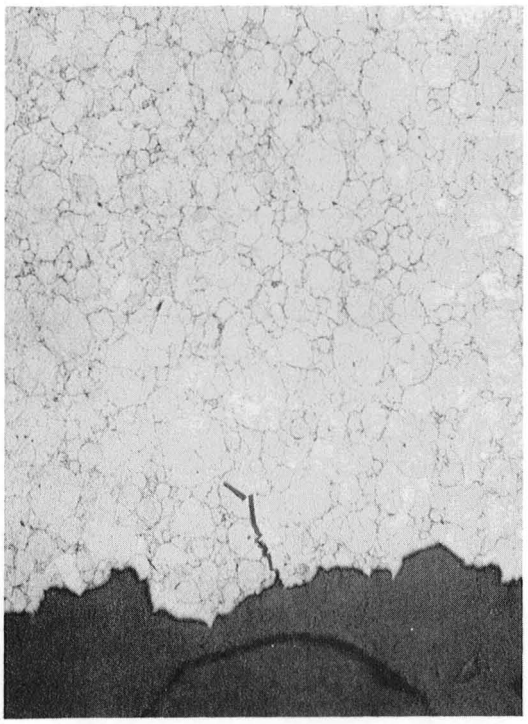

(a) Rene' 95, 100X

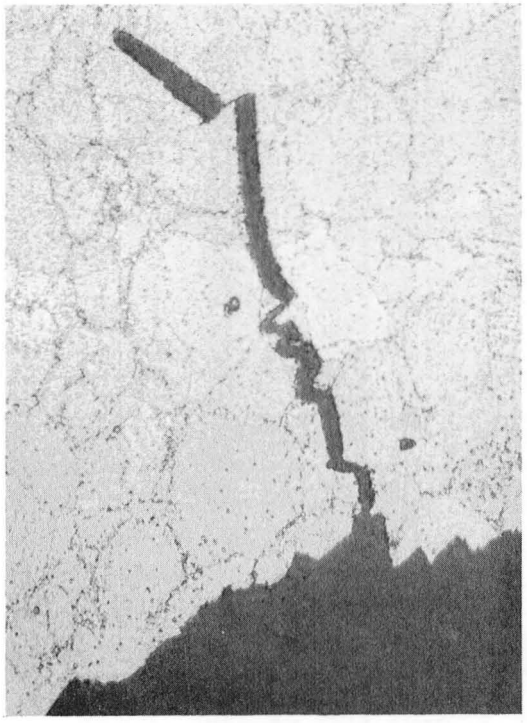

(b) Rene' 95, 500X

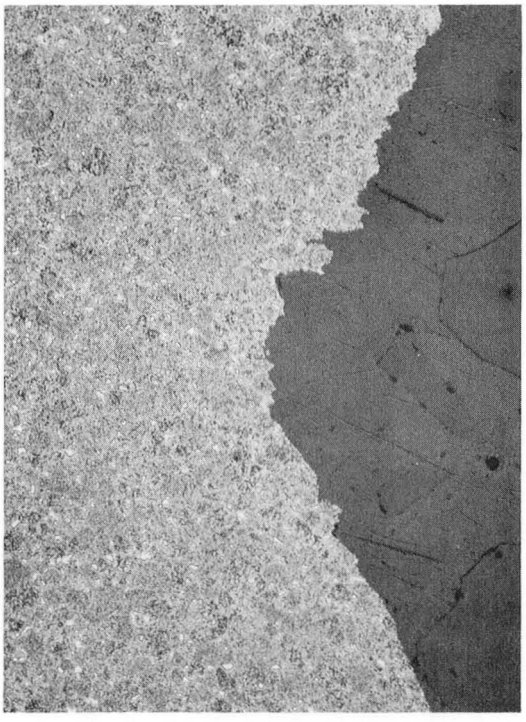

(c) AF-115, 100X

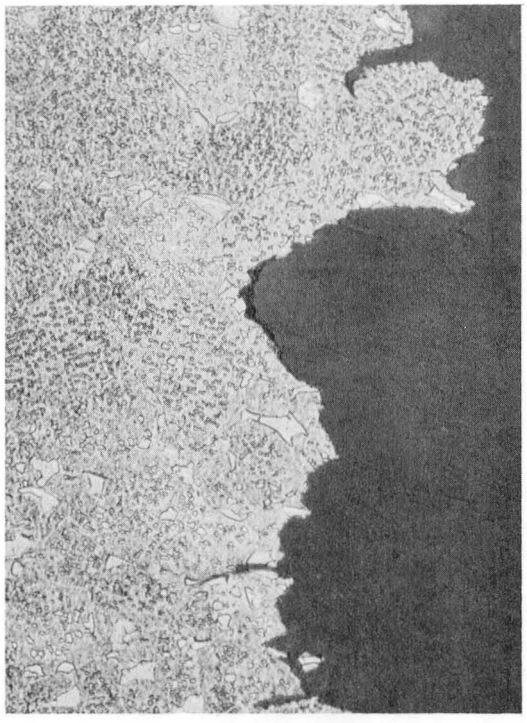

(d) AF-115, 500X

Figure 78. Light Photomicrographs of Typical Fracture Surfaces of Rene' 95 and AF-115 Stress Rupture Specimens from CFM-56 Disk Tested at 650°C (1200°F)/1035 MPa (150 ksi).

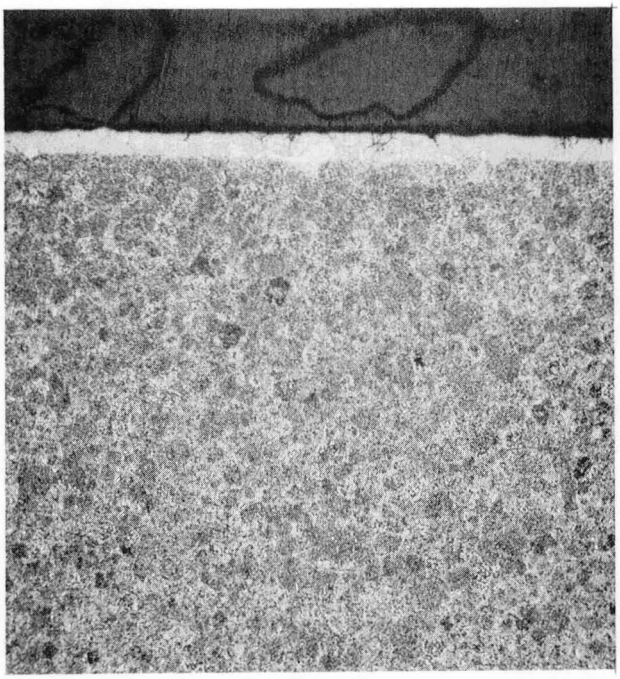

(a) 100X

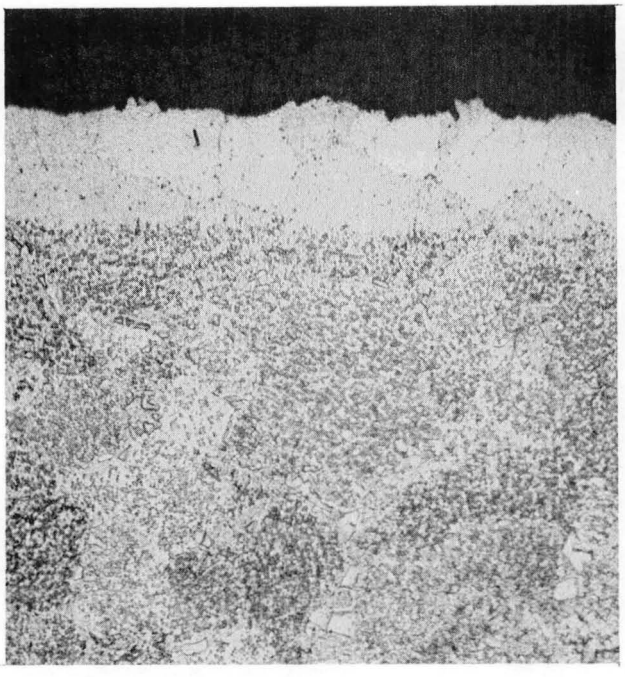

(b) 500X

Figure 79. Light Photomicrographs of Typical Fracture Surface of Joint Stress Rupture Specimen from CFM-56 Disk Tested at 650°C (1200°F)/1035 MPa (150 ksi).

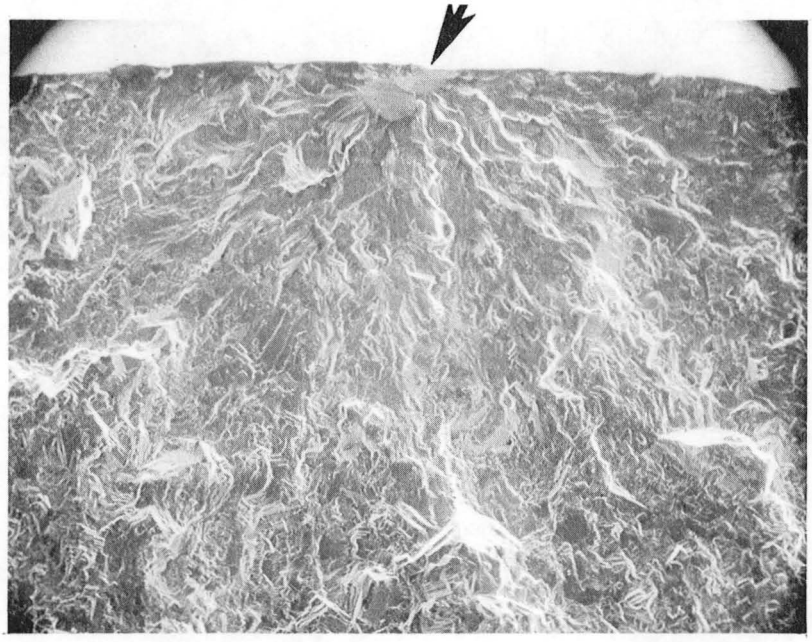

(a) 100X

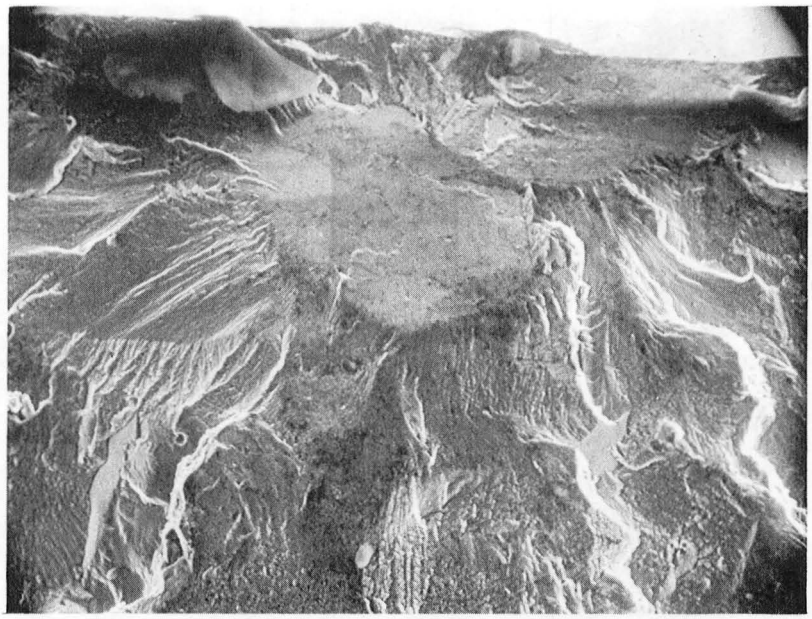

(b) 500X

Figure 80. SEM Fractographs of Fracture Initiation Site of Rene' 95 480°C (900°F) Low Cycle Fatigue Specimen Exhibiting Failure Life of 24,966 Cycles.

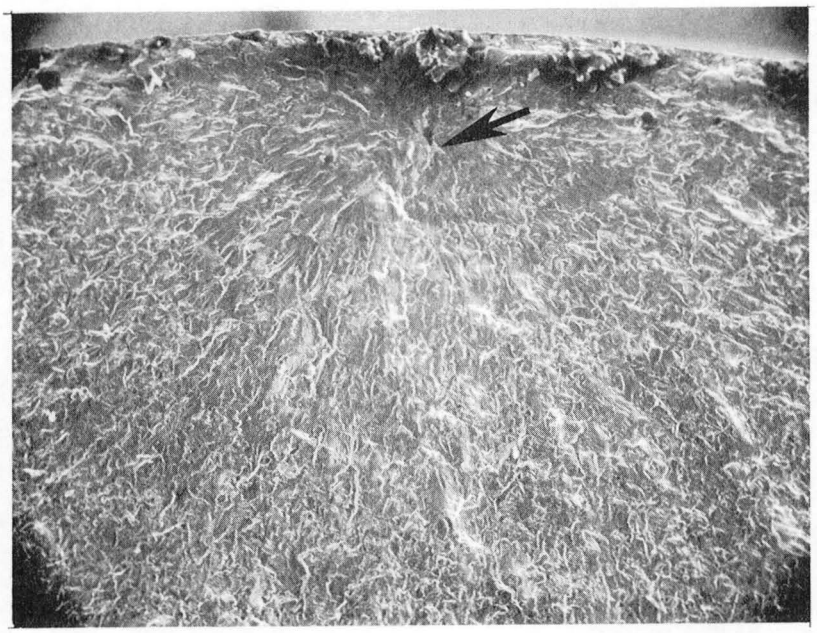

(a) 100X

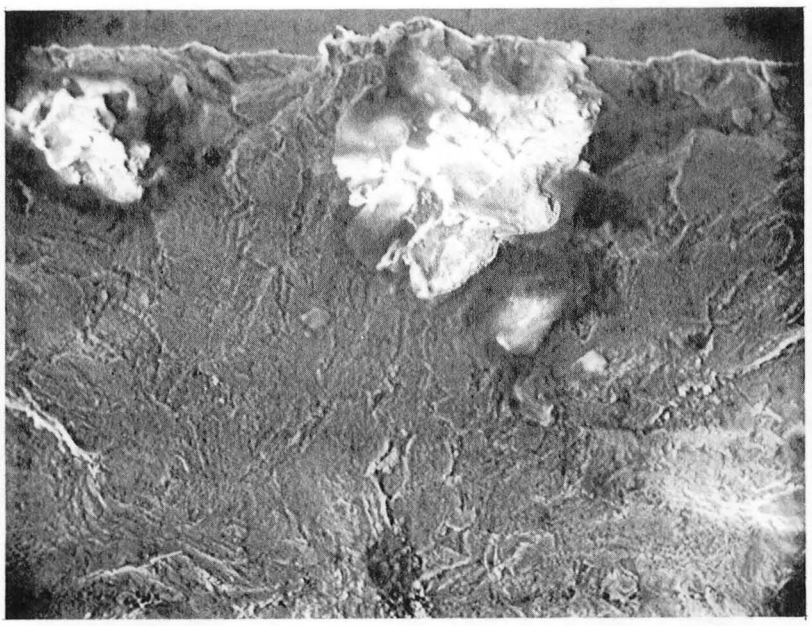

(b) 500X

Figure 81. SEM Fractographs of Fracture Initiation Site of AF-115 650°C (900°F) Low Cycle Fatigue Specimen Exhibiting Failure Life of 44,318 Cycles.

DISTRIBUTION LIST FOR NASA CR-165224

CONTRACT NAS 3-21351

(THE NUMBER IN PARENTHESES SHOWS HOW MANY COPIES IF MORE THAN ONE ARE TO BE SENT TO AN ADDRESS.)

MR. J. ACURIO
MS 77-5
NASA LEWIS RESEARCH CTR.
21000 BROOKPARK ROAD
CLEVELAND, OHIO 44135

MR. R.L. DAVIES
MS 106-1
NASA LEWIS RESEARCH CTR
21000 BROOKPARK ROAD
CLEVELAND, OH 44135

DR. R.L. DRESHFIELD
MS 105-1
NASA LEWIS RESEARCH CTR.
21000 BROOKPARK ROAD
CLEVELAND, OHIO 44135

DR.J. GAYDA
MS 49-3
NASA LEWIS RESEARCH CTR.
21000 BROOKPARK ROAD
CLEVELAND, OHIO 44135

DR. H.R. GRAY
MS 49-3
NASA LEWIS RESEARCH CTR.
21000 BROOKPARK ROAD
CLEVELAND, OHIO 44135

MR. S.J. GRISAFFE
MS 105-1
NASA LEWIS RESEARCH CTR
21000 BROOKPARK ROAD
CLEVELAND, OHIO 44135

MR. F.H. HARF (9)
MS ~~49-3~~ 105-1
NASA LEWIS RESEARCH CTR
21000 BROOKPARK ROAD
CLEVELAND, OHIO 44135

MR. M.J. HARTMAN
MS 3-7
NASA LEWIS RESEARCH CTR
21000 BROOKPARK ROAD
CLEVELAND, OHIO 44135

MR. M.H. HIRSCHBERG
MS 49-6
NASA LEWIS RESEARCH CTR.
21000 BROOKPARK ROAD
CLEVELAND, OHIO 44135

MR. C.E. LOWELL
MS 49-1
NASA LEWIS RESEARCH CTR.
21000 BROOKPARK ROAD
CLEVELAND, OHIO 44135

MATLS DIVISION FILES
MS 49-1
NASA LEWIS RESEARCH CTR
21000 BROOKPARK ROAD
CLEVELAND, OHIO 44135

DR. R.V. MINER
MS 49-3
NASA LEWIS RESEARCH CTR.
21000 BROOKPARK ROAD
CLEVELAND, OHIO 44135

DR. H.B. PROBST
MS 49-3
NASA LEWIS RESEARCH CTR.
21000 BROOKPARK ROAD
CLEVELAND, OHIO 44135

MR. R.A. SIGNORELLI
MS 106-1
NASA LEWIS RESEARCH CTR.
21000 BROOKPARK ROAD
CLEVELAND, OHIO 44135

MR. J.R. STEPHENS
MS 105-1
NASA LEWIS RESEARCH CTR.
21000 BROOKPARK ROAD
CLEVELAND, OHIO 44135

M. & S. CONTRACT SECTION
MS 501-11
NASA LEWIS RESEARCH CTR
21000 BROOKPARK ROAD
CLEVELAND, OH 44135

LIBRARY (2)
MS 60-3
NASA LEWIS RESEARCH CTR
21000 BROOKPARK ROAD
CLEVELAND, OHIO 44135

PATENT COUNSEL
MS 500-113
NASA LEWIS RESEARCH CTR
21000 BROOKPARK ROAD
CLEVELAND, OHIO 44135

REPORT CONTROL OFFICE
MS 5-5
NASA LEWIS RESEARCH CTR
21000 BROOKPARK ROAD
CLEVELAND, OHIO 44135

TECHNOLOGY UTILIZATION
MS 7-3
NASA LEWIS RESEARCH CTR
21000 BROOKPARK ROAD
CLEVELAND, OHIO 44135

CHIEF
AFSC LIAISON MS 501-3
NASA LEWIS RESEARCH CTR
21000 BROOKPARK ROAD
CLEVELAND, OHIO 44135

DR. M.A. GREENFIELD /RTM-6
NASA HEADQUARTERS
WASHINGTON, DC
20546

DR. L.A. HARRIS / RTM-6
NASA HEADQUARTERS
WASHINGTON, DC
20546

LIBRARY
NASA
GODDARD SPACE FLIGHT CTR
GREENBELT, MARYLAND 20771

LIBRARY
NASA
LANGLEY RESEARCH CENTER
HAMPTON, VA 23365

LIBRARY
NASA
MARSHALL SPACE FLIGHT CENTER
AL 35812

TECHNICAL LIBRARY / JM6
NASA
JOHNSON SPACE CENTER
HOUSTON, TX 77058

LIBRARY - ACQUISITIONS
JET PROPULSION LAB.
4800 OAK GROVE DRIVE
PASADENA, CA 91102

LIBRARY
NASA
DRYDEN FLIGHT RES. CTR
P. O. BOX 272
EDWARDS, CA 93523

LIBRARY - REPORTS
MS 202-3
NASA AMES RESEARCH CENTER
MOFFETT FIELD, CA 94035

ACCESSIONING DEPT (25)
NASA SCIENTIFIC & TECHN.
INFORMATION FACILITY
BOX 8757
BALTIMORE, MD 21240

DEFENCE DOCUMENTATION CTR
CAMERON STATION
5010 DUKE STREET
ALEXANDRIA, VIRGINIA
22314

DR. A. ROSENSTEIN
AFOSR (NE)
BOLLING AIR FORCE BASE
WASHINGTON, DC 20332

MR. A.M. ADAIR
AFWAL/MLLM
WRIGHT PATTERSON AFB.
OH 45433

MR. E.E. BAILEY
AFWAL/PO/NASA
WRIGHT PATTERSON AFB.
OH 45433

MR. J.K. ELBAUM
AFWAL/MLTM
WRIGHT PATTERSON AFB.
OH 45433

MR. N.M. GEYER
AFWAL/MLLN
WRIGHT PATTERSON AFB.
OH 45433

MR. H.A. JOHNSON
AFWAL/MLTM
WRIGHT PATTERSON AFB.
OH 45433

MR. C.A. LOMBARD
AFWAL/MLTM
WRIGHT PATTERSON AFB.
OH 45433

MR. W.T. O'HARA
AFWAL/MLLM
WRIGHT PATTERSON AFB.
OH 45433

MR. R.J. ONDERCIN
AFWAL/MLTM
WRIGHT PATTERSON AFB.
OH 45433

LIBRARY
AFWAL/TST
WRIGHT PATTERSON AFB.
OH 45433

DR. S. ISSEROW
ARMY MATERIALS AND
MECHANICS RESEARCH CTR.
WATERTOWN, MA 02172

LIBRARY
ARMY MATERIALS AND
MECHANICS RESEARCH CTR.
WATERTOWN, MA 02172

MR. J. LANE
ATL-ATP
AVRADCOM
USARTL
FORT EUSTIS, VA 23604

DR. J.C. HURT
ARMY RESEARCH OFFICE
BOX CM
DURHAM, NC 27706

MR. T.F. KEARNS AIR-320A
NAVAL AIR SYSTEMS COMMAND
NAVY DEPARTMENT
WASHINGTON, DC 20361

DR. B. MCDONALD
CODE 471, ONR
DEPARTMENT OF THE NAVY
ARLINGTON, VA 22217

MR. J.R. LANE
MATERIALS ADV. BD.
NAT. ACAD. OF SCIENCES
2101 CONSTITUTION AVE.
WASHINGTON, DC 20418

MR. F.W. BOULGER
BATTELLE MEMORIAL INST.
505 KING AVENUE
COLUMBUS, OHIO 43201

MCIC
BATTELLE MEMORIAL INST.
505 KING AVENUE
COLUMBUS, OHIO 43201

PROF. J.C. WILLIAMS
CARNEGIE MELLON
UNIVERSITY
PITTSBURGH, PA 15213

PROF. L.J. EBERT
DEPT. OF MET. & MAT. SCI.
CASE - WESTERN RESERVE U.
CLEVELAND, OH 44106

PROF. J.F. WALLACE
DEPT. OF MET. & MAT. SCI.
CASE - WESTERN RESERVE U.
CLEVELAND, OH 44106

DR. J.K. TIEN
HENRY KRUMB SCH. OF MINES
COLUMBIA UNIVERSITY
520 WEST 120 STREET
NEW YORK, NY 10027

LIBRARY
DENVER RESEARCH INSTITUTE
UNIVERSITY PARK
DENVER, COLORADO 80210

DR. R.I. JAFFEE
ELECTRIC POWER RESEARCH
INSTITUTE
BOX 10412
PALO ALTO, CA 94304

MR. K. KULKARNI
IIT RESEARCH INSTITUTE
10 WEST 35TH STREET
CHICAGO, ILLINOIS 60616

PROF. N.J. GRANT
DEPT. OF METALLURGY
MASS. INST. OF TECHNOLOGY
CAMBRIDGE, MA 02139

PROF. R.A. RAPP
DEPT. OF METALL. ENGRG.
OHIO STATE UNIVERSITY
COLUMBUS, OHIO 43210

PROF. G.S. ANSELL
RENSSELAER POLYTECHNICAL INSTITUTE
TROY, NY 12181

PROF. O. SHERBY
DEPT. OF MATERIALS SCI.
STANFORD UNIVERSITY
PALO ALTO, CALIF. 94305

MR. R.A. LULA RES. CTR.
ALLEGHENY LUDLUM STEEL CORP.
BRACKENRIDGE, PENNA. 15014

LIBRARY
AVCO SYSTEMS DIVISION
201 LOWELL STREET
WILMINGTON, MA 01887

MR. J. WALTERS
AVCO LYCOMING DIV.
550 S. MAIN STREET
STRATFORD, CT 06497

MR. L. ENGEL
BROWN-BOVERI TURBO, INC.
711 ANDERSON AVE, N.
ST. CLOUD, MN 56301

LIBRARY
CABOT CORPORATION
STELLITE DIVISION
P.O. BOX 746
KOKOMO, INDIANA 46901

MR. D.A. NAIL
CAMERON IRON WORKS, INC
P.O. BOX 1212
HOUSTON, TX 77001

MR. R.E. SCHWER
CANNON-MUSKEGON
MUSKEGON, MI 49443

DR. D.R. MUZYKA
CARPENTER TECHNOLOGY CORP
RES. & DEV. CENTER
P.O. BOX 662
READING, PA 19603

DR. A. ROY
CHRYSLER CORPORATION
P.O. BOX 1118
DETROIT, MI 48231

MR. H. MORROW
CLIMAX MOLYBDENUM CORP.
1, GREENWICH PLACE
GREENWICH ,CT 06830

DR. E.P. WHELAN
CLIMAX MOLYBDENUM COMPANY
1600 HURON PARKWAY
ANN ARBOR, MICHIGAN 48106

MR. E.J. DULIS, PRESIDENT
COLT INDUSTRIES
CRUCIBLE MAT RES CTR
P.O. BOX 88
PITTSBURGH, PA 15230

MR. J. MOGUL
DIR - MATLS ENGRG
CURTISS-WRIGHT
1 PASSAIC ST
WOOD-RIDGE, NJ 07075

POWDER METALS RESEARCH
FIRTH STERLING, INC.
P.O. BOX 71
PITTSBURGH, PENNA. 15230

DR. C.E. FELTNER
FORD MOTOR COMPANY
P.O. BOX 2053
DEARBORN, MI 48121

DR. Y.P. TELANG
MATERIALS DEVELOPMENT
FORD MOTOR COMPANY
ROUGE OFFICE BUILDING
DEARBORN, MICHIGAN 48121

DR. R.F. KIRBY
CHIEF, MATERIALS ENG.
GARRETT TURBINE ENGINE CO
P.O. BOX 5217
PHOENIX, AZ 85010

MR. J. HSIA
AEG/GED
1000 WESTERN AVENUE
LYNN, MA 01905

DR. M. KAUFMAN
AEG/GED
1000 WESTERN AVE
LYNN, MA 01905

LIBRARY
R. & D. CENTER
GENERAL ELECTRIC COMPANY
P.O. BOX 8
SCHENECTADY, N.Y. 12301

MR. C.T. SIMS
GAS TURBINE PROD.DIV.
GENERAL ELECTRIC COMPANY
SCHENECTADY, N.Y. 12345

MR. D. CHANG
AEG/GED
GENERAL ELECTRIC COMPANY
CINCINNATI, OHIO 45215

MR. G.E. WASIELEWSKI
AEG/GED
GENERAL ELECTRIC COMPANY
CINCINNATI, OH 45215

DR. M. HERMAN
DETROIT DIESEL ALLISON DV
P.O. BOX 894
INDIANAPOLIS, IN 46206

MR. E.S. NICHOLS
DETROIT DIESEL ALLISON DV
P.O. BOX 894
INDIANAPOLIS, IN 46206

LIBRARY
MATERIALS SCIENCE LAB.W5
DETROIT DIESEL ALLISON
GENERAL MOTORS
INDIANAPOLIS,IN 46206

MRS. V. SCHMIDT
GOULD LABORATORIES
GOULD INC.
540 EAST 105TH STREET
CLEVELAND, OH 44108

LIBRARY - RESEARCH CENTER
HERCULES, INC
910 MARKET STREET
WILMINGTON, DE 19899

MR. W.R. FREEMAN
HOWMET TURB. COMP. CORP.
47500 STEAMBOAT ROAD
GREENWICH, CT 06830

DR. J.R. MIHALISIN
HOWMET
AUSTENAL-DOVER DIVISION
P.O. BOX 371
DOVER, NJ 07801

DR. L.F. NORRIS
HOWMET TURB. COMP. CORP.
699 BENSON ROAD
WHITEHALL, MI 49461

MR. F.L. PERRY
HUNTINGTON ALLOYS INC.
HUNTINGTON, WV
25720

DR. R. WIDMER
INDUSTR. MATLS. TECHNOL.
19 WHEELING AVENUE
WOBURN, MA 01801

DR. R.F. DECKER
INTERNATIONAL NICKEL CO.
ONE NEW YORK PLAZA
NEW YORK, NY 10004

DR. J.H. BROPHY
INTERNATIONAL NICKEL CO.
RES. & DEV. CENTER
STERLING FOREST
SUFFERN, NY 10901

MR. T.E. MILES
KELSEY HAYES CORPORATION
38481 HURON RIVER DRIVE
ROMULUS, MI 48174

MR. R. DAYKIN
LADISH COMPANY
5481 SOUTH PACKARD AVE
CUDAHY, WISCONSIN 53110

DR. J.F. RADAVICH
MICROMET LABORATORIES
202 SOUTH STREET
WEST LAFAYETTE,
INDIANA 47906

MR. T.G. MCNAMARA
ROCKWELL INTERNATIONAL
ROCKETDYNE DIVISION
6633 CANOGA AVENUE
CANOGA PARK, CA 91304

MR. N. PATON
ROCKWELL INTERNATIONAL
SCIENCE CENTER
THOUSAND OAKS, CALIFORNIA
91360

DR. J.W. PRIDGEON
SPECIAL METALS
CORPORATION
NEW HARTFORD, N.Y. 13413

MR. R. BECK
TELEDYNE-CAE
P.O. BOX 6971
TOLEDO, OH 43612

RESEARCH LIBRARY
UNITED TECHNOLOGIES CORP
400 MAIN STREET
EAST HARTFORD, CT
06108

MR. D.J. EVANS
PRATT & WHITNEY AIRCRAFT
UNITED TECHNOLOGIES CORP
400 MAIN STREET
EAST HARTFORD, CT 06108

MR. R.L. ATHEY
PRATT & WHITNEY AIRCRAFT
UNITED TECHNOLOGIES CORP
WEST PALM BEACH,
FLORIDA 33402

LIBRARY
PRATT & WHITNEY AIRCRAFT
UNITED TECHNOLOGIES CORP
WEST PALM BEACH, FLORIDA
33402

MR. J. B. MOORE
PRATT & WHITNEY AIRCRAFT
UNITED TECHNOLOGIES CORP
WEST PALM BEACH,
FLORIDA 33402

MR. W.B. KENT
UNIVERSAL CYCLOPS STEEL
RES. & DEV. DEPARTMENT
BRIDGEVILLE, PENNA 15017

MR. L.W. LHERBIER
UNIVERSAL CYCLOPS STEEL
RES. & DEV. DEPARTMENT
BRIDGEVILLE, PENNA 15017

MR. F.J. WALL
WESTINGHOUSE ELECTRIC
STEAM DIVISION
P.O. BOX 9175
LESTER, PENNA. 19113

LIBRARY
WILLIAMS RESEARCH CORP.
2280 W. MAPLE ROAD
WALLED LAKE, MI 48088

MR. J. COYNE
WYMAN-GORDON COMPANY
NORTH GRAFTON,MA 01536

MR. M. WHITE
WYMAN-GORDON COMPANY
NORTH GRAFTON,MA 01536

MR. J. GANGLER
CONSULTANT AIAA
6730 KENWOOD FOREST LANE
CHEVY CHASE,MD 20815

MR. C.H. LUND
CONSULTANT
15 N. WINDSOR ROAD
ARLINGTON HEIGHTS, IL
60004